Universidade de Aveiro
Ano 2012
Departamento de Electrónica, Telecomunicações e Informática

Hugo Miguel Cravo Gomes

ESTUDO DO IMPACTO DA DISTORÇÃO NÃO-LINEAR EM ARQUITECTURAS DE RECEPÇÃO RÁDIO

Universidade de Aveiro
Ano 2012
Departamento de Electrónica, Telecomunicações e Informática

Hugo Miguel Cravo Gomes

Estudo do Impacto da distorção Não-Linear em Arquitecturas de Recepção Rádio

(STUDY OF THE IMPACT FROM NONLINEAR DISTORTION IN RADIO RECEIVER ARCHITECTURES)

Dissertação apresentada à Universidade de Aveiro para cumprimento dos requisitos necessários à obtenção do grau de Doutor em Eng. Electrotécnica, realizada sob a orientação científica do Doutor Nuno Miguel Gonçalves Borges de Carvalho, Professor Associado com Agregação do Departamento de Electrónica, Telecomunicações e Informática da Universidade de Aveiro e Coorientação do Doutor Rafael Ferreira da Silva Caldeirinha, Professor Coordenador do Departamento de Engenharia Electrotécnica da Escola Superior de Tecnologia e Gestão do Instituto Politécnico de Leiria

Apoio financeiro da Fundação para Ciência e Tecnologia

Dedico este trabalho aos meus três tesouros: a minha esposa e as minhas filhas.

(Dedicated to my three treasures: my wife and my daughters.)

o júri

presidente

Prof. Doutor Artur Manuel Soares da Silva
Professor Catedrático da Universidade de Aveiro

vogais

Prof. Doutora Mónica Fernández Barciela
Professora Titular no Departamento de Teoria de la Señal y Comunicaciones, Escuela Técnica Superior de Ingenieros de Telecomunicación, Universidade de Vigo

Prof. Doutor Vitor Manuel Grade Tavares
Professor Auxiliar da Faculdade de Engenharia da Universidade do Porto

Prof. Doutor João Nuno Pimentel da Silva Matos
Professor Associado da Universidade do Aveiro

Prof. Doutor Nuno Miguel Gonçalves Borges de Carvalho (Orientador)
Professor Associado com Agregação da Universidade do Aveiro

Prof. Doutor Rafael Ferreira da Silva Caldeirinha (Co-orientador)
Professor Coordenador do Instituto Politécnico de Leiria

agradecimentos

Todo o presente trabalho doutoral não teria sido possível sem a constante orientação, força e incentivo do Professor Nuno Borges de Carvalho, que a toda a hora se mostrou disponível para comigo ultrapassar as dificuldades e nos momentos mais difíceis sempre me encorajou a avançar e contornar os obstáculos. Para ele o meu muito obrigado.

Quero agradecer também ao Professor Rafael Caldeirinha pelos conselhos e ajudas durante o trabalho doutoral e na redacção da presente tese.

Quero ainda deixar aqui um agradecimento aos colegas que comigo colaboraram, quer disponibilizando materiais necessários para as experiências laboratoriais realizadas, quer contribuindo com ideias para a resolução das dificuldades.

Por fim, quero agradecer a toda a minha família que sempre teve presente, me apoiou e incentivou, me proporcionou “paz e sossego” nos momentos mais críticos e que sempre acreditou que seria capaz.

palavras-chave

Electrónica de radiofrequência, sistemas nãolineares, distorção de intermodulação, arquitecturas de conversão directa, cancelamento de interferidores.

resumo

A dissertação de doutoramento apresentada insere-se na área de electrónica não-linear de rádio-frequência (RF), UHF e microondas, tendo como principal campo de acção o estudo da distorção não-linear em arquitecturas de recepção rádio, nomeadamente receptores de conversão directa como Power Meters, RFID (Radio Frequency IDentification) ou SDR (Software Define Radio) front-ends. Partindo de um estudo exaustivo das actuais arquitecturas de recepção de radiofrequência e revendo todos os conceitos teóricos relacionados com o desempenho não-linear dos sistemas/componentes electrónicos, foram desenvolvidos algoritmos matemáticos de modulação dos comportamentos não-lineares destas arquitecturas, simulados e testados em laboratório e propostas novas arquitecturas para a minimização ou cancelamento do impacto negativo de grandes interferidores em frequências vizinhas ao do sistema pretendido.

keywords

Radiofrequency electronics , nonlinear systems, IMD (intermodulation distortion), direct-conversion architectures, interference cancellation

abstract

The doctoral dissertation presented is inserted in the area of electronic non-linear radio frequency (RF), microwave and UHF, with the main field of action focus in the study of nonlinear distortion in radio reception architectures, including direct-conversion receivers like Power Meters, RFID (Radio Frequency Identification) or SDR (Software Defined Radio) front-ends. Started with on an exhaustive study of current radio reception architectures and the review from all the theoretical concepts related to nonlinear systems / electronics, it were developed mathematical algorithms for modulating the nonlinear behaviour of these architectures, simulated and tested in the laboratory and proposed new architectures for reduction or cancellation of the negative impact of large jammers at frequencies surrounding the system of choice.

Index

Index of figures

Index of Tables

Abbreviations

IF – Intermediate Frequency

RF – Radio Frequency

RFID – Radio Frequency Identification

LNA – Low Noise Amplifier

I/Q – Phase /Quadrature mixing

BS – Base Station

IMD – Intermodulation distortion

SDR – Software Define Radio

PAPR – Peak-to-Average Power Ratio

LO – Local Oscillator

SNR – Signal to Noise Ratio

CHAPTER 1

Introduction

In today's world, the exponential growth in communications between people/companies in different places (at the same time), the increasing requirements to measure and control all processes, the analysis in real time, the mandatory requirement to provide information and entertainment data to electronic devices that must be increasingly smaller and more complex, requires a continuous and nonstop searching for new technologies with greater capacity, lower cost, reduced size and improved reliability.

The communication systems based on radio-frequency (RF) transmission are one of the greatest examples of this challenging demand. These systems, present in almost all equipment used in daily life as mobile phones, Personal Digital Assistants (PDAs), notebooks, Radio Frequency Identification (RFID), sensors, among others, require an increasing versatility and ability to storage of data, huge transmission rates of information and size reduction.

All these needs for more sophisticated equipment, along with a greater number of services available in a single equipment (preferably portable), besides the drastic size reductions from the electronic components, requires a constant search for new architectures and new materials in order to maximize the features offered.

Associated to this almost survival need to the development of new radio architectures and systems for data transmission, researchers will have to take special care to the several problems that arise from the nonlinear phenomena of "key" components from receiver's architectures such as Low Noise Amplifiers (LNA), Mixers and Oscillators [1][2]. This nonlinear behaviour is responsible for degradation from the received signal both in amplitude and phase, directly affecting the good reception quality and correct demodulation [3]. Another problem in RF systems that is intrinsically linked to nonlinear behaviour is interference between different systems. When several systems have to coexist in a narrow bandwidth of operation, if the system's power levels involved is significant different, there is a huge probability that one system can severely degrade the receiver's signal quality from its neighbours, even the systems are in distinct frequencies [4]. Those

interference characteristics arise from the nonlinear intermodulation products (IMD) generated in several RF components, mainly in receiver's RF block, because the nonlinear response from components like Low Noise Amplifiers (LNA) have the capability to generate new spectral products that will fall in the operation frequency band of the desire system.

As refer, the nonlinear behaviour in RF transceivers has a significant impact in the correct functioning of the designed architecture but also in systems that can operate in adjacent frequency bands. Furthermore, these interference problems are also common among the broadband emitting systems, which although operating at very distinct frequency band than other RF systems, continue to cause severe problems in high sensitivity receivers, since the high power levels transmitted and the harmonic products resulting from nonlinear transmitters (the Power Amplifier is a good example) will assume the jammer's role in their neighbours communications systems.

1.1 - Motivation

For all the reasons previous presented is clearly imperious the preparation of a meticulous study and analysis to nonlinear behaviour in RF architectures (especially in receiver's front-ends), since nonlinear products play a major role in the performance and reliability from radio systems.

At first glance all nonlinear products are seen as harmful to the proper functioning of an RF system. This idea is present in a common linearization's process from the impulse response of the Low Noise Amplifiers (LNA), to obtain a better replica of the input signal (minimization from the new spectral components generated), or in the cancellation of harmful contributions from signal jammers in the adjacent frequency bands from desired operating system [3][5]. However, these nonlinear products are also currently used in several simple applications, especially in architectures that use the spectral regrowth created to easily down-convert a RF signal to baseband frequency. As will be seen in next chapters, taking advantage from the even order intermodulation products, there is a replica from the original signal in "near DC" frequencies, allowing performing a acceptable and reliable directly conversion without the use of oscillators and mixers, making the architecture simple, cheaper and reducing energy consumption.

One of the most known applications of this concept is the diode power meter, present in several RF systems, like the well know Global System for Mobile communication (GSM). This power meters are used in base-stations to manage the process of power control between the mobile and base-station [6]. Other typical system that uses a similar operation principle is the Radio Frequency Identification (RFID) Tags, in particularly the Passive Tags, where, due to lack of battery, the main concern is the minimum energy consumption. In these small tags with no batteries, the nonlinear phenomena has a double importance: it allows harvesting energy from the received RF signal (direct conversion from RF to DC) and permit the retransmission of RF signal using the second harmonics created in a process similar to conversion RF → baseband described above but in two times the original frequency operation [7][8][39].

Several others applications use this phenomena, especially when the size minimization and very low cost is an imperative in the production of this RF system. Software Define Radio front-ends is another scenario where nonlinear products could have an interesting application in future applications.

Returning to "bad effect side" of the nonlinear products, the interference in neighbours systems is one of the most concern problems that nonlinear behaviour is responsible for. This issue is even more important since the exponential increase of RF systems concentrated in a narrow band frequency, emphasized the interference problems that occur between systems due the nonlinearities of strong power active elements that exist in the radio frequency receiver's. This type of interference is so problematic that there are real systems, both commercial and military, whose performance is seriously affected by the co-existence of interfering radio signal near its frequency band with relatively high power values. Typical examples are the broadband band transmitter or powerful RF transceivers (like radar for instance), where the interferer will have a tremendous huge power compare with desire signal power level. Although separate in frequency, the products generated by nonlinear active components at receiver's entry (typically the LNA block) will cause the "masking" of the lower power signal and consequently degradation in quality reception. This problem appears to be especially difficult in prioritized communications (like military) that lead to the emergence of point solutions useful for specific cases, but very limited scope and innovation [9]. It is therefore important to study the origin of this interference, completely modelling the nonlinear behaviour with mathematical approaches, test the robustness and reliability of these models and finally

design and propose some new receiver's radio architectures more robust to interference and less subject to loss the communication signal.

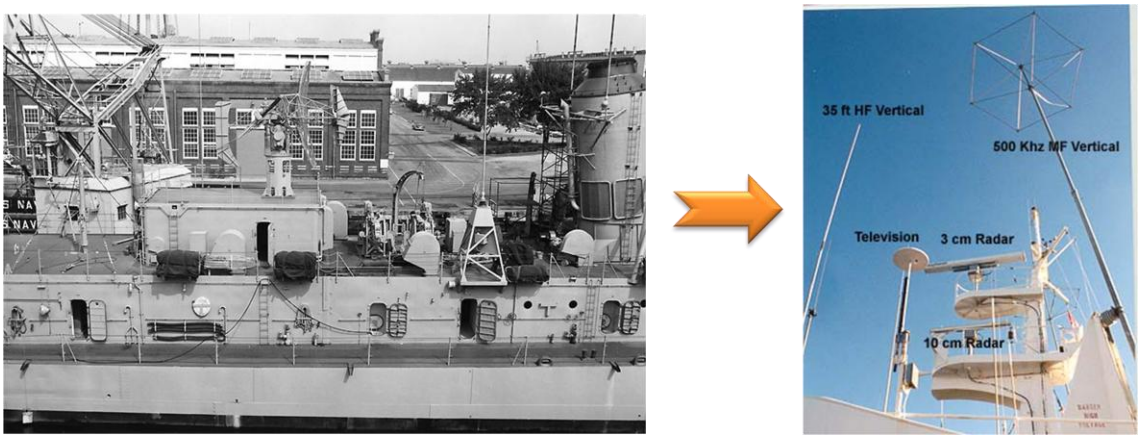

Fig 1.1 – A war boat: a typical scenario where the interference between systems is a very critical problem.

One more time, this issue is also of greater importance in the case of RFID systems, because the harmful interference has direct implications in the identification of objects and/or people (ex. passports), severely affecting the performance of the entire system. Thus, the reduction of ambiguity in such systems is critical to its future success, especially if passive tags are used (much more dependent on the RF signal from the Reader, and as such, much more "exposed" to external interference).

A third scenario where the interferer's nonlinear products have an important impact in the reception is Software Define Radio (SDR), and more recently Cognitive Radio. The main objective of these systems is to receive a signal with a wide range of bandwidth and, by using digital tools, be able to separate the different radio signals embedded in the wide spectral received without the need for different analogue front ends for each system. For these reasons, these architectures are extremely sensitive to large jammers and heavily affected by the nonlinear products generated by the RF components before digitalization (the presence of harmonics and intermodulation products have here a role even more harmful than in discrete systems). In these systems, the direct conversion architecture (RF→baseband) or RF direct digitalization are typically used in front-end receivers. The presence of undesired LNA's nonlinear products can severely corrupt the received signal, degrading a proper conversion to the digital domain and making it impossible to correct separate the different frequency spectrums from desired signals without quality degradation.

The study of jammers associated with the nonlinear behaviour of the RF receiver's front-ends, led to the definition of two paths that have been combined during the work of this thesis: the first path was oriented to the development of new of mathematical formulas that allowed a more reliable and complete approach to real results with fast modelling algorithms; the second path was more focused to the creation of new discrete interference's cancellation architectures using as starting point well known architectures such as image rejection architectures and techniques for linearization of performance nonlinear active components [10].

By assuming the importance of a serious study from the phenomenon that occur in nonlinear radio receivers (particularly in the presence of strong signal interferers) and knowing the absence of a deep and structured scientific research within this area, it was imperative a thorough and meticulous study from all the hypotheses proposed earlier.

1.2 - Objectives

Considering the problems and scenarios presented in last section, there are two main paths well identify in this doctoral thesis: one is the clearly identification and modulation off all nonlinear products in major types of RF receiver front-ends, namely architectures that used the nonlinear behaviour in their operation to down-convert RF signals to baseband; the other path is minimize RF interference generated in the receivers by strong nonlinear devices.

To achieve these major goals, it was essential to conduct a comprehensive study of systems architectures from the major radio-frequency receivers used in RF communications, RFID systems or generic wireless communications. This initial study was crucial for the correct identification from the most important and problematic nonlinear products in these systems.

One crucial task is the mathematical characterization from all the impacts caused by nonlinear elements in the signal receivers and understanding the role of those components in the treatment of interference. Through an exhaustive and deductive study, it was possible to create mathematical algorithms to model the nonlinear response from typical nonlinear systems. Through these algorithms will be possible to easily predict and simulate system response, especially in direct-conversion systems focused on second and fourth nonlinear order products (as Power Meters or some RFID systems) and

prove/justify some results sometimes wrongly ignored or not compensate. In Figure 1.2 is shown an example from the aforementioned Power Meter front-end (studied in detail in chapter 5), where it is demonstrated that the load impedance has an important role in the nonlinear response of the system.

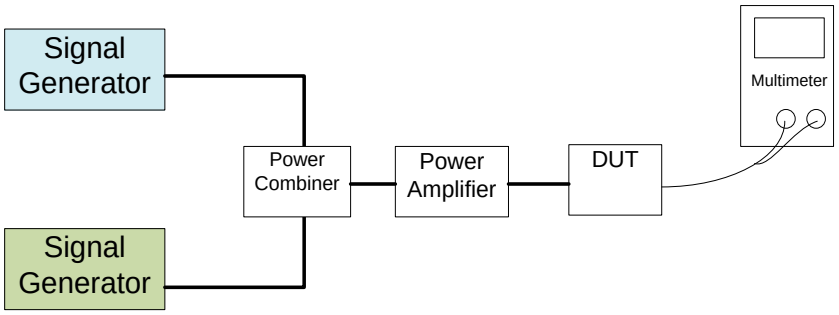

Fig 1.2 - Block diagram from a case study of a nonlinear system (RF power meter) in the presence of two input tones.

As already mention, the second major objective of this thesis is the creation of new architectures capable of mitigating the effects of interferences caused by jammer systems that works in neighbour frequencies. When there is a big difference between power levels from the two operating systems, even with a good band-selection filter in the receiver's entry, the signal jammer could not be sufficient attenuated to a level that does not influence the correct reception of the signal desired. Other possible scenario is that frequency separation between the two signals isn't larger enough to allow the use of a regular bandpass filter. With these issues, despite being on distinct frequency from the desired signal, the jammer will have a great influence on the LNA's response, namely in the intermodulation products between the two signals.

As result, using the well known Hartley and Weaver configuration as a starting point to the cancellation methods study, the main goal is create one or more architectures capable not only to mitigate the interferer's effects (the interferer signal and the nonlinear products near the desire signal or at least the IMD that fall over the desire signal) but also to have a low-cost, be universal and adaptable (to allow a extensive range of applications and systems), capable to be socket/integrated into any type of radio system and (if possible) with small size. The last goal is validate the proposed architectures using some simulation multi-tone tests (able to represent much of the RF signals) with several iterations and different parameters. The reliability and robustness from the proposed

interference cancelation configurations should be the first priority in these tests but it's also important to open new paths of development into the future.

1.3 - Structure of the thesis

The present doctoral thesis is structured in seven chapters. In the introductory chapter is presented the motivation and the reason to study the nonlinear phenomenon present in communication system and shown the major problems caused by nonlinear behaviour in most known RF architectures. In this chapter is also established the fundamental action points, the main objectives, targets and architectures under test. At the end, besides the structure of the thesis, is presented the major scientific contributions published during the course of the doctoral program.

In the second chapter is all devoted to a detailed study of all front-end receivers used in today's systems, highlighting the main features of each approach, promoting a study of performance between different architectures. The impact from the LNA's nonlinear response (and other nonlinear RF components) in the overall system performance is also pointed out. This study, initiated already during the Master's doctoral dissertation, is essential as background to the new proposals presented in Chapter 6.

Chapter 3 is full dedicated to the characterization of nonlinear phenomena existing in almost radio frequency systems known and the study from their main contributions to the overall performance of the system itself and neighbour frequency systems. This study made based on dedicated scientific books, scientific journals publications and major conference proceedings, present the main mathematical tools to nonlinear theory and launches the structural basis for Chapter 4, where mathematical algorithms were developed to predict all impacts created by the weak nonlinear components (based in the Taylor's Series) in the presence of a multi-tone signal received in a direct conversion system.

In Chapter 5 a new view of diode power probes is presented as proof of concept of the previous chapters. The main objective is shown that an RF power probe (or other similar system) calibrated with a single-tone sinusoidal excitation can provide erroneous values when used with modulated signals. Using an theoretical analyze based on the Harmonic Input Method (introduced in chapter 3), prove by simulations and validated with

laboratory measurements, it is shown that calibration procedures for diode power probes should be rethought when measuring new wireless standard types of signals.

Finally, in Chapter 6, two new architectures capable of reducing the impact of interference of strong signals that coexist in neighbour bands are presented. These architectures ensure the requirement of universality, since they are constructed with standard RF components, allowing the integration in almost any radio system. Several simulations (with some variation points) are presented to analyze the robustness of the proposed architectures and future ideas that may be performed.

The final chapter presents the developed work conclusions and some considerations about future work.

1.4 - Scientific contribution during PhD program

During the PhD program were written several contributions to the major scientific magazines in the RF and Microwave electronics, conference proceedings, electronic journals and a contribution for a chapter in a book of electronics and radio systems. In this section we present the summary data from these contributions.

1.4.1 - Book chapters

- Cruz, P.M.; Gomes, H.G.; Carvalho, N.B.C.; "Receiver Front-End Architectures - Analysis and Evaluation" - Chapter in *Advanced Microwave and Millimeter Wave Technologies Semiconductor Devices Circuits and Systems*, Moumita Mukherjee, In-Tech, Austria, 2010.

1.4.2 - Papers in Journals

- Gomes, H.G.; A. R. T. Testera; Carvalho, N.B.C.; M. B. Barciela; K. R. Remley; "Diode Power Probe Measurements of Wireless Signals", *IEEE Trans. on Microwave Theory and Tech.*, Vol. 59, No. 4, pp. 987 - 997, April, 2011.

- Gomes, H.G.; Carvalho, N.B.C.; "RFID for Location Proposes Based on the Intermodulation Distortion", *Sensors & Transducers Magazine*, Vol. 106, No. 7, pp. 85 - 96, July, 2009.

1.4.3 - Papers in Conference Proceedings

- Gomes, H.G.; A. R. T. Testera; Carvalho, N.B.C.; M. B. Barciela; K. R. Remley; "The Impact of Long-term Memory Effects on Diode Power Probes", Proc *IEEE International Symp. on Microwave Theory and Tech.*, Anaheim, United States, Vol. 1, pp. 596 - 599, May, 2010.

- Gomes, H.G.; Carvalho, N.B.C.; "Interference cancellation: New configuration technique for cancellation of strong interferences from adjacent frequency bands", Proc *International Workshop on Integrated Nonlinear Microwave and Millimeter-Wave Circuits - INMMIC*, Malaga, Spain, Vol. 1, pp. 65 - 68, November, 2008

CHAPTER 2

Receivers Architectures

As mention in the introduction, the RF systems are one of the main sources of development from the last decades. The numerous new services and the constant demanding for better and smaller devices make these systems one of the most important and desirable goals in the World of Telecommunications.

One of the most important parts from a RF system is the receiver. In receivers, the entry block has a key role in performance and reliability of the system. Any unresolved issue caused by/in this block, generates enormous problems in the following blocks of the transceiver architecture. For this reason, considering the constant increase of services available for the same frequency bands, associated with the growing number of users for each service, the entry receiver architecture must be capable to resolve issues such as blocking problems, Peak-to-Average Power Ratio (PAPR) problems, among others. In other hand, must be capable to offer good selectivity, sensitivity, lower energy consumption at a small price.

This chapter is intended to make a review of the main receiver's architectures known up to now, explain the major applications and study their main advantages and limitations.

It will start with a brief review about what we call the mixing process, being that real mode or complex mode. Next, the main section of this chapter will show in detail a study of the common receiving architectures using in RF telecommunication systems, emphasizing its main advantages and drawbacks. Moreover, some enhancements to these architectures are also presented and its principal benefits explained, such as the Hartley and Weaver configurations. In the last section, the major problems in RF architectures are studied and its advantages/disadvantages are resumed in a table with all the RF receiver architectures explored in this chapter. It is also draw a few guidelines for next chapters.

2.1 – The Mixing Concept Review

Before starting the presentation of the receiver's architectures, is important to remember some concepts related to frequency mixing which can help to understand some of the differences between the architectures that will be studied afterwards. In Figure 2.1 a simple architecture of a basic RF system is presented. In the transmitter, the modulating signal (message) must pass through a mixing block that translates the signal from baseband to RF frequency. The signal is than amplified and filtered before being transmitted by the antenna. In the receiver the process repeats, but in reverse direction. The received RF signal, after been filter and amplified, must be translated to baseband frequency in the de-mixing block.

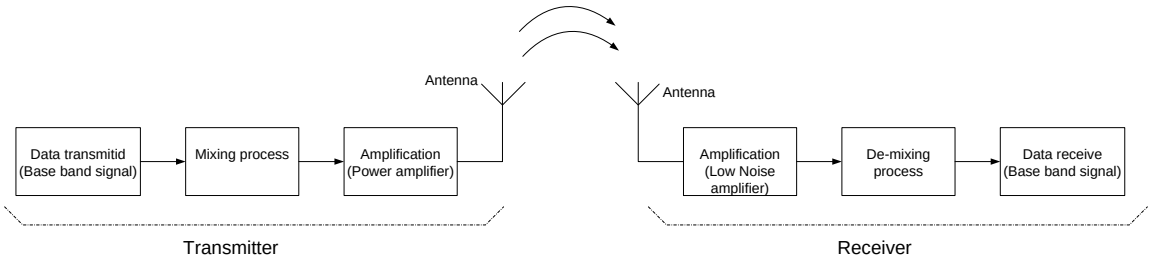

Fig. 2.1 – Typical architecture for a radiofrequency system

As mentioned above, the mixing process involves the translation from baseband to intermediate frequency or directly for RF frequency. There are two different types of mixing (each one can be held once or twice depending on the type of architecture chosen): **real mixing** and **complex mixing** [11].

2.1.1 - The Real Mixing Concept

The first mixing process that will be explained is the *real mixing*, shown in Figure 2.2. In this case the input signal $x(t)$ is multiplied by a sinusoid carrier $c(t)$ with frequency f_{LO}. As known, in frequency, the convolution between the $X(f)$ (spectrum from $x(t)$) and $C(f)$ (spectrum from $c(t)$) results in a replica from $X(f)$ center at $-f_C$ and f_C frequency.

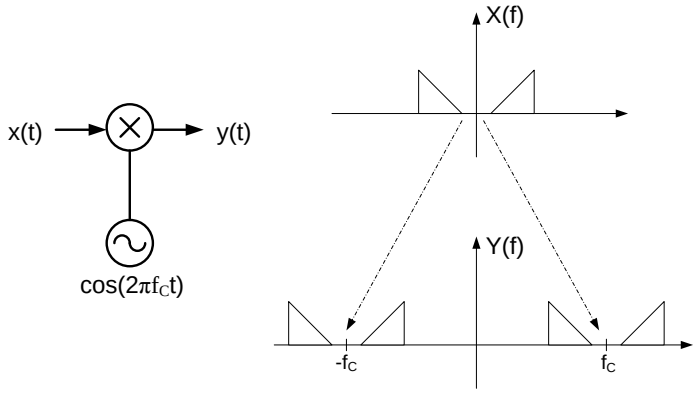

Fig. 2.2 – Real mixing process - up-conversion

Since the RF signal is typically in a higher frequency than the baseband signal, this process is called up-conversion. In the up-conversion process the real mixing has a reasonable behaviour and do not cause major problems in transmitting the modulated signal. The major disadvantages occur in the down-conversion process, because the two spectra are centred at $-f_C$ and f_C and will be overlapping at the baseband signal (figure 2.3). If the desired signal has a small power (white) and is in presence of a strong power interference appearing at the so-called image frequency (grey), even with the use of good image frequency rejection filter, the desired signal at baseband or DC could be strongly corrupted by the image frequency interference signal. This problem could be even more relevant when the desire signal's bandwidth is much smaller than the carrier frequency (like direct conversion for example) because image rejection's filter could be extremely complex to assure a good attenuation from the image frequency interference signal.

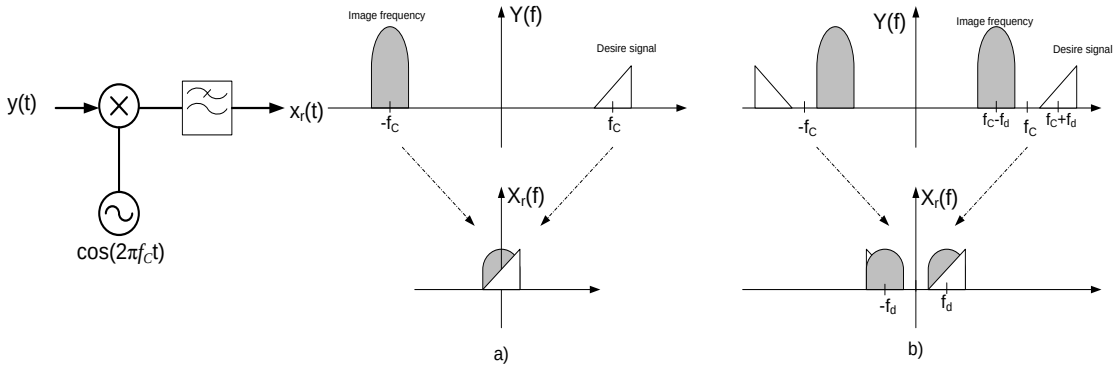

Fig. 2.3 – Real mixing process - down-conversion. a) complex signal; b)real signal;

The real mixing is preferably used in simpler systems, where energy consumption and low cost are imperative characteristics in the production of the RF transceiver.

2.1.2 - The Complex Mixing Concept (In-phase and Quadrature mixing)

The complex mixing was developed to minimize the problems arising with the real mixing. This process can actually assure a increased immunity to image frequency without needing a complex mixing image rejection filters. In this new mixing process, also known as In-phase and Quadrature mixing (I & Q), the carrier is a complex signal ($e^{-j2\pi f_c t}$, typically) instead of a sinusoidal. As a result, the baseband spectrum is center only in the carrier frequency *fc*, without any replica in symmetric carrier frequency *–fc*.

As shown in Figure 2.4, the complex mixing don't used a true complex carrier (because exponential generators doesn't exist) but a combination of two carriers with 90º shift between them to create a phase and quadrature signals that combined has the same effect than a complex carrier.

To demonstrate this technique let assume an input signal *x(t)* mixing with two carriers shift by 90º and given by:

$$c_1(t) = \cos\left(2\pi f_c t\right) = \frac{e^{j2\pi f_c t} + e^{-j2\pi f_c t}}{2}; \tag{2.1}$$

$$c_2(t) = \cos\left(2\pi f_c t - 90^{\circ}\right) = \sin\left(2\pi f_c t\right) = \frac{e^{j2\pi f_c t} - e^{-j2\pi f_c t}}{2j}; \tag{2.2}$$

The resultant phase and quadrature signals are then:

$$y_I(t) = x(t) \times \frac{e^{j2\pi f_c t} + e^{-j2\pi f_c t}}{2} = \frac{1}{2} x(t) \times e^{j2\pi f_c t} + \frac{1}{2} x(t) \times e^{-j2\pi f_c t}; \tag{2.3}$$

$$y_Q(t) = x(t) \times \frac{e^{j2\pi f_c t} + e^{-j2\pi f_c t}}{2} = \frac{1}{2j} x(t) \times e^{j2\pi f_c t} - \frac{1}{2j} x(t) \times e^{-j2\pi f_c t}; \tag{2.4}$$

Combining these two components, the final signal will be:

$$\begin{aligned} & y(t) = y_I(t) + j y_Q(t) = \\ & = \frac{1}{2} x(t) \times e^{j2\pi f_c t} + \frac{1}{2} x(t) \times e^{-j2\pi f_c t} + j \times \left(\frac{1}{2j} x(t) \times e^{j2\pi f_c t} - \frac{1}{2j} x(t) \times e^{-j2\pi f_c t} \right) \\ & = \frac{1}{2} x(t) \times e^{j2\pi f_c t} + \frac{1}{2} x(t) \times e^{-j2\pi f_c t} + \frac{1}{2} x(t) \times e^{j2\pi f_c t} - \frac{1}{2} x(t) \times e^{-j2\pi f_c t} \\ & = x(t) \times e^{j2\pi f_c t} \end{aligned} \tag{2.5}$$

This demonstration shows that using the phase and quadrature components produces the same result as the mixing process between the input signal and a complex exponential

carrier, making the translation from the input signal spectrum to the f_C frequency without replica in $-f_C$.

The complex mixing is especially useful in de-mixing process. As already discussed, the image frequency has a great impact in the down-conversion process using the real mixing technique. When we made a complex mixing, the spectrum of the desired signal will be simply translated from the *fc* to baseband frequency without any contribution from the spectrum in the negative frequency *–fc*, since this spectrum will be translated to *–2fc* (figure 2.5).

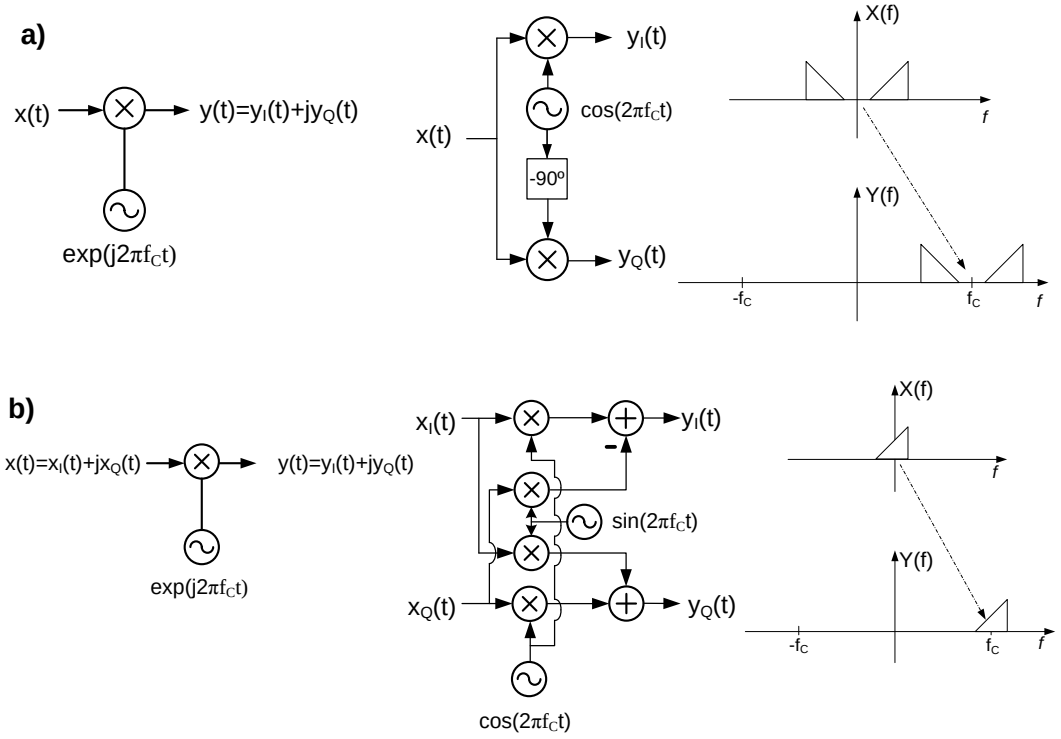

Fig. 2.4 – Complex mixing process - up-conversion. a) real signal; b) complex signal;

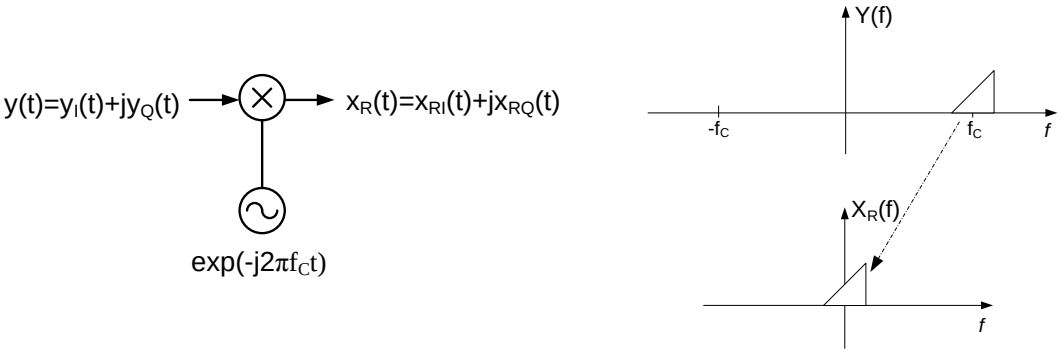

Fig. 2.5 – Complex mixing process - down-conversion. (complex signal)

Using the signal from equation 2.5, the down-conversion process is given by:

$$\begin{aligned} x_{RI}(t) &= y_I(t)\times\cos\left(2\pi f_c t\right)+y_Q(t)\times sin\left(2\pi f_c t\right) \\ &= \frac{1}{2}y_I(t)\times e^{j2\pi f_c t}+\frac{1}{2}y_I(t)\times e^{-j2\pi f_c t}+\left(\frac{1}{2j}y_Q(t)\times e^{j2\pi f_c t}-\frac{1}{2j}y_Q(t)\times e^{-j2\pi f_c t}\right) \end{aligned} \tag{2.6}$$

$$\begin{aligned} x_{RQ}(t) &= y_Q(t)\times\cos\left(2\pi f_c t\right)-y_I(t)\times sin\left(2\pi f_c t\right) \\ &= \frac{1}{2}y_Q(t)\times e^{j2\pi f_c t}+\frac{1}{2}y_Q(t)\times e^{-j2\pi f_c t}-\left(\frac{1}{2j}y_I(t)\times e^{j2\pi f_c t}-\frac{1}{2j}y_I(t)\times e^{-j2\pi f_c t}\right) \end{aligned} \tag{2.7}$$

Using equations 2.3 and 2.4, $x_{RI}(t)$ and $x_{RQ}(t)$ will be determine by :

$$\begin{aligned} x_{RI}(t) = &\left(\frac{1}{2}x(t)\times e^{j2\pi f_c t}+\frac{1}{2}x(t)\times e^{-j2\pi f_c t}\right)\times\frac{1}{2}e^{j2\pi f_c t} \\ &+\left(\frac{1}{2}x(t)\times e^{j2\pi f_c t}+\frac{1}{2}x(t)\times e^{-j2\pi f_c t}\right)\times\frac{1}{2}e^{-j2\pi f_c t} \\ &+\left(\frac{1}{2j}x(t)\times e^{j2\pi f_c t}-\frac{1}{2j}x(t)\times e^{-j2\pi f_c t}\right)\times\frac{1}{2j}e^{j2\pi f_c t} \\ &-\left(\frac{1}{2j}x(t)\times e^{j2\pi f_c t}-\frac{1}{2j}x(t)\times e^{-j2\pi f_c t}\right)\times\frac{1}{2j}e^{-j2\pi f_c t} \end{aligned} \tag{2.8}$$

$$\begin{aligned} x_{RI}(t) &= \frac{1}{4}x(t)\times e^{j4\pi f_c t}+\frac{1}{2}x(t)+\frac{1}{4}x(t)\times e^{-j4\pi f_c t} \\ &\quad -\frac{1}{4}x(t)\times e^{j4\pi f_c t}+\frac{1}{2}x(t)-\frac{1}{4}x(t)\times e^{-j4\pi f_c t} \\ &\quad = x(t); \end{aligned} \tag{2.9}$$

$$\begin{aligned} x_{RQ}(t) = &\left(\frac{1}{2j}x(t)\times e^{j2\pi f_c t}-\frac{1}{2j}x(t)\times e^{-j2\pi f_c t}\right)\times\frac{1}{2}e^{j2\pi f_c t} \\ &+\left(\frac{1}{2j}x(t)\times e^{j2\pi f_c t}-\frac{1}{2j}x(t)\times e^{-j2\pi f_c t}\right)\times\frac{1}{2}e^{-j2\pi f_c t} \\ &-\left(\frac{1}{2}x(t)\times e^{j2\pi f_c t}+\frac{1}{2}x(t)\times e^{-j2\pi f_c t}\right)\times\frac{1}{2j}e^{j2\pi f_c t} \\ &+\left(\frac{1}{2}x(t)\times e^{j2\pi f_c t}+\frac{1}{2}x(t)\times e^{-j2\pi f_c t}\right)\times\frac{1}{2j}e^{-j2\pi f_c t} \end{aligned} \tag{2.10}$$

$$\begin{aligned} x_{RQ}(t) &= \frac{1}{4j}x(t)\times e^{j4\pi f_c t}-\frac{1}{4j}x(t)+\frac{1}{4j}x(t)-\frac{1}{4j}x(t)\times e^{-j4\pi f_c t} \\ &\quad -\frac{1}{4j}x(t)\times e^{j4\pi f_c t}-\frac{1}{4j}x(t)+\frac{1}{4j}x(t)+\frac{1}{4j}x(t)\times e^{-j4\pi f_c t} \\ &\quad = 0; \end{aligned} \tag{2.11}$$

As expected, the resulting signal from the down-conversion process will be identical to *x(t)* without any replicas in other frequencies. This also demonstrates that complex mixing can dramatically reduce the problem with image frequency, since there is only translation in frequency from the desire signal's spectrum.

However, its complexity and need for greater number of components can limit its use for the more simplest and low cost systems. By making the system more complex, it will requires a higher and costly number of electronic components and a bigger energy demanding, limiting this type of mixing to be used mainly in more robust and complex systems. However, in last years, with the migration from several RF tranceiver's parts to digital domain (where process are more easily done), the complex mixing has increase their application in RF transceivers, even in the lowest cost architectures.

2.2 - Receiver's Front-Ends Architectures

As refer before in this section a review of the main receiver's architectures known will be presented, main applications will be showed and their main advantages and limitations are studied.

A special attention will be given to the envelop detector receiver because it will be one that will be used as support example for next chapters.

2.2.1 - Envelop Detector

The most simple RF receiver used in our days is the envelop detector receiver (or simple detector). Used in the first AM radios, this reduced architecture was reused for the development of very small tags (with reduced consumption) on RFID systems, for power meters in communication's base stations or even in Cognitive Radio Systems [12].

As refered, the envelope detector configuration (figure 2.6) is the most simple receiver architecture used in RF receiver's front-ends because avoids the use of problematic and expensive components like mixers and local oscillators, making this topology very simple and cheap. The down-conversion method used in this architecture is based in the strong nonlinear behaviour from basic electronics components such diodes or transistors. An interesting property of nonlinear systems is the spectral regrowth capability, which means that the system has the capability to create new frequency components in the output signal that do not exist at the input side. As result of this propriety, if we use a nonlinear

generator such a diode, the received RF signal (X_1) will present several replicas from the original signal in the harmonics and baseband frequencies at diode's output response.

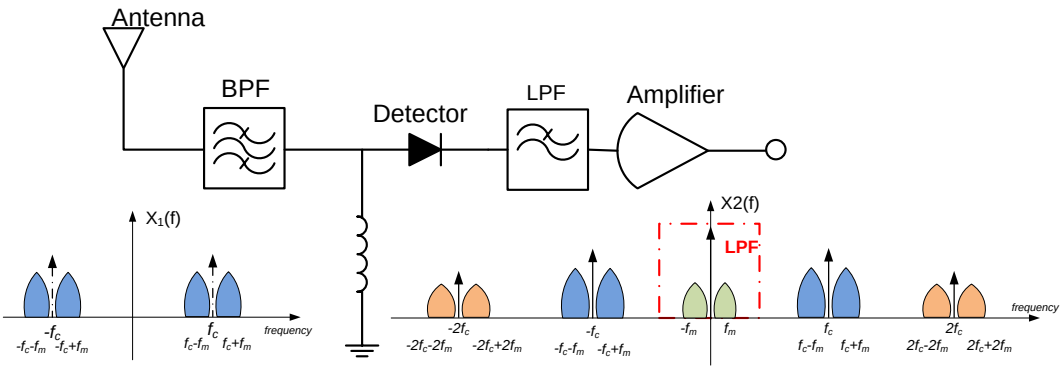

Fig. 2.6 – Envelope detector configuration and frequency domain operation

To demonstrate the concept, let assume an input message $v_m(t)$ and a carrier $v_C(t)$given by [13]:

$$v_m(t) = A_m \sin(\omega_m t) \tag{2.12}$$

$$v_C(t) = A_C \sin(\omega_C t) \tag{2.13}$$

The result signal will be:

$$v_Y(t) = \left(A_C + A_m \sin(\omega_m t)\right) \times \sin(\omega_C t) \tag{2.14}$$

$$v_Y(t) = A_C \left(1 + \frac{A_m}{A_C} \sin(\omega_m t)\right) \times \sin(\omega_C t) \tag{2.15}$$

$$v_Y(t) = A_C \left(1 + m \sin(\omega_m t)\right) \times \sin(\omega_C t), \tag{2.16}$$

where m is the modulation factor given by $\frac{A_m}{A_C}$ (figure 2.7) .

If this RF signal passes through a nonlinear device such a diode (figure 2.8), the result signal could be approached by the Taylor's Series expansion to diode's biased voltage as (v_D=v_Y):

$$i_D(t) = a_1 v_D + a_2 v_D^2 + a_2 v_D^3 + \ldots \tag{2.17}$$

Assuming de diode's biased voltage equal to v_Y, the diode's current is given by:

$$i_D(t) = a_1 A_C \left(1 + \frac{A_m}{A_C}\sin(\omega_m t)\right) \times \sin(\omega_C t) + a_2 \left[A_C \left(1 + \frac{A_m}{A_C}\sin(\omega_m t)\right) \times \sin(\omega_C t)\right]^2 + \ldots \quad (2.18)$$

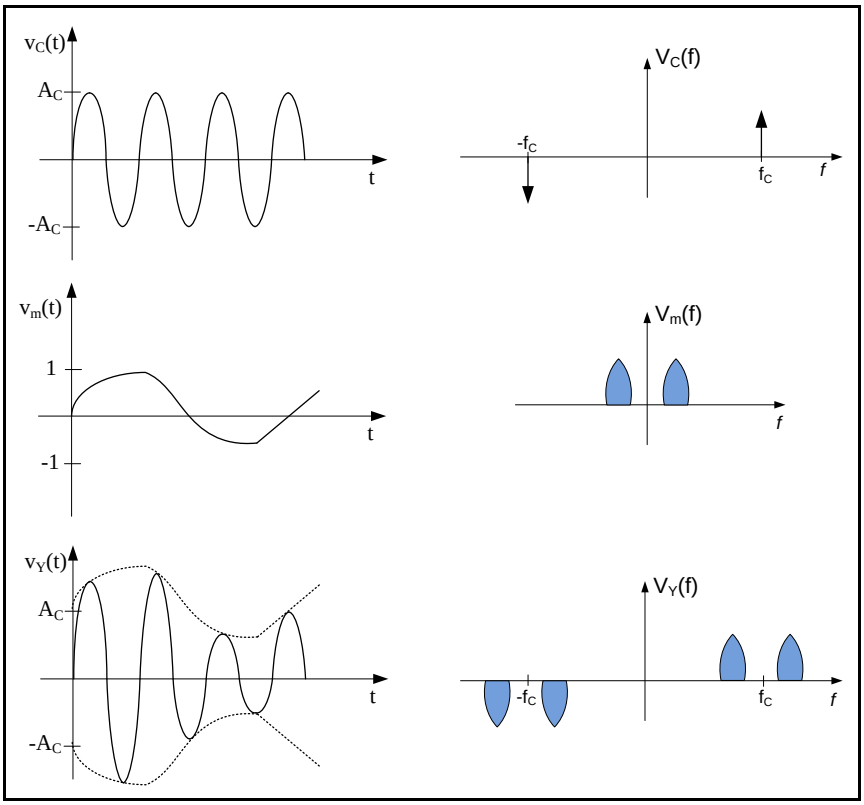

Fig. 2.7 – Modulation process in time and frequency domain

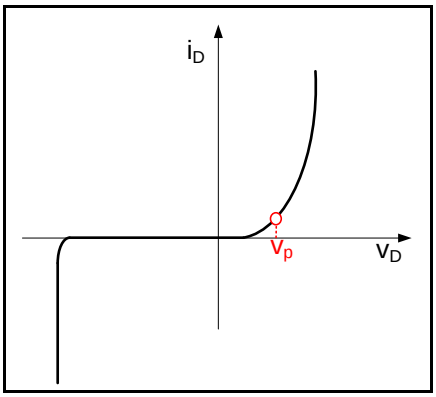

Fig. 2.8 – Diode characteristic behaviour (current versus bias voltage)

If the diode is biased in the "knee" voltage *Vp* (figure 2.8), that maximizes the second and fourth order component in Taylor's series. As stated above, these non-first order components generate new products in frequency that does not exist in the input signal. In

this case the second and forth order will generate a replica of the desired signal at baseband frequency (figure 2.9).

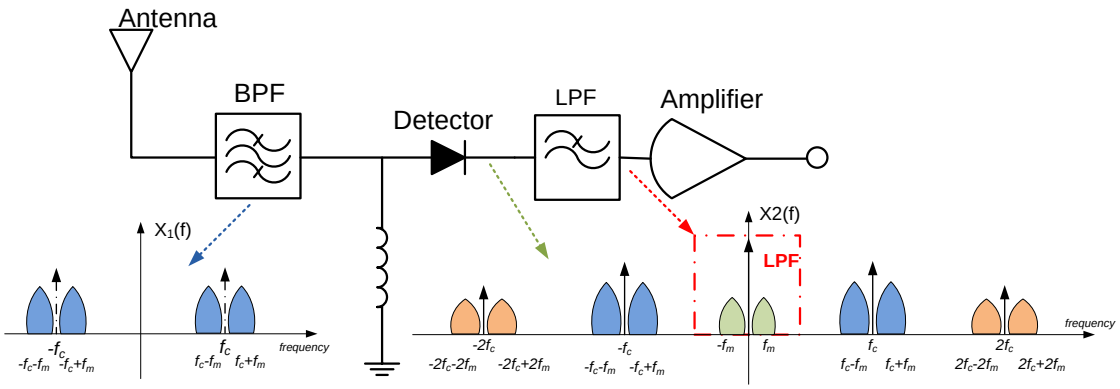

Fig. 2.9 - Un-mixing process using the envelope detector

With the help of a low pass filter it is possible to eliminate all undesired frequencies and achieve the down-conversion of the desired signal at baseband without the use of mixers and local oscillators.

This architecture is very useful in systems that require an extremely low energy consumption such as passive RFID tags or even Cognitive Radio entry modules [14][15][16]. The mains limitations of this architecture are the intolerance to interferences, some DC problems (as zero-IF receiver) and very low sensitivity and selectivity.

2.2.2 - Zero-IF Receiver

One of the most typical receiver's architecture used is the Zero-IF receiver [12][17][18], also known as Homodyne receiver or Direct Conversion receiver (figure 2.10). Like envelope detectors, the zero-IF Receiver coverts the RF signal directly to baseband (using only one stage) with the help of a Mixer and a Local Oscillator. This architecture gives greater stability in the desired RF signal reception, although it is more complex, expensive and with higher energy consumption than the Envelope Detector. As shown in Figure 2.11, the RF received signal (figure 2.11a) is selected by a bandpass filter (similar to the previous architecture) and then it is amplified by an LNA (figure 2.11b). The result signal is directly down converted to DC by a mixer (or two mixers if used in an I/Q conversion) and, if desired, could be transformed into the digital domain using a straightforward ADC (figure 2.11c). The main difference between this architecture and the previous one is the use of oscillators and mixers that gives more reliability and stability to the receiver. In

the opposite way, this front end has a significantly increase in the number of components (increasing its cost and energy consumption), bringing some new problems that was not presented in the simple detector.

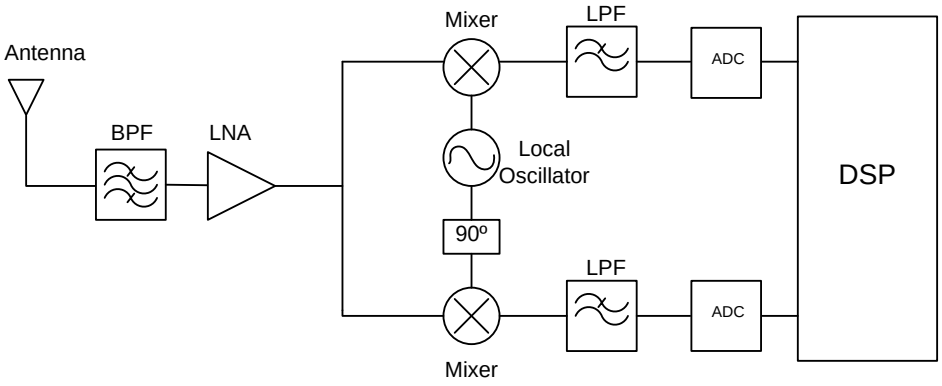

Fig. 2.10 - A zero-IF receiver architecture

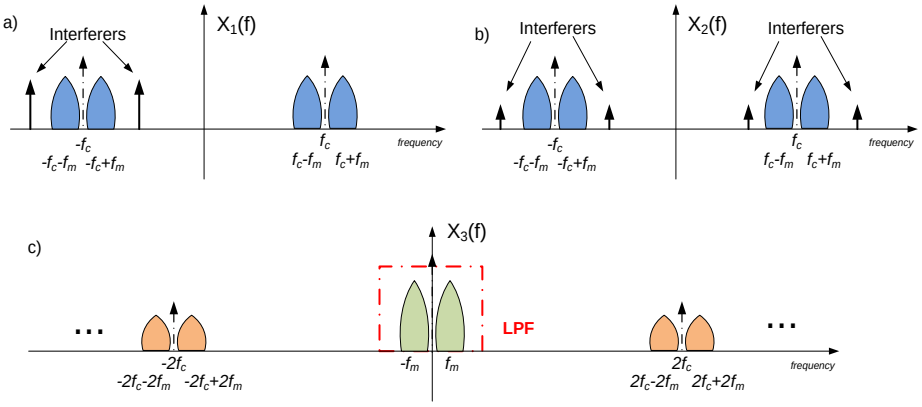

Fig. 2.11 – Frequency domain operation of a zero-IF receiver architecture

Compared with Heterodyne architecture (next in presentation line), the Homodyne receiver has a clear reduction in the number of analogue components and guarantees a high level of integration thanks to its simplicity. However this simplicity has a non despicable cost, since many components from the zero-IF receiver are more complex to deploy and brings some difficult problems to solve. Some of these problems start right at input selective filter. Using only one stage to convert the RF signal to baseband frequency, the bandwidth of the input filter must be much smaller than the carrier frequency. This can create serious problems in the construction of this filter, greatly increasing its complexity and cost.

In addition, the direct conversion to DC can generate several problems that strongly conditioned the use of this architecture over the super-heterodyne one. Problems as DC

offset, such as LO leakage (non-ideal isolation between the port from the mixer) or interferer leakage (non-ideal isolation between the port from the mixer), I/Q mismatch (errors in I&Q modulation), Even/Odd-order distortion (non-linear components generated several products in harmonic frequencies, especially second-order intermodulation products that arise around DC) and large flicker noise from the mixer can easily corrupt the output baseband signal. These problems will be discussed in detail on section 2.3.

Although this, the emergence of new techniques to reduce these problems, associated with the increasing integration of the components, has contributed to better performance and thus increased the use of this RF architecture in several types of RF systems at different frequency bands as seen in [19][20][21][22][23].

2.2.3 - Super-Heterodyne Receiver

The most popular configuration used in RF receivers is the well known Super-Heterodyne architecture (figure 2.12) [12][18]. This configuration is based in two down-conversion stages, i.e., the RF receive signal is first translated to an Intermediate Frequency (IF) and then converted to baseband signal. The received signal (figure 2.13a) is first filtered by a pre-selection filter and amplified in the LNA. The resultant signal passes through another filter to reduce the image frequency effects before the first translation from RF to IF (figures 2.13b e 2.13c). After this stage, the signal is filtered again and demodulated to baseband (fig. 2.13d), where can be converted to the digital domain (if wanted) to be processed. Like Homodyne configuration, in this stage some architectures use a phase/quadrature mixing stage in order to achieve better amplitude/phase information from the received signal.

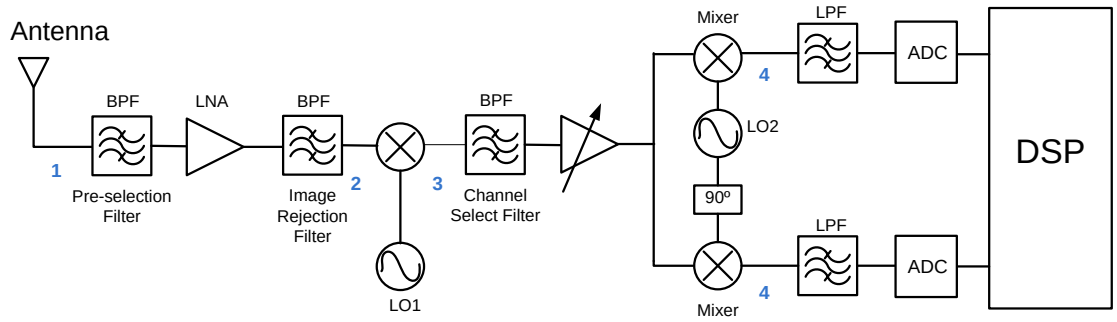

Fig. 2.12 – A super-heterodyne receiver architecture with I/Q mixing in second stage

As referred above, this architecture is currently adopted in most radio receivers due to the availability of low cost narrowband RF and IF components with low power consumption. Furthermore, this architecture can ensure good levels of sensitivity (allows the good reception from a lower power signal at receiver input for which there is sufficient signal-to-noise ratio at the receiver output), selectivity (better ability to separate the desired band from signals received at other frequencies) and it is immune to most DC problems affecting Homodyne architectures.

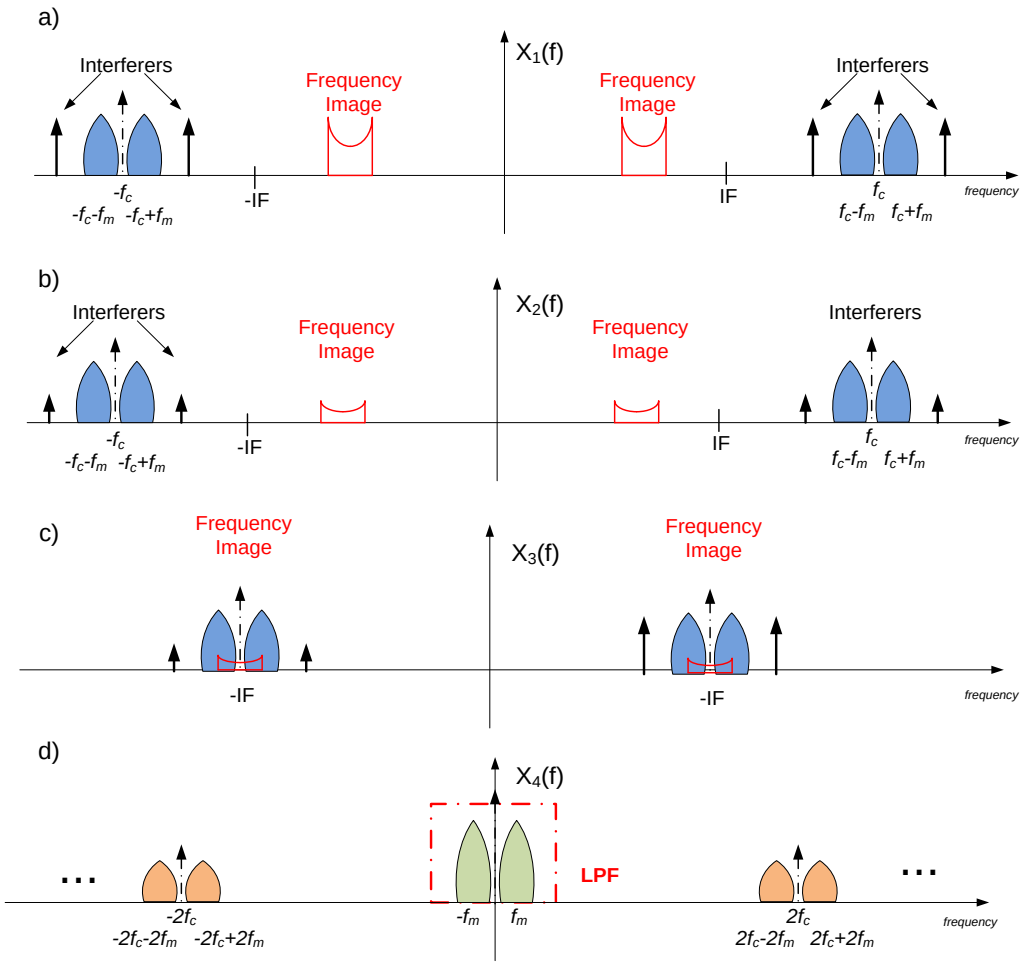

Fig. 2.13 – Frequency domain operation of a super-heterodyne receiver architecture

However Super-Heterodyne receivers have also a number of substantial problems. The most important problem in this architecture is the cancellation of the image frequency, previously discussed during the presentation from the real mixing concept. For a good signal/image ratio it is imperative that the image rejection filter has a reduced transition band. To achieve this goal these filters must be performed using high-Q discrete components (SAW or ceramic filters), unpractical in today's IC technologies. For this

reason, it is not possible to do a full integration on-chip, resulting in problems like the inexistence of a perfect LNA 50 Ω load, increased noise figure values and nonlinear behaviour appearing in discrete components.

Fortunately other ways exists to solve image frequency problems, as the use of cancellation architectures such as Hartley or Weaver configurations, presented in section 2.2.6.

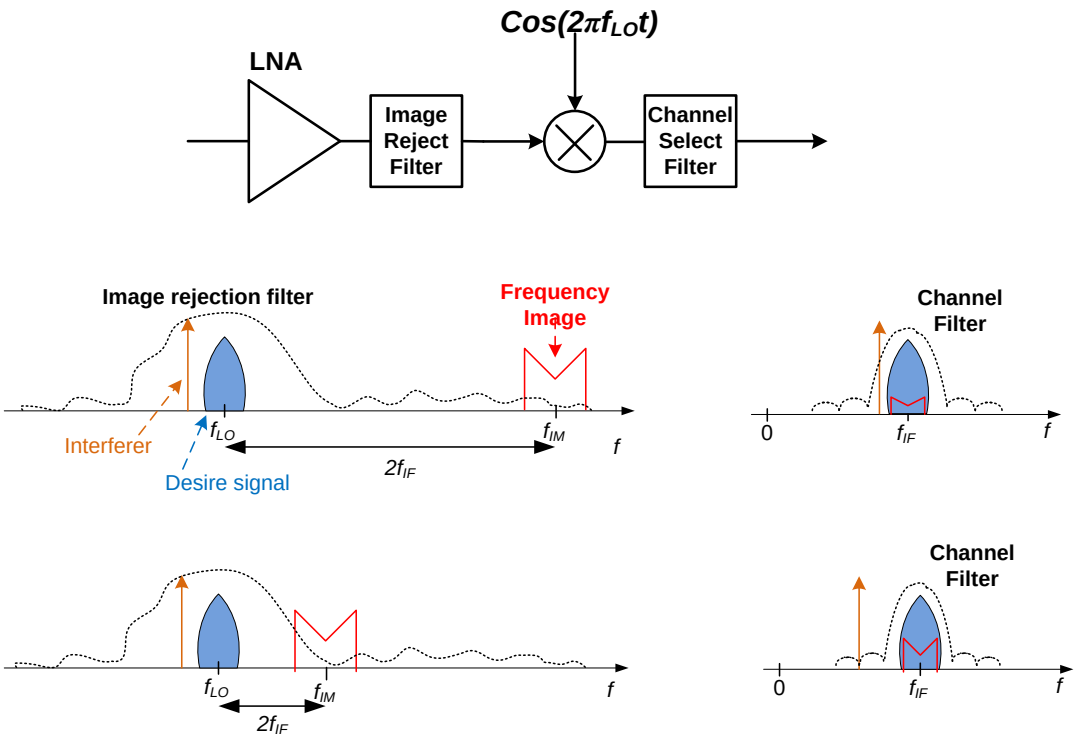

Fig. 2.14 - Low/High IF analyze effects in the receive signal

One of the most important parameters to choose in the Heterodyne receiver is the IF. As can be seen from Figure 2.14, if we chose a High IF, we reduce the image frequency problem but near interferes will have greater impact in baseband signals. Otherwise, if a Low IF is chosen, the interference impact will be minimized but the image frequency will have an important role in the mixing process. For that reason the IF must be carefully chosen to minimize the impact of both problems.

Finally, despite its greater complexity, the fact that it is designed for a specific channel (in a particular wireless standard) prevents the expansion of the receiving band.

2.2.4 - Low-IF Receiver

It can be say that Low-IF receivers is a hybrid between Homodyne and Heterodyne architectures [24] (figure 2.15), because the RF signal is mixed down to a nonzero low or moderate IF (few hundred kHz to several MHz) instead of going directly to DC, preferably using I/Q down-conversion. This solution tries to combine the advantages from the Zero-IF and the Super-Heterodyne configurations. Like both architectures, the received signal (figure 2.16a) passes through a channel-selection filter at RF and is amplified by a LNA (figure 2.16b). After this stage, the signal is down-converted to a low IF, instead of zero IF (figure. 2.16c), and used an image suppression block in order to cancel the negative effects from the image frequency. Finally, an ADC converts the signal to digital domain, allowing the use of digital signal processing algorithms. In some low-IF architecture the image suppression block is also transferred to the digital domain.

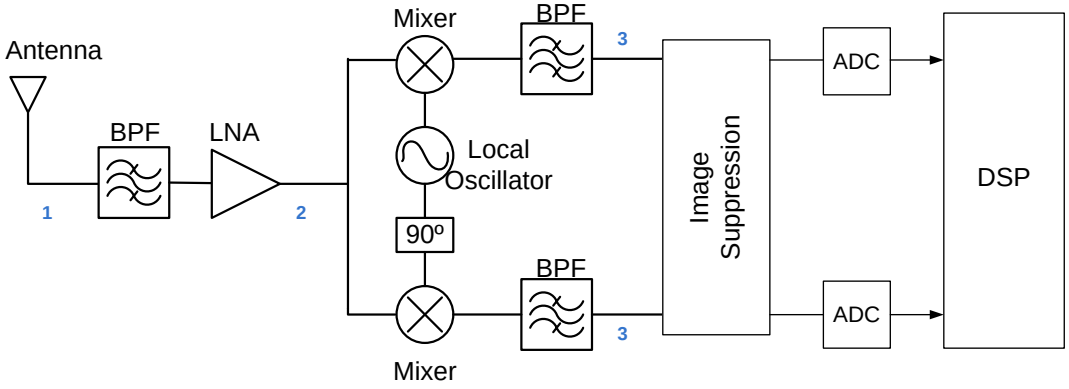

Fig. 2.15 – A low-IF receiver architecture

This architecture still allows a high level of integration (advantage from zero-IF) but does not suffer from the DC problems (advantage from Super-Heterodyne), since the desired signal is not situated around DC. However, this architecture continued to suffer from the image frequency and I/Q mismatch problems (with a greater impact than in previous architectures) and the ADC power consumption is increased since now a high conversion rate is required.

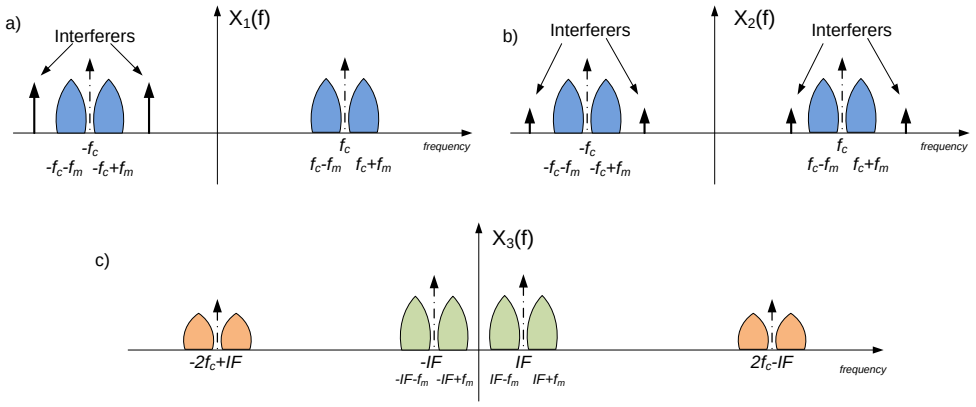

Fig. 2.16 – Frequency domain operation of a low-IF receiver architecture

2.2.5 - Bandpass Sampling Receiver

An alternative to the previous configurations is the bandpass sampling receiver (also known as Digital receiver) [25][26][27][28]. This type of architecture is so named because much of the process of de-multiplexing is done in the digital domain. However, there are several types of configurations that fit within this profile.

These receivers can be divided in terms of its maximum input frequency: RF digital receiver or IF digital receiver. In the RF digital receiver (figure 2.17), the input signal is filtered by an RF bandpass filter (that can be a tuneable filter or a bank of filters), amplified using a wideband LNA and is then converted to the digital domain by a high sampling rate ADC and digitally processed.

On the other hand, the IF digital receiver (figure 2.18) makes the first translation in the analog domain to an IF frequency and then convert it to the digital domain where the I/Q mixing is made. This architecture is similar to Low-IF Receiver, however the I/Q process is made in the digital domain, achieving better performance and avoid much of the I/Q mismatch problems present in analogue devices.

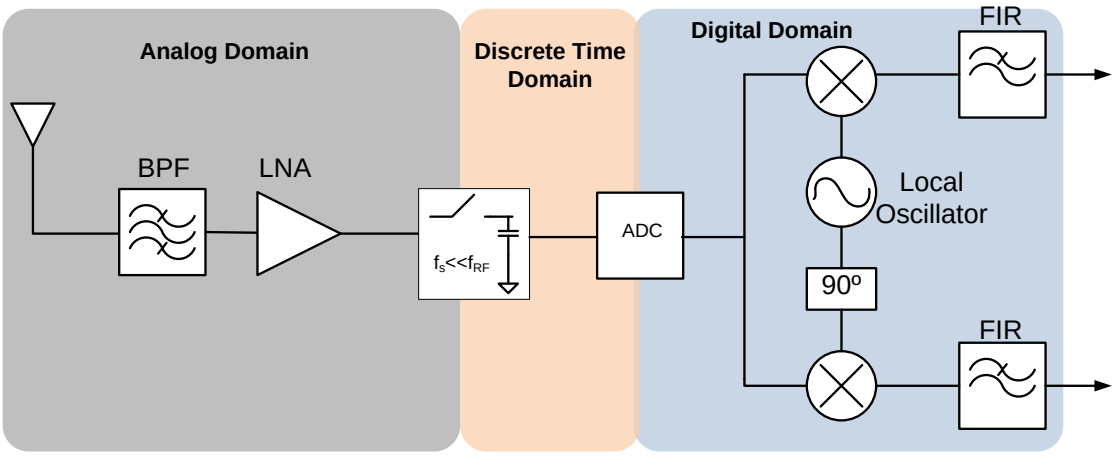

Fig. 2.17 – A RF bandpass sampling receiver architecture

Another main division in digital receivers is the digital sampling receiver and the sub-sampling digital receiver (both are used in RF or IF receivers). In RF (or IF) sampling receivers the sampling frequency is at least twice the RF maximum frequency (Nyquist law). In RF sub-sampling receivers the sampling frequency is twice (or greater) than the RF bandwidth of the receive signal. Table 1 presents a brief comparison between RF and IF sampling receivers as presented in [27].

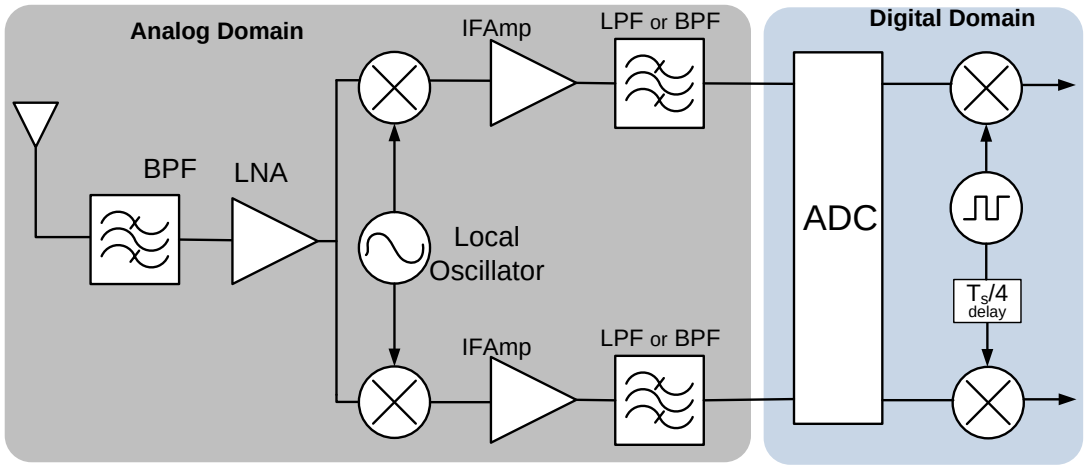

Fig. 2.18 – An IF band-pass sampling receiver architecture

As refer, one of the most important advantages of sampling receivers is the I/Q process that is done in the digital domain. As seen before, with analogue architectures this process brings important problems as I/Q mismatch. In the digital domain this complex mixing is easier to realize with a good matching accuracy in the two digital signal paths, using for instance the Hilbert transform [29] during the process.

IF Sampling	RF Sampling
Lower susceptibility to aperture jitter	Potential advantages in circuit complexity and area, power consumption, and re-configurability
Anti-aliasing filters and ADCs can be implemented with improved performance at lower frequencies	Their use is currently limited to lower performance applications where the effects of aperture jitter, and the limited performance of current ADC's and anti-aliasing filters at RF frequencies can be tolerated.

Table 2.1 – Comparison between RF and IF sampling receivers

Thus, as in the low-IF architecture, here we can take advantage of digital signal processing to alleviate some issues of the analogue front-end. Moreover, pushing the analogue-to-digital conversion closer to the antenna provides an increased flexibility.

This configuration is based on the fact that all energy from DC to the input analogue bandwidth of the ADC will be folded back to the first Nyquist zone [0, $f_S/2$] without any mixing down conversion needed because a sampling circuit is replacing the mixer module. Figure 2.19 shows the frequency domain operation of the band-pass sub-sampling receiver. Whether a correct sampling frequency is chosen, it is possible to receive more than one RF signal at same time and then make its processing in the digital domain. Nevertheless, it is mandatory to include RF bandpass filtering in order to avoid overlap of other undesirable signals.

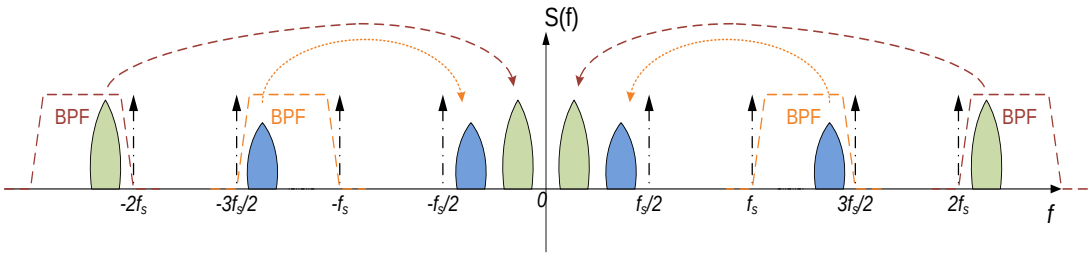

Fig. 2.19 – Frequency domain operation of a band-pass sampling receiver

As was described in [26], it is possible to pinpoint the resulting intermediate frequencies, f_{IF}, based on the following relationship

$$\text{if } f_{ix}\left(\frac{f_c}{f_s/2}\right) \text{ is } \begin{cases} even,\ f_{IF} = rem(f_c, f_s) \\ odd,\ f_{IF} = f_s - rem(f_c, f_s) \end{cases} \tag{2.19}$$

where f_C is the carrier frequency, f_S is the sampling frequency, *fix(a)* is the truncated portion of argument *a*, and *rem*(*a*,*b*) is the remainder after division of *a* by *b*.

In this case, the RF bandpass signal filtering plays an important role because it must reduce all signal energy (essentially noise) outside the Nyquist zone of the desired frequency band that otherwise would be aliased. If not filtered, the signal energy (noise) outside the desired Nyquist zone is folded back to the first zone together with the desired signal, producing a degradation of the signal-to-noise ratio (SNR). This may be given by

$$SNR = 10 \times \log_{10}\left(\frac{S}{N_i + (n-1) \times N_0}\right) \tag{2.20}$$

where S represents the desired-signal power, N_i and N_0 are in-band and out-of-band noise, respectively, and n is the number of aliased Nyquist zones.

The advantage of this configuration is the sampling frequency needed and the subsequent processing rate are proportional to the information bandwidth, rather than to the carrier frequency. This reduces the number of components required, the cost and energy consumption. This architecture also reduces substantially the RF problems and DC offsets. However, some critical requirements exist. For example, the analogue input bandwidth of the sample and hold circuit inside the ADC must include the RF carrier, which is a serious problem, considering the sampling rate of modern ADCs. Clock jitter and aperture distortion can also be a vital problem when high frequencies implementations are considered.

2.2.6 - Hartley and Weaver architectures

In addition to the main receiver architectures presented, there are other architectures or sub-architectures that are currently used (or been developed) to minimize problems existing in the "traditional" ones. Two of these solutions are Hartley's and Weaver's configurations.

The Hartley's and Weaver's configurations are sub-architectures especially developed to reduce/cancel the problems with the image frequency that affects especially the Super-Heterodyne receiver. These architectures are similar but in recent years Weaver architecture has gained an advantage over the Hartley architecture, especially because of their better performance when integrated into Integrated Circuits (IC).

The Hartley's architecture (figure 2.20) uses an I/Q modulation in first stage and, after the low-pass filter, make a 90º time shift (Hartley shift) to invert the negative part from the spectrum.

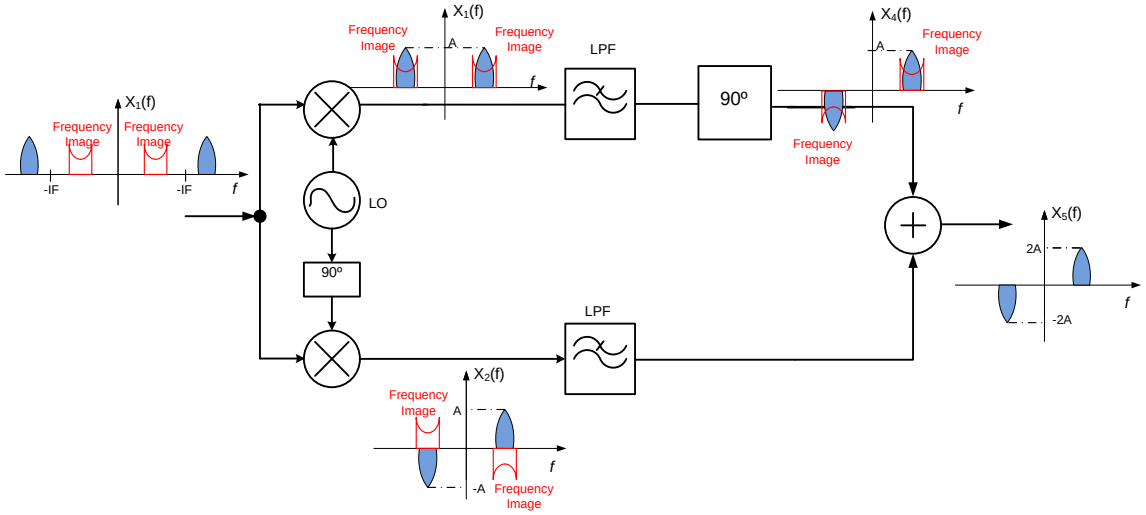

Fig. 2.20 – Hartley image rejection configuration and frequency domain operation

Combining the I and Q components results in the cancellation from the image frequency and also strengthen the desired signal. The main advantages from this architecture are good image rejection ratio (IRR) and the immunity to load problems that results from the needless of high quality discrete components (needed in Super-Heterodyne). Although this configuration is very sensitive to I/Q mismatch and non-linear behaviour of the 90º delay process and it is also affected by the adder blocks that can be extremely deteriorative to the output signal. The 90º delay block it is also difficult to realize and its behaviour is severely affected by the variation of each component. The Weaver architecture is similar to Harley in the first stage, although the 90º delay block is replaced by a second I/Q modulation. The two resulting signals can be subtracted and achieve the desired signal (with cancelation from the image frequency).

The Weaver arrangement has the advantage that not depends from the 90º delay block, bringing some flexibility to the architecture because with a simple switch from the adder it is possible to achieve the desire signal or the image frequency signal. With a most certain digitalization from several parts, this configuration can ensure better results in technologies such as Software Defined Radio.

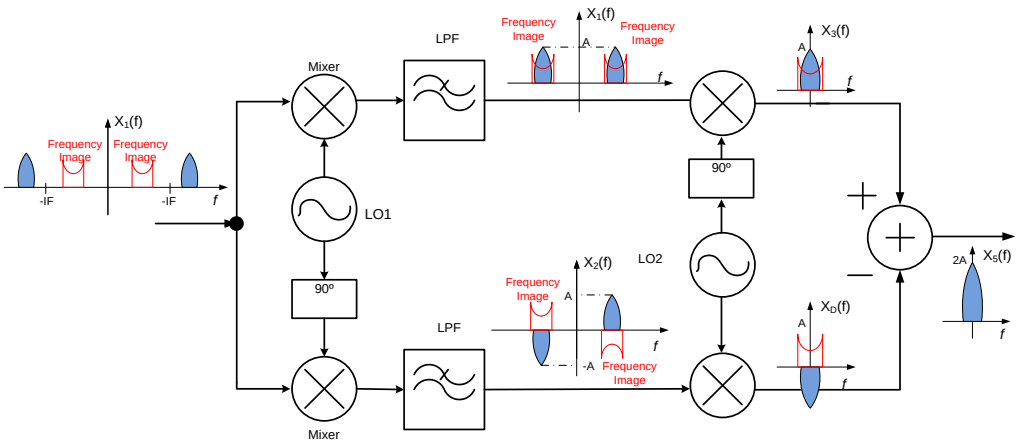

Fig. 2.21 – Weaver image rejection configuration and frequency domain operation

Nevertheless, the Weaver architecture has some limitations. Firstly, suffer the same I/Q mismatch problem as Hartley but with double. Secondly, the huge number of mixers and LO increases the energy consumption and the cost of the topology. Finally, the temperature and process variation can significantly degrade the desired signal. Several examples of this architecture are present in [28][30][31][32].

2.3 - Major Problems in Receiver's Architectures

As shown previously, all the studied architectures have advantages and problems that limit its behaviour and conditioned the selection of the most correct RF front-end for a certain system. Most of those problems are common to several architectures. For that reason it was decided to resume all in this sub-chapter.

2.3.1 - DC Offsets

The DC offset, such as LO leakage (figure 2.22a) or Interferer leakage (figure 2.22b) is one of the most important problem that affects the direct-conversion architectures. The LO leakage results from a non-ideal isolation between the ports from the mixer, causing that the local oscillator's signal flowing to the entry port corrupting the received RF signal (arises from capacitive and substrate coupling and bond wire coupling when LO is external). This non-ideal isolation between the mixer's ports is also the source of the Interference leakage. However in this case, the input signal is the signal that flow to local oscillator, corrupting the mixing process. This problem is particularly more visible in the presence of large interferes in the input signal.

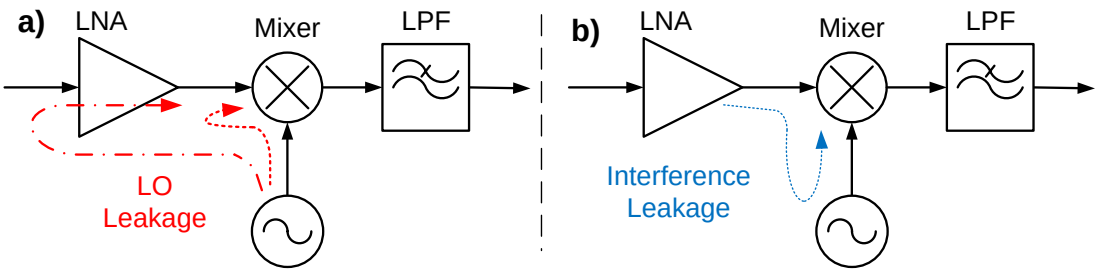

Fig. 2.22 – DC Offsets problems – a)LO Leakage; b) Interference Leakage

To minimize the effects of DC Offsets problems, several techniques/architectures has been developed such as AC coupling, DC offsets or DC compensation feedback, although these solutions are more oriented for specifics types of modulation.

2.3.2 - In-Phase/Quadrature Mismatch

Other problem very common in receiver's architectures that use complex mixers are the I/Q mismatch (errors in I&Q mixing).

This type of problem results from small synchronization differences from the LO signal in the mixing process or even in the RF path (if a 90º delay block is used) (figure 2.23). Let assume that we have an entry signal given by:

$$x_{IN}(t) = a\cos(\omega_C t) + b\sin(\omega_C t) \tag{2.21}$$

If the LO signals used in mixing process have a small synchronization difference:

$$C_{LO,I}(t) = 2\cos(\omega_C t) \tag{2.22}$$

$$C_{LO,Q}(t) = 2\times(1+\varepsilon)\times\sin(\omega_C t + \theta) \tag{2.23}$$

The amplitude and phase from the result signal will be different than expected (figure 2.24):

$$x_{BB,I}(t) = a \tag{2.24}$$

$$x_{BB,Q} = (1+\varepsilon)\times b\cos\theta - (1+\varepsilon)\times a\sin\theta \tag{2.25}$$

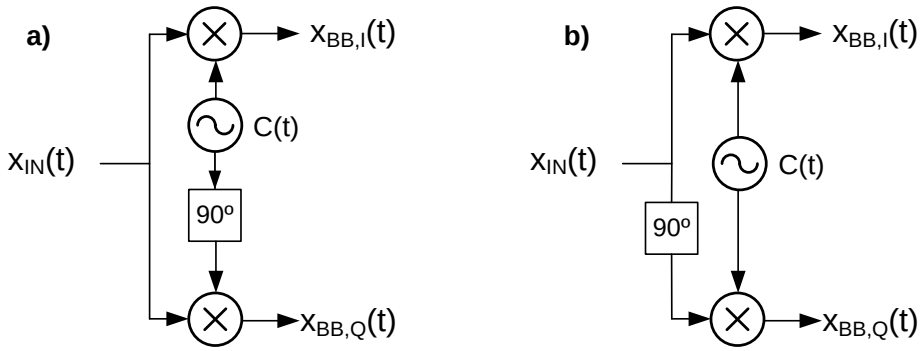

Fig. 2.23 – Quadrature generation problems – a)LO Path; b) RF Path

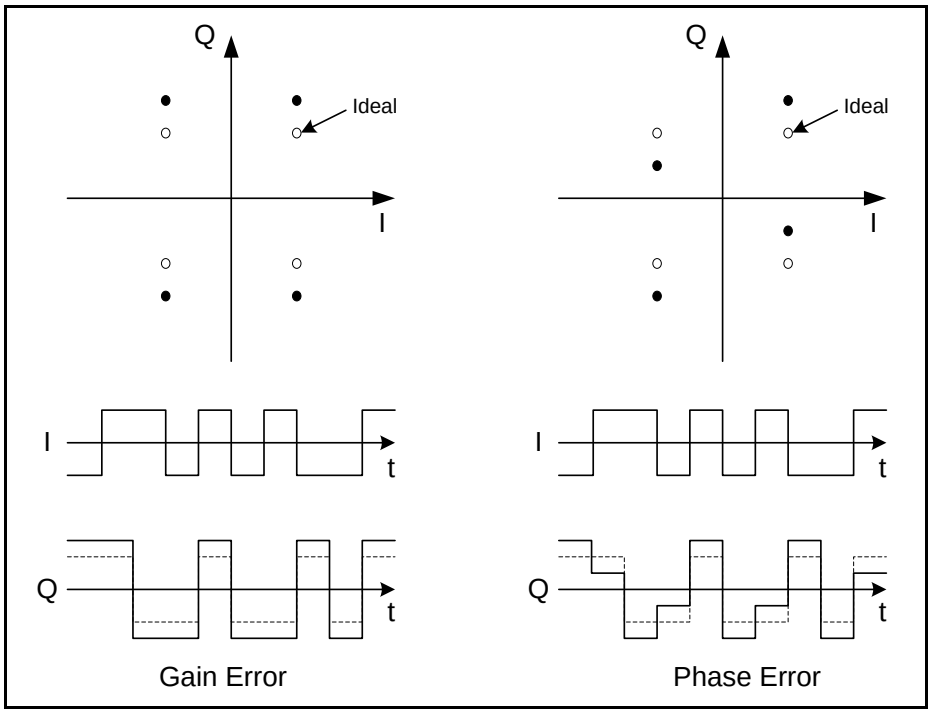

Fig. 2.24 – Quadrature generation problems – Gain and phase errors

The I/Q Mismatch has been one of the major obstacle in discrete designs, especially critical in the connection between the different discrete components, but this problem has been drastically reduced with higher levels of integration.

2.3.3 - Even/Odd-order Distortion

The Even/Odd-order distortions are other common problem in RF architectures based in discrete components. This distortion is generated by the nonlinear behaviour from the RF components that generated several products in harmonic frequencies, at baseband and even in the band of the signal. Products arising from the even order (especially the second and fourth) affect the signal at DC and baseband frequencies (figure 2.25) and the odd

order products (also known as intermodulation products) have major influence on the frequency of the received signal (figure 2.26). This problem will be one of the main focus of this theses and will be analyze in detail in next chapter.

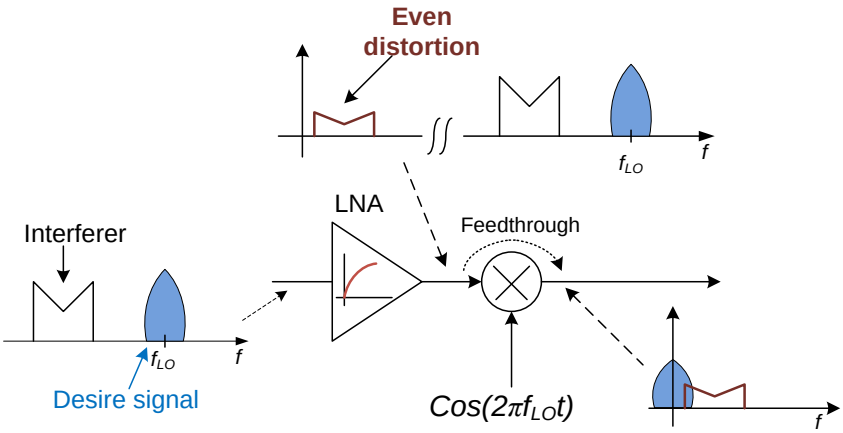

Fig. 2.25 – Even-order distortion caused by the nonlinear behaviour of the LNA

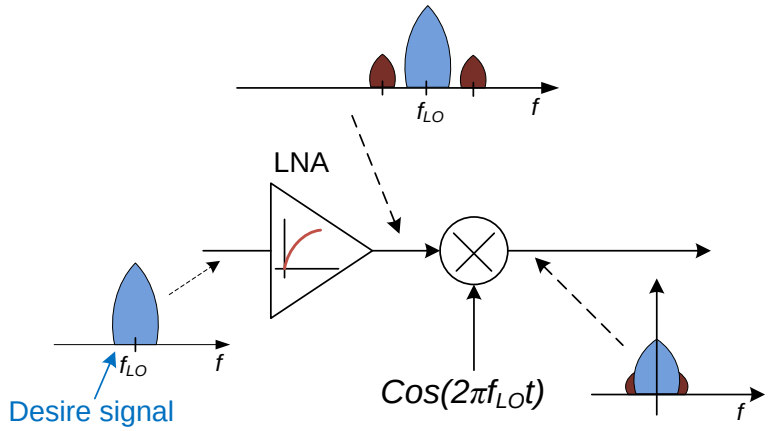

Fig. 2.26 – Odd-order distortion caused by the nonlinear behaviour of the LNA

2.3.4 - Clock Aperture Jitter and Aperture distortion

Some of the exclusivity problems from digital receivers are the Clock aperture jitter and the aperture distortion [16]. The clock jitter is a variation between of sampling instants relative an ideal clock. This small variation causes the degradation from the signal-to-noise ratio (SNR) in comparison with an ideal sampling system. Assuming a sinusoidal input signal, this SNR is given by the expression:

$$SNR = -20\log_{10}(2\pi f_a t_{jrms})^2 \qquad (6.26)$$

where f_a is the input signal frequency and t_{jrms} is the root mean square of the jitter (is assume that mean of t_{jrms} is 0).

Clock jitter can cause degradation especially in sub-sampling systems performance, forcing the use of anti-aliasing filtering to avoid bigger problems. The jitter requirements imposed by the sub-sampling process become more stringent as the frequency being sampled increases but are independent of the jitter requirements imposed by the required ADC resolution.

The aperture distortion is mainly cause by transition of control signals from track to hold. Is strongly influenced by clock signal transition time, signal characteristics, the sampling circuit architecture and fabrication technology. It is difficult to quantify because it depends from several factors, could only be quantify for specific sampling architectures.

2.3.5 - Minor problems

There are other problems with lower relevance, than the previous presented, but can have a significant role in the chosen of the RF architecture. Problems like large flicker noise of the mixer that can easily corrupt the output in a baseband signal or Noise Figure associated with the number of the components and the quality from the first electronic components after the receiver's antenna (Filter and LNA) [33].

In this section it is also good to remember more practical problems as transversality, reliability, complexity and size reduction which are always taken into account when choosing a particular architecture.

2.4 - Final comparison between all architectures

This chapter presented the principals configurations known and used as receivers in RF systems. As can been seen in table 2.2, there is not an ideal configuration for all types of RF systems but the chosen architecture will depends on the application, the minimum requirements, working scenarios, cost, size among others. These parameters are directly connected to the performance and reliability of the RF system and the influence in their frequency neighbours. It is important to first outline the minimum requirements of the system to easily choose the configuration that best suits it. Is also important not forget that more technical factors and best results usually are associated with a higher cost and bigger size.

Architecture	Advantages	Major Problems
Simple Detector	- Simplicity - Low cost	- Huge degradation with interferes - Low selectivity, sensitivity - Some DC problems
Zero-IF	- Simplicity - IC integration	- Strong DC problems - I/Q mismatch - Even/Odd distortion - Flicker noise
Super-Heterodyne	- Selectivity - Sensitivity - Immune DC problems	- Image frequency - I/Q mismatch - High quality discrete components - Perfect LNA 50Ω load - Complexity - Noise figure - Nonlinear behaviour in components
Low-IF	- No DC problems - Simplicity - Less high quality discrete components	- I/Q mismatch - Image frequency - Requires high performance ADC
Band-Pass Sampling	- Flexibility - Signal manipulation - Low cost, circuit area - Minimize DC problems and RF problems (in digital domain)	- Susceptibility to clock aperture jitter - Noise figure degradation - Aperture distortion - Power consumption
Hartley	- Good IRR - Less discrete components - Reduce load problems	- I/Q mismatch - Shift-by-90^{o} block and adder - Variation R &C in RC-CR network - Increased number of components
Weaver	- Similar to Hartley - Avoid RC-CR network	- Huge number of mixers - I/Q mismatch - Dependent VCO - Strong adjacent channel interferes - Increased number of components

Table 2.2 – Comparison between the receiver's architectures presented in this chapter

There are some others architectures being proposed for use in the actual and future receivers mainly involving the use of direct RF sampling techniques based on discrete-time analogue signal processing to receive the signal, such as the ones developed in [34][35]. These methods are still in a very immature stage but should be further studied due to their potential efficiency in implementing reconfigurable receivers.

2.5 - Conclusions and guidelines for next chapters

As presented in Chapter 1 and referred to throughout this chapter, the main objective of this doctoral work is the study of nonlinear phenomena present in RF communication systems, its impacts, problems and consequences. For that reason it was important to made this comparative study between the most typical receiver architectures in order to better understand the true impact of the nonlinear products in receiver performance, identify the most responsible for this behaviour (like LNA), be able to model mathematically the nonlinear response, explain and analyze in detail some measurement methods based on this nonlinear phenomenon (and also correcting the methods of their calibration), and finally propose new architectures capable to minimize some of the adverse nonlinear impacts to the reliability of systems.

To develop all this goals, this chapter is also useful to select the most important architectures study along the doctoral work, their major applications and limitations. In this context, the envelope detector configuration was chosen to analyze and characterize the measurements of well known Power Meter in order to understand their dependence from the output impedance, the unreliability of the common calibration methods used and fluctuations in measured quantities with the variation of output impedance. Other selected configurations are Hartley's and Weaver's configurations as a starting point to support new interference cancellation architectures proposed in Chapter 6.

CHAPTER 3

Nonlinear behaviour - Theoretical principles and characterization

As referred in the previous chapters, the nonlinear behaviour from the electronic devices could be an important problem in receiver's architecture but also a way to simplify the conversion process from RF frequency to DC. The nonlinear phenomenon is present in almost all communication systems and RF components will be the main subject of analyses from this thesis. One of the goals is achieve several reasonable mathematical models with extensive applications, mainly in simulation of RF systems or calibration from measurements instruments.

This chapter is so dedicated to introduce nonlinear theory approaches to receiver circuits. In order to identify all nonlinear products in most common RF systems, a detailed study of the characteristics of a nonlinear system especially focused on the response to two input tones will be presented.

3.1 - Linear systems vs nonlinear systems

When we analyse the RF output response of a communication circuit, all radio systems can be divided into two major groups: linear or nonlinear response.

A linear system is characterized by presenting the principle of superposition, or in other words, the system has a linear response in magnitude and phase for each constituent component of the input signal. The superposition principle states that the response of a linear system to an input signal composed by the sum of two or more components is equal to the sum of the system's individual response to each component of the signal. To demonstrate this concept, let us assuming an input signal with two components (equation 3.1). The response of a linear system is given by equation 3.2 [2]:

$$x(t) = k_1 x_1(t) + k_2 x_2(t) \tag{3.1}$$

where k_1 and k_2 are arbitrary constants (real or complex) and

$$\delta_L\left[x(t)\right]=\delta_L\left[k_1x_1(t)+k_2x_2(t)\right]=k_1\delta_L\left[x_1(t)\right]+k_2\delta_L\left[x_2(t)\right] \quad (3.2)$$

Thus, if the system is time invariant, since there is only linear variation in magnitude and phase, there is no creation of new spectral products in output's spectrum. In other words, the output spectrum will have the same components than the input signal spectrum, only suffer a change in amplitude and/or in phase.

Although these systems are easier to characterize and parameterize, they are a minority of radio systems. This linear superposition theorem is often used as an accurate approximation for systems with very weak nonlinear performance (defined as *quasi-linear).* Example of these types of systems are the passive components like resistors, capacitors, coils, filters and others, although many of these elements start to have nonlinear characteristics when subjected to extreme conditions (weather, temperature, age,...) [36].

The Nonlinear systems, predominant in nature, can also be divided in two major groups: weak nonlinearity and strong nonlinearity.

A weak nonlinear system have an output, that despite not obeying the principle of superposition, can be mathematically approach (with an error below a certain threshold) by a Taylor (or Volterra) series expansion of the current/voltage ratio (I/V), load/voltage (Q/V), etc ... around a reference point, whether it is current or voltage [37][38]. This definition requires that the nonlinearity under study is continuous, has continuous derivatives and for most practical applications, response's approach does not require many Taylor's series terms.

Many electronic components based on semiconductors like diodes or transistors (and some passive components) may be enclosed in this definition since the excitation voltages are within normal operating parameters of the component.

For systems with strong nonlinear characteristics, the Taylor's series could not be used as the approach method, since the number of terms necessary would be too high and do not give guarantees of convergence. Such circuits must be simulated using *harmonic balance* methods or *time domain* [2] and modulated with measurement models based on laboratory result tests.

3.2 - Nonlinear systems: Characterization

As mentioned in the previous section, when a system has weakly nonlinear behaviour, it can be mathematically approached by a Taylor's (or Volterra) series expansion. The Taylor series states that the system's nonlinear behaviour can be represented by a weighted sum of different exponential contributions from the input signal. In other words, as can be seen in equation 3.3, each term is a function (linear, quadratic, cubic, etc...) of the input signal with order (k) and a degree of importance given by a_k.

$$y_{NL} = \sum_{k=1}^{+\infty} a_k x(t-\tau_k)^k = a_1 x(t-\tau_1) + a_2 x(t-\tau_2)^2 + a_3 x(t-\tau_3)^3 + \ldots \quad (3.3)$$

As already said, the Taylor series is a practical tool to modulate nonlinear system's behaviour if it is used with only a small number of terms. If we use reasonable number of series' terms to modulate our nonlinear system we could achieved almost identical results as the real ones. However the complexity of the response results (especially if the input signal is not a simple sum of sinusoids) and the computation time needed to do such number of iterations can make the process painful and too slow for a acceptable time window process. For that reason, it is important to define a maximum truncation order from Taylor series that achieve good accuracy but also guaranties the simplicity of the analysis processes. In some systems this truncation order is not easy to define and could only be achieved after several iterations and comparisons with measurements results.
It is easy to see that the products resulting from those Taylor series terms will affect distinctly our output signal. In section 3.2.1 the different types of nonlinear products and their greatest impact on nonlinear response of the system are presented.

3.2.1 –Description of the main nonlinear products

In a nonlinear phenomenon there are several new products that affect differently the output resulting signal. Since there is generation of new spectral components, as already been mentioned in previous sections, some of these new created products will fall over the fundamental signal frequencies strongly affecting system performance [2][3][36]. Starting with this knowledge, this section is dedicated to identify all main products arise in a nonlinear response, in order to understand this role in spectral efficiency, high power importance and relation between signal/jammer. Each product will be presented in a

separate subsection, enhancing their main disadvantages to the conventional radio systems. The section will be finalized with a brief comparison between all of them.

3.2.1.1 - Generation of Harmonics

One of the most known products resulting from a nonlinear system is the generation of harmonics in the multiple frequencies of the fundamental (input's signal frequency). It is easy to realize that these harmonics are directly related to the exponents of the terms from the Taylor series presented before. If we have a nonlinear system represented by a Taylor series and the input signal has a fundamental frequency at ω_k, the 2nd order term will generate harmonics at $2\omega_k$, the 3rd order harmonics will fall at $3\omega_k$ and so on.

If the starting harmonics of 2nd and 3rd order seems do not have a great impact on system performance (it could easily be filtered by a bandpass filter, centred on the fundamental frequency), they become especially critical when it starts to interact with intermodulation components of lower order creating in-band distortion, that is, nonlinear products with the same frequency as fundamental spectrum components (or near), strongly condition the magnitude and phase from the output signal spectrum.

The n-order harmonics can also be harmful for other communication systems that operate in area, because the transmitted harmonics can fall in fundamental frequencies of those systems. This is especially critical in broadband systems (like television transmitters) that have a very high power widespread. Even a bandpass filter is used to strongly attenuate the generated harmonics, a neighbour system that has a very low sensitivity (like -90dBm) will be strongly affected by these harmonics, because their power levels could be higher than sensitivity of those systems.

3.2.1.2 - Intermodulation Distortion

The intermodulation distortion present in nonlinear systems could be one of the most problematic types of distortion in communication systems, but also the operating principle of the simplest circuits like envelope detectors as shown in Chapter 2. These products (that appears only in signals more complicated than a single sinusoid) result from the intermodulation process (cross-modulation) between the several spectral products from the input signal.

To better understand the origin and the impact of this distortion let assume a typical two-tones input signal at the entry of our nonlinear system. All components generated in a nonlinear process can be mathematically represented by:

$$\omega = m\omega_1 + n\omega_2 \tag{3.4}$$

The order of the created component is defined by $|m| + |n|$ where m and n are integers that depend on the maximum order of the Taylor series. The resulting intermodulation products may fall close to DC, like $\omega_1-\omega_1$ or $\omega_2-\omega_1$, or near the core of the system, like $2\omega_2-\omega_1$. If the first products, resulting from even order terms, can be explored for a rapid conversion from RF band to baseband (or DC) or simply removed with a common bandpass filter, the last intermodulation products could be problematic because they are in the neighbourship of the fundamentals components. These last products, also known as in-band Intermodulation Distortion (IMD) arises from the odd order terms of Taylor series. Because they actually fall near the fundamental spectrum of the system, it is extremely difficult to eliminate them by regular filtering (even using very selective filters), reason why they have a very strong influence in system's output response.

The location and importance from the major intermodulation products is present in figure 3.1. Using the same two-tone example and considering a nonlinear system truncated to order 5, the intermodulation products that falls near DC (when the input has two-tones) will be:

$$\omega_1-\omega_2;\omega_2-\omega_1;\ 2\omega_1-2\omega_2;\ 2\omega_2-2\omega_1; \tag{3.5}$$

The intermodulation products that fall near the fundamentals of the signal will be:

$$2\omega_1-\omega_2;\ 2\omega_2-\omega_1;\ 3\omega_1-2\omega_2;\ 3\omega_1-2\omega_2; \tag{3.6}$$

Joining these products the output's signal spectra is present in figure 3.1.

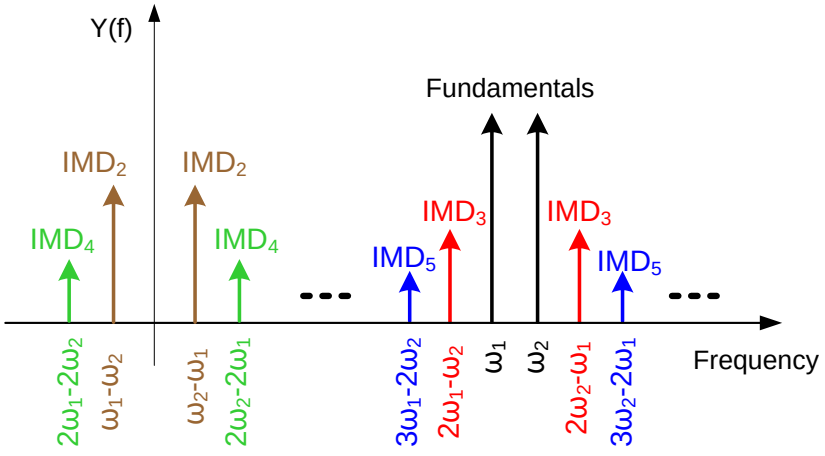

Fig. 3.1 - Components of the resulting spectral intermodulation to 5th order (principal products)

At this point, the magnitude and phase from each product is not relevant. Although, as will be seen latter, it could constitute one of the main concern in system performance, because not only the magnitude of these products can affect the correct interpretation of desire signal, but also the product's phase can clearly corrupt the good reception in systems based in phase measuring. The magnitude of each term will be calculated later with a two-tone complete test present in section 3.3.

3.2.1.3 - Desensitization and cross-modulation

In radio-frequency systems, another class of nonlinear distortion products is called desensitization. This characteristic phenomenon from odd products has a great impact when we processing a strong signal outside the band of the carrier with the weak signal within the band. Its importance becomes even greater when there are strong signals in adjacent bands to the band's operating system. Due to this nonlinear effect of the system, the output signal can suffer what is called a blocking effect.

Returning to the example of a nonlinear system excited by a two-tone signal, the products responsible for desensitization will be:

$$\begin{aligned} &\omega_2 - \omega_1 + \omega_1;\ \omega_1 + \omega_2 - \omega_2 \ \text{(3rd order)} \\ &\omega_2 - 2\omega_1 + 2\omega_1;\ \omega_1 + 2\omega_2 - 2\omega_2 \ \text{(5th order)} \end{aligned} \tag{3.7}$$

As referred, these distortion products will fall on the fundamental frequencies causing generally a reduction of system gain. Using the system represented on equation 3.3, when a_3 and a_5 are negative, the system response will eventually compress, because these component, as a product of superior order, increases in the order proportion to the input power. Therefore, the presence of large jammers in adjacent bands can be a major contribution for attenuation of the desired signal, despite being at different frequencies and a_3 or a_5 much smaller than a_1 (linear gain of the system).

Similar to desensitization is the cross-modulation. With the same origins, the cross-modulation results from the transfer of information from one carrier to another carrier, from a channel located adjacent to another or, in the case of two tones, from one to another tone. This also results from nonlinear effects of odd orders.

To emphasize these two nonlinear problems, let consider again the nonlinear system of equation 3.3 and the following input signal [2]:

$$x(t) = b_1 \cos(\omega_1 t) + b_2 \left(1 + m(t)\right) \cos(\omega_2 t) \tag{3.8}$$

where $m(t)$ is a modulated signal with a frequency ω_m and $|m(t)|<1$. Passing this signal by a nonlinear system, the 3rd order component that will fall over the ω_1 tone, resulting from $\omega_2 - \omega_2 - \omega_1$, is:

$$y_3(t) = \frac{3}{2} a_3 b_1 b_2^2 \left(1 + 2m(t) + m^2(t)\right) \cos(\omega_1 t) \tag{3.9}$$

As reflected in equation 3.9, in these 3rd order distorted version the component ω_2 is transferred to the component ω_1. The cross-modulation interference is much more pronounced as higher the odd nonlinear coefficient is and/or with the increasing magnitude from the jammer signal.

3.2.1.4 - Phase distortion (AM-PM)

The phase distortion, also known as AM-PM conversion, is a phenomenon that can change both the amplitude and the phase from the signal applied to a nonlinear system.

Like previous desentization and cross-modulation distortion, this phenomenon also falls over the fundamentals frequency but in this case the distortion is caused only by the proper signal to itself. As previously presented, there are odd-order products that fall within the range of operation of the system, like $\omega_1 - \omega_1 + \omega_1$ or $\omega_2 - \omega_2 + \omega_2$. If these products have large phase changes, even if their amplitude is substantially lower than the fundamental, the impact on the output signal can be significant as we see in Figure 3.2.

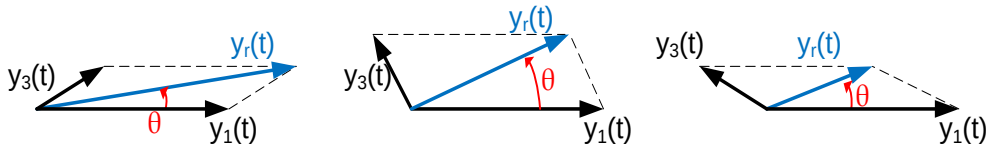

Fig. 3.2 – Illustration of AM-PM distortion: $y_1(t)$ – linear component; $y_3(t)$ – third-order signal correlated distortion component; $y_r(t)$ – resultant output component; θ – resultant output phase;

Observing figure 3.2, it becomes clear that, although the third order component always has the same amplitude, as we increase the phase difference between them and the fundamental and third-order product, the impact on the output signal also increases significantly.

This distortion is also very harmful for systems that strongly depend from the variation of phase, like communications signals modulated in phase (PSM or PSK) or frequency (FM or FSK).

3.3 - Nonlinear analyses for a Two-tone excitation

To illustrate all the features presented previously, in this section will be shown a detailed study of the nonlinear response from the system of equation 3.3 excited by a common two-tones input signal [2][8].

In order to simplify the equations and to easily demonstrate the concepts, it is assumed that the Taylor series can be truncated to the third order and behave memoryless, so the delay τ_k could be removed. Thus the studied $y_{NL}(t)$ is:

$$y_{NL}(t) = \sum_{k=1}^{3} a_k x(t)^k = a_1 x(t) + a_2 x(t)^2 + a_3 x(t)^3 \tag{3.10}$$

Considering the input signal is composed of two tones (closed in frequency) given by:

$$x(t) = b_1 \times \cos(\omega_1 t) + b_2 \times \cos(\omega_2 t) = \frac{1}{2} b_1 e^{-j\omega_1 t} + \frac{1}{2} b_1 e^{j\omega_1 t} + \frac{1}{2} b_2 e^{-j\omega_2 t} + \frac{1}{2} b_2 e^{j\omega_2 t} \tag{3.11}$$

The mathematical response of the system will be:

$$\begin{aligned} y_{NT}(t) = & \underbrace{a_1 \left(b_1 \times \cos(\omega_1 t) + b_2 \times \cos(\omega_2 t) \right)}_{y_1 = 1^{st}\ order} + \underbrace{a_2 \left(b_1 \times \cos(\omega_1 t) + b_2 \times \cos(\omega_2 t) \right)^2}_{y_2 = 2^{nd}\ order} + \\ & + \underbrace{a_3 \left(b_1 \times \cos(\omega_1 t) + b_2 \times \cos(\omega_2 t) \right)^3}_{y_3 = 3^{rd}\ order} \end{aligned} \tag{3.12}$$

The resulting spectrum is presented in Figure 3.3.

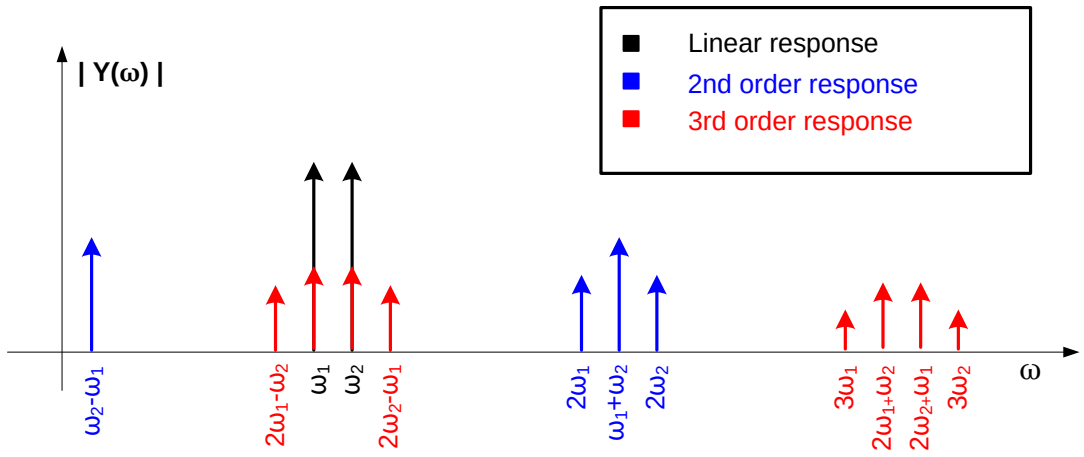

Fig. 3.3 – Nonlinear system response (trunk to 3rd order) from a two-tones input signal

For better analysis and organization of the products resulting from the nonlinear behaviour of the system, the several nonlinear contributions will be presented by the order response.

3.3.1 – Linear response

The system's linear (first-order) response to this input signal will be:

$$y_L = a_1\left(b_1 \times \cos(\omega_1 t) + b_2 \times \cos(\omega_2 t)\right) = a_1 b_1 \times \cos(\omega_1 t) + a_1 b_2 \times \cos(\omega_2 t) \tag{3.13}$$

and in (Euler's) exponential mode:

$$y_L = \frac{1}{2} a_1 b_1 e^{-j\omega_1 t} + \frac{1}{2} a_1 b_1 e^{j\omega_1 t} + \frac{1}{2} a_1 b_2 e^{-j\omega_2 t} + \frac{1}{2} a_1 b_2 e^{j\omega_2 t} \tag{3.14}$$

This is a typical linear response of the system and could be a reasonable approach if we know that $a_1 x(t)$ >>> $a_n x^n(t)$. As expected this first order response does not create new spectral components beyond those already existing in the original signal and the output signal only differs in amplitude from the input signal.

3.3.2 – Second-order response

Consider now what happens in the 2nd-order nonlinear behaviour. The 2nd-order products will be given by:

$$\begin{aligned} y_2 &= a_2\left(b_1 \times \cos(\omega_1 t) + b_2 \times \cos(\omega_2 t)\right)^2 \\ &= a_2\left(b_1^2 \times \cos^2(\omega_1 t) + b_2^2 \times \cos^2(\omega_2 t) + 2 \times b_1 \times b_2 \times \cos(\omega_1 t) \times \cos(\omega_2 t)\right) \end{aligned} \tag{3.15}$$

which, using the following trigonometric relations:

$$\begin{aligned} \cos^2(\omega) &= \frac{1+\cos(2\omega)}{2} \\ \cos(\omega_2)\cos(\omega_1) &= \frac{1}{2}\left[\cos(\omega_2+\omega_1) + \cos(\omega_2-\omega_1)\right] \end{aligned} \tag{3.16}$$

results in:

$$y_2 = a_2\left[b_1^2\left(\frac{1+\cos(2\omega_1 t)}{2}\right) + b_2^2\left(\frac{1+\cos(2\omega_2 t)}{2}\right) + b_1 b_2\left(\cos(\omega_2 t+\omega_1 t) + \cos(\omega_2 t-\omega_1 t)\right)\right] \tag{3.17}$$

$$y_2 = \frac{1}{2}a_2\left(b_1^2 + b_2^2\right) + \frac{1}{2}a_2 b_1^2\cos\left(2\omega_1 t\right) + \frac{1}{2}a_2 b_2^2\cos\left(2\omega_2 t\right) + \\ + a_2 b_1 b_2\cos\left((\omega_1 + \omega_2)t\right) + a_2 b_1 b_2\cos\left((\omega_2 - \omega_1)t\right) \tag{3.18}$$

$$y_2 = \frac{1}{2}a_2\left(b_1^2 + b_2^2\right) + \frac{1}{4}a_2 b_1^2 e^{-j2\omega_1 t} + \frac{1}{4}a_2 b_1^2 e^{j2\omega_1 t} + \frac{1}{4}a_2 b_2^2 e^{-j2\omega_2 t} + \frac{1}{4}a_2 b_2^2 e^{j2\omega_2 t} \\ \frac{1}{2}a_2 b_1 b_2 e^{-j(-\omega_2 - \omega_1)t} + \frac{1}{2}a_2 b_1 b_2 e^{-j(-\omega_2 + \omega_1)t} + \frac{1}{2}a_2 b_1 b_2 e^{-j(\omega_2 - \omega_1)t} + \frac{1}{2}a_2 b_1 b_2 e^{-j(\omega_2 + \omega_1)t} \tag{3.19}$$

Looking to equation 3.19, it is possible to distinguish the creation of new spectral components: one DC component (which changes the bias point of the system), two harmonics appearing at the double of fundamental frequencies ($2\omega_1$; $2\omega_2$), two intermodulation products (ω_2-ω_1; ω_1-ω_2) that falls at baseband (near DC) and two other intermodulation products near the 2nd harmonics are also created (ω_2+ω_1; -ω_1-ω_2).

If was considered a nonlinear system of order different from two, there will be others even order terms that would match the 2nd order components at DC and baseband frequencies, attenuating or expanding them depending from the input signal and ratio between Taylor's coefficients.

The relationship between the fundamental and the 2nd order components (resulting from the sum or difference) is called the ratio of 2nd-order intermodulation (IM_2). In this case, because is only considered the second order products, the ratio is given by:

$$IM_2 = \frac{\frac{1}{2}a_2 b_1 b_2}{\frac{1}{2}a_1 b_1} = \frac{a_2 b_2}{a_1} \vee IM_2 = \frac{\frac{1}{2}a_2 b_1 b_2}{\frac{1}{2}a_1 b_2} = \frac{a_2 b_1}{a_1} \tag{3.20}$$

This equation shows that the second order intermodulation ratio is directly proportional to the input signal amplitude (for this example). Knowing that usually the linear coefficient (a_1) is much bigger then de second order coefficient (a_2), this relationship can be neglected for low-amplitude signals. However, as the amplitude of the input signal increases, this relationship begins to have a greater degree of significance. For systems that use the second order products to quickly convert a signal from RF frequency for DC, this relation must be as bigger as possible to maximize the quality of the signal's replica at baseband frequency.

3.3.3 – Third-order response

Finally the 3rd order products are showed in equation 3.21:

$$\begin{aligned} y_3(t) &= a_3\left(b_1\times\cos(\omega_1 t)+b_2\times\cos(\omega_2 t)\right)^3 \\ &= a_3\left(b_1\times\cos(\omega_1 t)+b_2\times\cos(\omega_2 t)\right)\left(b_1\times\cos(\omega_1 t)+b_2\times\cos(\omega_2 t)\right)^2 \end{aligned} \tag{3.21}$$

Using equation 3.17, the 3rd order response will be:

$$\begin{aligned} &y_3(t) = a_3\left(b_1\times\cos(\omega_1 t)+b_2\times\cos(\omega_2 t)\right)\times \\ &\left[b_1^2\left(\frac{1+\cos(2\omega_1 t)}{2}\right)+b_2^2\left(\frac{1+\cos(2\omega_2 t)}{2}\right)+b_1 b_2\left(\cos(\omega_2 t+\omega_1 t)+\cos(\omega_2 t-\omega_1 t)\right)\right] \end{aligned} \tag{3.22}$$

Extending this equation:

$$\begin{aligned} &y_3(t) = \frac{1}{2}a_3 b_1^3\cos(\omega_1 t)+\frac{1}{4}a_3 b_1^3\cos(3\omega_1 t)+\frac{1}{4}a_3 b_1^3\cos(2\omega_1 t-\omega_1 t) \\ &+\frac{1}{2}a_3 b_1 b_2^2\cos(\omega_1 t)+\frac{1}{4}a_3 b_1 b_2^2\cos(2\omega_2 t-\omega_1 t)+a_3 b_1 b_2^2\cos(2\omega_2 t+\omega_1 t) \\ &+\frac{1}{2}a_3 b_1^2 b_2\cos(\omega_2 t)+\frac{1}{4}a_3 b_1^2 b_2\cos(2\omega_1 t-\omega_2 t)+a_3 b_1^2 b_2\cos(2\omega_1 t+\omega_2 t) \\ &+\frac{1}{2}a_3 b_2^3\cos(\omega_2 t)+\frac{1}{4}a_3 b_2^3\cos(3\omega_2 t)+\frac{1}{4}a_3 b_2^3\cos(2\omega_2 t-\omega_2 t) \\ &+\frac{1}{2}a_3 b_1^2 b_2\cos(\omega_1 t+\omega_2 t+\omega_1 t)+\frac{1}{2}a_3 b_1^2 b_2\cos(\omega_1 t-\omega_2 t-\omega_1 t) \\ &+\frac{1}{2}a_3 b_1^2 b_2\cos(\omega_1 t+\omega_2 t-\omega_1 t)+\frac{1}{2}a_3 b_1^2 b_2\cos(\omega_1 t-\omega_2 t+\omega_1 t) \\ &+\frac{1}{2}a_3 b_1 b_2^2\cos(\omega_2 t+\omega_2 t+\omega_1 t)+\frac{1}{2}a_3 b_1 b_2^2\cos(\omega_2 t-\omega_2 t-\omega_1 t) \\ &+\frac{1}{2}a_3 b_1 b_2^2\cos(\omega_2 t+\omega_2 t-\omega_1 t)+\frac{1}{2}a_3 b_1 b_2^2\cos(\omega_2 t-\omega_2 t+\omega_1 t) \end{aligned} \tag{3.23}$$

And finally:

$$\begin{aligned} &y_3(t) = \frac{3}{4}a_3 b_1^3\cos(\omega_1 t)+\frac{3}{4}a_3 b_2^3\cos(\omega_2 t)+\frac{1}{4}a_3 b_1^3\cos(3\omega_1 t)+\frac{1}{4}a_3 b_2^3\cos(3\omega_2 t) \\ &+\frac{3}{2}a_3 b_1 b_2^2\cos(\omega_1 t)+\frac{3}{4}a_3 b_1 b_2^2\cos(2\omega_2 t-\omega_1 t)+\frac{3}{2}a_3 b_1 b_2^2\cos(2\omega_2 t+\omega_1 t) \\ &+\frac{3}{2}a_3 b_1^2 b_2\cos(\omega_2 t)+\frac{3}{4}a_3 b_1^2 b_2\cos(2\omega_1 t-\omega_2 t)+\frac{3}{2}a_3 b_1^2 b_2\cos(2\omega_1 t+\omega_2 t) \end{aligned} \tag{3.24}$$

As seen in equation 3.24, the resulting 3rd order products will also create new spectral components beyond the linear and the 2nd order spectrum tones.

Thus, carefully analyzing the equation, there are 4 types of emerging spectral components: two harmonics of 3rd order appearing at $3\omega_1$ and $3\omega_2$; intermodulation distortion components that fall near the fundamental (ex: $2\omega_2-\omega_1$); conversion AM/AM and AM/PM components that will affect (attenuate or expand) their own fundamentals (ex: $2\omega_2-\omega_2$); cross-modulation components that also fall at fundamentals frequency but depends from both tones (and not only one as AM/PM components) as seen in previously.

These last two distortion products are undetectable by observing the spectrum, since they coincides with the fundamental tones from input signal. As referred, those products may result in the expansion or attenuation of the gain depending on whether they are in phase with the fundamental components (or not). If the input signal has two-tones with the same amplitude, the cross-modulation products have twice the amplitude than the AM-AM/AM-PM products, but this last products could have a significant difference role due to their phase difference to the fundamentals. The equations 3.25 and 3.26 show the AM/PM distortion and cross-modulation equation respectively:

$$\frac{3}{4}a_3 b_1^3 \cos\left(\pm 2\omega_1 t \mp \omega_1 t\right); \quad \frac{3}{4}a_3 b_2^3 \cos\left(\pm 2\omega_2 t \mp \omega_2 t\right) \tag{3.25}$$

$$\frac{3}{2}a_3 b_1 b_2^2 \cos\left(\pm \omega_1 t + \omega_2 t - \omega_2 t\right); \quad \frac{3}{2}a_3 b_1^2 b_2 \cos\left(\pm \omega_2 t + \omega_1 t - \omega_1 t\right) \tag{3.26}$$

Once again, AM/AM distortion is always present in the nonlinear response of a system (isn't attach to the type of input signal), since depends only from signal spectrum and is characterization enables the evaluation of an important figure of merit called the 1-dB compression point [1]. This figure marks the reference level from which the output signal power is 1 dB below the equivalent when calculate only with the linear response for small signals. This is a very important point for system characterization, particularly in amplifier devices. The AM/AM characterization is usually expressed as a certain dB/dB deviation at a predetermined input power [40]. This point is also generally assumed as the maximum output power from the amplifier (from this point on the response of the amplifier becomes strongly nonlinear).

The intermodulation products in band also appear very close to the fundamental frequency and could have a significant importance in degradation of the output signal.

These products have the contribution from both fundamental tones, mixing the information between them. From 3.24, their equation is given by:

$$\frac{3}{4}a_3 b_1 b_2^2 \cos\left(\omega_1 t \pm 2\omega_2 t\right); \qquad \frac{3}{4}a_3 b_1^2 b_2 \cos\left(\omega_2 t \pm 2\omega_1 t\right) \tag{3.27}$$

Being close to the fundamental tones (which justify the designation of nonlinear distortion in band), their spectral distance to ω_1 and ω_2 is the same as the spectral distance between the two fundamental tones. They have a strong importance in the characterization of the nonlinear system and are generally known as intermodulation distortion (IMD). Their power varies with the triple power of the input signals (with equal input tones) or the product of twice the power from one tone multiplied by other tone. The power of the intermodulation product of 3rd order is given by:

$$P_{IMD}\left(2\omega_1 - \omega_2\right) = \frac{1}{T_{2\omega_1-\omega_2}} \int_0^{T_{2\omega_1-\omega_2}} \left(\frac{3}{4}a_3 b_1^2 b_2 \cos\left((2\omega_1 - \omega_2)t\right)\right)^2 dt = \frac{9}{32}a_3^2 b_1^4 b_2^2 \tag{3.28}$$

with the power of the input signals been given by:

$$\begin{aligned} P_{1IN} &= \frac{1}{T_{\omega_1}} \int_0^{T_{\omega_1}} \left(b_1 \cos(\omega_1 t)\right)^2 dt = \frac{b_1^2}{2} \\ P_{2IN} &= \ldots = \frac{b_2^2}{2} \end{aligned} \tag{3.29}$$

The formula 3.28 can be rewritten by:

$$P_{IMD}\left(2\omega_2 - \omega_1\right) = \frac{9}{32}a_3^2 b_1^4 b_2^2 = \frac{9}{4}a_3^2 \times \frac{b_1^4}{4} \times \frac{b_2^2}{2} = \frac{9}{4}a_3^2 \times P_{1IN}^2 \times P_{2IN} \tag{3.30}$$

Considering the amplitude of the tones identical ($b_1 = b_2 = b$), the final equation for the power of the intermodulation products at $2\omega_2 - \omega_1$ is:

$$P_{IMD}\left(2\omega_2 - \omega_1\right) = \frac{9}{4}a_3^2 \times P_{IN}^3 \tag{3.31}$$

To evaluate the impact of these products in the output signal, the intermodulation ratio (IMR) can be used. IMR compares the power of fundamental tone (P_S) with their intermodulation neighbour tone:

$$IMR = \frac{P_S}{P_{IMD}} = \frac{P(\omega_1)}{P(2\omega_1 - \omega_2)} = \frac{P(\omega_2)}{P(2\omega_2 - \omega_1)} \tag{3.32}$$

Using equation 3.28 and assuming that the power of the fundamental tone just depends on the linear response of the system (ignoring here the contribution of the AM/AM and cross-modulation distortion), then:

$$IMR = \frac{\frac{1}{2} b_1^2 a_1^2}{\frac{9}{32} a_3^2 b_1^4 b_2^2} = \frac{\frac{1}{2} b_2^2 a_1^2}{\frac{9}{32} a_3^2 b_2^4 b_1^2} = \frac{9}{16} \frac{a_1^2}{a_3^2 b_1^2 b_2^2} \tag{3.33}$$

The IMR is directly linked to the so called 3rd order point intercept point (IP3).

3.3.3.1 - Third-order Intermodulation Characterization

At this point is important to make a more thorough study to the impact and relevance of intermodulation products in the performance of such a system, especially important to the development of new interference cancellation present in chapter 6.

As demonstrated above, the intermodulation products (resulting from a two-tones excitation) that fall within the frequency band of the fundamental tones will strongly increasing with the raise of input signal power. However, this relationship is not always linear, or in other words, the intermodulation products power not always increase 3 dB with 1 dB increase of input tones (assuming equal amplitude tones).

It is intended of this section to present some relations between power levels of intermodulation products with power levels of the input/output linear system.

Figure 3.4 shows the principal relationships between the fundamental components (P_S) and 3rd order intermodulation products (P_{IMD}) [36].

The first observation from figure 3.4 is that there are two distinct operation zones on the system: a weak signal area where P_{IMD} has a linear behaviour and a strong signal area where the P_{IMD} has response anything less linear. In the weak signal area, P_{IMD} has a linear increase of 3 dB per 1 dB increase in input signal and P_S (power from fundamental tones) has also a linear behaviour (the AM-AM and cross-modulation distortion are not yet significant due the low a_3 coefficient and input power).

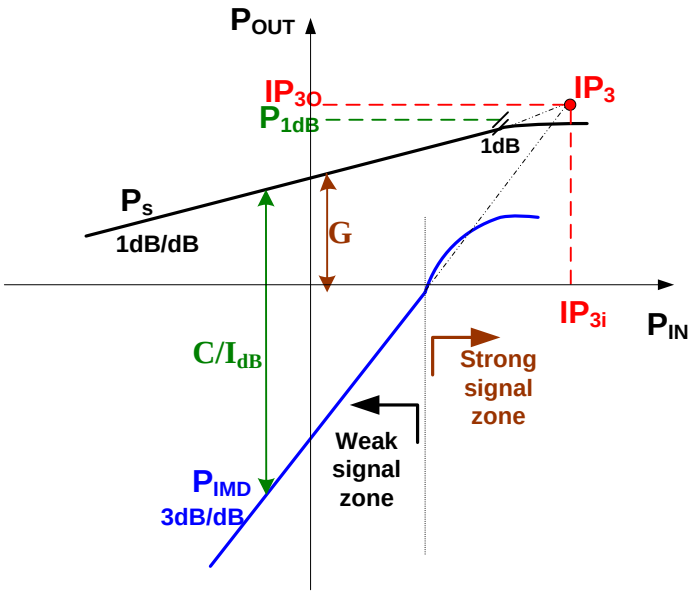

Fig. 3.4 - Relationship between power output and power intermodulation with the input power.

For this zone, using equation 3.31, P_S and P_{IMD} can be calculated by:

$$P_S = G \times P_{IN} \tag{3.34}$$

$$P_{IMD} = P_{IMD_0} + 3 \times (P_{IN} - P_{IN_0}) \tag{3.35}$$

where P_{IN0} and P_{IMD0} are, respectively, the initial input power and initial intermodulation power of the system, reflected by the third component of equation 3.31.

In the strong signal area, the system behaviour is completely different. The P_S starts to be reduced by AM/AM and cross-modulation nonlinear products, leading to compression of the system. As mention before, one important value in this region is the 1dB compression point, that reflects 1dB difference between the real P_S and the fundamental power if only a linear response is considered.

In this region another important value is the 3rd order intercept point (IP3). This fictitious point marks the intersection point from the two linear lines P_S and P_{IMD} from weak signal area. From equations 3.28 and 3.33 and using equal amplitude for both input tones (b_1=b_2=b), then:

$$\frac{1}{2} b_1^2 a_1^2 = \frac{9}{32} a_3^2 b_1^4 b_2^2 \Leftrightarrow \frac{1}{2} b^2 a_1^2 = \frac{9}{32} a_3^2 b^6 \Leftrightarrow b^2 = \frac{4}{3} \frac{a_1}{a_3} \tag{3.36}$$

Thus, substituting the b_1^2 in $P_s(\omega_1)$, then the IP3 point is given by:

$$IP_3 = P_s(\omega_1) = \frac{2}{3}\frac{a_1^3}{a_3} \tag{3.37}$$

This extrapolation is very important because knowing the system's IP3 point we can quickly calculate the signal/jammer for a given power level of the output signal using equation 3.38.

$$C/I\Big|_{dB} = P_{S_{dB}} - P_{IMD_{dB}} = IMR_{dB} = 2\left(IP_3 - P_{S_{dB}}\right) \tag{3.38}$$

or

$$IP_{3_{dB}} = P_{S_{dB}} + \frac{1}{2}IMR_{dB} \tag{3.39}$$

where $P_{S_{dB}}$ is the fundamental output power per tone (in dB units) at which IMR_{dB} was measured. It should be stated that this is only valid for the weak region.

In the strong signal zone the intermodulation products clearly abandon the linear behaviour because other orders bigger then 3rd start to have significant influence on the intermodulation power [36][41].

3.3.4 - Global analyses

To resume all the information presented in this chapter, Table 3.1 summarized all products generated by a nonlinear system with behaviour approach to a Taylor series trunked to 3rd order, when excited by an input signal with two-tones.

As a conclusion, the nonlinear response to a two-tones input signal shows the creation of several spectral components that did not exist in the original signal and a degradation of output signal both in amplitude and in phase. The third order nonlinear products (and higher odd orders) are the main sources of signal degradation within the band of fundamental frequencies. Despite that, the even-order products are also relevant in a system, because not only can affect performance at baseband, but also contribute to changing the bias point of the system. These products can also be used to quick transitions from RF frequencies to baseband domain.

	Vector				Frequency component	Output Amplitude	Response Type
	m_{-2}	m_{-1}	m_1	m_2			
Linear	1	0	0	0	$-\omega_2$	$\frac{1}{2}a_1b_2$	Linear
	0	1	0	0	$-\omega_1$	$\frac{1}{2}a_1b_1$	
	0	0	1	0	ω_1	$\frac{1}{2}a_1b_1$	
	0	0	0	1	ω_2	$\frac{1}{2}a_1b_2$	
2ª order	2	0	0	0	$-2\omega_2$	$\frac{1}{4}a_2b_2^2$	2nd order Harmonic Distortion
	0	2	0	0	$-2\omega_1$	$\frac{1}{4}a_2b_1^2$	
	0	0	2	0	$2\omega_1$	$\frac{1}{4}a_2b_1^2$	
	0	0	0	2	ω_2	$\frac{1}{4}a_2b_2^2$	
	1	1	0	0	$-\omega_2-\omega_1$	$\frac{1}{2}a_2b_1b_2$	2nd order intermodulation distortion
	1	0	1	0	$-\omega_2+\omega_1$	$\frac{1}{2}a_2b_1b_2$	
	0	1	0	1	$-\omega_1+\omega_2$	$\frac{1}{2}a_2b_1b_2$	
	0	0	1	1	$\omega_1+\omega_2$	$\frac{1}{2}a_2b_1b_2$	
	0	1	1	0	$-\omega_1+\omega_1$	$\frac{1}{2}a_2b_1^2$	Change of bias popup
	1	0	0	1	$-\omega_2+\omega_2$	$\frac{1}{2}a_2b_2^2$	
3ª order	3	0	0	0	$-3\omega_2$	$\frac{1}{8}a_3b_2^3$	3rd order Harmonic Distortion
	0	3	0	0	$-3\omega_1$	$\frac{1}{8}a_3b_1^3$	
	0	0	3	0	$3\omega_1$	$\frac{1}{8}a_3b_1^3$	
	0	0	0	3	$3\omega_2$	$\frac{1}{8}a_3b_2^3$	
	2	1	0	0	$-2\omega_2-\omega_1$	$\frac{3}{8}a_3b_1b_2^2$	3rd order Intermodulation distortion
	1	2	0	0	$-\omega_2-2\omega_1$	$\frac{3}{8}a_3b_1^2b_2$	
	2	0	1	0	$-2\omega_2+\omega_1$	$\frac{3}{8}a_3b_1b_2^2$	
	0	2	0	1	$2\omega_1+\omega_2$	$\frac{3}{8}a_3b_1^2b_2$	
	1	0	2	0	$-\omega_2+2\omega_1$	$\frac{3}{8}a_3b_1^2b_2$	

	0	1	0	2	$-\omega_1+2\omega_2$	$\frac{3}{8}a_3b_1b_2^2$	
	0	0	2	1	$2\omega_1+\omega_2$	$\frac{3}{8}a_3b_1^2b_2$	
	0	0	1	2	$\omega_1+2\omega_2$	$\frac{3}{8}a_3b_1b_2^2$	
	2	0	0	1	$-2\omega_2+\omega_2$	$\frac{3}{8}a_3b_2^3$	AM/AM e AM/PM conversion
	0	2	1	0	$-2\omega_1+\omega_1$	$\frac{3}{8}a_3b_1^3$	
	0	1	2	0	$-\omega_1+2\omega_1$	$\frac{3}{8}a_3b_1^3$	
	1	0	0	2	$-\omega_2+2\omega_2$	$\frac{3}{8}a_3b_2^3$	
	1	1	1	0	$-\omega_2-\omega_1+\omega_1$	$\frac{3}{4}a_3b_1^2b_2$	Desentization and croos-modulation
	1	1	0	1	$-\omega_2-\omega_1+\omega_2$	$\frac{3}{4}a_3b_1b_2^2$	
	1	0	1	1	$-\omega_2+\omega_1+\omega_2$	$\frac{3}{4}a_3b_1b_2^2$	
	0	1	1	1	$-\omega_1+\omega_1+\omega_2$	$\frac{3}{4}a_3b_1^2b_2$	

Table 3.1 - Summary table of the response of a nonlinear system truncated to the 3rd order

The use of a 3rd order approximation clearly serves the purpose of identifying all products resulting from the nonlinear system response. Normally this is a sufficient/good approximation for the analysis of nonlinear systems, especially when in presence of weak input signals. However, in some real scenarios, this approach becomes insufficient and does not accurately reflect the behaviour of the system to study. As will be seen in subsequent chapters, it is sometimes necessary to use higher order (4th and 5th order) to get better and reliable results approximations to real measurements.

3.4 – Nonlinear method analyzes for small-signal excitation

During the doctoral program, one of the main objectives was the study and modelling of nonlinear behaviour of radio-frequency systems, especially in the RF receiver. As these systems work in most cases with small input signals, it is desirable to finish this chapter with a short presentation of the main methods of analysis of nonlinear systems when excited by small signals.

There are two major methods to analyze nonlinear circuits under small-signal excitation: the Current method and the Harmonic Input method. Both methods are based on the

Taylor/Volterra series, but while the Current method seeks to use currents sources to modulate nonlinear circuits elements, the Harmonic Input method prefers the frequency domain representation of the Volterra kernels, because it's more appropriated for the analysis and design of RF and microwave circuits [2][42].

In this sub-chapter will be show a simple explanation of each method giving preference to the method of Harmonic Input, since this is the method used in chapter 5.

3.4.1 – Nonlinear Currents Method

The nonlinear Currents method is an approaching process to achieve a solution in time domain. In this method, each nonlinear circuit element is modulated as a linear element that is in parallel with a set of current sources. Each current source represents a unique order (greater than 1) of the mixing products, and its current is a nonlinear function of the node-voltage components at lower-order mixing frequencies. The weakly nonlinear circuit is reduced to a linear circuit, one that contains the linear elements and the linear parts of the nonlinear elements, as well as a set of excitation sources [42][43].

As expected, the first-order response is simply the response of the linear circuit. Although for second order mixing frequencies is used the first-order node voltage to achieved an acceptable solution. To demonstrate this method let use a simple voltage-controlled conductance having the small-signal I/V characteristic, based in Volterra series and given by expression 3.40:

$$i(t) = g_1 v(t) + g_2 v^2(t) + g_3 v^3(t) + \ldots \tag{3.40}$$

The first-order terminal voltage is given by:

$$v_1(t) = \frac{1}{2} \times \sum_{n=-Q}^{Q} V_{s,n} e^{i\omega_n t} \tag{3.41}$$

And second-order current is:

$$i_2(t) = g_2 v_1^2(t) = \frac{g_2}{4} \sum_{n1=-Q}^{Q} \sum_{n2=-Q}^{Q} V_{1,n1} V_{1,n2} e^{j(\omega_{n1}+\omega_{n2})t} \tag{3.42}$$

In the case of a capacitor having the charge/voltage characteristic

$$q(t) = C_1 v(t) + C_2 v^2(t) + C_3 v^3(t) + \ldots$$

The second-order current $i_2(t)$ is then:

$$i_2(t) = C_2 \frac{d\left(v_1^2(t)\right)}{dt} = \frac{C_2}{4} \sum_{n1=-Q}^{Q} \sum_{n2=-Q}^{Q} j\left(\omega_{n1} + \omega_{n2}\right) \times V_{1,n1} V_{1,n2} e^{j(\omega_{n1}+\omega_{n2})t} \tag{3.43}$$

One can find the second-order node voltages by solving the linear network's admittance equations with the second-order sources used as excitations. The process is repeated to find the third- and higher-order node voltages.

For Stephen Maas [42], great authority in nonlinear theory, "*… is considerably more efficient than generalized harmonic-balance analysis, because it requires neither Fourier transformation nor iteration: when the nonlinear-current method is used, the source currents are found directly in the frequency domain.*"

3.4.2 – Harmonic Input Method

Although the Current method has some good applications and used in certain types of circuits, the Harmonic Input method is the most known and used analyzes for simulation of nonlinear system behaviour.

This method, also known as probing method, is used to achieved the nonlinear transfer function in frequency-domain H(ω) and is a generalization of the linear system harmonic input with a cosine or exponential excitation.

As know, all systems obey to equation 3.44 in time domain or 3.45 in frequency domain.

$$y(t) = h(t) * x(t) = \int_{-\infty}^{\infty} h(\tau) \times x(t-\tau) d\tau \tag{3.44}$$

$$Y(\omega) = H(\omega) \times X(\omega) \Rightarrow H(\omega) = \frac{Y(\omega)}{X(\omega)} \tag{3.45}$$

In linear systems, the $H(\omega)$ transfer function is easily determine using a input exponential voltage $1.exp(j\omega t)$ and transform the output signal as $H(\omega).exp(j\omega t)$. The ratio between the two signal gives us the linear transfer function $H(\omega)$ [2][36][43].

The calculation from the transfer function of a nonlinear circuit is a process very similar to the linear response but, as expected, more complicated and has to obey to certain assumptions. For instance, to determine the second-order transfer function it will be

necessary two independent frequencies in the bi-dimensional Fourier Transform. For that reason, the input excitation signal must be:

$$x(t) = e^{j(\omega_1 t)} + e^{j(\omega_2 t)} \tag{3.46}$$

Using equation 3.46 and knowing that we must perform two times the Fourier transform (because this is a bi-dimensional transform through the independence of the terms), the resultant second order response will be:

$$y_{o2}(t) = \int_{-\infty}^{\infty}\int_{-\infty}^{\infty} h_2(\tau_1,\tau_2)\times\left(e^{j\omega_1(t-\tau_1)} + e^{j\omega_2(t-\tau_1)}\right)\times\left(e^{j\omega_1(t-\tau_2)} + e^{j\omega_2(t-\tau_2)}\right)d\tau_1 d\tau_2 \tag{3.47}$$

Since $h_2(\tau_1, \tau_2)$ and $H_2(\omega_1, \omega_2)$ are symmetric in their arguments, the previous equation can be simplified to:

$$\begin{aligned} y_{o2}(t) = {} & e^{j2\omega_1 t}\int_{-\infty}^{\infty}\int_{-\infty}^{\infty} h_2(\tau_1,\tau_2)\times e^{-j\omega_1(\tau_1+\tau_2)}d\tau_1 d\tau_2 \\ & + 2.e^{j(\omega_1+\tau_2)t}\int_{-\infty}^{\infty}\int_{-\infty}^{\infty} h_2(\tau_1,\tau_2)\times e^{-j(\omega_1\tau_1+\omega_2\tau_2)}d\tau_1 d\tau_2 \\ & + e^{j2\omega_2 t}\int_{-\infty}^{\infty}\int_{-\infty}^{\infty} h_2(\tau_1,\tau_2)\times e^{-j\omega_2(\tau_1+\tau_2)}d\tau_1 d\tau_2 \end{aligned} \tag{3.48}$$

$$y_{o2}(t) = H_2(\omega_1,\omega_2)\times e^{j2\omega_1 t} + 2H_2(\omega_1,\omega_2)\times e^{j(\omega_1+\omega_2)t} + H_2(\omega_1,\omega_2)\times e^{j2\omega_2 t} \tag{3.49}$$

which shows that the second-order nonlinear transfer function can be calculated by dividing the output component at the sum frequency by $2.e^{j(\omega_1+\omega_2)t}$.

In order to find the nth-order part of the response, the excitation signal must be:

$$x_i(t) = \sum_{n=1}^{n} e^{j(\omega_n t)} \tag{3.50}$$

Using equations 3.48 and 3.49, the nth-order output response will be:

$$y_{on}(t) = n!H_n(\omega_1,\ldots,\omega_n)\times e^{j(\omega_1,\ldots,\omega_n)t} \tag{3.51}$$

The Harmonic Input method will be used and explorer in detail on chapter 5, where will be needed to demonstrate theoretically the dependence of measure results from output impedance in a power meter (based on Schocty diodes).

3.5 – Conclusions

The nonlinear phenomenon is present in almost all communication systems because they are few electronic elements that have a purely linear behaviour. The most used tools to mathematically characterize the nonlinear behaviour are the Taylor's or Volterra's series, if the system in analyses doesn't have a very strong nonlinear behaviour. With these series is possible to identify the various types of nonlinear products generated, their places in the spectrum frequency and the influences on the performance of the RF system. As shown, the nonlinear response modelled by Taylor's series presents new spectral components at DC and baseband frequencies, several new intermodulation products that fall within the frequency band of operating system and several harmonics in multiples of the fundamental frequency. Intermodulation distortion, AM-PM and cross-modulation are the major problems inside fundamental band, the harmonic products can create interferences in neighbour systems and DC (and/or baseband) products could be use in direct conversion of the signal but also can change the bios point of the receiver circuit. In systems without own battery (like passive tags) the RF→DC conversion also allows the energization of the system (the Tag harvest their own energy from the RF signal emitted by the Reader).

There are two major methods to make a nonlinear analyze for small-signal excitation: Current method and Harmonic Input method. In the Current method each nonlinear circuit element is modulated as a linear element that is in parallel with a set of current sources and is calculated a solution for witch node of iteration. In Harmonic Input method the goal is to achieve the nonlinear transfer function in frequency-domain $H(\omega)$. The calculation from the transfer function of a nonlinear circuit is a process very similar to the linear response but, to determine the n-order transfer function it will be necessary n independent frequencies in the n-dimensional Fourier Transform.

As final conclusion, this chapter presents the main theory of nonlinear phenomena in radio frequency communications, main influences and consequences for the proper functioning of systems as essential basis for the following chapters.

CHAPTER 4

DC and Baseband nonlinear distortion generation.

Finish in last chapter the presentation from all major nonlinear products that traditional affects good reliability of RF receivers, it's time to embrace one of the biggest challenges in the study of nonlinear phenomena (beyond their understanding): the constant call to develop new mathematical models able to parameterize and simulate all the output response from a nonlinear RF entire system or a single electronic component.

This need is also intrinsically linked to the development of new technologies and, above all, require that the models are reliable and achieve results identical (or near as possible) to the real response of the nonlinear device. Furthermore these models should be wide open and universal, having a greater scope as possible and easily customizable with adjustable factors for each configuration and/or type of system under test. These models are very important for example in the development and test of new technologies, allowing premier simulations to prediction of results and evaluate the impact of these systems in real implementations, which can prevent many hours/man in the field tests.

As already mentioned several times throughout this thesis, one of the main objectives of the work developed during the doctoral program was to study and explore the nonlinear generation of products that enable the direct conversion of an RF signal to baseband (or DC). This technique is the operating principle in simple systems like envelope detectors or power meters. Although, in present days the simplicity of this type of conversion makes this configuration very attractive for systems that has a very low energy consumption like SDR architectures and passive (or semi-passive) RFID devices. This technique beyond requiring less energy to down-covert the signal, it also reduce the costs associated to oscillators and mixers present in traditional settings, allowing the size reduction and mass production.

This chapter is thus devoted to the study and analysis of the nonlinear products responsible for this translation in frequency from RF to DC and baseband frequencies.

Several mathematical equations able to predict (with good accuracy) the number of tones and the influence of each tone in the resulting product on base band is also presented.

4.1 – Nonlinear products in base band and DC frequencies

As seen in the previous chapter, one of the models used to parameterize the nonlinear response of a system is the Taylor (or Volterra) series, if the under-test system does not present a strongly nonlinear behaviour (eq. 3.3). As shown this model is a weighted power series in which the weight of each contribution defines nonlinear "degree" of the system under analysis. For the majority of RF components the Taylor series are typical trunked to third order, assuming that a4 and a5 are much smaller than a1, that their weight in final signal is negligible. Some studies even show nonlinear behaviour prediction equations only for the third order [44][45] and specialize books support this assumption.

However, this Taylor's series simplification can cause significant deviations from the real nonlinear response in several devices and cause higher differences in final readings, as will be demonstrated in next chapter. In addition, the largest contributions in the area are mainly focus in the 3rd order in-band products, (or in remote 5th order possibly), summarizing the direct conversion only to products of the 2nd order (the typical x^2 from a diode).

As will be shown in chapter 5, this assumption brings several measurement mistakes in systems based in this conversion like the Power Meter. For all these reasons, if we assume the goal to study the direct-conversion using the nonlinear theory, is important to develop formulas that can predict the contribution of several products that fall at baseband into a nonlinear system, when the system is excited by the simple two-tones test or a more complicated multi-tone signal (able to mimic several typical RF signals).

As noted above, a nonlinear system contributions that fall at baseband (or DC) are the result of even order products like 2nd, 4th, etc... in combinations like $\omega_2 - \omega_1$; $2\omega_2 - 2\omega_1$ as presented in the previous chapter.

If when we have an input two-tones signal we can easily see the number of nonlinear products that will hit a certain baseband tone, for an input multi-tones signal, this contribution is not so intuitive and can even require the use of more complex mathematical formulas that are not present in scientific architecture, especially the fourth

order behaviour, since in the majority of the cases their contribution is erroneously ignored

4.1.1 - Definition of variables and explanation of the model

Over the next sections will be explored and modelled all nonlinear contributions generated in direct-converters when excited with a multisine input signal. The main goal is achieve mathematical formulas than can calculate the amplitude and the number of contributors tones for DC or any baseband tone. Before moving to the presentation of these formulas that enables the calculation from the number of contributions in each tone, it is essential to explain the principle model used to connect number of tones from our multi-tones input signal with baseband bandwidth.

In our model exists three major variables that are intrinsically connected and have the main role in the mathematical analyses. The first parameter (represented by N) is the number of tones from our input signal. The second main parameter is the frequency-separation between tones, currently designated Δ. At this point is important to note that we assuming a well calibrated multisine signal with equidistant tones. With this signal we can represent both simple signals (like the two-tones test) as well more complex signals with larger bandwidths. The last parameter is the position off the tone that we are referring, either in RF either the baseband. This variable is designated by k and assumes the form of ω_k for a RF tone and $k\Delta$ for a baseband tone. This information is summarized in Figure 4.1 to better understanding.

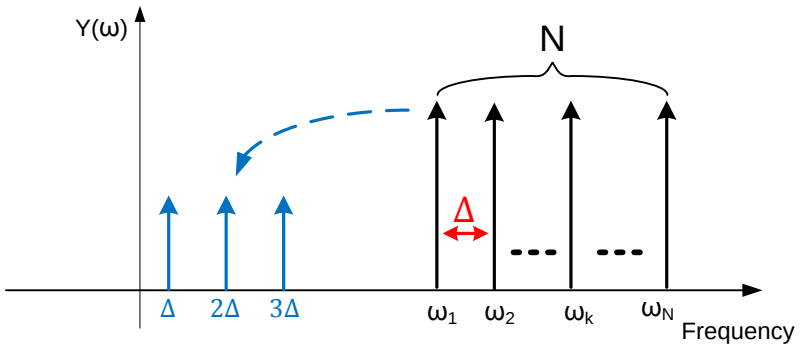

Fig. 4.1 – Model representation from the variables present in equations

For now, we assuming an equal amplitude for all tones and ignore the phase (making him equal to 0) because the goal is knowing the number and the quality from tones that fall at $k\Delta$ and not it's amplitude or phase.

Present the variables that will help in formulation of the equations, it's also important to distinguish the types of tones that will appear in 2nd and 4th order nonlinear response. At this point isn't possible to achieve the formulas by specific tone or baseband product, reason why we group the contributions in different types according to the combination from the tones.

In the second order response is only possible to distinguish two types of contribution: (a-a) and (a-b). The first results the combination from one tone with them self, like $\omega_1 - \omega_1$. The second one represents the combination with two distinct tones like $\omega_3 - \omega_1$ or $\omega_6 - \omega_2$ for example. The first type always falls at DC and the second one at baseband.

As expected, the forth order response is more complex and can generate several different types of products:

- (a-a)+(a-a) – represents the fourth order combination of a single tone like $(\omega_1-\omega_1)+(\omega_1-\omega_1)$.
- (a-a)+(a-b) or (a-a)+(b-a)– represents the three time combination of a single tone with other tone, as $(\omega_1-\omega_1)+(\omega_1-\omega_3)$ or $(\omega_1-\omega_1)+(\omega_3-\omega_1)$.
- (a-a)+(b-b) – represents the combination between two tones after the combination with them self, as $(\omega_1-\omega_1)+(\omega_2-\omega_2)$.
- (a-b)+(a-b) – represents the combination between two different tones, like $(\omega_1-\omega_2)+(\omega_1-\omega_2)$.
- (a-a)+(b-c) – represents the combination between three different tones, such as $(\omega_1-\omega_1)+(\omega_3-\omega_4)$.
- (a-b)+(a-c) or (b-a)+(c-a) – represents the combination of distinct tones with a common tone, such as $(\omega_3-\omega_1)+(\omega_3-\omega_2)$ or $(\omega_3-\omega_1)+(\omega_4-\omega_1)$.
- (a-b)+(c-d) - represents the full intermodulation of four distinct tones, like $(\omega_1-\omega_2)+(\omega_3-\omega_4)$.
- (-a+b)+(b-c) – represents the combination where the "bigger" tone is negative and there is a tone use twice, such as $(-\omega_5+\omega_4)+(\omega_4-\omega_1)$
- (-a+b)+(c-d) – similar to the previous one but with contribution from 4 different tones, as $(-\omega_6+\omega_5)+(\omega_4-\omega_1)$.

This distinction in types of product has a very important role because they allow the creation of different equations for each type of product. To predict the total number of contributions to a particular $k\Delta$ baseband tone only need to combine the result from all

formulas made to each type. Several of this terms could be fuse in one type only but the complexity of the formulas will be such higher that we prefer to use it separately.

From the all possible combinations presented for 4th order response, not all will eligible for DC or baseband nonlinear tone calculation. For instance, for DC only the first, third, sixth and seventh product type will have influence in its nonlinear product, making their calculating more easier than other baseband tone. On the other hand the first and third combination does not enter into the calculation of baseband tones.

As already mention, the specification by tone becomes far more complex and almost impossible to modulate.

4.2 – Equations for calculation DC nonlinear terms

Since the DC and baseband tones don't share the same properties, or in other words, don't be affected for all the same type of combination previous presented, we decide to separate presentation of the formulas to each specific case. Other reason to separate the DC equations from the baseband formulas is because some products have doubled impact at DC, ie, the combination from positive and negative terms result in a double term in DC (example: ω_1-ω_1+ω_1-ω_1 and -ω_1+ω_1-ω_1-ω_1 both fall in DC), that doesn't happen in other baseband tones. This special property prohibits the creation of a single equation (especially for products of 4th order) that characterizes simultaneously the DC and baseband products. The major 4th order nonlinear products through the 8Δ could be view in Appendix D.

Before enter the equations presentation is important to briefly explain the nomenclature used in the formulas. All formulas will be identify by:

$Nt(k\Delta)_{(a-a)} \rightarrow$ number of 2nd order terms from (a-a) type that will be present at $k\Delta$ frequency.

$Nt(k\Delta)_{(a-a)+(b-b)} \rightarrow$ number of 4th order terms from (a-a)+(b-b) type that will be present at $k\Delta$ frequency.

Other uncommon symbols present in equations are:

$\lceil x \rceil \rightarrow$ represents the next biggest integer near x (ex: $\lceil 2.4 \rceil = 3$)

$\lfloor x \rfloor \rightarrow$ represents the next lower integer near x (ex: $\lfloor 2.4 \rfloor = 2$)

$rest(k,x) \rightarrow$ represents the rest of the division from k with x (ex: $rest(5,2)=1$)

All other symbols are wide known.

4.2.1 - Second order terms

As refer in the beginning of the chapter, the equations to determine the number of tones of second order is easy to achieve. At DC, only the (a-a) combination contributes to the nonlinear product generated, making the number of contributions equal to the number of tones of the input signal. So, in the presence of a N-tone input signal, will be N contributions to DC nonlinear product

$$Nt(0)_{(a-a)} = N \tag{4.1}$$

These terms depend only from one single tone and have a weight contribution of $A^2/2$ has will be seen in section 4.2.3.

4.2.2 - Fourth order terms

As expected the mathematical equations for forth order response are more complex and with higher restrictions than previous one. In 4th order response, as already mentioned, there are four nonlinear contributors: (a-a)+(a-a); (a-a)+(b-b); (a-b)+(a-c); (a-b)+(c-d).

The (a-a)+(a-a) term is the most simple one since its equation that represents the number of terms at DC is simple as previous one:

$$Nt(0)_{(a-a)+(a-a)} = N \tag{4.2}$$

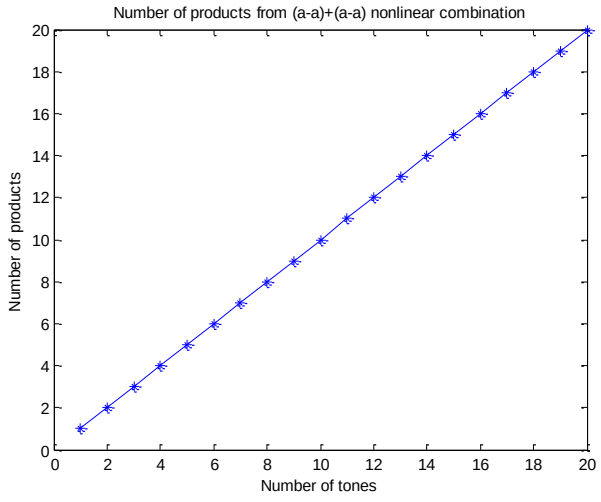

Fig. 4.2 – Number of DC products from (a+a) and (a-a)+(a-a) nonlinear terms

To note this nonlinear term always appears even if the signal is a single sinusoid (like second order term). The behaviour of these two equations is obvious linear (figure 4.2).
From this point, the equations that represent the nonlinear term contribution obviously started to become more complex and extensive, since they always depend from more than one tone. For example, in products such (a-a)+(b-b), the number of tones in DC is given by:

$$Nt(0)_{(a-a)+(b-b)} = 2 \times \sum_{i=1}^{N} (i-1) \Leftarrow N \geq 2 \tag{4.3}$$

Unlike the previous formulas, this equation is already formed by a sum, which gives it a completely nonlinear characteristic with the increase number of tones in the input signal (much different from eq. 4.1 and 4.2), as can be seen in Figure 4.3.

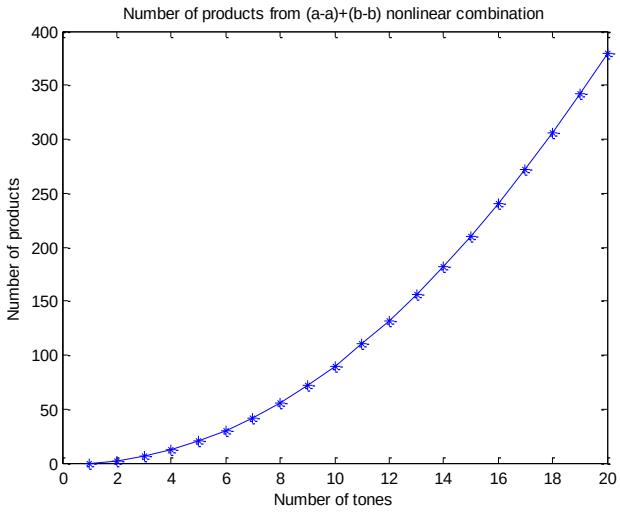

Fig. 4.3 – Number of DC products from (a-a)+(b-b) nonlinear combination

The next 4th order term that contributes to DC nonlinear product is (a-b)+(a-c) . At first impression, these terms not seem to influence the DC. However, combinations like $(\omega_2-\omega_3)+(\omega_2-\omega_1)$ enters in this "non-evident" group and have direct influence in nonlinear DC contribution. With few differences to the previous formula, the equation that reflects the (a-b)+(b-c) contribution is:

$$Nt(0)_{(a-b)+(a-c)} = 2 \times \sum_{i=3}^{N} \left\lceil \frac{(i-2)}{2} \right\rceil \Leftarrow N \geq 3 \tag{4.4}$$

As can be seen from eq. 4.4 and shown in figure 4.4, this nonlinear contribution would only appear if the input signal has at least three tones. In a typical two-tones test, this kind of product would not appear.

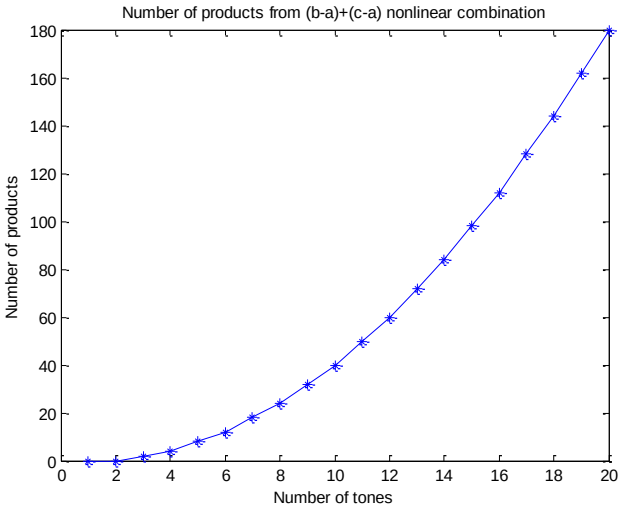

Fig. 4.4 – Number of DC products from (a-b)+(a-c) nonlinear combination

The last forth order product that falls at DC depends from four different nonlinear products. The equation that predicts the number of tones is:

$$Nt(0)_{(a-b)+(c-d)} = 2\times\sum_{i=4}^{N}\left(\left\lfloor\frac{(i-2)}{2}\right\rfloor+\sum_{j=4}^{i-1}\left\lfloor\frac{(j-2)}{2}\right\rfloor\right) \Leftarrow N \geq 4 \qquad (4.5)$$

As expect this is the most complex equation in nonlinear DC calculation and start to show an interesting recursion property. In other words, to calculate the number of terms that arise from a N-tones input signal, we need to calculate all contributions from since 4-tones to (N-1)-tones, since we have a sum function inside other sum function. Although its graphic seems to be similar to the previous ones, if we carefully look to the number of nonlinear tones generated, we realize an exponential increase of them. For that reason, with the N increase, this term becomes the most important four order product in DC frequency.

All presented equations able to predict the number of tones that fall at DC frequency, independent the number of tones from the input multisine. With these formulas, would be simple to determinate the nonlinear response from a power meter or similar RF→DC converter.

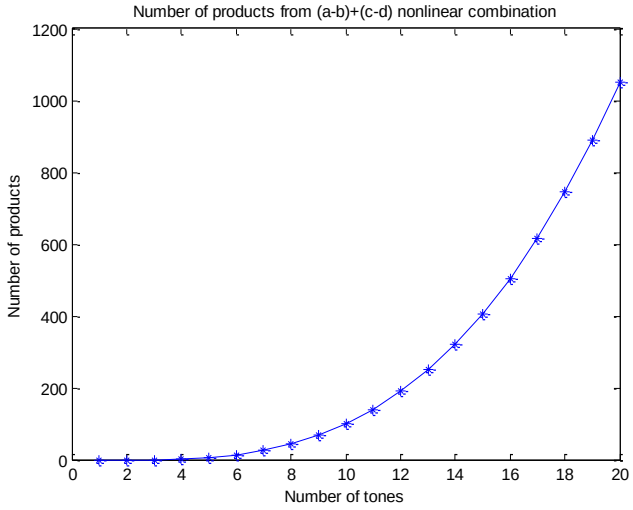

Fig. 4.5 – Number of DC products from (a-b)+(c-d) nonlinear combination

4.2.3 - Amplitude value from each term

Before proceeding to the practical application of the formulas presented it is imperative to point out another important issue that we only achieve after several iterations and many comparisons between the formula's results and actual values. We already suspect that the several types of terms presented wouldn't have the same impact because this was already present in equations 3.9 and 3.24 from last chapter. Although we don't known the impact of each type of term and if is constant for all terms of the same type.

After an extensive battery of tests and several analyses between formula's results and real values, we could understand that the weight of each term doesn't change inside the type but is different between the four types of term defined. The results are present in Table 4.1.

This different contribution from terms is the "mirror" from the way that we separate the tones, because we only distinguish the different type of combinations and never the number of times that they appear in the calculation. Moreover some of the tones, through the development from the series, seem to have a greater importance (appears more than one time) in the DC calculation. For example, we only count one time the ω5-ω4+ω3-ω2 combination in (a-b)+(c-d), but it could appear more than one time in DC nonlinear prediction. For this reason the contribution of each type are different and the final weight seems to increase with increasing diversity of the tones in the term, that is, terms with more different tones has a higher contribution.

Type of DC term	Weight in DC calculation
(a-a)	$\frac{A^2}{2}$
(a-a)+(a-a)	$\frac{3}{8}A^4$
(a-a)+(b-b)	$\frac{3}{4}A^4$
(a-b)+(a-c)	$\frac{3}{4}A^4$
(a-b)+(c-d)	$\frac{3}{2}A^4$

Table 4.1 – Amplitude contribution for DC nonlinear product

4.2.4 - Application example

At this point, it will be useful to make a small practical calculation to prove the utility and reliability from the presented formulas and weight terms.

Assuming an input five-tones signal, where all tones have the same amplitude A, no phase deviation and Δ (ω_k-ω_{k-1}) is much smaller than any ω_k, the input signal is given by:

$$x(t)=\sum_{l=1}^{5}A_l\cos(\omega_l t+\phi)=A\times\sum_{l=1}^{5}\cos(\omega_l t) \tag{4.6}$$

Using the Taylor's series (eq. 3.2), the 2nd and 4th order products will be given by:

$$\begin{aligned} c_2x^2(t)&=c_2A^2\times\left(\sum_{l=1}^{5}\cos(\omega_l t)\right)^2 \\ c_4x^4(t)&=c_4A^4\times\left(\sum_{l=1}^{5}\cos(\omega_l t)\right)^4 \end{aligned} \tag{4.7}$$

Using the formulas from 4.1 to 4.5, the number of tones that fall at DC will be:

$$Nt(0)_{(a\text{-}a)}=5 \tag{4.8}$$

$$Nt(0)_{(a\text{-}a)+(a\text{-}a)}=5 \tag{4.9}$$

$$\mathrm{Nt}(0)_{(a-a)+(b-b)} = 2\times\sum_{i=2}^{5}(i-1)=2\times(1+2+3+4)=20 \tag{4.10}$$

$$\mathrm{Nt}(0)_{(b-a)+(c-b)} = 2\times\sum_{i=3}^{5}\left\lceil\frac{(i-2)}{2}\right\rceil=2\times(1+1+2)=8 \tag{4.11}$$

$$\mathrm{Nt}(0)_{(a-b)+(c-d)} = 2\times\sum_{i=4}^{5}\left(\left\lceil\frac{(i-2)}{2}\right\rceil+\sum_{j=4}^{i-1}\left\lceil\frac{(j-2)}{2}\right\rceil\right)=2\times(2+1)=6 \tag{4.12}$$

That results in a total number of 5 second order terms and 29 fourth order terms (5+10+8+6). Combining these terms with their respective weights, the output DC products will be given by:

$$\begin{aligned} y_{DC}(t) &= c_2\times 5\times\frac{A^2}{2}+c_4\times\left(5\times\frac{3}{8}A^4+20\times\frac{6}{8}A^4+8\times\frac{6}{8}A^4+6\times\frac{12}{8}A^4\right) \\ &= c_2\times\frac{5}{2}\times A^2+c_4\times\frac{237}{8}\times A^4 \end{aligned} \tag{4.13}$$

This simple example shows the utility of the presented equations for estimation of nonlinear DC voltage when we have an input RF signal. If we desire a way to understand the influence from a signal in the DC Bias point from the system, these formulas could be a reasonable and quick tool to achieve the contribution value without using complex and lengthy simulation methods. As will be seen in next sections, this method allows the computation of several results from a huge number of input tones in a very small time.

4.3 - Equations for calculation the number of tones at baseband

Finish the presentation of DC equations is time to move to the study of the baseband formulas. One of the requirements that make these equations more complex and extensive than previous DC is the fact that they have to be generic, i.e., they must be capable of determinate the number of 2nd and 4th order terms for any $k\Delta$ (baseband tone) for any N (number of input tones). As expected the complexity will increase greatly with the raise of N and the formulas start to depend from k also.

Assuming only the 2nd and 4th order response we also can say that the maximum baseband tone generated will be at frequency $(\omega_N - \omega_1)+(\omega_N - \omega_1)\Delta$, or, from the separation point of view, k couldn't be greater than $2(N-1)$.

4.3.1 - Second order terms

As occurs in section 4.2.1, the equation that represents the number of second order products that fall in a generic $k\Delta$ is very simple and intuitive (note that all terms are from type (a-b) now):

$$Nt(k\Delta)_{(a-b)} = N - k \Leftarrow N \geq k; \tag{4.14}$$

From eq. 4.14 it's easy to realize that if we have a input signal with N tones, the maximum 2nd order baseband term will be k=N-1, in other words, the maximum 2nd order tone at baseband will be (N-1)Δ.

4.3.2 - Fourth order terms

Like in the previous section, the equation that represents the fourth order (a-a)+(a-b) that fall in a generic $k\Delta$ is simple as:

$$Nt(k\Delta)_{(a-a)+(a-b)} = N - k \Leftarrow N \geq 2 \ \wedge \ N \geq k; \tag{4.15}$$

As expected, the equation that represents the fourth order (a-a)+(b-a) terms is identical to the previous one:

$$Nt(k\Delta)_{(a-a)+(b-a)} = N - k \Leftarrow N \geq 2 \ \wedge \ N \geq k; \tag{4.16}$$

These two products can be seen as complementary and could be represented together. However in a way to achieve better comprehension and avoid certain confusion it was decided to present them separately.

The figure 4.6 represents a 3-D graphic with the evolution from the number of products at baseband frequency $k\Delta$ as function the number of input tones N and k. The graphic is similar for both terms. The function has a linear behaviour and they have no null terms since the two-tone input signal.

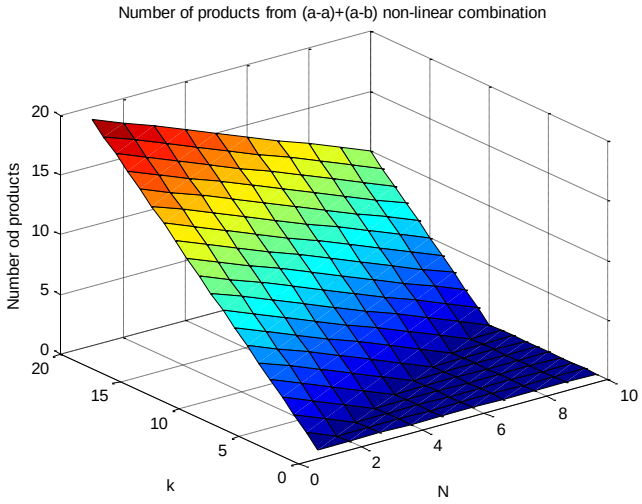

Fig. 4.6 – Number of nonlinear products from (a-a)+(a-b) and (a-a)+(b-a) in kΔ tone

The next 4th order nonlinear terms results from the contribution of three different tones, (a-a)+(b-c). For this specific product, the equation that represents the number of tones in a generic $k\Delta$ isn't yet true complex, although definitely abandon the linear behaviour from their predecessors. The equation is given by:

$$Nt(k\Delta)_{(a-a)+(b-c)} = \sum_{i=(k+1)}^{N} (2i-k-3) \Leftarrow N \geq (k+1); \tag{4.17}$$

Another characteristic noted on equation 4.16 is that this term only arise at baseband tones one or more times lower (in coefficient) than the number of input tones. For instance if you have a 5-tones input signal, this term will never be present over k=4. The eq. 4.17 behaviour is represented in Figure 4.7.

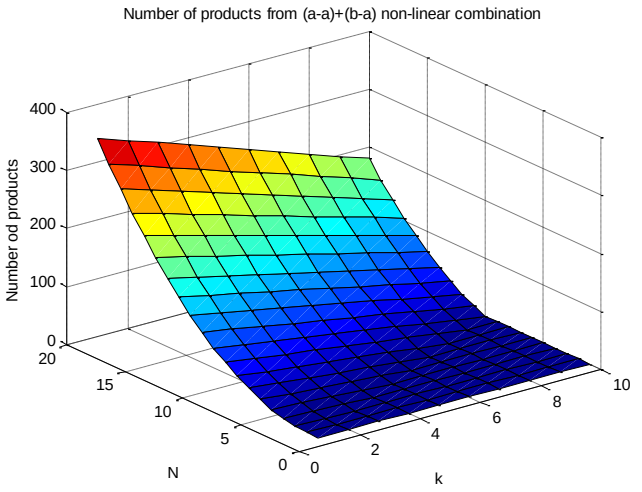

Fig. 4.7 – Number of nonlinear products from (a-a)+(b-c) in kΔ tone

The next term is the only one that will be conditioned by *k* parity. This special term is the (a-b)+(a-b) combination and is exclusive from even baseband tones since the sum of two equal differences will always give a even result (ex: $(\omega_2-\omega_1+\omega_2-\omega_1 = \Delta + \Delta = 2\Delta)$. The compensation from odd tones is done in the next equations. The (a-b)+(a-b) equation is given by:

$$Nt(k\Delta)_{(a-b)+(a-b)} = N - \frac{k}{2} \Leftarrow N \geq (k+1) \wedge k \text{ is Even} \tag{4.18}$$

The figure 4.18 is very clearly that only even tones have a non-zero contribution from (a-b)+(a-b) terms. For all odd *k* the results are null.

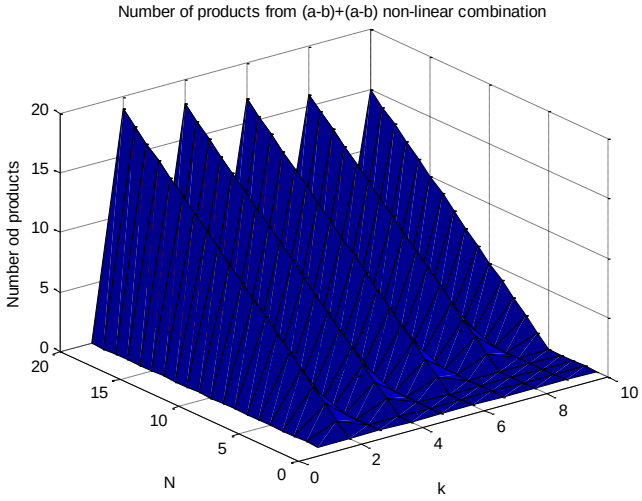

Fig. 4.8 – Number of nonlinear products from (a-b)+(a-b) in kΔ tone

Although the (a-b)+(a-c) term seems similar to the previous (a-b)+(a-b), they presents a completely different behaviour and don't have the parity restriction. This term starts a new level of complexity in the equations that characterize the number of fourth order terms in a particular *k*Δ tone. The formulas abandon the single equation, become more and more complex, with several restrictions interconnected. To this specific nonlinear product (a-b)+(a-b), the number of tones will be give by a system with two equations:

$$Nt(k\Delta)_{(a-b)+(a-c)} = \begin{cases} \sum_{i=\left\lfloor \frac{k+4}{2} \right\rfloor}^{N} i - \left\lfloor \frac{k+2}{2} \right\rfloor \Leftarrow N < k \wedge \left\lfloor \frac{k+4}{2} \right\rfloor > 0 \\ \sum_{i=\left\lfloor \frac{k+4}{2} \right\rfloor}^{k-1} \left(i - \left\lfloor \frac{k+2}{2} \right\rfloor \right) + \left\lfloor \frac{k-1}{2} \right\rfloor \times \left(N - (k-1) \right) \Leftarrow N \geq k \end{cases} \tag{4.19}$$

It's possible to see that some of the odd products that not fall in the last product category are there present. This effect is perceptible in Figure 4.9, where the "stair" effect seems to be lightly reduced when we pass from a even tone to a odd tone.

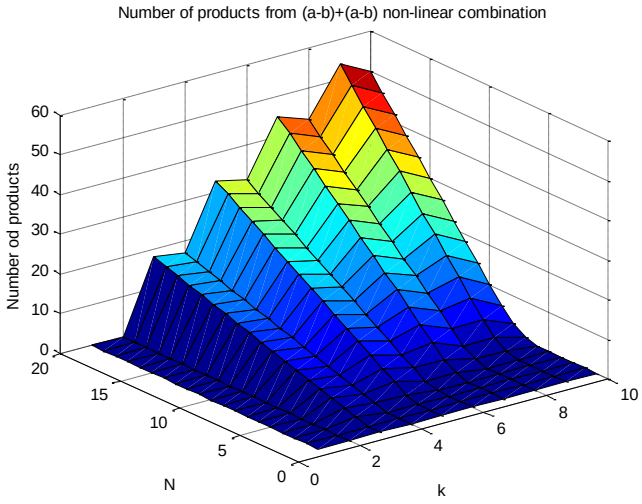

Fig. 4.9 – Number of nonlinear products from (a-b)+(a-c) in kΔ tone

We enter now in main difficulty of this prediction method. The next two nonlinear combinations are the more complex and with more restrictions from all formulas. The first example is the (b-a)+(c-a) forth order product that depends from 3 distinct tones and the number of terms that contributes to $k\Delta$ is given by a system with 6 equation:

$$Nt(k\Delta)_{(b-a)+(b-c)} = \begin{cases} \sum_{i=k+3}^{N}\left\lfloor \frac{i-(k+1)}{2}\right\rfloor + \left\lfloor \frac{k-1}{2}\right\rfloor \Leftarrow 1\le k\le 2 \wedge N\ge k+3 \\ \sum_{l=k}^{N}\left\lfloor \frac{k-1}{2}\right\rfloor \Leftarrow 3\le k\le 4 \wedge 3\le N\le k+2 \\ \sum_{l=k}^{k+2}\left\lfloor \frac{k-1}{2}\right\rfloor + \sum_{i=k+3}^{N}\left\lfloor \frac{i-(k+1)}{2}\right\rfloor + \left\lfloor \frac{k-1}{2}\right\rfloor \Leftarrow 3\le k\le 4 \wedge N\ge k+3 \\ \sum_{j=\left\lceil \frac{k+3}{2}\right\rceil}^{N}\left(j-\left\lceil \frac{k+1}{2}\right\rceil\right) \Leftarrow k\ge 5 \wedge \left\lceil \frac{k+3}{2}\right\rceil \le N\le k-1 \\ \sum_{j=\left\lceil \frac{k+3}{2}\right\rceil}^{k-1}\left(j-\left\lceil \frac{k+1}{2}\right\rceil\right) + \sum_{l=k}^{N}\left\lfloor \frac{k-1}{2}\right\rfloor \Leftarrow k\ge 5 \wedge k\le N\le k+2 \\ \sum_{j=\left\lceil \frac{k+3}{2}\right\rceil}^{k-1}\left(j-\left\lceil \frac{k+1}{2}\right\rceil\right) + \sum_{l=k}^{N}\left\lfloor \frac{k-1}{2}\right\rfloor + \sum_{i=k+3}^{N}\left\lfloor \frac{i-(k+1)}{2}\right\rfloor + \left\lfloor \frac{k-1}{2}\right\rfloor \Leftarrow k\ge 5 \wedge N\ge k+3 \end{cases} \quad (4.20)$$

Like the previous equation, this product covers the last odd baseband tones that cannot be insert in previous equation. Number of constraints is huge and requires a forced concentration when choosing the correct equation to the proper *k* and N. The figure shows us that the number of components is almost independent from the valour *k*.

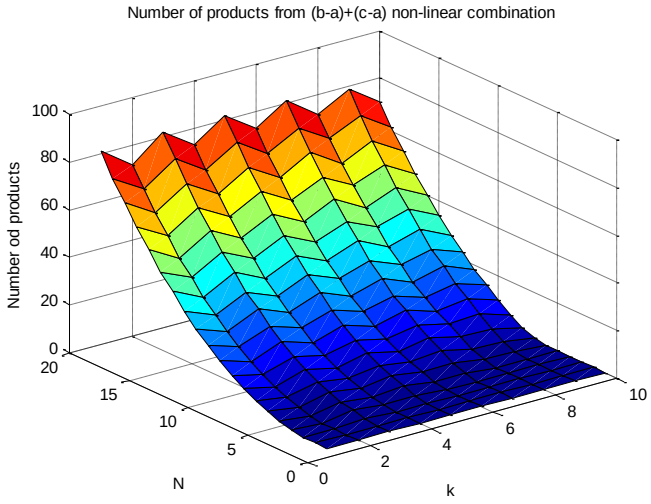

Fig. 4.10 – Number of nonlinear products from (b-a)+(c-a) in kΔ tone

The second most complex nonlinear reproduction that falls at *k*Δ baseband frequency will be a intermodulation between four distinct tones, (a-b)+(c-d), and generate the most complex mathematical system from all products. We need four equations with a high complexity degree to correct modulate the behaviour of this product for a certain *k*Δ. The system of equations is then:

$$Nt(k\Delta)_{(a-b)+(c-d)} = \sum_{i=k+2}^{N}\left[(k-1)+\left\lfloor\frac{i-k}{2}-1\right\rfloor+\sum_{l=k+2}^{i-1}(k-1)+\left\lfloor\frac{l-k}{2}-1\right\rfloor\right] \Leftarrow k\le 3\wedge N\ge 2$$

$$\sum_{j=\left\lceil\frac{k+4}{2}\right\rceil}^{N}\left[\left(j-\left\lceil\frac{k+1}{2}\right\rceil\right)^2-rest(k,2)\times\left(j-\left\lceil\frac{k+1}{2}\right\rceil\right)\right] \Leftarrow k\ge 4\wedge\left\lfloor\frac{k+4}{2}\right\rfloor\le N\le k$$

$$\sum_{j=\left\lceil\frac{k+4}{2}\right\rceil}^{k}\left[\left(j-\left\lceil\frac{k+1}{2}\right\rceil\right)^2-rest(k,2)\times\left(j-\left\lceil\frac{k+1}{2}\right\rceil\right)\right]+\left(k-\left\lceil\frac{k+1}{2}\right\rceil\right)^2- \tag{4.21}$$

$$-rest(k,2)\times\left(j-\left\lceil\frac{k+1}{2}\right\rceil\right) \Leftarrow k\ge 4\wedge N=k+1$$

$$\sum_{j=\left\lceil\frac{k+4}{2}\right\rceil}^{k}\left[\left(j-\left\lceil\frac{k+1}{2}\right\rceil\right)^2-rest(k,2)\times\left(j-\left\lceil\frac{k+1}{2}\right\rceil\right)\right]+\left(k-\left\lceil\frac{k+1}{2}\right\rceil\right)^2-rest(k,2)\times\left(i-\left\lceil\frac{k+1}{2}\right\rceil\right)+$$

$$+\sum_{i=k+2}^{N}\left[(k-1)+\left\lfloor\frac{i-k}{2}-1\right\rfloor+\sum_{l=k+2}^{i-1}(k-1)+\left\lfloor\frac{l-k}{2}-1\right\rfloor\right] \Leftarrow k\ge 4\wedge N\ge k+1$$

As shown in figure 4.11, the fluency of the graphic is uncommon, with a irregular format, reflecting the complexity of equation 4.20.

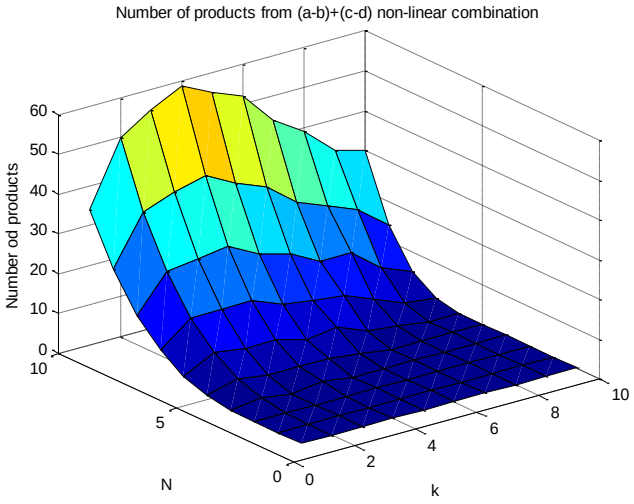

Fig. 4.11 – Number of nonlinear products from (a-b)+(c-d) in kΔ tone

Showing all the equations where the biggest tone (in frequency) was positive, it's time to present the two types of equation where it is negative.

The (-a+b)+(b-c) is the first of the combinations with a (**-a**) and it was discover lately in RF→DC modelling. Compare with the last two presented, this formula is simple and give by:

$$Nt(k\Delta)_{(-a+b)+(b-c)} = \sum_{i=k+3}^{N} \left\lceil \frac{i-(k+2)}{2} \right\rceil \Leftarrow N \geq k+3 \qquad (4.22)$$

As expected, the graphic in figure 4.12 is simple and shows a variation almost linear.

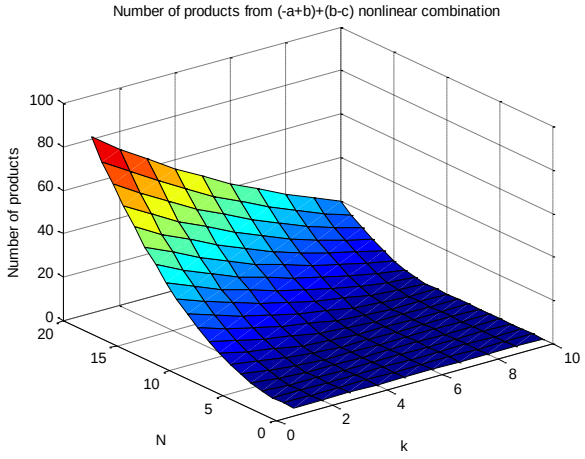

Fig. 4.12 – Number of nonlinear products from (-a+b)+(b-c) in kΔ tone

One interesting point in this type of combination is the fact the number of terms will decrease with the increase of k and will be only present in signals with more than four tones.

The last formula to calculate a baseband nonlinear tone is from the (-a+b)+(c-d). This formula shows a little more complexity than the previous one but is simpler than its "congener" from equation 4.21. The equation is:

$$Nt(k\Delta)_{(-a+b)+(c-d)} = \sum_{i=k+4}^{N}\left(\left\lceil \frac{i-(k+3)}{2} \right\rceil + \sum_{j=k+4}^{i-1}\left\lceil \frac{j-(k+3)}{2} \right\rceil\right) \Leftarrow N \geq k+4 \qquad (4.23)$$

The correspondent behaviour graphic is presented in Figure 4.13.

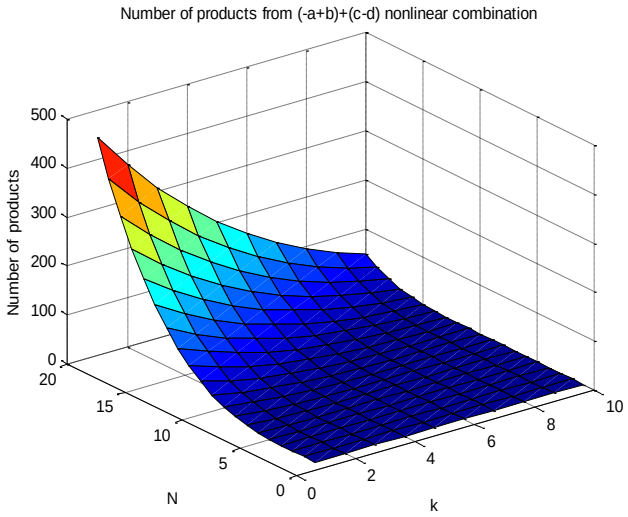

Fig. 4.13 – Number of nonlinear products from (-a+b)+(c-d) in kΔ tone

Although it seems similar to previous term, a closed and careful analyse from both figures, is clear the differences between's graphics behaviour, since the number of tones from the last term is much higher than the other terms.

4.3.3 - Amplitude value from each term

Like as in DC formulas, the several types of combination previously presented don't have the same impact at the baseband's nonlinear tone in analyses. Although they obey to the same rule: terms from the same type has an equal contribution. With these arguments we were able to find the weights from each type of combination summarized in Table 4.2.

Baseband term	Weight in baseband calculation
(a-b)	A^2
(a-a)+(a-b)	$\frac{3}{2}A^4$
(a-a)+(b-a)	$\frac{3}{2}A^4$
(a-b)+(b-c)	$3A^4$
(a-b)+(a-b)	$\frac{3}{4}A^4$
(a-b)+(a-c)	$\frac{3}{2}A^4$
(b-a)+(c-a)	$\frac{3}{2}A^4$
(a-b)+(c-d)	$3A^4$
(-a+b)+(b-c)	$\frac{3}{2}A^4$
(-a+b)+(c-d)	$3A^4$

Table 4.2 – Amplitude contribution for baseband nonlinear products

As DC terms, the combination that depends from more different tones has a bigger influence in the nonlinear baseband prediction than the ones that depends only form two different tones. Generally these tones have a bigger contribution in amplitude than the tones at DC and 4th order terms bigger than the 2nd order. Although these last suffer a big reduction since c_4 is generally much smaller than c_2.

4.3.4 - Application example

At the end of this chapter, it's imperative (like was done in the previous DC calculation) to conduct one example to prove the relevance of these equations, demonstrating its usefulness and easy calculation as quickly nonlinear calculator from baseband nonlinear phenomenon. In order to present a full result at the end of the section, let's assuming the same input signal with 5 tones and we want to know how many tones will fall in 2Δ. Using the equations from 4.13 to 4.20, the number of nonlinear products that fall in baseband wanted will be:

$$Nt(k\Delta)_{(a-b)} = 5-2=3 \tag{4.24}$$

$$Nt(k\Delta)_{(a-a)+(a-b)} = 5-2=3 \tag{4.25}$$

$$Nt(k\Delta)_{(a-b)+(b-a)} = 5-2=3 \tag{4.26}$$

$$Nt(k\Delta)_{(a-a)+(b-c)} = \sum_{i=3}^{5}(2i-2-3) = 1+3+5=9 \ \left(\text{knowing that } N \geq 3\right) \tag{4.27}$$

$$Nt(k\Delta)_{(a-b)+(a-b)} = 5-\frac{2}{2} = 4 \ \left(\text{because } k \text{ is even}\right) \tag{4.28}$$

$$\begin{aligned} Nt(k\Delta)_{(a-b)+(a-c)} &= \sum_{i=\left\lfloor\frac{2+4}{2}\right\rfloor}^{2-1}\left(i-\left\lfloor\frac{2+2}{2}\right\rfloor\right)+\left\lfloor\frac{2-1}{2}\right\rfloor\times\left(5-(2-1)\right) \ \left(\text{knowing that } N \geq 2\right) \\ &= \sum_{i=\lfloor 3\rfloor}^{1}\left(i-\lfloor 2\rfloor\right)+\left\lfloor\frac{1}{2}\right\rfloor\times 4 = 0+0=0 \end{aligned} \tag{4.29}$$

$$Nt(k\Delta)_{(b-a)+(c-a)} = \sum_{i=5}^{5}\left\lfloor\frac{i-(2+1)}{2}\right\rfloor+\left\lfloor\frac{2-1}{2}\right\rfloor=\sum_{i=5}^{5}\left\lfloor\frac{i-3}{2}\right\rfloor+\left\lfloor\frac{1}{2}\right\rfloor=1+0=1 \tag{4.30}$$

$$Nt(k\Delta)_{(a-b)+(c-d)} = \sum_{i=4}^{5}\left[1+\left\lfloor\frac{i-2}{2}-1\right\rfloor+\left(\sum_{l=4}^{i-1}1+\left\lfloor\frac{l-2}{2}-1\right\rfloor\right)\right]=1+(1+1)=3 \tag{4.31}$$

$$Nt(k\Delta)_{(-a+b)+(b-c)} = \sum_{i=5}^{5}\left\lceil\frac{i-(2+2)}{2}\right\rceil=1 \ \left(\text{knowing that } N \geq 5\right) \tag{4.31}$$

$$Nt(k\Delta)_{(-a+b)+(c-d)} = 0 \ \left(\text{knowing that } N < k+4\right) \tag{4.32}$$

With fives tones we realize that for the 2Δ baseband tone we have 3 second order terms and 23 fourth order terms (3+3+9+4+1+3). Assuming an input signal with equal tone amplitude and using terms weight from table 4.2, the amplitude at 2Δ will be given by:

$$\begin{aligned} A_{2\Delta} &= C_2\times 3\times A^2 + C_4\times\left(3\times\frac{3}{2}\times A^4+3\times\frac{3}{2}\times A^4+9\times 3\times A^4+4\times\frac{3}{4}\times A^4\right. \\ &\qquad \left.+1\times\frac{3}{2}\times A^4+3\times 3\times A^4+1\times\frac{3}{2}\times A^4\right) \\ &= c_2\times 3\times A^2 + c_4\times 51.0\times A^4 \end{aligned} \tag{4.33}$$

This simple example shows the utility of the developed equations to estimation of 2Δ nonlinear voltage when we have an input RF signal.

The compute time dispended to predict the result was extremely lower compare with regular simulators. To achieve the complete baseband nonlinear spectrum, all other nonlinear baseband products in the presence of a five-tones input signal are presented in table 4.3 (remember that the last tone will be 2(*N*-1)).

	Δ	3Δ	4Δ	5Δ	6Δ	7Δ	8Δ
(a-b)	4	2	1	0	0	0	0
(a-a)+(a-b)	4	2	1	0	0	0	0
(a-a)+(b-a)	4	2	1	0	0	0	0
(a-b)+(b-c)	12	6	3	0	0	0	0
(a-b)+(a-b)	0	0	3	0	2	0	1
(a-b)+(a-c)	0	3	2	3	1	1	0
(b-a)+(c-a)	2	3	2	3	1	1	0
(a-b)+(c-d)	1	2	2	2	1	0	0
(-a+b)+(b-c)	2	0	0	0	0	0	0
(-a+b)+(c-d)	1	0	0	0	0	0	0

Table 4.3 – Baseband spectrum with a five-tones input signal

With all baseband nonlinear terms, the mathematical representation from the output signal at lower frequencies will be:

$$\begin{aligned} y_{DC+baseband}(t) = {} & c_2 \times \frac{5}{2} \times A^2 + c_4 \times 31.875 \times A^4 + \left(c_2 \times 4 \times A^2 + c_4 \times 60 \times A^4\right) \times \cos(\Delta t) + \\ & + \left(c_2 \times 3 \times A^2 + c_4 \times 51 \times A^4\right) \times \cos(2\Delta t) + \left(c_2 \times 2 \times A^2 + c_4 \times 39 \times A^4\right) \times \cos(3\Delta t) + \\ & + \left(c_2 \times 1 \times A^2 + c_4 \times 26.25 \times A^4\right) \times \cos(4\Delta t) + \left(c_4 \times 15 \times A^4\right) \times \cos(5\Delta t) + \\ & + \left(c_4 \times 7.5 \times A^4\right) \times \cos(6\Delta t) + \left(c_4 \times 3 \times A^4\right) \times \cos(7\Delta t) + \left(c_4 \times 0.75 \times A^4\right) \times \cos(8\Delta t) \end{aligned} \tag{4.34}$$

Considering a c2/c4 =100 and A= 1, the baseband spectrum form this signal is present on Figure 4.14.

To test the robustness and processing time to determine baseband nonlinear products using these formulas, several Matlab functions were drawn and can be found in the attachment of this thesis. The main functions are *coeficients(N,k).m* and *direct_conversion(N).m* (a brief explanation from MATLAB functions could be seen in Appendix C)

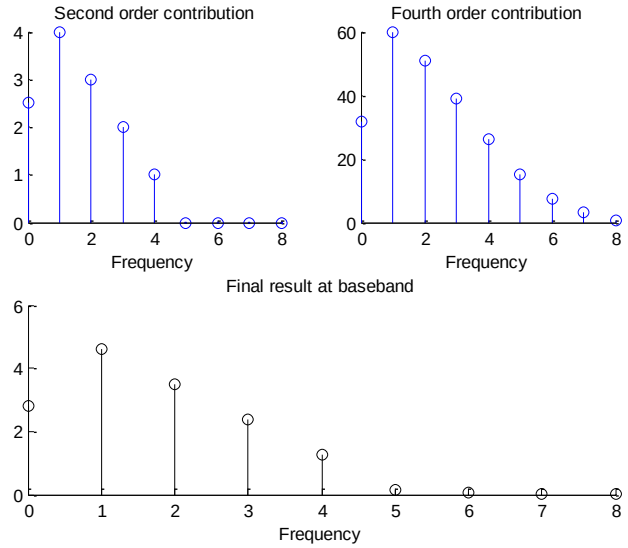

Fig. 4.14 – Baseband spectrum with a five-tones input signal

In the first function we can know the number and the type of terms which fall to a specific frequency (and baseband DC) for a given amount of input tones *N*. In second function, will be drawn all baseband nonlinear products generated thorough a N-tones input signal. This last function only requires the number of input tones *N*.

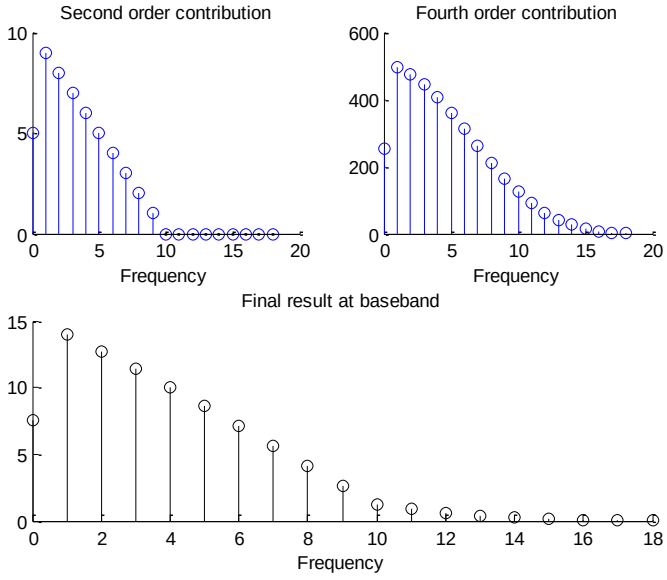

Fig. 4.15 – Baseband spectrum with a 10-tones input signal

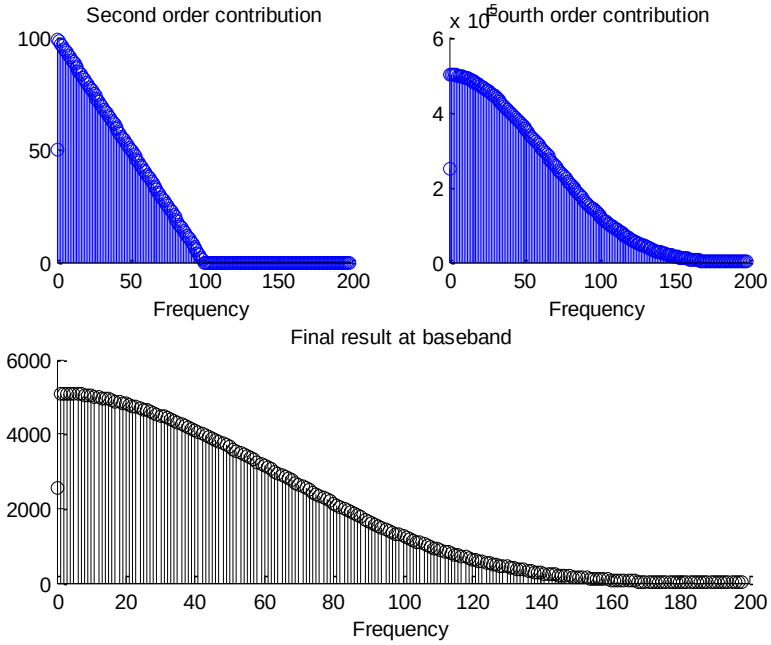

Fig. 4.16 – Baseband spectrum with a 100-tones input signal

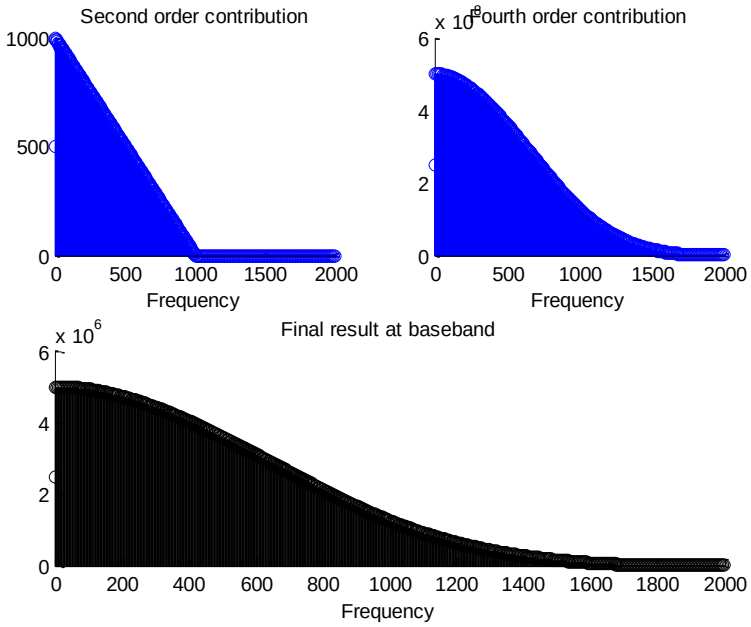

Fig. 4.17 – Baseband spectrum with a 1000-tones input signal

Figures 4.15, 4.16 and 4.17 show several examples of baseband results in the presence of several distinct input signals with 10, 100 and 1000 tones.

One of the most important characteristics is the computation time require, very small compare with other traditional simulators used, even if the number of tones was unusually high. Figure 4.17 shows this example, where the number of input tones is so

high that the resultant spectrum is almost continuous. The computation time for this example was about 2 -3 minutes when made with other simulator, will require several hours to realize the same conversion if the system doesn't overflow.

4.4 - Conclusions

This chapter was entire dedicated to the development of a new set of mathematical equations to parameterize the nonlinear behaviour of the second and fourth order that allow direct conversion of an RF signal to baseband or DC. The present nonlinear mathematical model tries to revolutionize the way of thinking (previous based only in response to the second order), to a higher level of reliability, since, as mentioned and shown in the next chapter, this assumption is erroneous and leads to results that are quite different in some cases. The achieve formulas allow a quick calculation from the contributions of these nonlinear products for any tone at baseband (including DC) making them very useful in the analysis of direct conversion systems. To prove the veracity of the equations presented, and estimate the advantages in computation time, a small MATLAB's library of functions was created for quick calculation from the number of nonlinear products in each nonlinear $k\Delta$. These Functions are attached to the present thesis.

There severe paths to follow after this first part of the work. One is explorer in next chapter, proving the importance from fourth order products in a nonlinear system's response. Other path could be the study and development of equations that reflect the impact that each individual tone in a particular tone at baseband frequency. This work would be much appreciated when we try to evaluate the influence of a single tone in our desire signal (principle of interference from an RF tone). Although this task appears to be involved in a unstoppable work because the number of variables involved and the transversality requirement make the task almost impossible and very painful to realize. One last path could be the introduction from the phase in the presented formulas, because as will be seen in section 5.7, the tone's phase could have an important role in DC or baseband tones determination.

CHAPTER 5

Diode Power Probe Measurements of Wireless Signals

After a extensive analytic analyses of the nonlinear behaviour from electronic devices and the study from algorithms to modulate this behaviour based on Taylor's Series, it is important to conduct a case study in order to verify and validate the conclusions from previous chapters, particularly regarding the importance of the fourth order nonlinear products, sometimes mistakenly ignored in the simulations and design of various receivers architectures. To obtain results as simple and clear as possible, this study is focus on the most simple receiver architecture present in chapter two - the simple detector working as diode probe. This architecture is the base off several circuits widely used today as the power probes in cell phone applications or RFID and front-ends of Software Define Radio devices. Take the example of the power probes. Power probes based on diodes have been used for many years for high-speed power measurements, and the results have been quite satisfactory when the measured power is the result from a simple signal such as a sinusoid [46][47][48]. The nonlinearity of the diode in these probes rectifies an RF signal, providing a representation of the RF power through the output DC voltage.

However, the nonlinear response of the power probe may be non-constant over the bandwidth of the RF input signal and may impact the time domain evolution of the signal. This can be an issue when measuring signals for state-of-the-art wireless systems that have wide bandwidths and high values of peak-to-average power ratio (PAPR).

The bandwidth-dependent behaviour of the power probe can be ascribed to the dynamic interaction of its baseband impedance response and the low-frequency voltage and current excited by the nonlinear device under test of a modulated-signal excitation [2]. If not corrected, these dynamic effects may impact the reliability of the measurements. Commercially available microwave power sensors have been designed to work in a 50Ω perfect environment, eliminating impedance mismatches. However, as refer, simple diode

power detector circuits are used in cell phone applications, to monitor the received power from the base station. For these circuits, the baseband embedding impedance can play a key role.

In other important scenarios like modern wireless signals, the high value of PAPR and switched performance may also interact with the nonlinear characteristic of the diode probe. Use of high PAPR signals may also yield erroneous power results, as was seen in [49] for code-division-multiple-access (CDMA) Intermediate Standard 1995 (IS-95) signals.

In this chapter, we will study and analyze the impact of dynamic long-term memory effects on measurements made with diode power probes. We will study their behaviour in the presence of high PAPR signals and provide methods for user characterization of diode power probes. This analysis will be conducted by comparing single-tone, two-tones and multisine excitations of a representative power probe. The DC voltage corresponding to the detected power will be studied to explain the changes caused by dynamic effects.

Long-term memory effects in power amplifiers have been studied for many years. They are normally attributed to the low-frequency behaviour of a transistor or amplifier, often due to the bias networks. Both input and output bias matching networks may cause these effects [50]. The frequency response of these external networks imposes a change in the nonlinear behaviour of the device, mainly introducing asymmetries in the upper and lower third-order intermodulation distortion products as a function of the excitation bandwidth.

In envelope detectors, this low-frequency interaction is also intuitively expected. This is because, for this case, the objective is to down-convert the signal from RF to the baseband.

The nonlinear distortion created by diode power probes is not so obvious. Because we are searching for the DC voltage created by the rectification of the diode, we may not expect that the effects of nonlinear distortion in the kilohertz or megahertz range would affect this DC value [46][47][48]. However, the nonlinearity of the junction capacitance of the diode means that the superposition theorem is not to represent the diode's response. As a result, the output of the diode is different for single or multiple tones. While the use of a single sinusoid does not create any baseband spurious signals, in a multisine arrangement, the baseband generated signals have a bandwidth equivalent to the RF one.

At the same time, new wireless standards are also imposing severe changes in the time-domain envelope, mainly evaluated using their PAPR, which can severely limit the range of operation of diode power sensors [51]. Unfortunately typical calibration procedures are

used for constant-envelope signals, such as single sinusoids, which do not create the fast variations of modern wireless signals.

In [52], the authors conducted a preliminary study of the effects of baseband impedance terminations on the accuracy of the DC voltage measured by the probe. In [53], a simple study of the differences between one tone measurements and modulated signals was carried out.

In the present work, we will further study the impact of these terminations, first for a single sinusoid and then for a multisine signal, including high PAPR signals having various statistical characteristics. We will also develop and improve methods to predict the effect of the baseband impedance on the measured DC values.

Actually the explanation of different behaviours of the probe when in presence of signals with quite different PAPR values is here firstly explained, and to the best knowledge of the authors it was never explained previously.

We will start by presenting, in Section 5.2, the problem of long-term memory effects with a mathematical approach based on Volterra series analysis. After that, in sections 5.3 and 5.4, an analysis of the impact of the baseband impedance will be carried out by use of both simulations and measurements when the system is excited by a single and a two-tone signal. This study continues in section 5.6, with the effects of high values of PAPR excitation using multisine signals with different statistics. Finally section 5.7 will presents results based on real communication signals. The chapter ends with the conclusions taken from all simulations and measurements results.

5.1 – Analytical Model of Long-Term Memory Effects

In order to understand the basic nonlinear mechanisms of diode power probes, consider the following circuit, in this case a very simple probe, used for demonstration purposes.

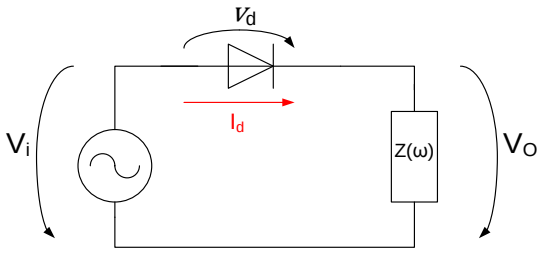

Fig. 5.1 - Schematic of a simple diode power probe.

A Volterra-series-based mathematical approach will be applied to the circuit of Figure 5.1, utilizing a minimum number of terms to simplify the understanding of the sought-after behaviour.

The measurement-based diode model described in [54] is first approximated by a polynomial series expansion around a quiescent operating point truncated to order four[1]. In this case, based on equation 3.3, the current through the diode is given by:

$$I_d = I_s + k_1 v_d + k_2 v_d^2 + k_3 v_d^3 + k_4 v_d^4 + \ldots \tag{5.1}$$

where $v_d = v_i - v_o$ and I_s is the diode quiescent point.

From this model we actually see that the terms that will contribute to DC are the even order terms, especially the second and fourth order coefficients in equation 5.1. The polynomial has been truncated to order four because we use the minimum number of terms for a correct understanding of the nonlinear mechanism, as we see latter on in this section. Considering that we would like to obtain the output voltage of the probe versus the input RF signal, we can develop the Volterra series [2], using the Harmonic Input method (section 3.4.2) as follows:

$$H_n(\omega_1, \omega_2, \ldots, \omega_n) = \frac{Y_{BB}(\omega_1, \omega_2, \ldots, \omega_n)}{X_{RF}(\omega_1, \omega_2, \ldots, \omega_n)} \tag{5.2}$$

where $Y_{BB}(.)$ is the output voltage at baseband plus DC, and $X_{RF}(.)$ is the input voltage at RF. This strategy was applied to the circuit of Figure 5.1, where four Volterra nonlinear operators were selected, because this is the minimum number of operators that are needed for the explanation of the impact of long-term memory effects in the DC value of the power probe. These operators are shown as representative examples in (5.3) to (5.6):

$$H_1(\omega_1) = Z(\omega_1)\frac{k_1}{1 + k_1 Z(\omega_1)} \tag{5.3}$$

$$H_2(\omega_1, \omega_2) = Z(\omega_1 + \omega_2)\frac{k_2\left[1 + H_1(\omega_1) + H_1(\omega_2) + H_1(\omega_1)H_1(\omega_2)\right]}{1 + k_1 Z(\omega_1 + \omega_2)} \tag{5.4}$$

[1] It should be stated that this polynomial approach is used mainly as a way to understand the mechanisms of the power measure itself, and not as a complete diode model.

$$H_3(\omega_1,\omega_2,\omega_3) = Z(\omega_1+\omega_2+\omega_3)\times$$
$$\frac{\left[\begin{array}{l} k_2\left(\begin{array}{l} -\frac{2}{3}H_2(\omega_1,\omega_2)-\frac{2}{3}H_2(\omega_1,\omega_3)-\frac{2}{3}H_2(\omega_2,\omega_3)+\frac{2}{3}H_1(\omega_3)H_2(\omega_1,\omega_2)+ \\ +\frac{2}{3}H_1(\omega_2)H_2(\omega_1,\omega_3)+\frac{2}{3}H_1(\omega_1)H_2(\omega_2,\omega_3) \end{array}\right)-\ldots \\ \ldots+k_3\left(\begin{array}{l} 1-H_1(\omega_1)-H_1(\omega_2)-H_1(\omega_3)+H_1(\omega_1)H_1(\omega_2)+H_1(\omega_1)H_1(\omega_3)+ \\ +H_1(\omega_2)H_1(\omega_3)-H_1(\omega_1)H_1(\omega_2)H_1(\omega_3) \end{array}\right) \end{array}\right]}{1+k_1Z(\omega_1+\omega_2+\omega_3)} \quad (5.5)$$

If we consider the terms whose frequencies will fall on DC, that is where $\sum\omega = 0$, we will have all components at $\omega_i - \omega_i = 0$. There are also other terms that correspond to the mixing of $\Delta\omega = \omega_2 - \omega_1$ and $\omega_3 - \omega_4$, that apparently wouldn´t have influence in DC (taking in consideration only the 2nd order response), now have an important contribute to the calculations of the resulting in DC signal as we can see by the equation (5.6). This means that terms falling on other components involving $\Delta\omega$ have a non-zero impact on the final DC value.

$$H_4(\omega_1,\omega_2,\omega_3,\omega_4) = Z(\omega_1+\omega_2+\omega_3+\omega_4)\times$$

$$\left[\begin{array}{l}
k_2\left(\begin{array}{l}
\frac{1}{3}H_2(\omega_1,\omega_2)H_2(\omega_3,\omega_4)+\frac{1}{3}H_2(\omega_1,\omega_3)H_2(\omega_2,\omega_4)+\frac{1}{3}H_2(\omega_1,\omega_4)H_2(\omega_2,\omega_3)\\
+\frac{1}{2}H_1(\omega_1)H_3(\omega_2,\omega_3,\omega_4)+\frac{1}{2}H_1(\omega_2)H_3(\omega_1,\omega_3,\omega_4)+\frac{1}{2}H_1(\omega_3)H_3(\omega_1,\omega_2,\omega_4)\\
+\frac{1}{2}H_1(\omega_4)H_3(\omega_1,\omega_2,\omega_3)-\frac{1}{2}H_3(\omega_1,\omega_2,\omega_3)-\frac{1}{2}H_3(\omega_1,\omega_2,\omega_4)\\
-\frac{1}{2}H_3(\omega_1,\omega_3,\omega_4)-\frac{1}{2}H_3(\omega_2,\omega_3,\omega_4)
\end{array}\right)+\\
+k_3\left(\begin{array}{l}
-\frac{1}{2}H_2(\omega_1,\omega_2)-\frac{1}{2}H_2(\omega_1,\omega_3)-\frac{1}{2}H_2(\omega_1,\omega_4)_2-\frac{1}{2}H_2(\omega_2,\omega_3)-\frac{1}{2}H_2(\omega_2,\omega_4)\\
-\frac{1}{2}H_2(\omega_3,\omega_4)+\frac{1}{2}H_1(\omega_1)H_2(\omega_2,\omega_3)+\frac{1}{2}H_1(\omega_1)H_2(\omega_2,\omega_4)+\frac{1}{2}H_1(\omega_1)H_2(\omega_3,\omega_4)\\
+\frac{1}{2}H_1(\omega_2)H_2(\omega_1,\omega_3)+\frac{1}{2}H_1(\omega_2)H_2(\omega_1,\omega_4)+\frac{1}{2}H_1(\omega_2)H_2(\omega_3,\omega_4)\\
+\frac{1}{2}H_1(\omega_3)H_2(\omega_1,\omega_2)+\frac{1}{2}H_1(\omega_3)H_2(\omega_1,\omega_4)+\frac{1}{2}H_1(\omega_3)H_2(\omega_2,\omega_4)\\
+\frac{1}{2}H_1(\omega_4)H_2(\omega_1,\omega_2)+\frac{1}{2}H_1(\omega_4)H_2(\omega_1,\omega_3)+\frac{1}{2}H_1(\omega_4)H_2(\omega_2,\omega_3)\\
-\frac{1}{2}H_1(\omega_1)H_1(\omega_2)H_2(\omega_3,\omega_4)-\frac{1}{2}H_1(\omega_1)H_1(\omega_3)H_2(\omega_2,\omega_4)\\
-\frac{1}{2}H_1(\omega_1)H_1(\omega_4)H_2(\omega_2,\omega_3)-\frac{1}{2}H_1(\omega_2)H_1(\omega_3)H_2(\omega_1,\omega_4)\\
-\frac{1}{2}H_1(\omega_2)H_1(\omega_4)H_2(\omega_1,\omega_3)-\frac{1}{2}H_1(\omega_3)H_1(\omega_4)H_2(\omega_1,\omega_2)
\end{array}\right)+\\
+k_4\left(\begin{array}{l}
1-H_1(\omega_1)-H_1(\omega_2)-H_1(\omega_3)-H_1(\omega_4)+H_1(\omega_1)H_1(\omega_2)+H_1(\omega_1)H_1(\omega_3)\\
+H_1(\omega_1)H_1(\omega_4)+H_1(\omega_2)H_1(\omega_3)+H_1(\omega_2)H_1(\omega_4)+H_1(\omega_3)H_1(\omega_4)\\
-H_1(\omega_1)H_1(\omega_2)H_1(\omega_3)-H_1(\omega_1)H_1(\omega_2)H_1(\omega_4)-H_1(\omega_2)H_1(\omega_3)H_1(\omega_4)\\
+H_1(\omega_1)H_1(\omega_2)H_1(\omega_3)H_1(\omega_4)
\end{array}\right)+\ldots
\end{array}\right]$$

$$1+k_1Z(\omega_1+\omega_2+\omega_3+\omega_4)$$

(5.6)

If the formulas of 5.3 to 5.6 are further simplified for a one-tone excitation, the change in DC voltage will be given by:

$$Y_{DC}(0) = H_2(\omega_1;-\omega_1)A_1^2 + H_4(\omega_1;-\omega_1;\omega_1;-\omega_1)A_1^4 \tag{5.7}$$

where A_1 is the amplitude from the input sinusoid. We see that the DC value is only dependent from ω_1-ω_1 or ω_2-ω_2, with the latter term approaching zero because of the low-pass behaviour of the output matching network.

If a two-tone signal is used as the excitation, the DC value will be

$$Y_{DC}(0) = 2!H_2(\omega_1;-\omega_1)A_1^2 + 2!H_2(\omega_2;-\omega_2)A_1^2 + 4!H_4(\omega_1;-\omega_1;\omega_1;-\omega_1)A_1^2A_2^2 + \\ + 4!H_4(\omega_2;-\omega_2;\omega_2;-\omega_2)A_1^2A_2^2 + 4!H_4(\omega_1;-\omega_1;\omega_2;-\omega_2)A_1^2A_2^2 \quad (5.8)$$

where A_1 and A_2 are the input signal amplitudes for each tone. In this case, some terms will depend on ω_1-ω_1, as in the single-tone case, but also on the nonlinear mixing product falling at ω_2-ω_1, present in four order transfer function.

From (5.8) we can also see that a second order expansion is not enough to describe the baseband impedance variation, since both $H_2(.)$ nonlinear operators exclusively depend on the beating frequencies, ω_1-ω_1 or ω_2-ω_2, and not on the base band frequency ω_2-ω_1. This actually proves that a minimum of forth order terms should be used to explain the base band impedance impact on diode power probes.

We also see that no matter what the relative phase offset between tones, the overall DC value is independent of the phase relationship, due to the fact that the $Y_{DC}(0)$ is always a group of complex conjugated mixing products, as can be seen by the fact that A_1 and A_2 always appear squared. Nevertheless, from equation (5.8) we see that the baseband impedance may also affect the DC value.

In order to better understand how the baseband impedance affects the DC value, consider that the output matching network presents a low-pass behaviour. This means that $Z(\omega)\approx 0$ for RF frequencies, but is different from zero at very low frequencies. In this case, H_2 and H_4 simplify to:

$$H_2(\omega_1,\omega_2) = k_2\frac{Z(\omega_1+\omega_2)}{1+k_1Z(\omega_1+\omega_2)} \quad (5.9)$$

$$H_4(\omega_1,\omega_2,\omega_3,\omega_4) = Z(\omega_1+\omega_2+\omega_3+\omega_4)\times \\ \frac{\left[\begin{array}{l} k_2\left(\frac{1}{3}H_2(\omega_1,\omega_2)H_2(\omega_3,\omega_4)+\frac{1}{3}H_2(\omega_1,\omega_4)H_2(\omega_2,\omega_3)+\ldots\right)+ \\ +k_3\left(-\frac{1}{2}H_2(\omega_1,\omega_2)-\frac{1}{2}H_2(\omega_1,\omega_4)-\frac{1}{2}H_2(\omega_2,\omega_4)-\frac{1}{2}H_2(\omega_3,\omega_4)+\ldots\right)+k_4 \end{array}\right]}{1+k_1Z(\omega_1+\omega_2+\omega_3+\omega_4)} \quad (5.10)$$

If equations (5.8) to (5.10) are closely studied, we see that, for a two-tone case, the term $H_4(\omega_1,-\omega_1,\omega_2,-\omega_2)$ will be:

$$H_4(\omega_1,-\omega_1,\omega_2,-\omega_2)=Z(\omega_1-\omega_1+\omega_2-\omega_2)\times \left[\begin{array}{l} k_2\left(\frac{1}{3}H_2(\omega_1,-\omega_1)H_2(\omega_2,-\omega_2)+\frac{1}{3}H_2(\omega_1,-\omega_2)H_2(-\omega_1,\omega_2)+\ldots\right)+ \\ +k_3\left(-\frac{1}{2}H_2(\omega_1,-\omega_1)-\frac{1}{2}H_2(\omega_2,-\omega_2)-\frac{1}{2}H_2(\omega_1,-\omega_2)-\frac{1}{2}H_2(-\omega_1,\omega_2)+\ldots\right)+k_4 \end{array}\right] \Big/ \left(1+k_1Z(\omega_1-\omega_1+\omega_2-\omega_2)\right) \quad (5.11)$$

Looking further, for instance, at $H_2(\omega_1,-\omega_2)$, it can be seen that

$$H_2(\omega_1,-\omega_2)=k_2\frac{Z(\omega_1-\omega_2)}{1+k_1Z(\omega_1-\omega_2)} \quad (5.12)$$

This clearly illustrates that the DC value depends on the impedance that appears at ω_1-ω_2. To illustrate the concept behind these formulas, an output matching circuit presenting a load impedance having the response shown in Fig. 2 will be used. This impedance was designed to exhibit a resonance around 750 kHz, to simulate the memory effect pattern. We use this impedance in (5.4) to (5.7), together with standard diode model values [50]. In this case, $Y_{DC}(0)$ will have different values for different excitations, as expected.

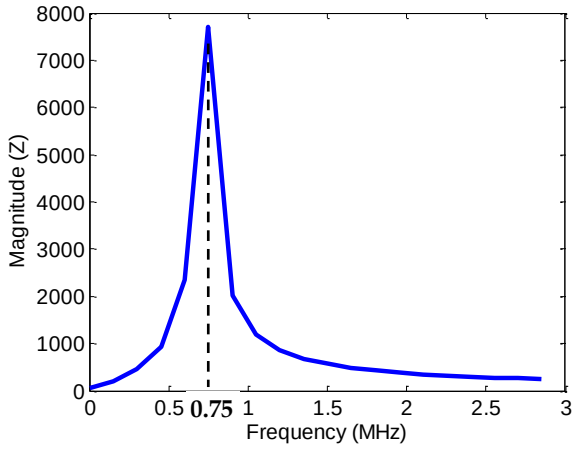

Fig. 5.2 - Output load impedance used as an illustrative example.

The DC response for single-tone and two-tone excitations is shown in Figure 5.3. In the one-tone case, we sweep the frequency of the tone over a 2.5 MHz frequency range near the carrier. In the two-tone case, we sweep the tone spacing from near 0 Hz to 2.5MHz.

As shown Figure 5.3, with a single tone, the DC output voltage is equal for all values of frequency. With two excitation tones, the resonance in the baseband impedance has a

noticeable effect on the DC output. For the case shown here, the maximum deviation appears at the resonant frequency.

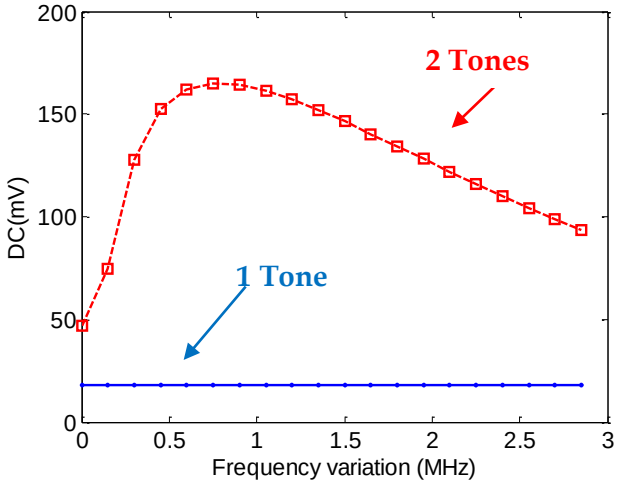

Fig. 5.3 - Output voltage of the diode probe obtained through the Volterra model.

This mathematical approach illustrates that the calibration of the overall system with a single sinusoid will not guarantee the calibration of the diode power probe for other types of excitations because they may be corrupted by long-term memory effects.

5.2 – Bandwidth-Dependent Probe Behaviour

In order to validate the mathematical concepts presented in the previous section, a diode power detector circuit designed for operation at 5.8 GHz, was simulated by using the Advance Design System simulator [63]. The schematic of the simulated circuit is presented in Figure 5.4. The bias circuit will be used as a way to guarantee that the circuit will work in its valid operating range, although the bias can be set to zero when desired.

For modelling the Schottky diode behaviour, it was used a Vigo measurement-based model that be presented in [54]. This model is a time-domain, table-based nonlinear model, extracted from DC and small signal S-parameters measurements.

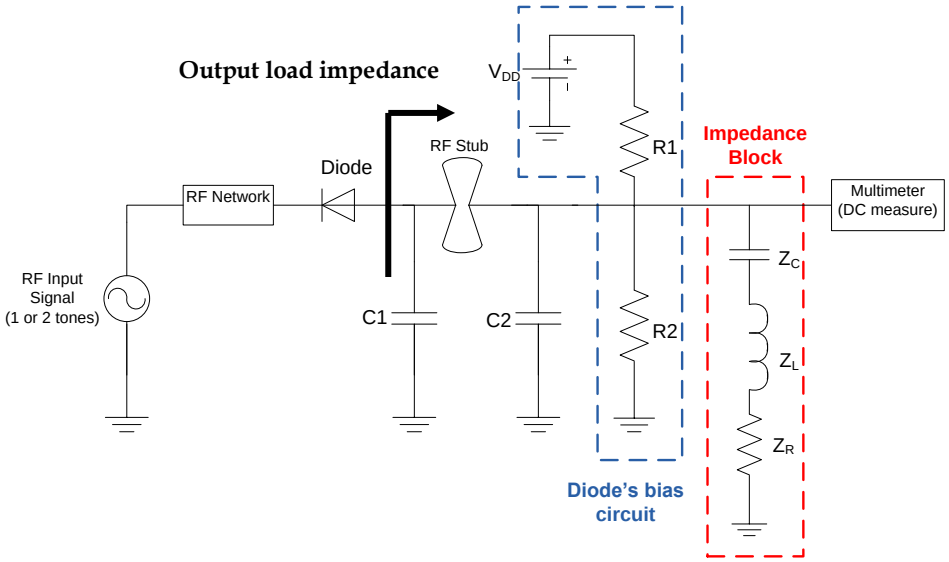

Fig. 5.4 – Schematic of the diode power detector circuit used in our simulations

An output-matching circuit was built in order to optimize the performance of the circuit, both at 5.8 GHz and at baseband, presenting a low-pass filter behaviour. An output load impedance with a resonance at 2.25 MHz was inserted in order to clearly mimic the effect of the baseband impedance, as illustrated in Figure 5.5.

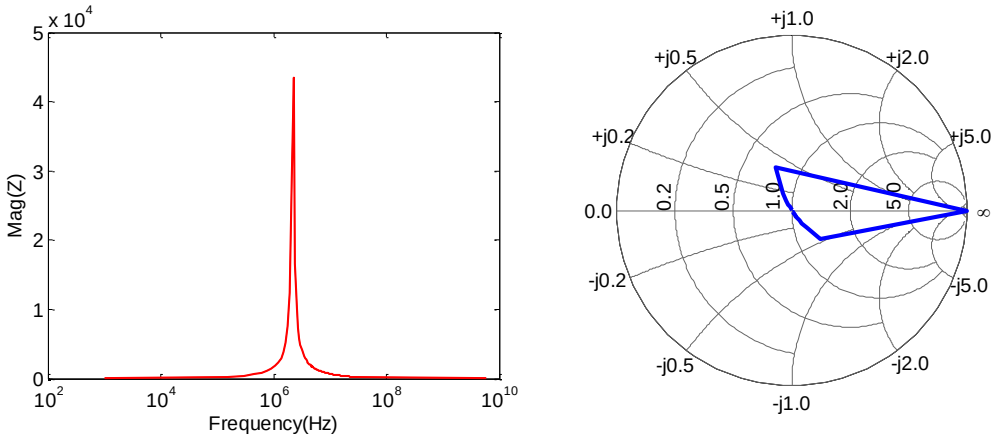

Fig. 5.5 – Diode's simulated output load impedance

To capture the behaviour of the diode power detector, two simulations were conducted. In the first, a one-tone excitation was centred at 5.8 GHz and swept in frequency within a 6 MHz band around the carrier. The results are shown in Figure 5.6(a). In the second simulation, a two-tone excitation was centred at 5.8 GHz. In this case, the tone separation was swept from 0 to 6 MHz. The power of each tone was varied from -20 dBm to -10 dBm. Results are shown in Figure 5.6(b).

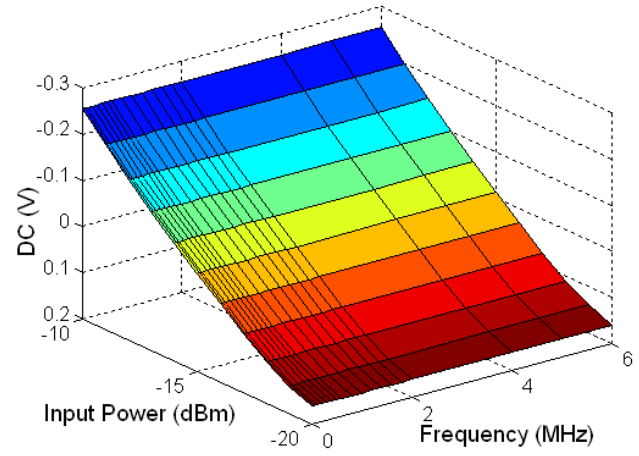

(a)

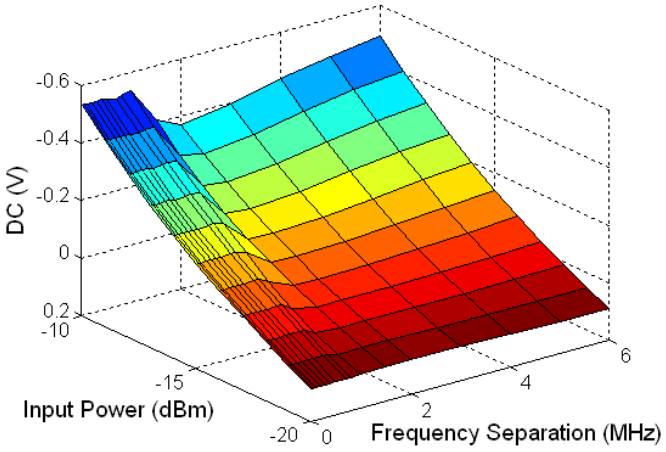

(b)

Fig. 5.6 – Simulated results showing the DC voltage measured at the output of the diode power detector with (a) one-tone(b) two-tones excitation. The various shades on the graph are included to aid in discerning similar DC output levels of the probe. The absolute scale corresponding to the colours is not significant.

It was expected that the voltage measured at the output of the diode probe for the two-tone excitation would be almost twice that of the voltage measured with the single tone, presenting the same power. In fact, this is the case for frequency separation near 0 Hz.

But for other frequency spacing values, especially close to the resonance frequency, the detector's output for the two-tone excitation changes significantly. The one-tone simulation is quite different from the two-tone behaviour, thus illustrating our initial idea and mathematical analyses. These indicate that a calibration for the one-tone case will not guarantee the correct calibration for more complex forms of excitations.

5.3 – Simulation of Probe Behaviour in Presence of Signals with Different Statistical Characteristics

Until now we have evaluated the behaviour of diode probes with changes in the bandwidth of the excitation signal. Nevertheless, modern wireless signals are also imposing strong amplitude variations over time. The effects of these signals on system behaviour can be evaluated by analyzing its statistical pattern[2]. One-tone calibration procedures, due to their constant amplitude, may significantly reduce the accuracy of the calibration.

Thus, the analysis of the behaviour of power probes when excited with different PAPR values should also be studied, and carefully evaluated when compared with a one-tone excitation.

Continuing further with the study of the nonlinear terms that will fall on DC, again using equations (5.3) to (5.6), we see that for a two-tone signal, we will have the impact of the difference frequency. As discussed before, the phase of each contribution is always equal, that is the mixing products do not depend on the relative phase between tones. Both $H_2(.)$ and $H_4(.)$ will multiply by $A_1A_1^*=|A_1|^2$, or $A_2A_2^*=|A_2|^2$ in the second-order terms and by $A_1A_1^*A_2A_2^*=|A_1|^2|A_2|^2$ in the fourth-order term, which means that they are independent of the phase of either.

However, if a more complex and rich signal is inserted in the system, such as, for instance, a uniform multisine [55], the outcome will be somewhat different. In order to explain this phenomenon, consider Figure 5.7.

The DC component will depend on several terms that are, in turn, dependent on the phase relationship between tones in the multisine. This can result in values of the DC voltage that are not the true average RF power.

[2] By statistic pattern we are referring to its amplitude statistical distribution, and thus from a practical view point to the probability distribution function, and its complementary cumulative distribution function. These functions actually represent the amplitude behaviour in terms of variation over time.

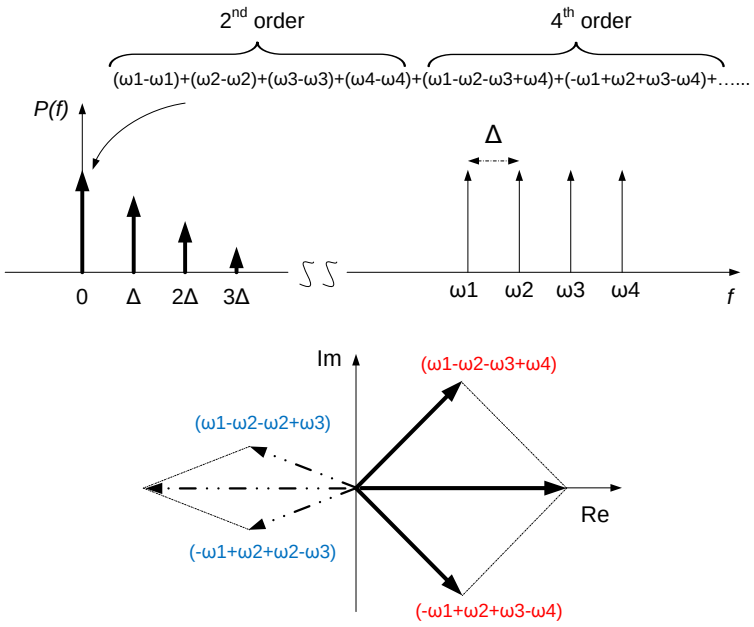

Fig. 5.7 – Example of second- and fourth-order products at DC with a four-tones excitation signal.

For instance, as shown in Figure 5.7, a fourth-order product resulting from the combination of ω_1-ω_2-ω_3+ω_4 could have a phase that actually is different from 0^o. This is counter-intuitive, because we will apparently have a DC component that has a phase different from 0^o or 180^o: a complex number! To explain this, we note that because the signal is real, a similar component arising from –(ω_1-ω_2-ω_3+ω_4) is exactly equal to the previous component at this frequency, but complex conjugated. Their addition will become a real number, as expected.

However, the amplitude will be substantially different depending on the phases arising from each tone as seen in Figure 5.7. Eventually, the resulting vector may even be negative and affect the DC voltage that is measured at output diode probe.

To take this hypothesis further, let us generate several different multisines, using different phase arrangements between tones, but with equal amplitudes. If this signal is measured using a spectrum analyzer the power spectral density will be equal for all the different multisines.

The three generated multisines are: a constant-phase multisine, where a 0^o relative phase exists between tones presenting a PAPR of 10dB; a normal (Gaussian) distribution of relative phases with PAPR of 5.6dB, and a uniform distribution of relative phases presenting a PAPR of 3.3dB. Their statistical probability density functions are present in Figure 5.8.

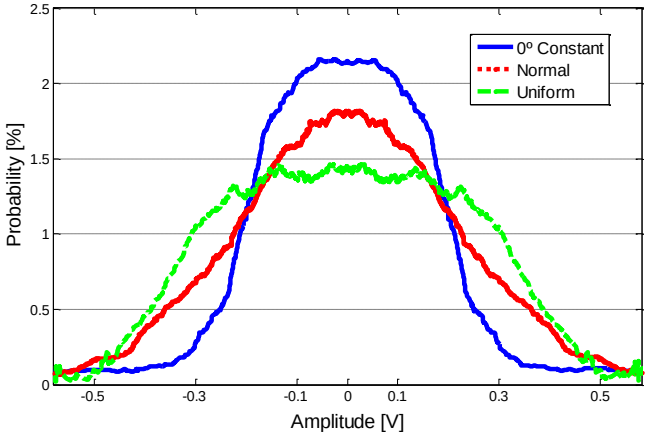

Fig. 5.8 – Probability density functions of the relative phase distributions of three multisine signals: 0º constant (blue); normal (red); uniform (green).

In Figure 5.8 the simulated DC values for a 10 component multisine signal (beginning at 5.9 GHz) having a normal phase distribution is presented. We again see the effect of the load's low-frequency resonances as was seen in the two-tone case. This indicates that memory effects are appearing also in multisine scenarios.

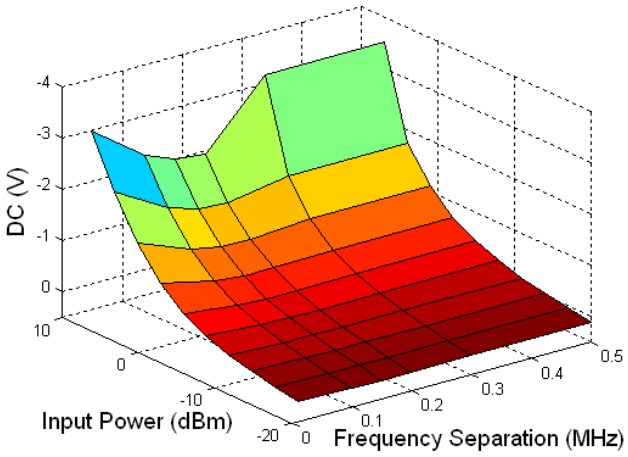

Fig. 5.9 – Simulation results for a multisine signal excitation with normal phase distribution.

The three multisines were simulated for a small frequency separation, where the resonance will have a mild impact in the final results. Figure 5.10 presents the simulated results, and, as discussed previously, the measured DC value is different for each phase distribution.

From same graphic, it's also clear that for low values of input power, where the second-order term is dominant, the DC voltage is similar for all of the phase arrangements. The

simulated voltage only starts to deviate for high values of input power, where higher-order terms start to be important, as was previously explained.

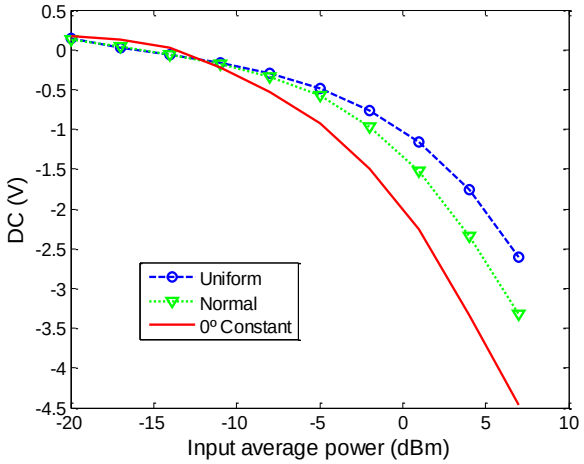

Fig. 5.10 – Simulation results with the three different multisines for 10 kHz separation of the 10 frequency components.

These simulations illustrate the previous assumption and further expand our first thought that a one-tone excitation is not sufficient for a diode power probe calibration when it is to be used with modulated signals.

5.4 – Measurements of the Bandwidth Effect

The under test circuit present on Figure 5.4 was fabricated and tested with the same conditions used in the simulations described above (figure 5.11).

The circuit has an input matching circuit that mainly guarantees the matching for input RF signals, in this case represented by a stub configuration, then the diode is actually the core of the frequency conversion circuit, from RF to DC, and the output is constructed with a matching circuit for DC and filtering for higher bandwidths.

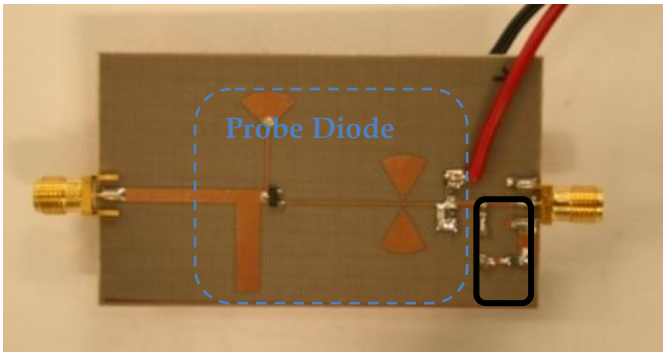

Fig. 5.11 – Power probe prototype used in laboratory tests.

Our measurement set-up (figures 5.12 and 5.13) consisted of two RF sources to generate a two-tone signal, a power combiner, a power amplifier to raise the signal and a voltmeter. The results presented here are intended to illustrate the trends regarding the use of different excitation signals on measurements made with diode power probes. The goal of the present work is to illustrate qualitative trends on the effects of excitation characteristics on diode power probe measurements.

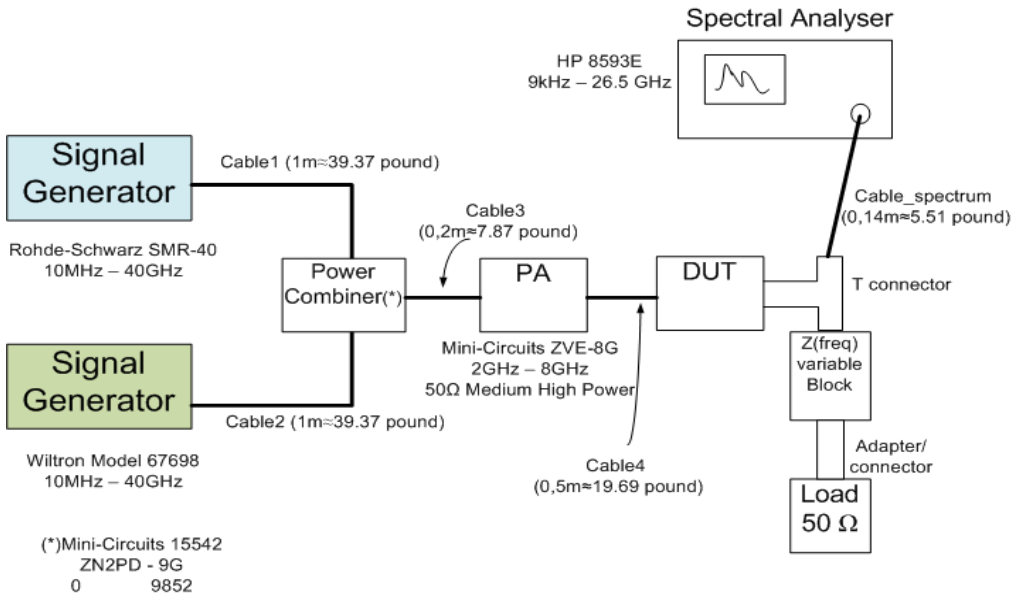

Fig. 5.12 - Block diagram of the laboratory measurement set-up for the two-tones measurement.

Fig. 5.13 - Laboratory measurement set-up.

In the case of multisines, only one signal generator was used, based on an arbitrary waveform generator (figure 5.14).

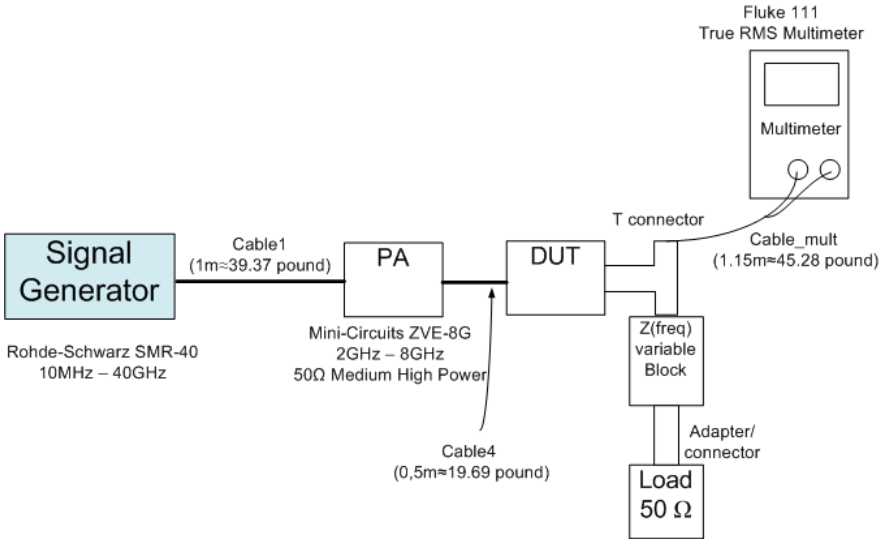

Fig. 5.14 - Block diagram of the laboratory measurement set-up for the multi-tones measurement.

First the output impedance of the diode power detector was measured with a vector network analyzer. This measurement was made both with and without a multimeter attached. Because the measurements were made at baseband frequencies, the multimeter's output impedance can actually play an important role, as shown in Figure 5.15.

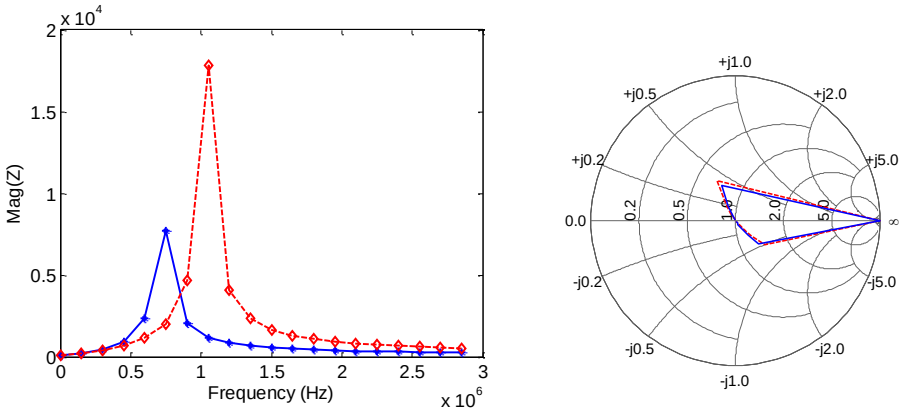

Fig. 5.15 – VNA measurements of the diode power detector's output load impedance: without multimeter attached (red dashed) and with multimeter attached (blue solid).

In Figure 5.16 (a) and 5.16 (b), the measurement results for a single sinusoidal signal and two-tone excitation are presented, respectively. The measured results are based on the assumptions that the DC voltmeter and signal generator are operating within manufacturers' specifications (+/- 0.7% for the DC voltmeter, and <0.9 dB for the signal sources), and that the sources of random error are negligible.

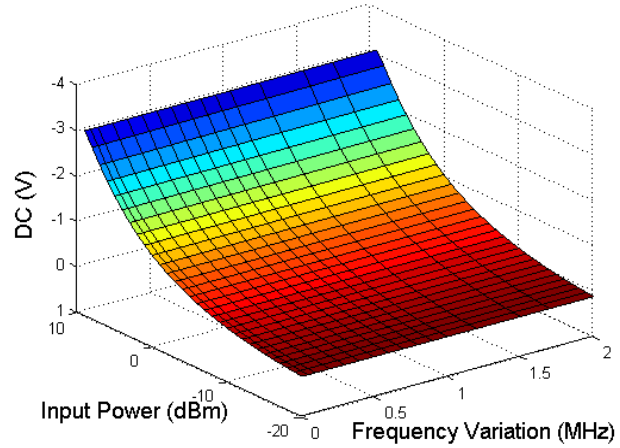

(a)

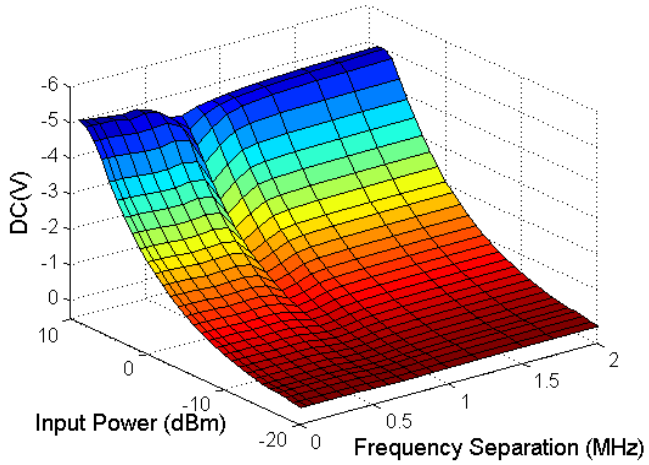

(b)

Fig. 5.16 – Illustrative measurement results with one-tone (a) and two-tone (b) excitations.

As can be seen in these figures, we observe a change in the DC value of almost 1 volt near the resonance frequency. The resonant frequency values are not equal to the simulated ones because of an inexact representation of the baseband impedance in the simulations. However, these results demonstrate our initial assumption, that if the probe is calibrated with a single tone, it can give incorrect results when excited by a two-tone signal when the baseband impedance is a function of frequency, as is often the case for reactive matching networks.

We should refer that as a rule of thumb to see if the base band has impact in your system behaviour, the experimental engineer can do these two type of measurements:

First use a single tone as the excitation and sweep its frequency in the bandwidth of interest, pointing out the measured DC values, this will allow the engineer to see the impact of the RF matching circuit and its behaviour over the band.

Secondly, using a two-tone signal, with half power in each tone compared with the single tone experiment, swept the frequency separation between the tones and measures the DC value again, if the value is the double of single tone over the band, then the base band impedance has little importance. Nevertheless is the DC value changes significantly then the base band is of strong importance, and can be identified as was pointed previously.

5.5 – Multisine Measurements

We now analyze the response of our probe to the multisine signals described in Section 5.4 to study the effect of different PAPR values. We also varied the multisines in both tone separation and power. Figures 5.17 and 5.18 present the results for the three multisines.

From the figures, a similar behaviour can be seen as in the two-tone case that is the graphs present a dip at the tone spacing on the order of the resonant frequency value. We also see that in the multisine case the dip is wider. This can be attributed to the fact that even if the tone separation is smaller than the resonant frequency, the signal can also present several multiples of the tone separation, some of which will fall on the resonant frequency. This effect will not occur for a two-tone excitation signal, because only one tone separation appears.

Even though we always excited the circuit with a ten-tones multisine having the same amplitude for each tone, the output DC values were different for each statistical arrangement. As a result a different power value will be reported for each multisine, even though the power should be equal for all of the excitations.

In order to better understand the effects of the statistical distribution in the nonlinear behaviour of the different multisines, a plot of the DC power for each multisine is presented in Figure 5.17.

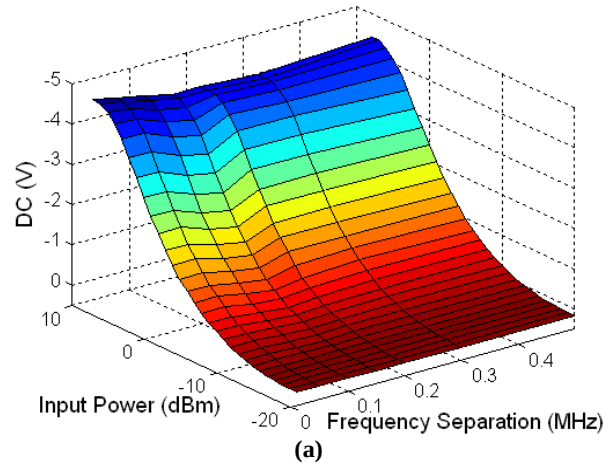

(a)

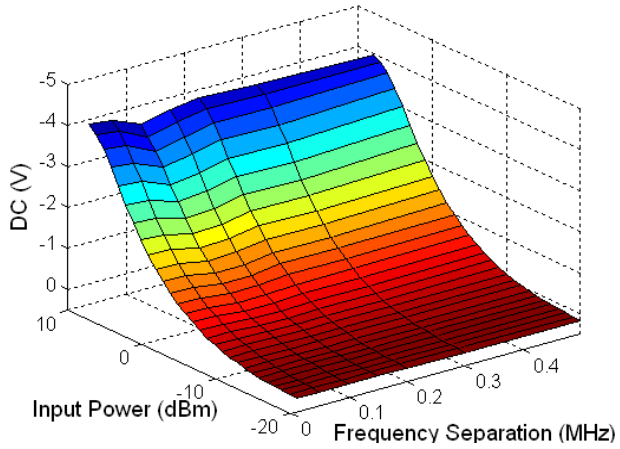

(b)

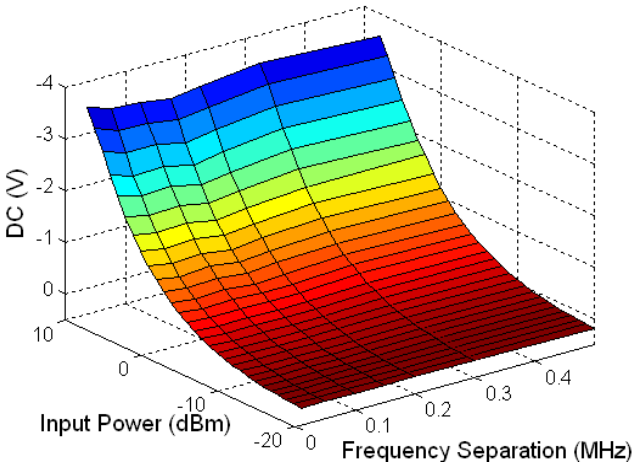

c)

Fig. 5.17 – Illustrative measurement results using multisine excitations with: (a) constant phase (0°); (b) normal phase distribution (c) uniform phase distribution.

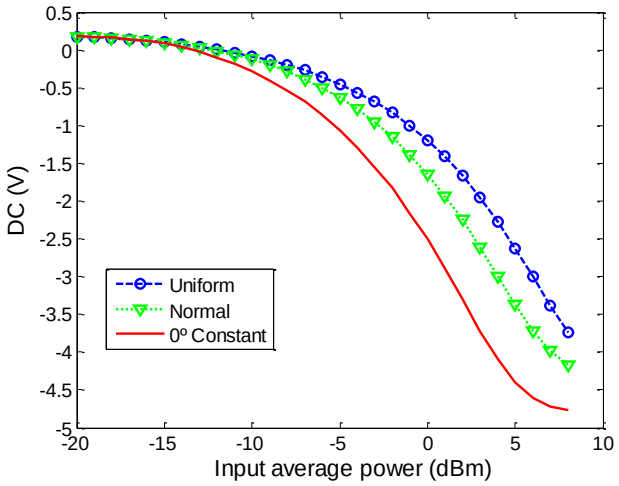

(a)

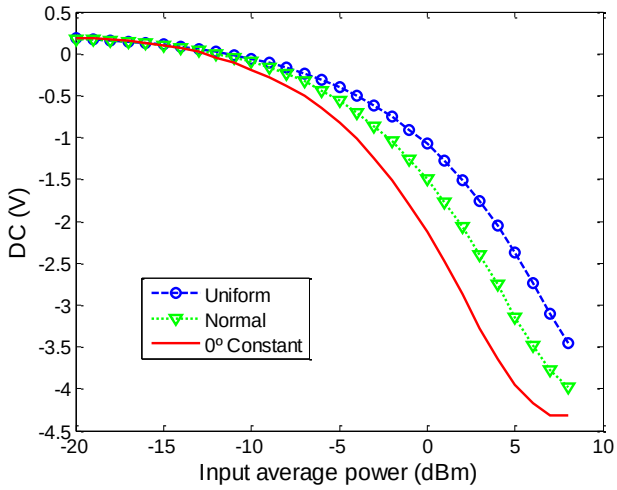

(b)

Fig. 5.18 – Qualitative comparison of measurements made with the power probe of multisines having three relative phase distributions: (a) for 10kHz separation between the tones; (b) for a separation between the tones corresponding to the resonant frequency.

As can be seen, for low values of average power, each distribution provides similar results. But when the signal power increases the nonlinear behaviour of the probe is excited. In this case, the obtained results present different behaviours. The DC values are also different in Figure 5.18 (a) and (b), corresponding to a different frequency separation, as expected.

5.6 – Probe Behaviour under Wireless Signal Excitation

Finally, and in order to evaluate the previous developed analysis with real signals, two digitally modulated signals were used, quadrature-phase-shift-keyed (QPSK) with near 4dB of PAPR and 256-quadrature-amplitude-modulation (QAM) modulation types with near 12dB of PAPR. These modulations were selected due to their difference in PAPR values.

Both of the signals were generated using a vector signal generator over different bandwidths and with the same integrated average power. Figure 5.19 presents the measured results.

As can be seen from Figure 5.19, similar results are obtained as those predicted from the previous analyses, in this case a dip continues to be visible when the bandwidth of the signals is changed. The DC value is also different for the different modulation formats. This can also be seen in Figure 5.20, which illustrates once again that the probe is sensitive to both PAPR and signal bandwidth.

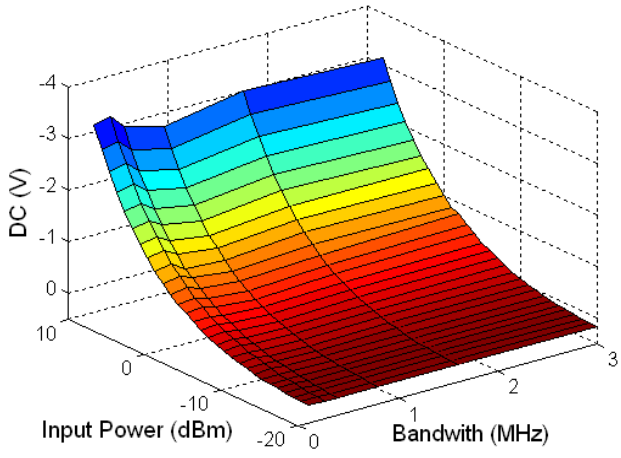

(a)

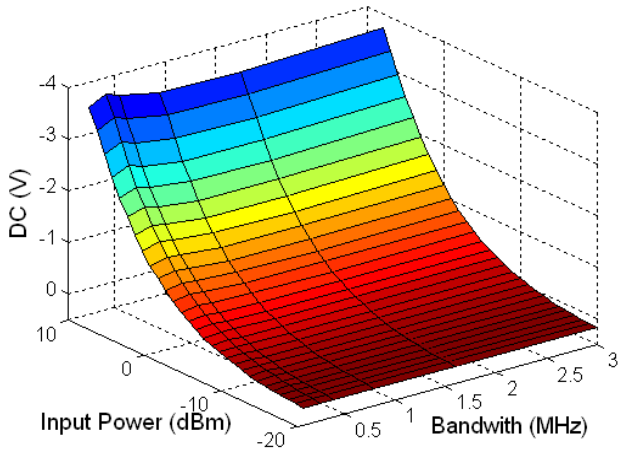

(b)

Fig. 5.19 – Illustrative power-probe measurement results using (a) QPSK signal; (b) 256-QAM signal.

The DC value is also different for the different modulation formats. This can also be seen in Figure 5.20, which illustrates once again that the probe is sensitive to both PAPR and signal bandwidth.

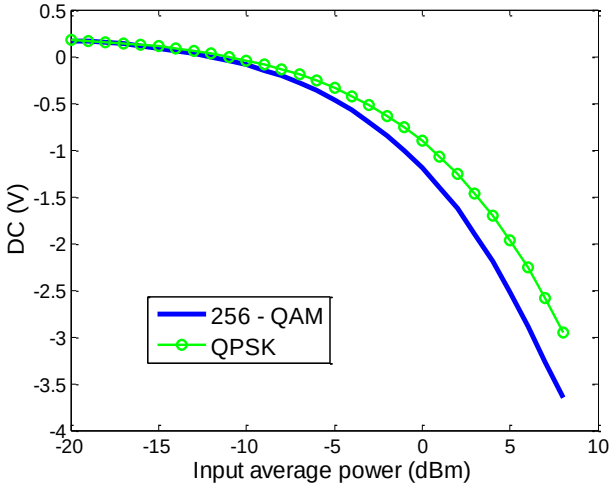

Fig. 5.20 – Qualitative comparison of power probe measurements of the two digitally modulated signals as a function of input power.

5.7 – Conclusions

This chapter demonstrates, with a practical example, analyzed issues on the use of diode power probes for measuring signals corresponding to new wireless standards. Two different aspects were studied, the effect of the signal's bandwidth and its PAPR on the power measurement.

Our analyses demonstrated mathematically, by simulations and by measurements, that the calibration of a power probe with a single-tone excitation does not guarantee the correct calibration for more complex forms of excitations. It's also proven that, as noted in chapter 4, the second order behaviour from the nonlinear generator isn't enough to modulate de Diode's nonlinear response, This incorrect assumption brings several erroneous results in its output measurements. This was then illustrated through measurement with digitally modulated signals, including a QPSK signal and a 256-QAM signal.

This chapter also demonstrate that a proper design of the diode power probe in order to account for low values of baseband impedance covering all the signal bandwidth is necessary. As well, the different values obtained with signals presenting high values of PAPR should be compensated for with different calibration approaches. Such calibrations

and measurement uncertainties are the subject of current research and is one of the major interests in future work.

CHAPTER 6

Interference Cancellation: New Configuration Technique for Cancellation of Strong Interferences from Adjacent Frequency Bands.

Beside all the issues that nonlinear behaviour brings to receivers architectures viewed in last chapters, other main problem that affects the RF communications systems is the cross-modulation interference between distinct systems that share near spectral frequency bands. If a system has a huge power level (relative to other system), even don't share the same frequency, it can entire collapse the reception of the desire signal. Besides the study from some known techniques of interference cancellation, the main objective of this chapter is the presentation and simulation/analyses from some new architectures able to mitigate the critical effects of these interferences, especially high jammers that associated with the nonlinear phenomenon can completely corrupt the good function of their "neighbours" systems. The idea is to build a interference canceller sub-system, that can be universal (works in any frequency) and adjustable to all RF technology known. To achieve this goal the main focus will be the compensation from the intermodulation distortion created in receiver's LNA, without using any pre-distortion subsystem and assuming the complete unknown from the jammer signal.

6.1 – Introduction

The co-existence of various technologies in the radio frequency spectrum has always led to problems of interference between systems. The regulatory authorities (whether national or international) try to avoid those interferences with rules and restrictions to radio frequency systems that coexist in the same band frequency or adjacent bands. However, even following all these standards and specifications, the presence of interference in a particular system is unavoidable, usually leading to degradation (or even the loss) of its quality and functionality.

Associated to the problem of loss of service quality, the developing of new technologies with high power densities, lower costs, able to "jamming" communications, "blind" locations and destroy the LNAs of receivers, either inadvertently, either as a product of technological warfare, lead to a constant concern of shielding of communications systems by preventing the failure of service or their destruction [56]. There are many scenarios where such interference is highly prejudicial and penalty in the performance of major systems. The most critical example is the military applications, where the role of communications is vital. The masking of a RF signal may have severe consequences and cause serious actions no less harmful. Other typical scenarios with interference problems are, for example, RFID, broadband systems or Software Defined Radio.

The RFID systems, especially the systems based on passive TAGs, are very sensitive to RF interferences. That happens because the transceiver TAG doesn't have own battery, harvesting their on energy to work and re-emitted the RF signal from the input signal received from the Reader. For that reason common RF systems or other ordinary fonts of jammer (like small appliances with a poor insulation) can severely damage both received/emitted signals [39][57][58].

The RF systems that are installed near big broadband systems (like TV or Radio emitters) can also suffer from interference problems, although the two systems work in very distinct frequency bands. The harmonics from broadband emitters could fall near the RF operation frequency and even their power level was significantly lower than their main broad signal, when the RF receiver has a good sensitivity, the power gap between both signals could be significant high, preventing a good and reliable signal reception.

The Software Defined Radio (or Cognitive Radio) as a system with a very wide bandwidth, it can experience some conflicts between different signals that share this band [59]. The main objective of the SDR is the construction of a radio frequency terminal capable of receiving and decoding all radio signals that are in the spectrum captured by it. Although the selection and decoding is done by software, the co-existence of several signals with different levels of power, raises serious problems in the ADC, where high intermodulation distortion products emerge, preventing the correct conversion of the signal from analogue to digital.

For all these reasons, the development from new techniques and sub-systems able to cancel (or at least mitigate strongly) the adverse effects caused by jammers in radio receivers architectures are extremely useful and even more important when the

interferences have high power densities such in military scenarios or near transmitters of broadband systems.

This chapter begins with a brief framework on the effects of intermodulation products in presence of strong radio frequency interference, that have been studied and presented in Chapter 3, using the same two-tones example. In next sections we presented and briefly discuss the techniques currently used to mitigate this issue and present the new configuration proposals, validated with several CAD/CAE simulations test. Finally we conclude the chapter with the main advantages and application from both configurations and draw some future work.

6.2 – Nonlinear distortion problems for huge interferences

As seen in chapter 2, in most radio architectures studied, one of the first components in a radio receiver's configuration is the LNA due to its low noise characteristics, allowing a system's Noise Figure of the as small as possible. In the receptor the Low Noise Amplifier component is always nonlinear, since for a certain input the output signal is no longer proportional, neither follows the super-position principle [2][36], as studied in Chapter 3. As presented in those chapter, the response from a nonlinear mechanism can be approximating by a Volterra series expansion if the system presents memory [2], represented by equation 6.1.

$$\delta_{NL}\left[y(x)\right] = K_0 + \underbrace{\frac{1}{1!}\frac{d\delta_{NL}\left[y(x)\right]}{dx}\bigg|_{x(t)=x_0}}_{C_1}\left(x-x_0\right) + \underbrace{\frac{1}{2!}\frac{d\delta_{NL}{}^2\left[y(x)\right]}{d^2x}\bigg|_{x(t)=x_0}}_{C_2}\left(x-x_0\right)^2 + \underbrace{\frac{1}{3!}\frac{d\delta_{NL}{}^3\left[y(x)\right]}{d^3x}\bigg|_{x(t)=x_0}}_{C_3}\left(x-x_0\right)^3 + \ldots \tag{6.1}$$

Using the two-tones input signal example (section 3.3) for better comprehension, let assume that our input signal *x(t)* is formed by two sinusoids, where ω_1 represents the interference frequency and ω_2 the desire signal frequency, assuming an interference amplitude (A_1) much bigger than the desire's one (A_2):

$$x(t) = \underbrace{A_1 \cos(\omega_1 t)}_{\text{Interference}} + \underbrace{A_2 \cos(\omega_2 t)}_{\text{Desire signal}} \tag{6.2}$$

Then, the LNA's output signal *y(t)* will be given by (assuming a memoryless system):

$$\begin{aligned} y(t) &= y_0 + y_1(t) + y_2(t) + y_3(t) + \ldots \\ y_1(t) &= c_1 x(t) = c_1.[A_1 \cos(\omega_1 t) + A_2 \cos(\omega_2 t)] \\ y_2(t) &= c_2 x^2(t) = c_2.[A_1 \cos(\omega_1 t) + A_2 \cos(\omega_2 t)]^2 \\ y_3(t) &= c_3 x^3(t) = c_3.[A_1 \cos(\omega_1 t) + A_2 \cos(\omega_2 t)]^3 \\ &\ldots \end{aligned} \tag{6.3}$$

As study, beyond linear response, there are third-order products that will fall within the band system. From them, the most problematic are the cross-modulation products because the interferer will have a double impact (in power) on the desired signal. To demonstrate the problem, let us observe only the output nonlinear products in-band, given by equation (6.4):

$$\begin{aligned} y(t) = &\underbrace{c_1 A_1 \cos(\omega_1 t) + c_1 A_2 \cos(\omega_2 t)]}_{\text{Linear response}} + \ldots \\ \ldots + &\underbrace{\frac{3}{2} c_3 A_1^2 A_2 \cos(\omega_1 t - \omega_1 t + \omega_2 t) + \frac{3}{2} c_3 A_1 A_2^2 \cos(\omega_2 t - \omega_2 t + \omega_1 t)}_{\text{Cross-modulation}} + \\ + &\underbrace{\frac{3}{4} c_3 A_1^3 \cos(2\omega_1 t - \omega_1 t) + \frac{3}{4} c_3 A_2^3 \cos(2\omega_2 t - \omega_2 t)}_{\text{AM/AM distortion}} + \\ + &\underbrace{\frac{3}{4} c_3 A_1^2 A_2 \cos(2\omega_1 t - \omega_2 t) + \frac{3}{4} c_3 A_1^2 A_2 \cos(2\omega_1 t - \omega_2 t)}_{\text{Intermodulation distortion}} + \ldots \end{aligned} \tag{6.4}$$

Since we are assuming a very strong interference (A_1 much higher than A_2), even if the LNA has of very small intermodulation coefficient (very low c3), the cross-modulation first element continues to strongly affect the signal reception. If the impact from the majority of these products can be mitigated (for certain cases) using bandpass filters (if there is a reasonable distance between ω_1 and ω_2), the effect of cross-modulation products that falls in ω_2 cannot be reduce by filtering or others common element, regardless the spectral distance between the signal and jammer.

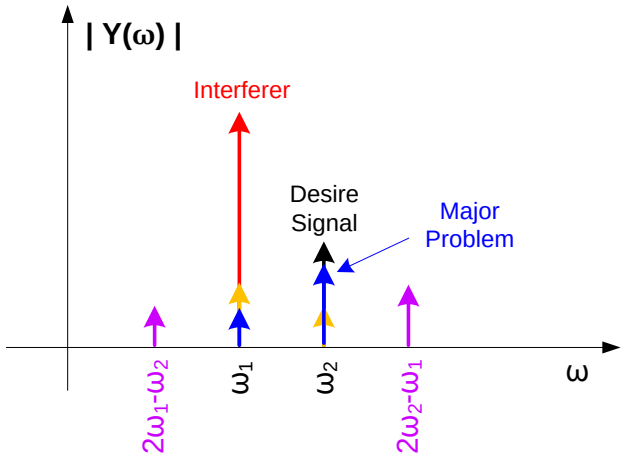

Fig. 6.1 - Spectrum components from a nonlinear system trunked to third order with two tones entry signal.

This impact is clearly visible in figure 6.1, where the cross-modulation product at $\omega_1 - \omega_1 + \omega_2$ could achieve a similar magnitude as the desire signal, since $c_3 A_1^2 A_2$ can be almost identical as $c_1 A_2$ (even $c_3 << c_1$).

For instance, if we have an interference signal with a power about 20dBm when the desired signal has a input power of -80dBm (using equation 3.29):

$$\begin{aligned} P_{1IN}\big|_{dB} = 20dBm \Rightarrow P_{1IN} = \frac{A_1^2}{2} = 10^{-1} \Leftrightarrow A_1 = \sqrt{0.2}\ (V) \\ P_{2IN}\big|_{dB} = -60dBm \Rightarrow P_{2IN} = \frac{A_2^2}{2} = 10^{-9} \Leftrightarrow A_2 = \sqrt{2\times10^{-9}} = \sqrt{0.2}\times10^{-4}\ (mV) \end{aligned} \tag{6.5}$$

and the c_1 and c_3 respectively 10 and 0.1 (100 times lower), the impact from the cross modulation product in desire signal will be:

$$\begin{aligned} & c_1 \times A_2 = 10\times\sqrt{0.2}\times10^{-4} = \sqrt{0.2}\times10^{-3} \rightarrow \text{desire signal amplitude} \\ & \left.\begin{aligned} & c_3 \times A_1^2 \times A_2 = 0.1\times\left(\sqrt{0.2}\right)^2 \times\sqrt{0.2}\times10^{-4} \\ & = 2\times100\times\sqrt{2}\times10^{-4} = 0.2\times\sqrt{0.2}\times10^{-4} \end{aligned}\right\} \text{cross-modulation amplitude} \end{aligned} \tag{6.6}$$

From equation 6.6, we see that the magnitude from the cross-modulation product is close from the linear response. Although it can be argue that the difference between power input tones is too high, it is undeniable that this intermodulation product can severally corrupt the desired signal and completely disabling the proper operation of the system.

Another affair identified with this example, it would be very difficult to significantly reduce the amplitude of the remaining nonlinear products in-band (relative to the desired signal) with a regular bandpass filter, particularly if frequency difference between the signals (jammer and desire) was too small. These products are not negligible since some of them could achieve a significant low signal/IMD relation.

6.3 – Implementation of interference cancellation system

As affirmed in the introduction, one of the goals from PhD. work will be the development of a new interference cancelation/attenuation architecture able to mitigate the impact of the intermodulation products resulting from the LNA in receiver's entry frontend. Although this problematic is well known in several real scenarios, there seems not exist extensive scientific studies that meets existing needs, particularly in cases where this problematic has a vital importance. The main studies/work developed in this area are focus in particular scenarios and systems, not looking for a wider solution with universal applications. For all these reasons, the study and development from new architectures are more tempting and a challenging work.

From the cancellation configurations known, we can distinguish the traditional Hartley and Weaver architectures, used to cancel the image frequency. Although these architectures (presented in the chapter 2) are not especially aimed to reduce the impact of the nonlinear products that affects the quality of radio systems, they can be used at starting point for the new architectures that will be present, using their sum cancellation principle in our configuration.

As more focus to reduce interference we can distinguish the configurations from Nightingale [60] or Raghavan [61]. Despite these architectures are especially designed for the cancellation of jammer signals, their settings depend on prior knowledge from the jammer signal(s) to their proper functioning, since their operating principle use a small interferer reference signal to cancel its effect on the desired signals. For this reason these architectures fail one of our goals: the principle that the jammer signal is unknown and/or could suffer several changes in several scenarios without affecting the system performance.

To achieve this goal the idea is to build a sub-system that will be couple in parallel with input LNA, as shown in Figure 6.2.

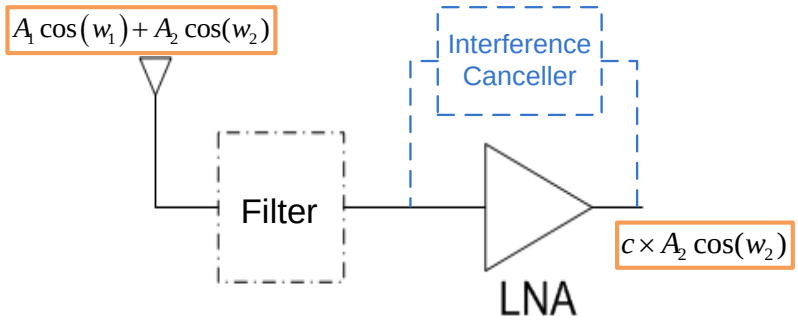

Fig. 6.2 - Main goal diagram.

As resume, the interference tries to linearize the LNA's behaviour and cancel the interferer signal, or in other words, mitigate not only the interferer signal but also all nonlinear products originated by LNA's behaviour, before the desire signal could be down-converted to an IF frequency or even baseband spectrum.

To fulfil this proposed goal we developed two new cancelation architectures that will be present in next sections. The first configuration is focused to satisfy all proposal targets: mitigate all nonlinear products and the interference signal, independently the frequency separation between jammer and desire signal. The second architecture is more oriented to only cancel the cross-modulation distortion, assuming in this case, that the jammer is sufficient far (in frequency) from desire signal frequency and their power level can be reasonable attenuated by filtering.

6.3.1 – Interference canceller proposal: first architecture

In figure 6.3 is shown our first proposal as an universal interference canceller. Based on RF components relatively well known, this configuration seems well adapted at any type of RF receiver and is completely independent from the input signal. The exception is the Frequency Limiter that could be replaced with a very tight band-pass filter (but with less effective results). Although it cannot properly be considered as constituent element from proposed architecture, since it's placed before the LNA and the desired architecture should only be connected in parallel with him, the Frequency Limiter restricts the input signal's power in frequency, changing the limitation coefficient with the correspondent frequency [62]. This different treatment in frequency allows a much lower offensive limiting technique and a reduction in amplitude of the intermodulation products on its output when compare with conventional limiters. This significant attenuation could also

be achieved with a cascade of filters but the negative impact in the Noise Figure of the system would be very harmful and completely undesired.

Besides the Frequency Limiter, the other RF components used such as Direct Couplers, Power Dividers/Combiners, Attenuators and Phase Shifters are common and widely used in RF architectures.

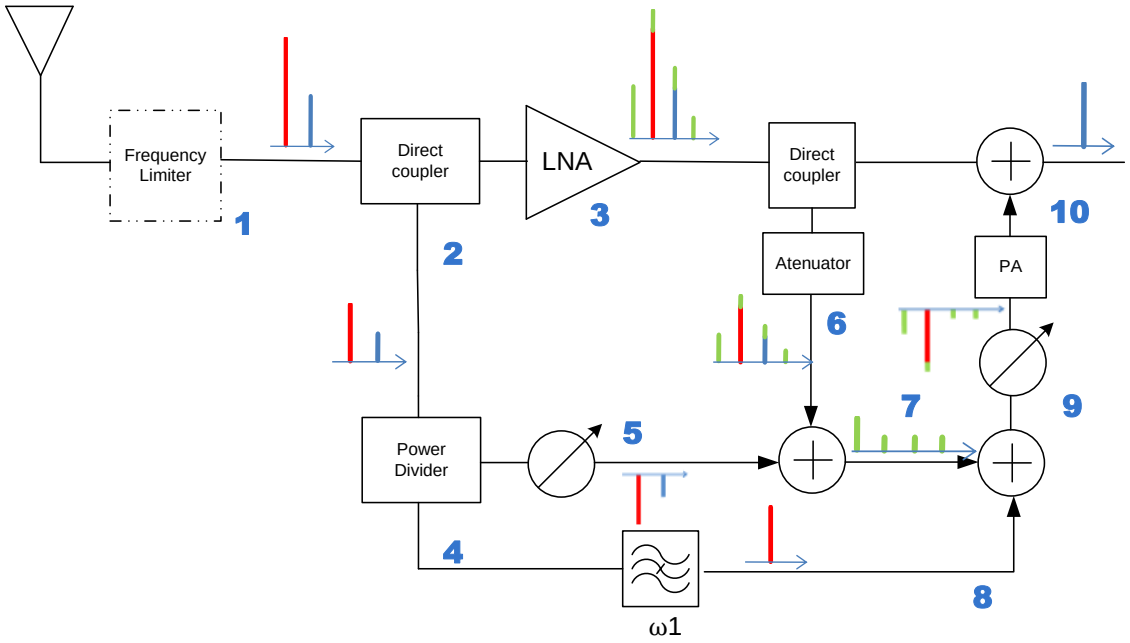

Fig. 6.3 – First proposed Interference Canceller schematic

To demonstrate the operational principle from this configuration let assume ideal components (that do not cause changes in amplitude or phase beyond expected). The well known two-tones signal is also used as introductory signal, where the interferer signal has a power level much higher than the desired signal.

$$x(t) = \underbrace{A_{r1}\cos(\omega_1 t)}_{\text{Interference}} + \underbrace{A_{r2}\cos(\omega_2 t)}_{\text{Desire signal}} \text{ (V)} \qquad (6.7)$$

$$P_{r1IN}\big|_{dB} >>> P_{r2IN}\big|_{dB}$$

In point 1, the Frequency Limiter has the function to reduce the interference signal of entrance (in ω_1). The Limiter threshold must be defined to reduce the intermodulation products but rather to guarantees that LNA does not enter in saturation mode. Although it is very important to be careful in the threshold definition in order to prevent the introduction of significant intermodulation products by the Frequency Limiter itself. Assuming 30dB attenuation in the interferer level (At) and 4dB for Insertion Loss (IL), the

resulting signal on 1 will be: (**note:** this will be our reference amplitude for the rest of the mathematical analyses)

$$x(t) = \underbrace{A_1 \cos(\omega_1 t)}_{\text{Interference}} + \underbrace{A_2 \cos(\omega_2 t)}_{\text{Desire signal}} \text{ (V)}$$
$$A_1 = \frac{A_{r1}}{At};\ A_2 = \frac{A_{r2}}{IL}; \tag{6.8}$$

When the signal arrives to the Directional Coupler, a small reference signal will be push to feedback way. Typically this reference is 20-30dB lower than the original signal. From now on we have two distinct signals. Let identify $x_p(t)$ as the signal from the main path and $x_s(t)$ as the signal in the secondary path. If $x_p(t)$ remain unchanged, the $x_s(t)$ undergoes a change of amplitude given by:

$$x_s(t) = \frac{A_1}{A_D}\cos(\omega_1 t) + \frac{A_2}{A_D}\cos(\omega_2 t) \text{ (V)} \tag{6.9}$$

where A_D is the reference attenuation in the Directional Coupler.

When the main signal passes through the LNA, the nonlinear products will emerge in LNA's output signal. Looking only for the components in-band, the resultant signal will be:

$$\begin{aligned} x_p(t) &= c_1 A_1 \cos(\omega_1 t) + c_1 A_2 \cos(\omega_2 t) \\ &\ldots + c_3 A_1^3 \cos(\omega_1 t) + \frac{3}{4} c_3 A_2^3 \cos(\omega_2 t) + \\ &+ \frac{3}{2} c_3 A_1 A_2^2 (1)\cos(\omega_1 t) + \frac{3}{4} c_3 A_1 A_2^2 \cos(2\omega_2 t - \omega_1 t) + \\ &+ \frac{3}{2} c_3 A_1^2 A_2 \cos(\omega_2 t) + \frac{3}{4} c_3 A_1^2 A_1 \cos(2\omega_1 t - \omega_2 t) + \ldots \end{aligned} \tag{6.10}$$

where c_1 and c_3 are the linear gain and third order gain coefficients respectively. The expression 6.10 can be simplified as:

$$\begin{aligned} x_p(t) &= \left[c_1 A_1 + \frac{3}{4} c_3 A_1^3 + \frac{3}{2} c_3 A_1 A_2^2 \right] \cos(\omega_1 t) + \left[c_1 A_2 + \frac{3}{4} c_3 A_2^3 + \frac{3}{2} c_3 A_1^2 A_2 \right] \cos(\omega_2 t) \\ &+ \frac{3}{4} c_3 A_1 A_2^2 \cos(2\omega_2 t - \omega_1 t) + \frac{3}{4} c_3 A_1^2 A_1 \cos(2\omega_1 t - \omega_2 t) + \ldots \end{aligned} \tag{6.11}$$

Back to secondary path, in point 4, the Power Divider is used to create a second reference signal for future interference cancellation. The two new signals ($x_{s1}(t)$ and $x_{s2}(t)$) have half the power of the signal $x_s(t)$.

$$\begin{aligned} x_{s1}(t) = x_{s2}(t) &= \frac{A_1 / A_D}{2}\cos(\omega_1 t) + \frac{A_2 / A_D}{2}\cos(\omega_2 t)\ \text{(V)} \\ &= \frac{A_1}{2A_D}\cos(\omega_1 t) + \frac{A_2}{2A_D}\cos(\omega_2 t)\ \text{(V)} \end{aligned} \tag{6.12}$$

The Phase Shifter present in point 5 makes a 180º shift delay in the reference phase signal. This change in phase will be use in cancellation of the two original tones, allowing obtaining a replica from the nonlinear products only generated in the LNA.

$$\begin{aligned} x_{s1}(t) &= \frac{A_1}{2A_D}\cos(\omega_1 t - 180^\circ) + \frac{A_2}{2A_D}\cos(\omega_2 t - 180^\circ)\ \text{(V)} \\ &= -\frac{A_1}{2A_D}\cos(\omega_1 t) - \frac{A_2}{2A_D}\cos(\omega_2 t)\ \text{(V)} \end{aligned} \tag{6.13}$$

In the main path another Direct Coupler pushes a replica from the LNA's output signal and reduces the power level of this replica with an attenuator. Once again, the Direct Coupler is chosen (instead of a power divider) to avoid reducing the power from the desire signal in main path and, on other hand, allows the use of a smaller attenuator. With this two RF components, the replica ($x_{s3}(t)$) present in 6 will be given by:

$$\begin{aligned} x_{s3}(t) = &\frac{\left[c_1 A_1 + \frac{3}{4}c_3 A_1^3 + \frac{3}{2}c_3 A_1 A_2^2\right]}{A_D \times A_{At}}\cos(\omega_1 t) + \frac{\left[c_1 A_2 + \frac{3}{4}c_3 A_2^3 + \frac{3}{2}c_3 A_1^2 A_2\right]}{A_D \times A_{At}}\cos(\omega_2 t) \\ &+ \frac{\frac{3}{4}c_3 A_1 A_2^2}{A_D \times A_{At}}\cos(2\omega_2 t - \omega_1 t) + \frac{\frac{3}{4}c_3 A_1^2 A_1}{A_D \times A_{At}}\cos(2\omega_1 t - \omega_2 t) + \ldots \end{aligned} \tag{6.14}$$

where A_D and A_{At} are the attenuation from the Direct Coupler and the Attenuator respectively.

The resulting signal $x_{s3}(t)$, is then added to $x_{s1}(t)$ in point 7.

$$x_s(t) = x_{s1}(t) + x_{s3}(t) = \\ = \frac{\left[c_1 A_1 + \frac{3}{4}c_3 A_1^3 + \frac{3}{2}c_3 A_1 A_2^2\right]}{A_D \times A_{At}}\cos(\omega_1 t) + \frac{\left[c_1 A_2 + \frac{3}{4}c_3 A_2^3 + \frac{3}{2}c_3 A_1^2 A_2\right]}{A_D \times A_{At}}\cos(\omega_2 t) \\ + \frac{\frac{3}{4}c_3 A_1 A_2^2}{A_D \times A_{At}}\cos(2\omega_2 t - \omega_1 t) + \frac{\frac{3}{4}c_3 A_1^2 A_1}{A_D \times A_{At}}\cos(2\omega_1 t - \omega_2 t) - \frac{A_1}{2A_D}\cos(\omega_1 t) - \frac{A_2}{2A_D}\cos(\omega_2 t) + \ldots \quad (6.15)$$

The idea is obtain a replica from the LNA's nonlinear products only. To obtain a "perfect" replica we must ensure that:

$$\underbrace{\left[\frac{c_1 A_1}{A_D \times A_{At}} - \frac{A_1}{2A_D}\right]}_{\approx 0}\cos(\omega_1 t) + \underbrace{\left[\frac{c_1 A_2}{A_D \times A_{At}} - \frac{A_2}{2A_D}\right]}_{\approx 0}\cos(\omega_2 t) \\ \Rightarrow \frac{c_1}{A_D \times A_{At}} \approx \frac{1}{2A_D} \Leftrightarrow \frac{c_1}{A_{At}} \approx \frac{1}{2} \quad (6.16)$$

then, $x_s(t)$ will be:

$$x_s(t) = \frac{3}{4}\frac{c_3}{(A_D \times A_{At})}\left[A_1^3 + 2A_1 A_2^2\right]\cos(\omega_1 t) + \frac{3}{4}\frac{c_3}{(A_D \times A_{At})}\left[A_2^3 + 2A_1^2 A_2\right]\cos(\omega_2 t) \\ + \frac{3}{4}\frac{c_3 A_1 A_2^2}{(A_D \times A_{At})}\cos(2\omega_2 t - \omega_1 t) + \frac{3}{4}\frac{c_3 A_1^2 A_1}{(A_D \times A_{At})}\cos(2\omega_1 t - \omega_2 t) + \ldots \quad (6.17)$$

In the third secondary path (at point 8) the stop-band filter is used to cut the desire signal, maintaining the interference signals. This is important because the resultant signal will be used as interferer canceller when combined with the main path signal. If the replica from desire signal isn't cut at this moment it will appear at the final stage and degrade the final desire signal. At first view it was possible to use a passband filter (centred at ω_1) instead of the less used stop-band filter. However it will be a mistake since this change will remove the universality characteristic from the configuration (will requires a pre-knowledge from jammer to achieve ω_1).

Considering IL_{RB} and A_{RB} as the filter's insertion lost and the attenuation in rejection band respectability, the algebraic equation from $x_{s2}(t)$ at point 8 is given by:

$$x_{s2}(t) = \frac{A_1}{2A_D \times IL_{RB}}\cos(\omega_1 t)\ (\mathrm{V}) \left(\text{assuming } \frac{A_2}{2A_D \times A_{RB}} \approx 0\right) \quad (6.18)$$

Combining these two last contributions results in a signal that contains a replica from the interference and the intermodulation products ($x_{sf}(t)$):

$$x_{sf}(t)=\frac{3}{4}\frac{c_3}{(A_D\times A_{At})}\left[A_1^3+2A_1A_2^2\right]\cos(\omega_1 t)+\frac{3}{4}\frac{c_3}{(A_D\times A_{At})}\left[A_2^3+2A_1^2A_2\right]\cos(\omega_2 t)$$
$$+\frac{3}{4}\frac{c_3A_1A_2^2}{(A_D\times A_{At})}\cos(2\omega_2 t-\omega_1 t)+\frac{3}{4}\frac{c_3A_1^2A_1}{(A_D\times A_{At})}\cos(2\omega_1 t-\omega_2 t)+\frac{A_1}{2A_D\times IL_{RB}}\cos(\omega_1 t)+\ldots \quad (6.19)$$

At this point, a second Phase Shifter is used to make another 180º delay and a Power Amplifier (PA) is use to raise this reference signal to the output power level from the LNA. Considering G_{PA} as gain from PA, the signal in 9 will be:

$$x_{sf}(t)=-\left[\frac{A_1\times G_{PA}}{2A_D\times IL_{RB}}+\frac{3}{4}\frac{c_3\times G_{PA}}{(A_D\times A_{At})}A_1^3+\frac{3}{2}\frac{c_3\times G_{PA}}{(A_D\times A_{At})}A_1A_2^2\right]\cos(\omega_1 t)$$
$$-\left[\frac{3}{4}\frac{c_3\times G_{PA}}{(A_D\times A_{At})}A_2^3+\frac{3}{2}\frac{c_3\times G_{PA}}{(A_D\times A_{At})}A_1^2A_2\right]\cos(\omega_2 t) \quad (6.20)$$
$$-\frac{3}{4}\frac{c_3A_1A_2^2\times G_{PA}}{(A_D\times A_{At})}\cos(2\omega_2 t-\omega_1 t)-\frac{3}{4}\frac{c_3A_1^2A_1\times G_{PA}}{(A_D\times A_{At})}\cos(2\omega_1 t-\omega_2 t)+\ldots$$

Finally, the main signal $x_p(t)$ and the final secondary signal $x_{sf}(t)$ are combine, resulting the cancellation from all undesired components. To guarantee this cancellation, is extremely important that:

$$\frac{3}{4}\frac{c_3\times G_{PA}}{(A_D\times A_{At})}A_1^3\approx\frac{3}{4}c_3A_1^3\Leftrightarrow\frac{G_{PA}}{(A_D\times A_{At})}\approx 1\Leftrightarrow G_{PA}\approx(A_D\times A_{At})$$
$$\frac{A_1\times G_{PA}}{2A_D\times IL_{RB}}\approx c_1A_1\Leftrightarrow\frac{G_{PA}}{2A_D\times IL_{RB}}\approx c_1\Leftrightarrow\frac{A_D\times A_{At}}{2A_D\times IL_{RB}}\approx c_1\Leftrightarrow\frac{A_{At}}{2\times IL_{RB}}\approx c_1 \quad (6.21)$$

The final output signal will be given by:

$$x_{ouput}(t)=x_p(t)+x_{sf}(t)=c_1A_2\cos(\omega_2 t)\ (\mathrm{V}) \quad (6.22)$$

Although has been considered ideal components in this theoretical analysis, even with the use of real components we expect that real phase deviations could be controlled in the Phase Shifters and the normal amplitude changes be compensated by the Attenuator and the Power Amplifier. This assumption will be proven in next section where simulations using real components parameters are tested in very though conditions (with more than 60dB between the jammer and the desire signal).

As expected, the proposed sub-system has the advantage that could be fully included in all types of operating systems and mitigate almost any type of interference (unless the interference and desire signal share the **same** frequency).

6.3.2 - Cad/Cae simulation

In order to validate the theory demonstrated in previous section, the proposed configuration was simulated in a CAD/CAE Simulator from Advance Design System (ADS) [63], using Harmonic Balance. The ADS model is present in Figure 6.4 and can be reviewed in more detail in Appendix A.

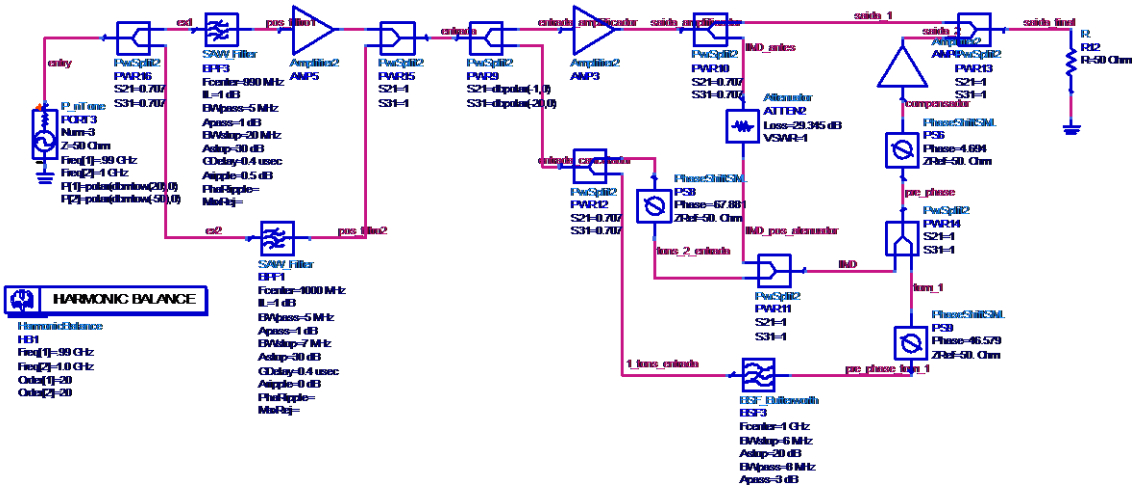

Fig. 6.4 – ADS schematic model from first proposal sub-system

6.3.2.1 – First simulation: huge interferer with well calibrated components

To test the limits of the proposed sub-system, in the first simulation (with all circuit well calibrated) we consider the interferer quite close to the desire signal (in frequency). The input signal has two tones: the interference signal with a power of 20dBm and the desired signal with -50dBm at 990Mhz and 1GHz respectively (figure 6.5).

Despite not being a focus in proposed architecture, in the first part of the configuration we simulate the behaviour of the frequency limiter. Since the interferer is so close in frequency from the desire signal, the goal is to attenuate the jammer by -30dB, which is difficult to achieve with a regular filtration in these specific cases. The resultant signal is shown in Figure 6.6.

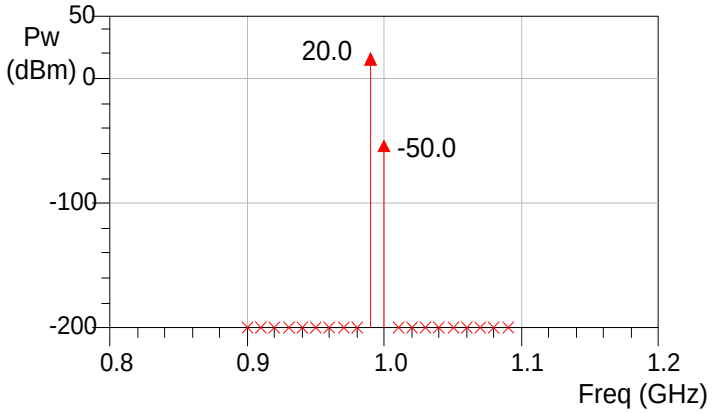

Fig. 6.5 – Input signal: the two-tones are very close in frequency and with 70 dB difference in power.

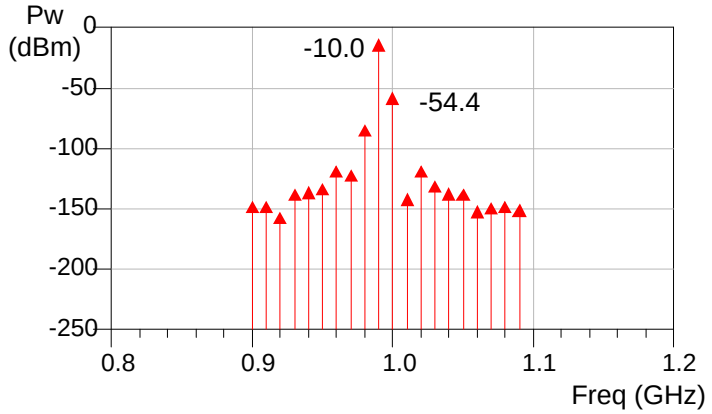

Fig. 6.6 – Signal at the entry of the second part of the configuration

As observe, the jammer was attenuated in 30dB (as wanted) but unfortunately the desire signal was also reduce 4-5 dB, due insertion losses and attenuation in band from the previous block.

Now we enter in the main focus of the circuit where the jammer and the nonlinear products will be mitigated. The Limiter's signal enters in nonlinear device (the LNA as already stated), not before a small replica is catch by direct coupler for further IMD cancellation. It is used a LNA's nonlinear model trunked to 20th order[3] and its output result shown in Figure 6.7.

As expected, in the LNA's output signal, we can observe the two original tones amplified (the jammer presents a high power level) in addition with several IMD products with levels close to the power of the desired signal.

[3] LNA's model parameters and other components are also present in appendix A

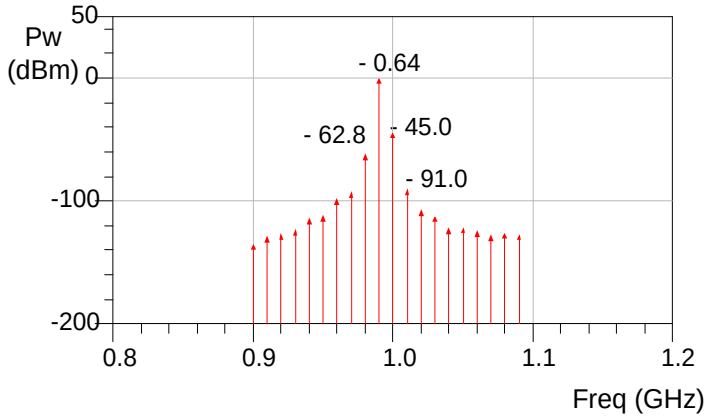

Fig. 6.7 – LNA's output signal.

Later, from paths 2 and 3 will be possible to create a replica from these IMD products and a single replica from the interferer that will cancel their contribution in main path.

The IMD replica (figure 6.8), as explain in previous section, has a crucial role in this architecture. To achieve reliable results at his point is essential a very good synchronization between both paths (either in magnitude and phase). For that reason the Phase Shifter and the Attenuator must have a good accuracy to guarantee a correct cancellation.

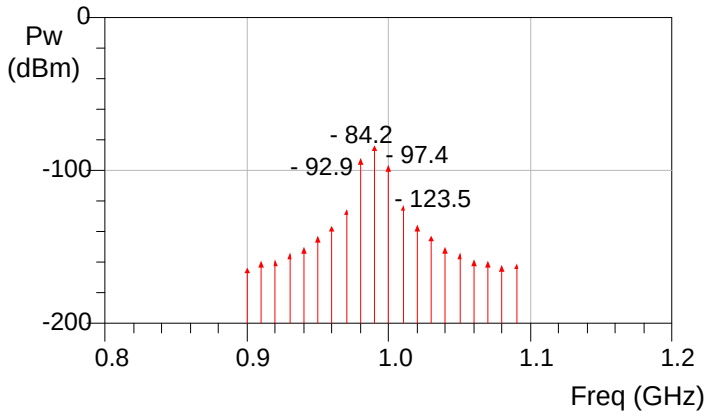

Fig. 6.8 – IMD replica of the output signal.

In third path, a stop-band filter cuts the desire tone, creating the interference's replica (figure 6.9), that will be used to mitigate LNA's output interference tone.

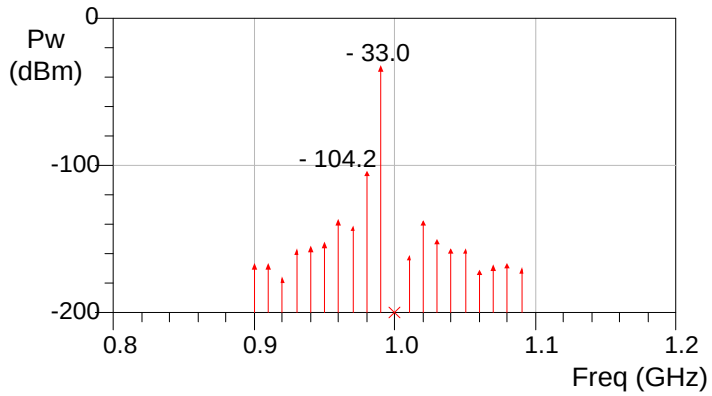

Fig. 6.9 – Interference replica.

Combining these two replicas with a properly adjusting in Phases Shifters and Amplifier's gain (in secondary path) is possible to obtain the secondary signal that contains a good "mirror" from jammer and IMD products in the main path signal (figure 6.10).

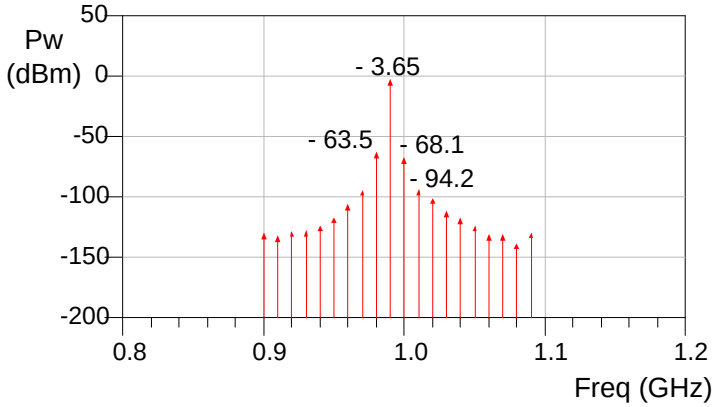

Fig. 6.10 – Secondary path final signal.

Finally the system output signal is the result from the main signal combination with the final secondary path signal (figure 6.11).

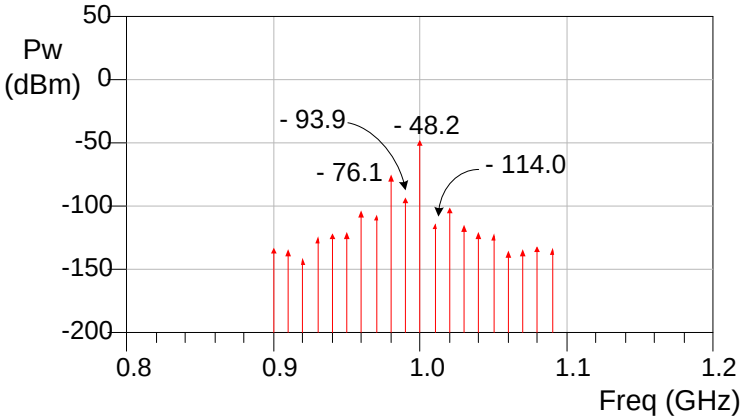

Fig. 6.11 – System final output signal.

This final signal presents a very low power level for interferer and also a good Signal/IMD ratio. This is a very good result with such difficult input conditions that give us hope in the good and reliable response for all scenarios from presented architecture. The main concern (that will be tested in next simulation) is the architecture's tolerance to variations in its own elements, since in this simulation the parameters were set very strict. Before moving to Monte Carlo simulation, it is important, to refer some small differences between the theoretical architecture introduced and the one used in the Harmonic Balance simulation. Comparing Figures 6.3 and 6.4, it is clear a displacement from a Phase Shifter in the second third path. This change was necessary to rectify the common imperfections present in the real components used. These imperfections cause unforeseen changes in the phases of both replicas, which not allow the phase adjustment after their combination as originally planned. This reason led to the individual adjustment of each replica forcing the existence of a Phase Shifter in every way before the junction of the two contributions. The Phase Shifter after combination is no longer necessary.

6.3.2.2 – Second simulation: Monte Carlo technique

To understand to potential of the proposed cancelation configuration and evaluate it robustness to variations in its elements own (especially the Phase Shifters), we made a Harmonic Balance simulation associated with the Monte Carlo technique to obtain results as close as possible to the real performance of the system. The simulations were doing with 250 iterations, with a variation of the ±1% in the most problematic electronic components.

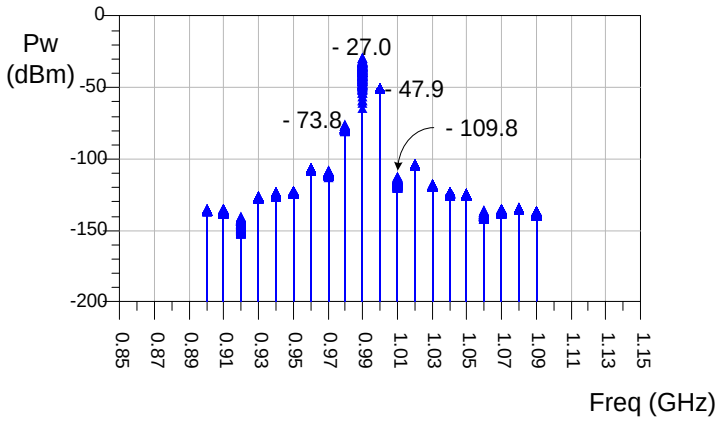

Fig. 6.12 – Final signal using Monte Carlo technique.

Observing the Figure 6.12, even in the worst scenario the jammer signal is 20 dB above the power level of the desired signal, this simulation shows that in the majority cases the

power from the interferer is lower (or at same level) as the desired signal, despite changes in the parameters from the architecture's components. Another good feature achieve with this configuration is the reasonable mitigation from IMD products, because even in the worst cases, their power don't exceed -74dBm, at least 16 dB below the desired signal. That represents a reduction in the interferer around than 50dB for worse cases and 70dB in the majority simulations and an attenuation of 11 dB (at least) in the closest IMD products relative to desire signal power.

In conclusion, the presented architecture reaches:

- a significant reduction from intermodulation products in band, allowing a good S/IMD ratio even in worst scenarios.
- a good interferer's power attenuation to the levels of the desire signal. This is especially important when the signal jammer is "frequency' neighbour" from the desired signal, hindering the use of regular filtering.

As drawbacks, this configuration has a substantial number of components used (which may make it unattractive for simplest systems and/or with reduced sources of energy) and requires very good calibration parameters in order to reach optimal results at interferer power levels (Phase Shifters and Power Amplifiers must be tightly controlled). The way to ensure satisfactory results requires the use of components with lower tolerances and a rigorous calibration of the system canceller. Regarding only the IMD products, this architecture reaches quite reasonable results even when conditions are not ideal and the constituent components show some variations.

6.4 – Implementation of interference cancellation system – second proposal

One of the main handicaps from the previously proposed architecture is the high number of RF components and the relatively high costs from some of them (for use in simplest and small circuits). This fact makes the typology not so cheap as wanted for certain systems.

Continuing the study and development from new strategies to make the previously presented architecture more simpler, with less components (especially the more expensive and intolerant ones like Phase Shifters) and reducing its cost, we realized that for certain scenarios with reasonable frequency separation between the interferer and desire signal

and a smaller power difference between them, the previous architecture could be more complex and expensive than necessary.

For these cases, the main focus will be the cross-modulation products that fall at the same frequency than desire signal, since they are completely independent from frequency's distance between the two signals and assuming that interferer and other intermodulation products can be mitigate by filtering. With this idea in mind, a more simple and easy to integrate topology was developed with similar goals but with less complexity and cheaper than the previous architecture. These new topology is presented in Figure 6.13.

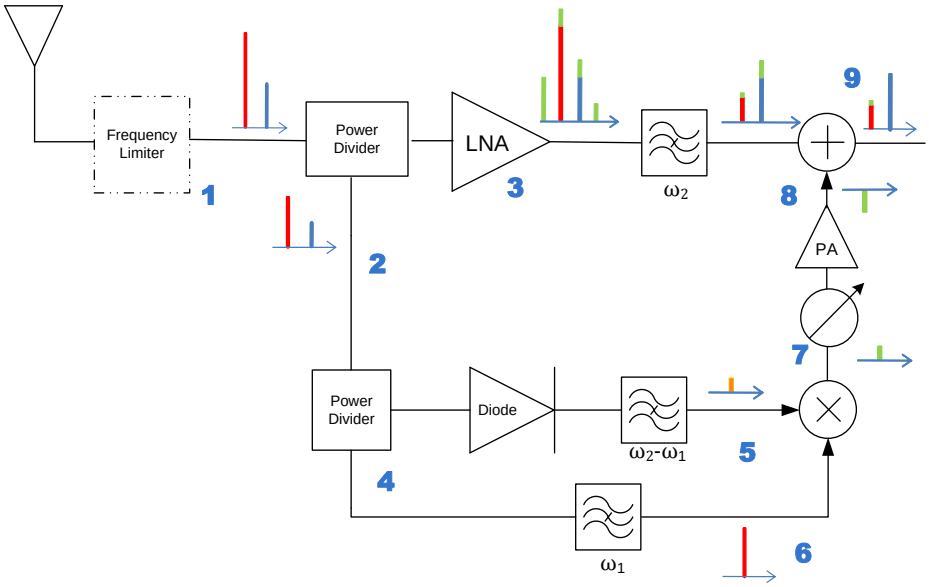

Fig. 6.13 - Second interference cancelation schematic propose

Since the system's main objective is the cancelation of the intermodulation products that fall over the desire signal frequency (ω_2) and $\Delta\omega$ (ω_2-ω_1) is reasonable larger, that allows the use of realistic filters with higher rejection attenuation levels. This fact enables the reduction from the number of elements used, minimizing the costs and decreasing possible variations in their constituent elements. In next section is presented the mathematical analyses from this second proposal.

6.4.1 – Second Interference Canceller proposal: Theoretical analysis

In this second architecture the first three steps are quite similar to the previous configuration. The only difference is the use of a Power Divider (in step 2) instead of a Direct Coupler, reduction even more the architecture's costs without an impact in the

performance of the device (as will be seen next). This configuration also allows the use of a regular band-selection filter (instead of the Frequency Limiter), since frequency diference between interferer tone and desire signal tone is five times bigger than used in last simulation. With this information and using the same two-tones input signal, $x_p(t)$, $x_{s1}(t)$ and $x_{s2}(t)$ will be almost identical to equations 6.9 and 6.11, with small differences in amplitude:

$$x_p(t)=\frac{1}{2}\left[c_1A_1+\frac{3}{4}c_3A_1^3+\frac{3}{2}c_3A_1A_2^2\right]\cos(\omega_1 t)+\frac{1}{2}\left[c_1A_2+\frac{3}{4}c_3A_2^3+\frac{3}{2}c_3A_1^2A_2\right]\cos(\omega_2 t)$$
$$+\frac{1}{2}\times\frac{3}{4}c_3A_1A_2^2\cos(2\omega_2 t-\omega_1 t)+\frac{1}{2}\times\frac{3}{4}c_3A_1^2A_1\cos(2\omega_1 t-\omega_2 t)+\ldots \quad (6.23)$$

$$x_{s1}(t)=x_{s2}(t)=\frac{A_1/2}{2}\cos(\omega_1 t)+\frac{A_2/2}{2}\cos(\omega_2 t)\ (\mathrm{V})$$
$$=\frac{A_1}{4}\cos(\omega_1 t)+\frac{A_2}{4}\cos(\omega_2 t)\ (\mathrm{V}) \quad (6.24)$$

Although the similarities between the two proposals stops here. In this second configuration we use a diode to work as a generator of nonlinearities. The aim is not to create replicas from all LNA's third order nonlinear products, but only the second order product(s) which subsequently multiplied by the jammer signal will originate a replica from the LNA's cross-modulation product(s) that falls at ω_2. This could be done with a Schottky diode because, as known, for their "knee" starting conducting voltage, the diode's second order products will be very strong due their similarity to a quadratic function. The diode's second order nonlinear products will be given by:

$$x_{s1}(t)\big|_{2nd}=c_2\left(\frac{A_1}{4}\cos(\omega_1 t)+\frac{A_2}{4}\cos(\omega_2 t)\right)^2$$
$$=c_2\frac{A_1^2}{16}\cos^2(\omega_1 t)+c_2\frac{A_1A_2}{8}\cos(\omega_1 t)\cos(\omega_2 t)+c_2\frac{A_1^2}{16}\cos^2(\omega_1 t) \quad (6.25)$$

Using the trigonometric equalities:

$$x_{s1}(t)\big|_{2nd}=c_2\frac{A_1^2}{16}\frac{1+\cos(2\omega_1 t)}{2}+c_2\frac{A_2^2}{16}\frac{1+\cos(2\omega_2 t)}{2}+$$
$$+c_2\frac{A_1A_2}{8}\frac{\cos(\omega_1 t+\omega_2 t)\times\cos(\omega_2 t-\omega_1 t)}{2} \quad (6.26)$$

Finally resulting:

$$x_{s1}(t)\big|_{2nd} = c_2\frac{A_1^2 + A_2^2}{32} + c_2\frac{A_1^2}{32}\cos(2\omega_1 t) + c_2\frac{A_2^2}{32}\cos(2\omega_2 t) + c_2\frac{A_1 A_2}{16}\cos((\omega_1+\omega_2)t) + c_2\frac{A_1 A_2}{16}\cos((\omega_2-\omega_1)t) \tag{6.27}$$

From the diode's output signal we filter the non-DC baseband products that, for the two-tone example, will be only the ω_2 - ω_1 tone. This product mixing with interferer signal will create a replica from the most problematic LNA's intermodulation product $\omega_2+\omega_1-\omega_1$ that will corrupt the desired signal tone. With this information, the $x_{s1}(t)$ at point 5 and $x_{s2}(t)$ at point 6 will be given by:

$$x_{s1}(t)\big|_5 = c_2\frac{A_1 A_2}{16}\cos((\omega_2-\omega_1)t) \tag{6.28}$$

$$x_{s2}(t)\big|_6 = \frac{A_1}{4}\cos(\omega_1 t) \tag{6.29}$$

The combination of these two signals will result in:

$$x_{sfinal}(t) = x_{s1}(t)\big|_5 \times x_{s2}(t)\big|_6 = c_2\frac{A_1 A_2}{16}\cos((\omega_2-\omega_1)t)\times\frac{A_1}{4}\cos(\omega_1 t); \tag{6.30}$$

$$x_{sfinal}(t) = c_2\frac{A_1^2 A_2}{64}\left[\cos((\omega_2-\omega_1+\omega_1)t) + \cos((\omega_2-\omega_1-\omega_1)t)\right] = c_2\frac{A_1^2 A_2}{64}\left[\cos(\omega_2 t) + \cos((\omega_2-2\omega_1)t)\right] \tag{6.31}$$

From equation 6.31, is possible to note that $x_{sfinal}(t)$ magnitude depends twice from interferer amplitude, revealing the importance when receiver's sensitivity is much lower than jammers power levels.

The next step is to change the replica's phase in order to be opposition with the LNA's intermodulation product. Ideally, the Shift Register should make a 180º phase delay in the $x_{sfinal}(t)$ signal, but, since we are using real components parameters, this delay must be adjust to reflect the LNA's phase response and the non-ideal behaviour from all architecture's RF components. This adjustment is important and could be one of the main adaptability focus for more demanding scenarios.

Before the final combination, it is still necessary to use a PA to raise the replica's power level to match with its contribution in main path. In this configuration the gain will be probably lower than in previous proposed architecture (allowing a significant reduction in energy consumption).

The final signal to cancel the intermodulation product at ω_2 will be:

$$x_{sfinal}(t) = -c_2 \frac{A_1^2 A_2 G_{PA}}{64}\left[\cos(\omega_2 t) + \cos\left((\omega_2 - 2\omega_1)t\right)\right] \tag{6.32}$$

In the main path, the $x_P(t)$ signal (from point 3) is filter with bandpass filter (or a cascade of filters) that must have a very good attenuation in rejection band to maximize the interference's attenuation. The use of this/these filter(s) after the LNA it´s not significant harmful to the system behaviour, because the LNA significantly reduces the filter's contribution for receiver's Noise Figure. Since we are assuming a reasonable frequency separation between tones, the common filtration process can drastically reduce the interferer power level and neighbours intermodulation products without using more complex and expensive components. The filter's output signal will be (considering the $2\omega_2 - \omega_1$ and $2\omega_1 - \omega_2$ power levels not relevant):

$$\begin{aligned} x_p(t) = {} & \frac{1}{2\times Af_{RB}}\left[c_1 A_1 + \frac{3}{4}c_3 A_1^3 + \frac{3}{2}c_3 A_1 A_2^2\right]\cos(\omega_1 t) + \\ & + \frac{1}{2\times Af_{PB}}\left[c_1 A_2 + \frac{3}{4}c_3 A_2^3 + \frac{3}{2}c_3 A_1^2 A_2\right]\cos(\omega_2 t) \end{aligned} \tag{6.33}$$

where Af_{PB} is the Insertion Loss and Attenuation in passband and Af_{RB} the attenuation in rejection-band.

Finally, combining both contributions, the output result has the desire signal and a small part from interferer and neighbour intermodulation products that can be eliminated with a second filter block (if not completely reduced with the previous one). The final output signal $x_O(t)$ is then given by:

$$\begin{aligned} x_O(t) = x_p(t) + x_{sfinal}(t) = {} & \frac{1}{2\times Af_{RB}}\left[c_1 A_1 + \frac{3}{4}c_3 A_1^3 + \frac{3}{2}c_3 A_1 A_2^2\right]\cos(\omega_1 t) + \\ & + \frac{1}{2\times Af_{PB}}\left[c_1 A_2 + \frac{3}{4}c_3 A_2^3 + \frac{3}{2}c_3 A_1^2 A_2\right]\cos(\omega_2 t) - c_2 \frac{A_1^2 A_2 G_{PA}}{64}\left[\cos(\omega_2 t)\right] \end{aligned} \tag{6.34}$$

To maximize the output signal's quality the coefficients must be adjust as shown in equation 6.35 in order to achieve a good IMD cancelation at ω_2.

$$\frac{3}{4}c_3A_2^3+\frac{3}{2}c_3A_1^2A_2=c_2\frac{A_1^2A_2G_{PA}}{64}\Leftrightarrow 3c_3\left(\frac{A_2^2}{2}+A_1^2\right)=c_2\frac{A_1^2G_{PA}}{32} \tag{6.35}$$

and knowing that $A_1>>A_2$, this equality can be simplify as:

$$3c_3\left(\frac{A_2^2}{2}+A_1^2\right)=c_2\frac{A_1^2G_{PA}}{32}\Leftrightarrow c_2=c_3\frac{96}{G_{PA}}\left(\frac{A_2^2}{2A_1^2}+1\right)\xrightarrow[A_2^2\ll A_1^2]{}c_2=c_3\frac{96}{G_{PA}} \tag{6.36}$$

Resulting a final signal given by:

$$x_O(t)=\underbrace{\frac{1}{2\times Af_{PB}}c_1A_2\cos(\omega_2t)}_{\text{Desire signal}}+\underbrace{\frac{1}{2\times Af_{RB}}\left[c_1A_1+\frac{3}{4}c_3A_1^3+\frac{3}{2}c_3A_1A_2^2\right]\cos(\omega_1t)}_{\text{Interferer}} \tag{6.37}$$

With equation 6.37 we able to de-mixing our desire signal, without great impact from the interferer (from this point it could be treat as a regular interferer). The desire signal is also "free" from any intermodulation product generated by LNA.

This theoretical analyse shows that, for certain scenarios where the main concern is the cross-modulation products that falls over the desire signal (instead of the interference itself), this smaller and cheaper architecture seems to achieve reasonable results, making them suitable for RF systems with less energy resources and simpler architectures.

6.4.2 – Cad/Cae simulation of the system

Like in previous architecture, to validate the mathematical analyses presented in section above, the proposed configuration was simulated in the ADS CAD/CAE Simulator, using the Harmonic Balance method and real values for the majority of the RF components.

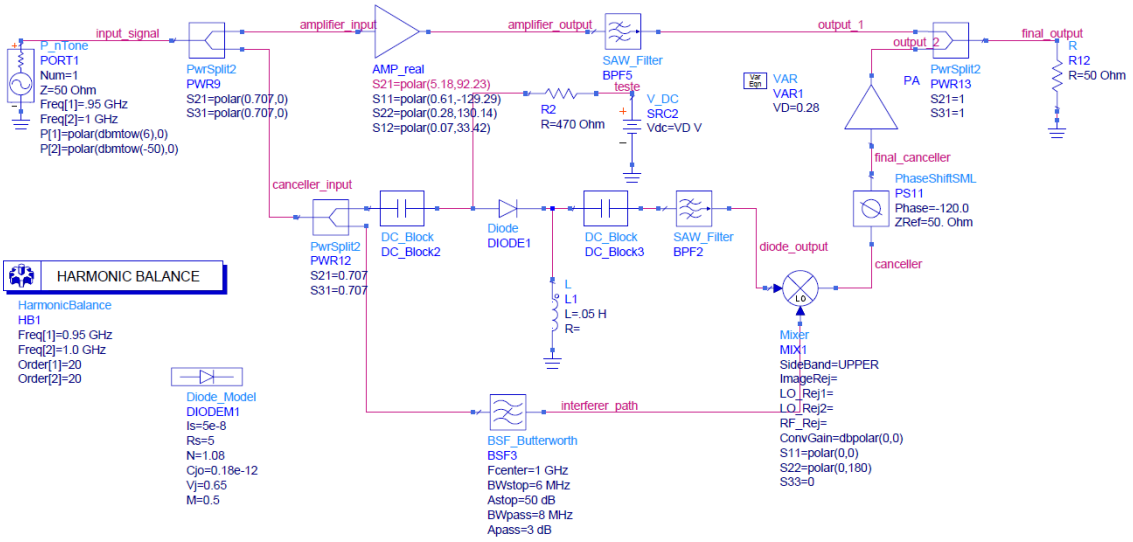

Fig. 6.14 – ADS schematic model from second proposal sub-system.

The ADS model created to the proposal architecture is shown at Figure 6.14 and could be analyze in more detail in Appendix B with components parameters also included.

6.4.2.1 - First simulation: One interferer tone

In first simulations we consider a two-tones input signal with of -50dBm to desire signal and 6 dBm to interferer and a frequency separation $\Delta\omega$ (ω_2-ω_1) of 50 MHz (5 times bigger than the 10MHz used in last simulation). These frequency gap allows the use of more realistic and common bandpass filters (even in cascade mode after LNA), capable to strongly mitigate the interference power in output signal. With these input values the power difference between both signals is nearly 56 dB at the entry of the LNA (figure 6.15).

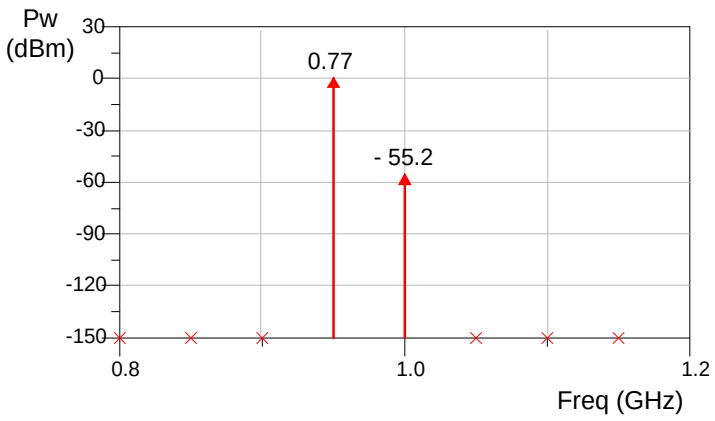

Fig. 6.15 – LNA's input signal

In ADS model we not included the typical frequency selection-band filter before the LNA, since wasn't bring any relevant information to system response analyse. Using a common filter with 25 dB attenuation in rejected band, it possible that the system's input signal would have in fact a difference around 80 dB between the desired component and the interferer.

The nonlinear device used in simulation is a real LNA with a 16dB gain and a phase shift of 92 degrees (the remain LNA's parameters could be consulted in appendix B). With these characteristics and the present input signal, it will expect that LNA's output signal clearly presents intermodulation products on the two original tones and in their neighbour's frequencies. As shown in Figure 6.16, the desire signal revels a significant attenuation compared to a linear response (-45.5 dBm against -39.2 dBm from linear response) proving a big influence from intermodulation products that falls at ω_2 in the LNA 's response.

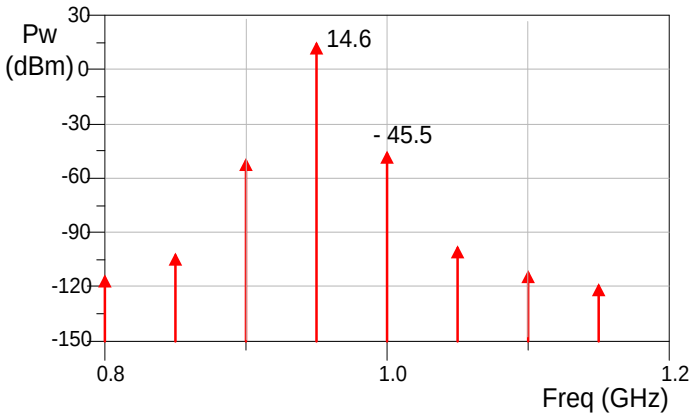

Fig. 6.16 – LNA's output signal.

Using a very good bandpass filter (or a cascade of filters) it's possible to strongly attenuate the interferer about 50 dB (remember that from this point on the component's noise contribution to the Noise Figure is already small) to, at least, match the level of two tones and mitigate all the neighbours nonlinear products (figure 6.17).

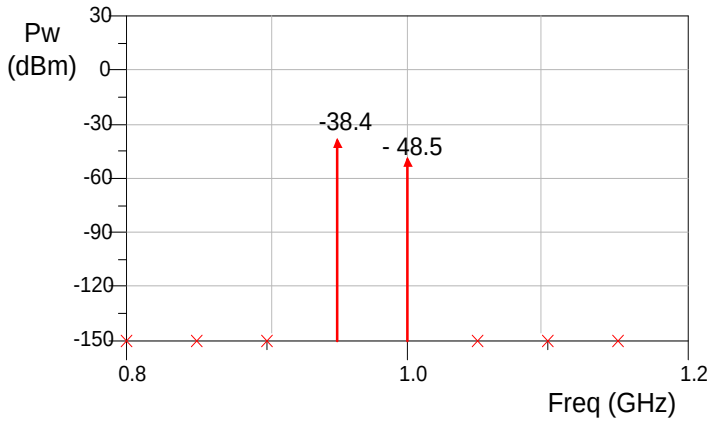

Fig. 6.17 – Bandpass output signal.

In the secondary path, as explain previously, the diode is used as a well known nonlinear generator to obtain the second order contribution that mixing with the interferer will generate IMD's replica at ω_2. In this particularly test we are only interesting in the ω_2-ω_1 products present in figure 6.18. In further simulations will we see that others second order tones will have a relevant importance too.

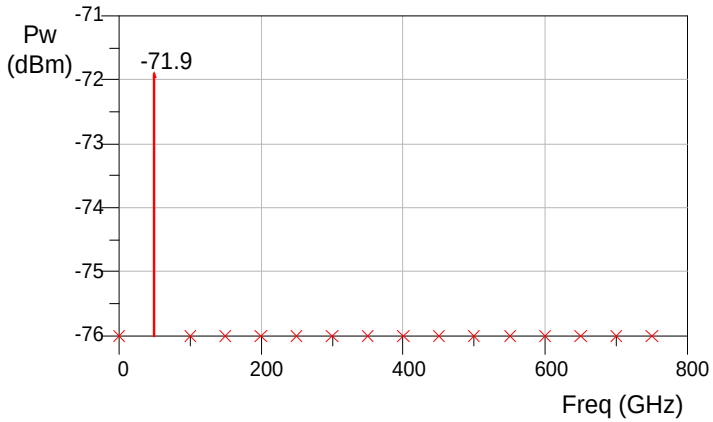

Fig. 6.18 – Diode's second order ω_2-ω_1 product (after filtration).

As refer, in this scenario *the cross-modulation* as a more important role at ω_2 than AM/AM or AM/PM conversion, because the interference power level is much higher than the power of desire signal and the magnitude from the first ones strongly depends from jammer's amplitude.

Mixing the diode's output signal with the interference (the desire signal was filter by a stopband filter at 1 GHz), adjusting the phase with a Phase Shifter (this replica must be in opposite phase against the LNA's cross-modulation products) and correcting the power

level with a Power Amplifier, the final secondary signal that will be used to mitigate LNA's third order nonlinear products at 1Ghz is present in figure 6.19.

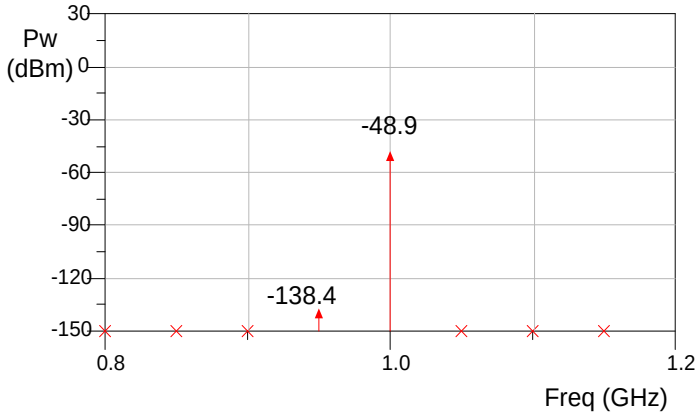

Fig. 6.19 – Final signal from secondary path.

The final step is the sum of the signals from the two paths (primary and secondary path), achieving the cancelation of cross-modulation generated in LNA (figure 6.20). As expected the desire signal has a significant rise of this power, almost identical to LNA's linear response (this result is 3dB lower due filter's attenuation in band after LNA). The two components (jammer and desire signal) are now at same power level.

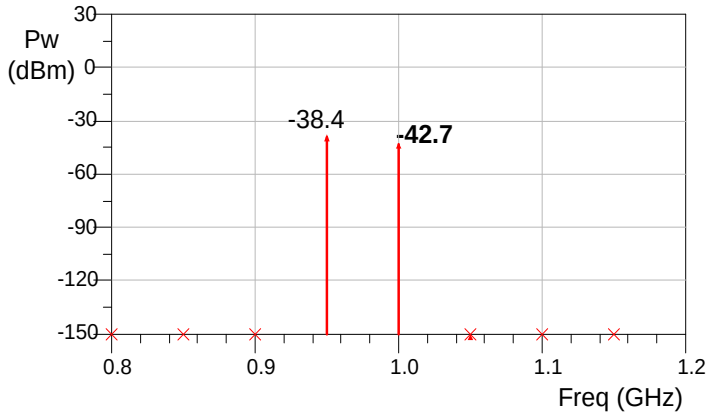

Fig. 6.20 – Final output signal.

Remind you that the input two-tones had about 56dB (80dB if considered the use of a band-selection filter) difference in their power and now have substantially the same power. From this point the jammer signal can be easily removed from our spectrum signal. The reason for using a jammer with such high power (almost unrealistic) is based on the fact that we want to test the setup in the worst possible scenarios. A radar signal could be one of this huge interferes examples for all neighbours communication systems.

Achieving acceptable results with very adverse conditions, we guarantee good results for normal situations. For instance, with a jammer 40dB above the desired signal power, their influence in the output signal would be much smaller than desired signal power.

6.4.2.2 - Secondary simulations: No interferer, Two-tone interferers and Monte Carlo simulation

After the first test with a very strong jammer (and architecture parameters calibrated), it is imperative to make other simulations with variation in architecture's elements parameters or using different interferes to involve other possible scenarios and more broad applications. With this goal we choose three new scenarios: the first with no interferer, the second with a two-tone interferer and the last with a Monte Carlo simulation identical to the one made in first architecture presented.

The "No interferer" test was made to evaluate the architecture response when no interference was present at entry and prove the similarity between the results in one and two-tones interference scenarios. In this simulation the interferer was minimize to a power level under -100dBm (without significance), maintaining the desire signal power. The signal at the entry of the LNA is present in next figure.

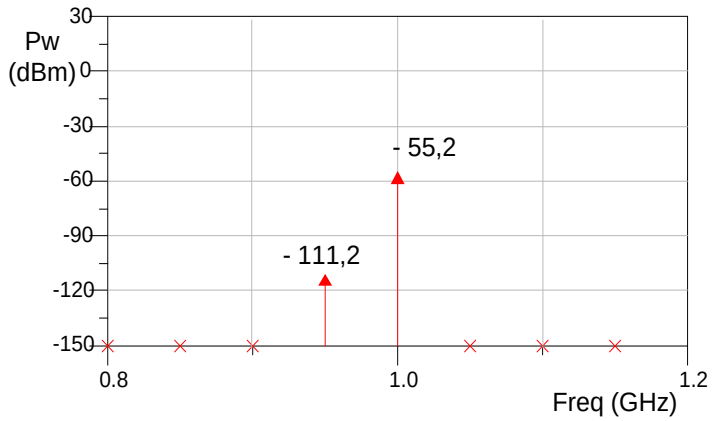

Fig. 6.21 – LNA's input signal "no jammer" simulation

With this very small interference power the nonlinear products will be negligible and the architecture must have an almost linear response in its frequency's operation band. The system output signal is present in Figure 6.22.

Comparing the final output signals from Figures 6.20 and 6.22, we observe a very small difference between the two signals power levels (about 1dB), proving the reliability of this presented sub-system either with or without a neighbour's jammers.

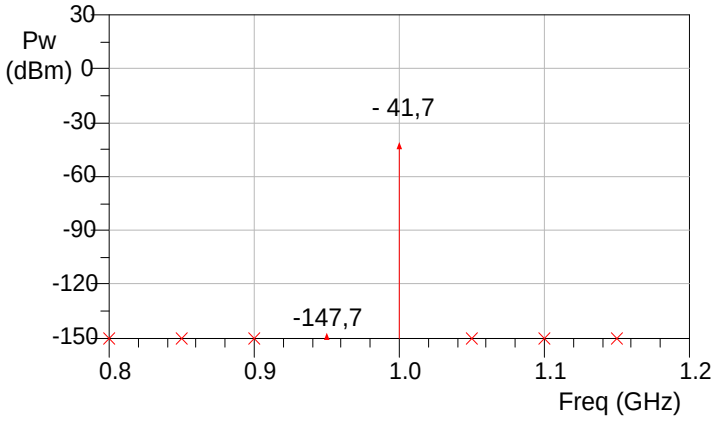

Fig. 6.22 – Final output signal in "no jammer" simulation

The second simulation in these "battery tests" is the "two-tones jammer", where we try to test the architecture's response in the presence of more complex interferers or two distinct jammers. The two-tones interference signal will have -20dBm each tone, maintaining the desire signal power. The signal that arrives to LNA is present in figure 6.23.

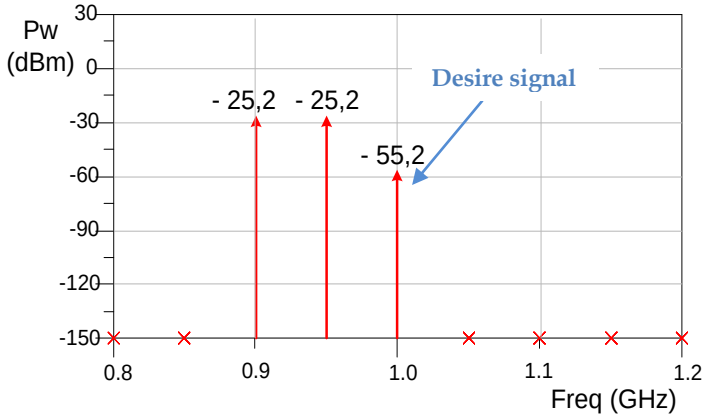

Fig. 6.23 – LNA's input signal in "two-tones jammer" simulation

An important feature desire with both presented architectures is its adaptability to the generality of the systems and the ability to be connected with the majority of them. With this test we also tried to understand whether or not be necessary to change one or more system's parameters when the jammer modifies.

For this particularly simulation was only necessary to change the bandpass filter after the diode, since in previous simulations we used a narrow bandwidth filter that not allows to pass all necessary nonlinear products generated in the diode (in this simulation), needed to produce the cross-modulation replica. Although, this is a minor change that cannot be

considered a system parameter modification since the system could perfectly work for both cases with this last filter's bandwidth.

The final output signal is then present in next figure.

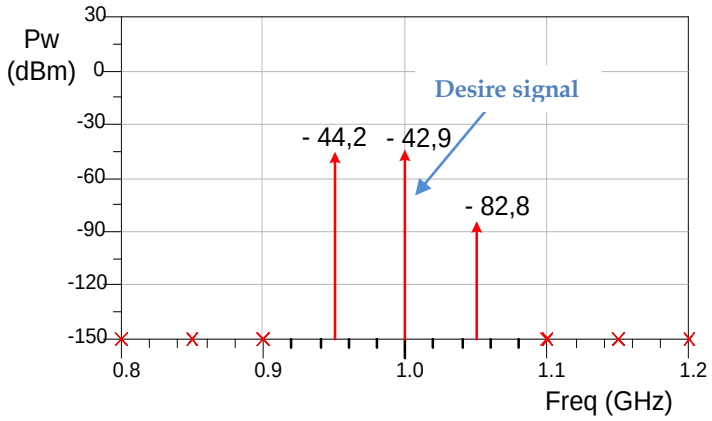

Fig. 6.24 – Output signal in "two-tones jammer" simulation

The results are almost identical to the simulation with a single interference tone, since the power levels achieved in the desire signal in both simulations are almost identical and the jammer power level maintains at same level than the desire signal.

This simulation shows that proposed architecture has a reasonable behaviour for other types of interferences (in adjacent frequencies) and could achieve similar results in other scenarios. More tests/simulations could be planned to prove this statement.

To finish the simulation tests it was essential to understand its robustness and tolerance to variations in electronic components like Amplifiers and Phase Shifters, as made in previous architecture. To evaluate the architecture's response to a non-ideal calibration in its components parameters, we made a final simulation based on a Monte Carlo technique with 250 interactions, allowing a 2% possible variation in LNA, PA e Phase Shifter (at this point we return for a single-tone interferer). The input signal is present in Figure 6.25 and final result in Figure 6.26.

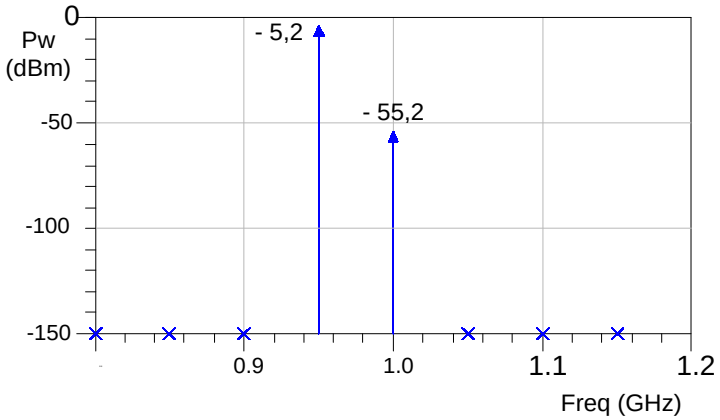

Fig. 6.25 – LNA's input signal "Monte Carlo" simulation

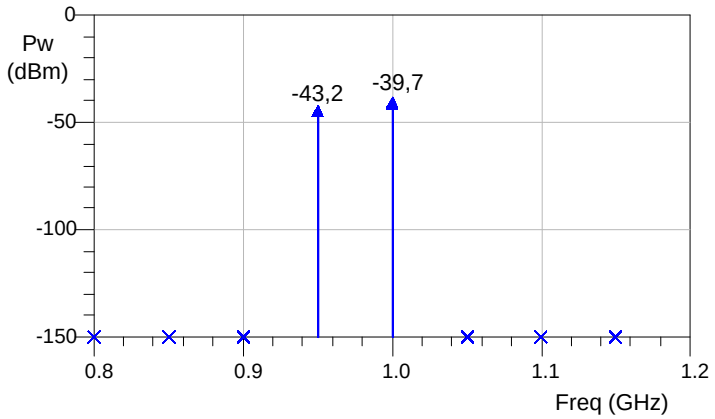

Fig. 6.26 – Output signal with "Monte Carlo" simulation

Even in worst scenario, the power level from the desire signal is similar to the levels obtain in previous simulations (no more than a small difference of 3dB). These results show a bigger robustness than first sub-system because it was possible to reduce the number of Phase Shifters and Atenuators/Amplifiers, the major contributors to the mismatches in system's parameters.

As resume, the last three simulations have shown that the proposed architecture is reliable, has good results for different types of jammers and is relatively immune to small variations in their constituent components (these variations can be easily observed in climate change, aging materials, external factors, etc ...).

6.5. Principal advantages/disadvantages and target applications

To end the current presentation from the two proposed sub-systems is essential to conduct a comparative study between them, knowing that like all systems, both configurations have their advantages and limitations when used in several RF systems.

The main difference between the two architectures is the focus target of each one. If in first architecture the goal is the reduction of all contributions that affects the good desire signal reception, i.e., interference signal and nonlinear products in band. The second configuration only focuses its attention on the cancellation from cross-modulation products that fall into the same frequency as the desired signal. This objective assumes that jammer's frequency is sufficiently distant from the desired signal allowing a regular attenuation with filtering before and after the LNA.

Another major difference between the two configurations is the number of elements used in each configuration and their corresponding cost. As expected, since the first configuration has wider objectives/applications, will require a bigger number and more complex components, raising the architecture cost due to the high expense from some components such as Phase Shifters. For this reason, it is expected that the number of possible applications will be more limited. However it will be a good "tool" to RF transceivers with high sensitivity near broadband systems such as radio transmitters, TV or similar. Its ability to cancel the jammer itself (even very close in frequency from the desired signal) could make it very useful in these scenarios.

As expected the second architecture presented, taking lower targets, presents a lower number of components, reducing especially the number from the most complex and expensive ones. Apart from the component's cost associated, is important to take into account the reduction of the energy needed and architecture size minimization. All these factors associated make the range of applications of this architecture greater than the first one since it can be used in the majority of RF systems without compromise their reliability and brings much cost associated. In future, it's possible that this second configuration with minor modifications could be applied to a RFID system with low energy consumption, increasing its efficiency.

To best evaluate all advantages and disadvantages of both architectures we resume the information in table 6.1.

Characteristic	First architecture	Second architecture
Main Goal	Mitigation from the jammer and all nonlinear products generated by LNA	Mitigation only from the IMD products that fall over the desire signal.
Main Advantages	- Greater attenuation in jammers (more than 80 dB). - Good interference mitigation results even in jammers very close in frequency. - Don't need pre-knowledge from interference signal. - Can be attached to several types of RF receivers without affecting their performance. - Operation Frequency Independence and transversality.	- Very good attenuation in nonlinear cross-modulation products. - Simple configuration with generic electronic devices. - Don't need pre-knowledge from interference signal. - Tolerant with variation in elements configurations. - Can be attached to main types of RF receivers. - Operation Frequency Independence and transversality.
Complexity and energy consumption	- Is more complex than the second architecture (through its higher requirements) and has a higher energy consumption. - Not suitable for low energy consumption system like RFID Tag's.	- Simple configuration with very few complex components. - Less energy consumption - More indicated to circuits with small energy resources - Small size due it's low number of elements
Major limitations	- Small tolerance to variations from its ideal settings. - Its performance is excessive dependent from the three Phase Shifters and the PA behaviour. - Could have a few reliability issues in the presence of more complex input jammers.	- Not ideal for jammers to close to the desire frequency signal. - Some elements like the Phase Shifter or Mixer could make this architecture a slightly more expensive than allowed to devices that must have a ridiculously low price like of passive or semi-passive RFID tags.

Possible application scenarios	- RF systems neighbours from broadband systems and/or systems with a huge transmitter power - Centers with several systems closed in frequency. - Very sensitive receivers	- Major RF systems to mitigate undesired nonlinear products - Suitable for systems that have near interferes with a significant power level (but far in operation frequency).

Table 6.1. Main characteristics from both presented architectures.

6.6 - Conclusions

As mentioned several times throughout this thesis, one of the most important issues in the study and treatment of nonlinear phenomena (that occur in RF receivers) is the adverse effect that the jammers may have on the correct reception of the desired signal, even if they are at distinct frequencies. Obviously this problem is worsened with the raising power from the interferers and the reduction sensitivity level from the system's receiver. Broadband communication systems or technologies with high power densities (with or without anti-work intentions) are typical scenarios where this problem arises as the main concern to achieve a reliable performance from other RF systems.

In this chapter was presented and analysed two new possible configurations for interference cancelation. This first configuration presented obtains reasonable results in the two-tones simulation with more than 80dB reduction in the interference signal, and acceptable marks when using a Monte Carlo technique (to simulate variations in several component's parameters). The second configuration, although simpler, cheaper and with more restricted goals than the previous one, also achieves good results in the four simulations done (one and two-tones interferer, no interferer and Monte Carlo). Aiming only for the mitigation from IMD products that falls over the desire signal this second sub-system could be a very good alternative for several types of interference signals since exists a reasonable frequency separation between desire and interferer signal.

Both sub-systems could be applied in locations with a huge density of interferences or in systems with very high sensitive levels that could be corrupted in the presence of a strong interference. However the applications/systems for the first architecture could be limited by its number of components that could be a major obstacle to implementing this topology in more simple RF systems. In other hand, the second configuration as less RF

electronic (especially the most critical ones), allowing good adaptability for many known RF receivers without compromise the expected and desire results.

CHAPTER 7

Conclusions

This PhD thesis presents a thorough and exhaustive study from the nonlinear behaviour typical in most radio-frequency transceivers that affects their performance oand reliability. This nonlinear phenomenon well known and study in RF amplifiers and similar crucial RF electronic components (ex: mixers and oscillators), is one of the major concerns is recent communication systems. Through the huge number of different technologies sharing the same spectrum bandwidth, several systems with restrictions and/or high sensitivity (like RFID or SDR) see their performances severely affected by the jammers that, even don't share the same operation band frequency, though the nonlinear's spectral regrowth capability, can generated products that will corrupt the correct reception from system's signals.

Chapter 2 was so used to introduce the main receivers used in today's technologies as a starting point in the nonlinear's analyse and comprehension. There we see some problems associated to their presence in key elements like LNA, where they could compromise the remainder receiver's architecture. Although, this behaviour also provide a quick and relative simple way to direct convert a RF signal to a baseband frequency. With this idea in mind, and through the advance study of the main algorithms for calculating the nonlinear behaviour of the RF system (especially the weakly nonlinear systems) mainly focused on Taylor or Volterra series (present in chapter 3), two ambitious and attractive paths arise to explore all the concepts learned.

One of these paths was the development from a new set of mathematical equations, capable of modulating the nonlinear response of a direct conversion system based on the even order products from a nonlinear generator. Starting to exclude the erroneous idea of using only the nonlinear second order products to realize RF→Baseband conversion, in chapter 4 we presented a new collection methods to calculate the number of second and fourth order products that falls at DC and Baseband, also handy to quickly estimate the impact of all terms in a predefined baseband tone. The formulas presented dramatically reduce the simulation time of the system response when excited with a multi-tones input

signal. Simulations with one thousand tonnes (almost impossible to realize with other common simulators) are realize in small time windows (lower than 2/3 minutes), allowing the program to use signals with a wide spectrum as SDR. This study opens a great window to demonstrate the incorrect calibration method that that has been used for calibration of common Power Detectors and similar RF circuits. Using some concepts introduced in the previous chapter, it was possible to prove that Power probe's measurements (associated with a voltmeter to measure the DC voltage) not only is strongly influenced by the device's output impedance (that could be variable in frequency) but also have a non-negligible dependence of fourth-order nonlinear response, unlike that normally done when only be consider the contributions of second order nonlinear generator. These conclusions shown that Power probes, wrongly calibrated with only a single tone signal during several years, not only have a for order influence in their measurements results but also depends from output's impedance mismatches. These incorrectness could provoke enormous errors in DC voltage measurements with differences about 20% between the real and measure result.

Finish this course, the second path taken after complete the study of nonlinear phenomena was the development of new configurations able to cancel the effects of strong signals in desire signal bandwidth. Being one of the main problems in the spectral "bandwidth fight" due to the large number of systems sharing the same RF frequency band, to cancel the interference signals in RF receivers two new architectures were developed with slight differences in their goals. The first architecture presented aim the reduction from all problematic nonlinear products and the jammer itself. Based in known electronic, although the good results depend from a reasonable/good match between phases from several path, it's demonstrated that a good equilibrated circuit could reduce the gap between Interferer and Desire Signal to almost 80dB, allowing their using in more demanding and sensitive receivers.

In opposite way, the second architecture tries to simplify their configuration in order to be more universal and diversify its applications. Only focus in mitigation of the cross-modulation products (assuming a bigger frequency separation between the system and the jammer that allows regular filtration), this architecture minimize the number of elements, complexity and energy consumption, also achieving a bigger tolerance to external and internal variations.

7.1 – Future Work

It is always difficult to exactly define the future work that may arise from a study that aims to be complete. However it is also true that a scientific works are never complete, since there are always points that can be improved and new paths to explore emerging from the older ones.

We start from the ending, or in other words, with chapter 6. One of points that seems to have continuous improved is the development of new architectures to cancel strong interferers. The two architectures presents fit in the mandatory requirements imposed in the beginning of the chapter. However, these present architectures still have some limitations, especially if the goal is to use in devices with very low energy resources. One of the future goals could be the even more simplification of the second architecture, allowing their use in devices like passive Tags or similar. We think that Phase Shifter could be excluded from this configuration and the integration in a IC could reduce some of the issues that we have to lead in discrete RF components. As example, if a perfect no-phase deviation could be achieved, the Phase Shifter could be replaced by a simple inverse amplifier configuration.

A second path in a possible future work is connected with the proof of concept present in Chapter 5. Knowing that power probe measurements will be conditioned by nonlinear fourth order response and low frequency impedance, it will be appreciated the elaboration of new several calibration methods to ensure reliable results in Power meters and system with direct conversion. These calibration methods necessarily have to pass through the use of more than one-tone signal in calibration process and by introducing several new parameters capable to modelling the frequency response from the power probe's output impedance.

The third and last path identified (for now) as a possible future work could be the introduction of new parameters such phase or amplitude variation (between the tones) in algorithms for baseband prediction present in Chapter 4. This could be a very hard task taking into account the complexity and difficulty in achieving the previous modeled formulas. Other possible scenario could be the fusion between these algorithms with the already developed for intermodulation distortion of 3rd and 5th order, creating the possibility of a new simple and faster simulation program capable to quickly predict the behaviour of a nonlinear system when exited with a signal that could be represented by a

multisine with a reasonable number of N tones. This could be a good pedagogic project for Master or PhD students that want be initiated in the Nonlinear World.

In addition to these possible scenarios, other paths can be taken, knowing that the problems associated with nonlinear phenomena are continually present in any radio-frequency system of that has to share the frequency spectrum with other communication systems.

References

[1] B. Razavi, *RF Microelectronics*, Prentice-Hall, Upper Saddle River, 1998.

[2] José Carlos Pedro, Nuno Borges Carvalho, "Intermodulation Distortion in Microwave and Wireless Circuits", 1th Edition ed. Norwood: Artech House, Inc., 2003

[3] Martins, João Paulo Tavares "Study of Linearization Techniques for RF Devices", Master Dissertation, Department of Electronics and Telecommunications at the University of Aveiro.

[4] S. Wu, B. Razavi, "A 900-MHz/1.8-GHz CMOS Receiver for Dual-Band Applications," IEEE Journal of Solid-State Circuits, Vol 33, pp. 2178-2185, Dec.1998.

[5] Kevin G. Gard, Member, IEEE, Lawrence E. Larson, Fellow, IEEE, and Michael B. Steer, Fellow, IEEE "*The Impact of RF Front-End Characteristics on the Spectral Regrowth of Communications Signals*" - IEEE Transactions on Microwave Theory and Techniques, vol 53, no. 6, pp.2179-2186, June 2005

[6] Scott, Allan W., Frobenius, Rex "*RF measurements for cellular phones and wireless data*", Hoboken, N.J. : IEEE : Wiley & Sons, c2008, ISBN: 9780470378014 , 0-470-37801-8

[7] Klaus Finkenzeller, *RFID Handbook*, 2nd Edition ed. Wiley, ISBN: 0-470-84402-7

[8] Gomes, Hugo Miguel Cravo "Construction of an RFID system with special tracking purposes," Master Dissertation, Department of Electronics and Telecommunications at the University of Aveiro.

[9] S. J. Nightingale, G S Sodhi, J. E. Austin & Shipton, "An Eight Channel Interference Cancellation System", ERA Technology Ltd, 2006 IEEE

[10] Lessing Luu, Babak Daneshrad, "An Adaptive Radio Architecture With Weaver Spectrum Sensing Capabilities to Relax RF Component Requirements ", IEEE Journal on Selected Areas in Communications, vol.25, no. 3, April 2007

[11] Mirabbasi, Shahriar; Martin, Ken (2000). "Classical and Modern Receiver Architectures", *IEEE Communications Magazine,* November 2000

[12] Besser, L. & Gilmore, R. (2003). *Practical RF Circuit Design for Modern Wireless Systems,* Artech House, ISBN 1-58053-521-6, Norwood, MA

[13] Chang, Kai (2000). *RF and Microwave Systems*, John Wiley & Sons, ISBN 0-471-35199-7,

[14] Gomes, Hugo; Carvalho, Nuno B (2007). "The use of Intermodulation Distortion for the Design of Passive RFID", *Proceedings of European Microwave Conference 2007,* ISBN: 978-2-87487-001-9, pp. 1656 – 1659, 9-12 October 2007

[15] Gomes, Hugo; Carvalho, Nuno B (2007). "RFID for Location Proposes Based on the Intermodulation Distortion", *Sensors & Transducers journal,* ISSN 1726-5479, Vol.105, No. 6, pp. 85-96, June 2009.

[16] Jamaluddin, M.H.; Rahim, M.K.A.; Aziz, M.Z.A.A.; Asrokin, A. ,(2005). "Direct conversion receiver with active integrated antenna", *Proceedings of Asia-Pacific Conference on Applied Electromagnetics,* ISBN: 0-7803-9431-3, 20-21 December 2005

[17] Ravazi, B. (1997). "Design Considerations for Direct–Conversion Receivers", *IEEE Transactions on Circuits and Systems – II: Analog and Digital Signal Processing*, ISSN: 1057-7130 Vol.44, No. 6, pp. 428-435, June 1997.

[18] Ravazi B. (1998). "Architectures and Circuits for RF CMOS Receivers", *Proceedings of IEEE 1998 Custom Integrated Circuits Conference*, ISBN: 0-7803-4292-5, pp. 393 – 400, 11-14 May 1998.

[19] Kyeongho Lee; Joonbae Park; Jeong-Woo Lee; Seung-Wook Lee; Hyung Ki Huh; Deog-Kyoon Jeong; Wonchan Kim; (2001). "A Single-Chip 2.4-GHz Direct-Conversion CMOS Receiver for Wireless Local Loop using Multiphase Reduced Frequency Conversion Technique", *IEEE Journal of Solid-state Circuits,* ISSN: 0018-9200, Vol. 36, No. 5, May 2001

[20] Kang-Yoon Lee; Seung-Wook Lee; Yido Koo; Hyoung-Ki Huh; Hee-Young Nam; Jeong-Woo Lee; Joonbae Park; Kyeongho Lee; Deog-Kyoon Jeong; Wonchan Kim (2003). "Full-CMOS 2-GHz WCDMA Direct Conversion Transmitter and Receiver", *IEEE Journal of Solid-state Circuits,* ISSN : 0018-9200, Vol. 38, No. 1, January 2003

[21] Lucero, R.; Pavio, A.; Penunuri, D.; Bost, J. (2002) "Design of an LTCC Integrated Tri-Band Direct Conversion Receiver Front-End Module" - *Microwave Symposium Digest, 2002 IEEE MTT-S International,* ISBN: 0-7803-7239-5, Vol. 3, pp. 1545 – 1548, 02-07 June 2002

[22] M. Mohajer, A. Mohammadi, R. Khosravi (2005). "A Five-Port Direct Conversion Receiver for Software Radio Applications," *Wireless and Optical Communications Networks, 2005. WOCN 2005. Second IFIP International Conference on,* ISBN: 0-7803-9019-9, pp. 589 - 593 *Dubai, UAE,* March 2005.

[23] Radio Amateurs Direct Convertion Receiver, http://www.qsl.net/vu2upx/Projects/dc_rx.htm

[24] James Tsui. *Digital Techniques for Wideband Receivers*. Artech House, 1995. ISBN 0-89006-808-9

[25] R.B. Staszewski, et al., "All-Digital TX Frequency Synthesizer and Discrete-Time Receiver for Bluetooth Radio in 130-nm CMOS," *IEEE J. Solid-State Circuits*, vol. 39, no. 12, pp. 2278-2291, 2004

[26] K. Muhammad, et al., "A Discrete Time Quad-Band GSM/GPRS Receiver in a 90nm Digital CMOS Process," *Custom IC Conference*, San Jose, CA, pp. 804-807, 2005

[27] Holly Pekau, Student Member IEEE and JamesW. HasLett, Fellow IEEE – "A Comparison of Analog Front End Architectures for Digital Receivers", *CCECE/CCGEI*, Saskatoon, May 2005

[28] Darius Jakonis, Kalle Folkesson, Jerzy Dabrowski, Patrick Eriksson - Member IEEE, Christer Svensson – Fellow IEEE- "A 2.4-GHz RF Sampling Receiver Front-End in 0.18-µm CMOS", *IEEE Journal of Solid-State Circuits*, vol. 40, no. 6, June 2005

[29] Zayed, A.I., "Hilbert transform associated with the fractional Fourier transform", *IEEE Signal Processing Letters*, vol. 5, no 8, pp 206 – 208, 1998

[30] K. Muhammad, D. Leipold, B. Staszewski, Y.-C. Ho, C. M. Hung, K. Maggio, C. Fernando, T. Jung, J. Wallberg, J.-S. Koh, S. John, I. Deng, O. Moreira, R. Staszewski, R. Katz, O. Friedman – "A Discrete-Time Bluetooth Receiver in a 0.13µm Digital CMOS Process" – *2004 IEEE International Solid-State Circuits Conference*

[31] Mohamed A.I. Mostafa, Sherif Embabi, Moderage C. Fernando, Wing Kan Chan, Charles Gore JR – "Subsampling RF Receiver Architecture" – *United States, Patent Application Publication No: 2002/0181614* – 5 December 2002

[32] Mehmet R. Yuce1, Wentai Liu2 – "Design and Implementation of a Multirate Sub-sampling Front-end in Software Radio Systems" – ISBN: 0-7803-8451-2/04/$20.00 ©2004 IEEE 529

[33] Sining Zhou, Mau-Chung Frank Chang, "A CMOS Passive Mixer With Low Flicker Noise for Low-Power Direct-Conversion Receiver", *IEEE Journal of Solid-State Circuits*, vol. 40, no. 5, May 2005

[34] Agilent Application Note, "Software Defined Radio Measurement Solutions," Agilent Technologies, Inc. 2007, July 13, 2007 – CHANGE TO CCDF application note

[35] Goldsmith, A.J.; Chua, S.-G. (1998). "Adaptive coded modulation for fading channels", *Communications, IEEE Transactions on*, ISSN: 0090-6778, pp. 595 – 602, May 1998

[36] Stephen A. Maas, *Nonlinear Microwave and RF Circuits*, 2nd Edition ed. Norwood: Artech House, Inc., 2003

[37] Tehrani, R.; Ludeman, L.C., "Use of generalized Taylor series expansion", *Circuits and Systems, 1992. ISCAS '92. Proceedings., 1992 IEEE International Symposium on,* ISBN: 0-7803-0593-0 vol. 2, pp. 979 - 982, May 1998

[38] Tehrani, R.; Ludeman, L.C., "Signal processing using the generalized Taylor series expansion", *Signals, Systems and Computers, 1993. 1993 Conference Record of The Twenty-Seventh Asilomar Conference on* ISBN: 0-8186-4120-7, vol. 2, pp.1446 – 1449, November 1993

[39] Steven Shepard, *RFID: Radio Frequency Identification*, McGraw-Hill Professional 2005, ISBN: 0-07-144299

[40] "Network Analyzer Measurements: Filter and Amplifier Examples," in Application Note Agilent, NA 1287-4, Agilent Technologies, 1997.

[41] Carvalho, Nuno Borges; Pedro, José Carlos, "Large- and Small-Signal IMD Behavior of Microwave Power Amplifiers", *IEEE Transactions on Microwave Theory and Techniques*, vol. 47, no. 12, December 1999

[42] Mass, S. A., "A General-Purpose computer Program for Volterra-Series Analysis of Nonlinear Microwave Circuits", *Microwave Symposium Digest, 1988, IEEE MTT-S International*, vol. 1, pp.311-314, May 1988.

[43] Maas, Stephen, "Measurements and Nonlinear Modeling", *ARFTG Conference Digest-Spring, 53rd*, ISBN: 0-7803-5686-1, vol. 35, pp.1-9, June 1999

[44] M. Leffel, "Intermodulation distortion in multi-signal environment" R.F.Des., pp. 78-84, June 1985

[45] Pedro, José Carlos; Carvalho, Nuno Borges, "On the Use of Multitone Techniques for Assessing RF Components Intermodulation Distortion" *IEEE Transactions of Microwave Theory and Techniques*, vol. 47, no. 12, pp. 2393-2402, December 1999

[46] M. Kanda and L.D. Driver, "An isotropic electric-field probe with tapered resistive dipoles for broad-band use, 100 kHz to 18 GHz", IEEE Trans. Microwave Theory Tech., vol. 35, no. 2, pp 124- 130, Feb 1987.

[47] M. Kanda, "Standard probes for electromagnetic field measurements", IEEE Trans. Antennas Prop., vol. 41, no. 10, pp. 1349-1364, Oct 1993.

[48] J.M. Ladbury and D.G. Camell, "Electrically short dipoles with a nonlinear load, a revisited analysis,"IEEE Trans. Electromagnetic Compatibility, vol. 44, no. 1, pp. 38-44, Feb 2002.

[49] C. D. Nallo and A. Faraone, "Effect of amplitude modulation of the CDMA IS-95 signal on SAR measurements," IEEE Trans. Electromagnetic Compatibility, vol. 48, no. 3, pp. 552-562, Aug. 2006.

[50] N. B. Carvalho and J. C. Pedro, "A comprehensive explanation of distortion side band asymmetries," IEEE Trans. Microwave Theory Tech., vol. 50, no.9, pp. 2090-2101, Sept. 2002.

[51] S. H. Han and J. H. Lee, "An overview of peak-to-average power ratio reduction techniques for multicarrier transmission," IEEE Trans. Wireless Comm., vol. 12, no. 2, pp. 56 – 65, April 2005.

[52] H. Gomes, A. R. Testera, N. B. Carvalho, M. F. Barciela and K. A. Remley, "The impact of long-term memory effects on diode power probes", IEEE Int. Microwave Symp. Dig, May, 2010, Anaheim, CA, USA.

[53] D. Adamson, D. Bownds, A. Fernández, E. Goodall, D. Humphreys, "The response of electric field probes to realistic RF environments,", IEEE Int. Microwave Symp. Dig, May, 2010, Anaheim, CA, USA.

[54] A. Rodriguez-Testera, O. Mojon, M. Fernandez-Barciela, E. Sanchez, "Robust packaged diode modelling with a table-based approach", Proc. European Microwave Integrated Circuit Conf., EuMIC, 27-28 Oct. 2008, pp. 131-134, Amsterdam, Netherlands.

[55] N.B. Carvalho, K.A. Remley, D. Schreurs, and K.C. Gard, "Multisine signals for wireless system test and design," IEEE Microwave Mag., vol. 9, no. 3 pp. 122 – 138, June 2008.

[56] A. Phommahaxay, G. Lissorgues, L. Rousseau, T. Bourouina, P. Nicole, "Tower a Frequency-Selective Microwave Power Limiter for Defense and Aerospace Applicaions", *4th European Radar Conference*, Munich, 2007

[57] Souryal, M. R.; Novotny, D. R.; Kuester, D. G.; Guerrieri, J.R.; Remley, K. A.; "Impact of RF interference between a passive RFID system and a frequency hopping communications system in the 900 MHz ISM band", *Electromagnetic Compatibility (EMC), 2010 IEEE International Symposium on*, ISBN: 978-1-4244-6305-3, vol. 1, pp.495-500, July 2010

[58] Wei Jiang; Yan Ma; "Interference Analysis of Microwave RFID and 802.11b WLAN", *Wireless Communications, Networking and Mobile Computing, 2007. WiCom 2007. International Conference on*, ISBN: 978-1-4244-1311-9, vol.1, pp. 2062 – 2065, September 2007

[59] Alan C. Tribble, "*The Software Defined Radio: Fact and Fiction*", Proceedings of the IRE, pp 1196-1204, October 2008.

[60] S.J:Nightingale, G: S. Sodhi, J. E. Autsin & R.D.Shipton, "An Eight Channel Interference Cancellation System", Microwave Sysmposium Digest, 2006, IEEE MTT-S International

[61] A. Raghavan, E. Gebara, E. M. Tentzeris, Joy Laskar, "Analysis and Design of an Interference Canceller for Collocated Radios", IEEE Transactions on Microwave Theory and Techniques, Vol.53, No 11, November 2005

[62] J. Douglas Adam, Steven N. Stitzer, "Frequency Selective Limiter for High Dynamic Range Microwave Receivers", IEEE Transactions on Microwave Theory and Techniques, Vol. 41, No 12, December 1993

[63] Advance Design System 2009A, Copyright (c) 1983-2009, Agilent Technologies - http://www.home.agilent.com/agilent/product.jspx?cc=PT&lc=eng&ckey=1297113&nid=-34346.0.00&id=1297113

[64] MATLAB, © 1994-2012 The MathWorks, Inc. - http://www.mathworks.com/products/matlab/

Appendix A

First Interference Cancellation architecture – ADS model (normal)

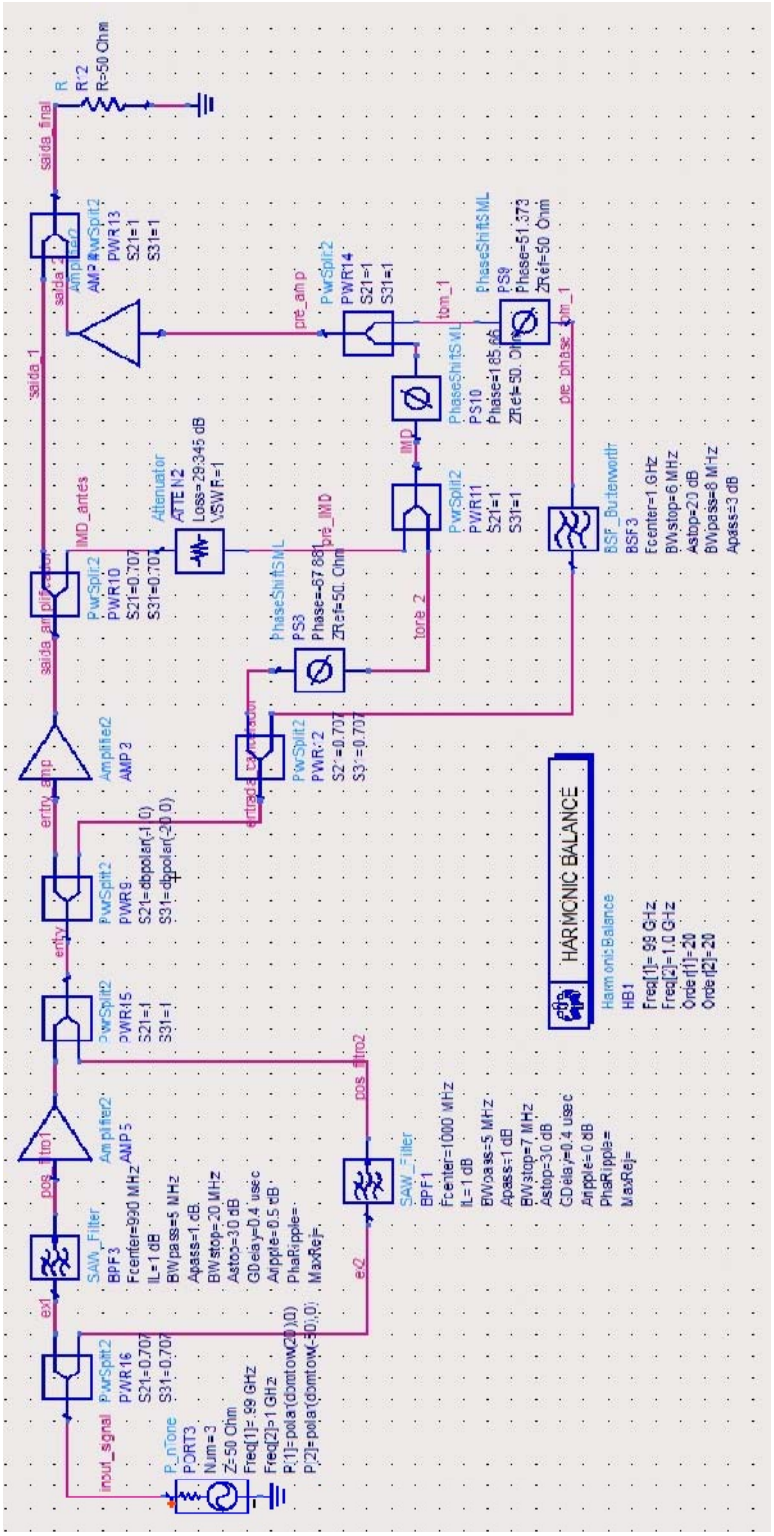

First Interference Cancellation architecture – ADS model (Monte Carlo)

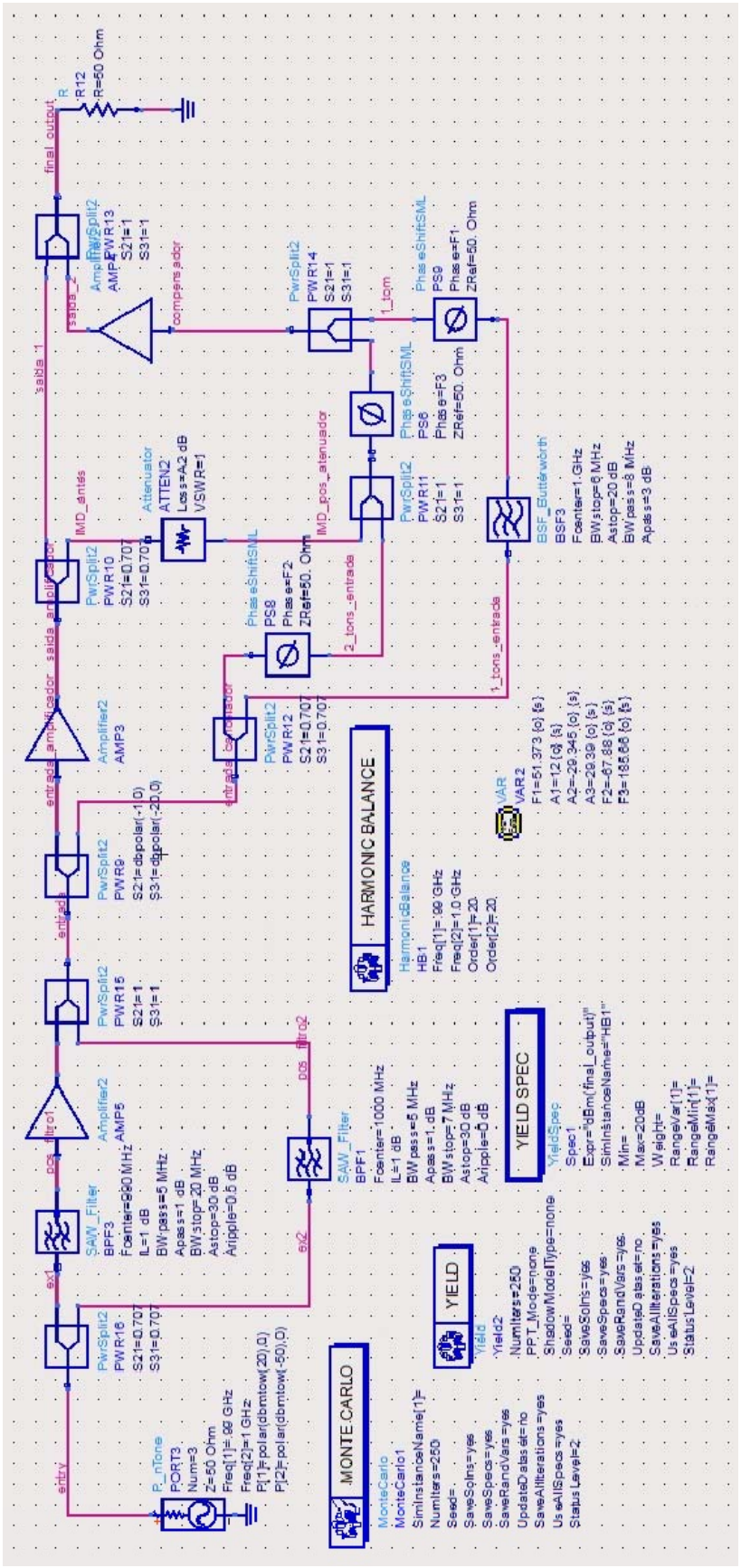

Appendix B

2nd Interference Cancellation architecture – ADS model (normal)

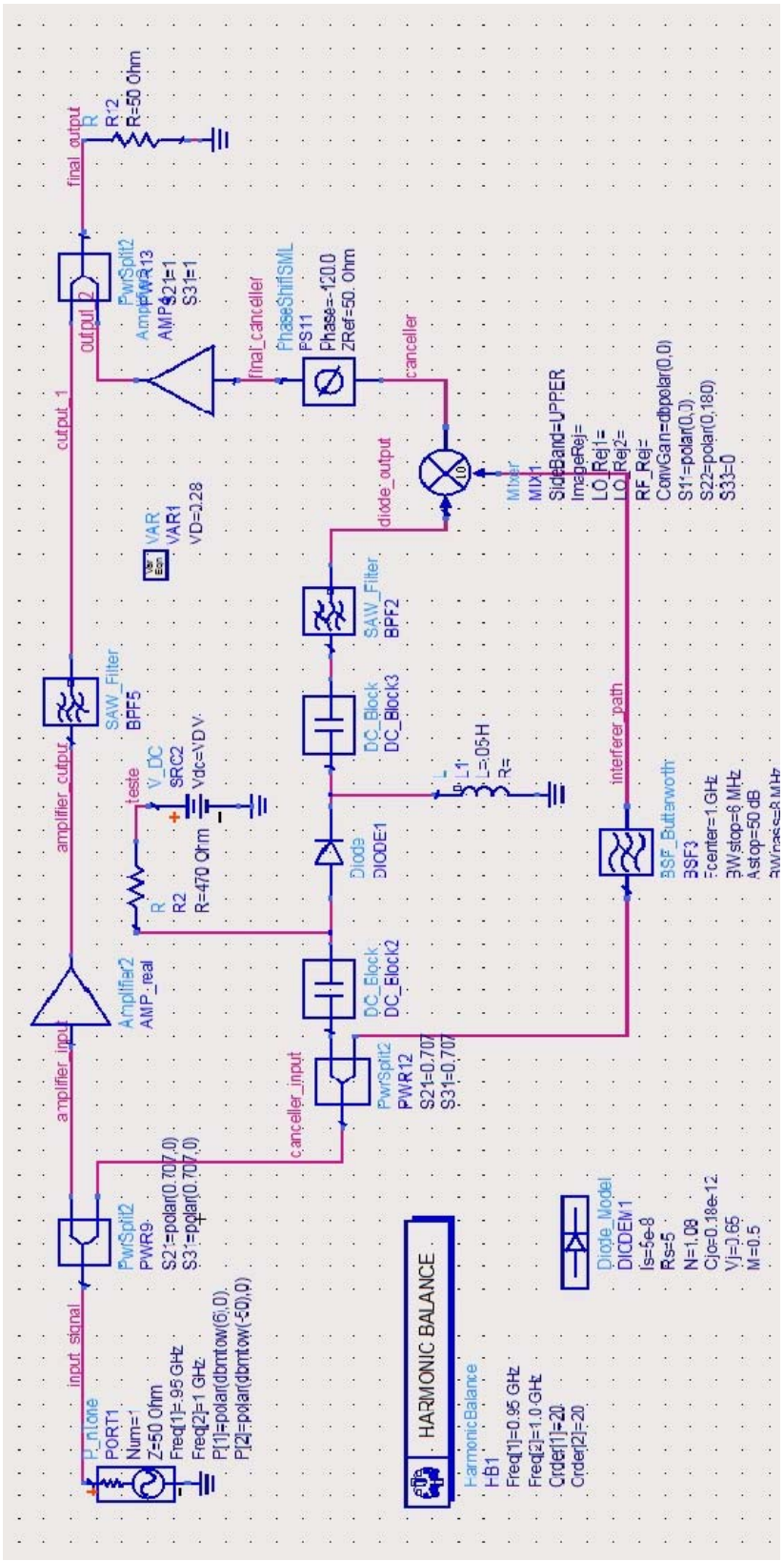

2nd Interference Cancellation architecture – ADS model (Two interferers)

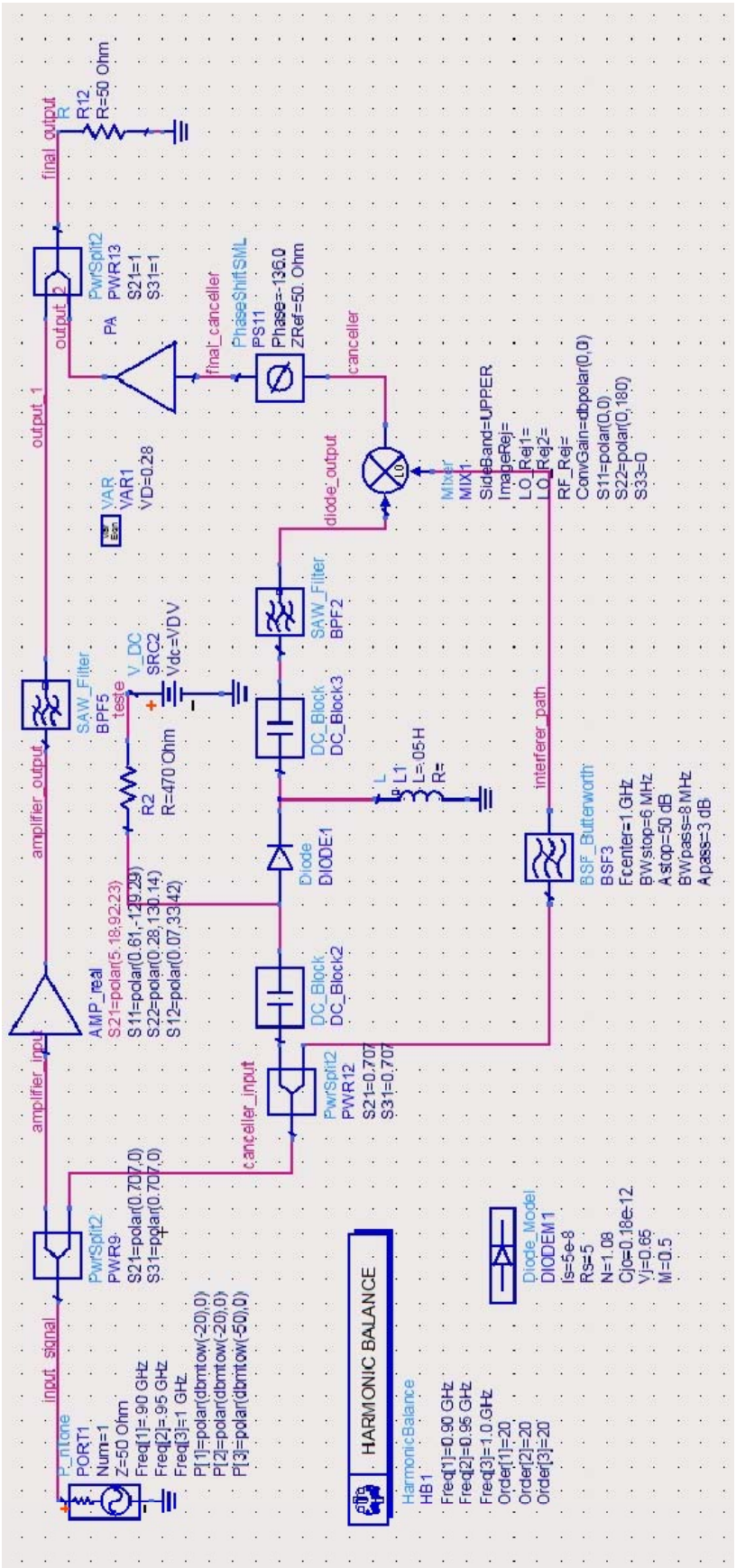

2nd Interference Cancellation architecture – ADS model (Monte Carlo)

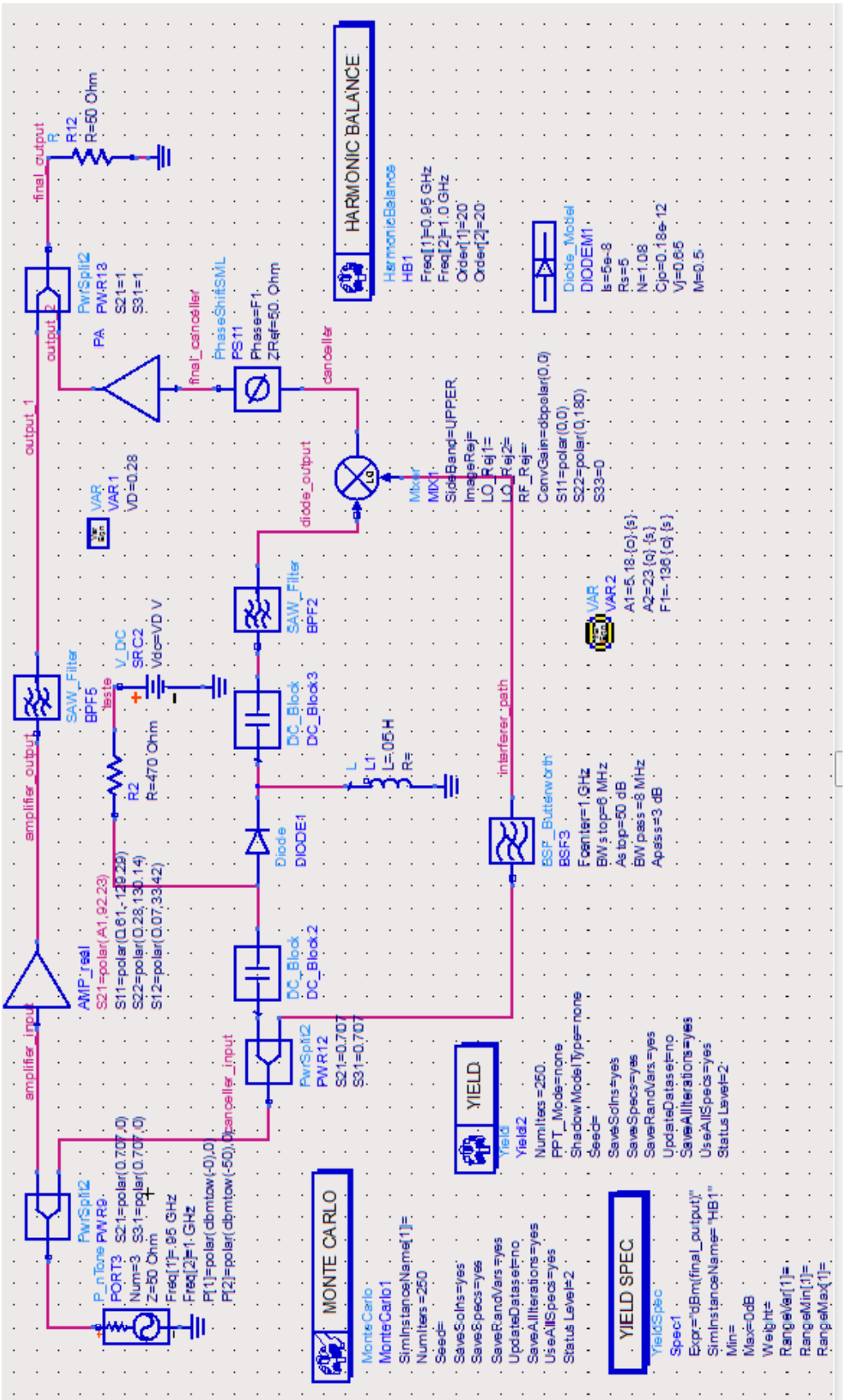

Appendix C

Resume from Matlab functions to RF→DC/Baseband conversion

(**Note:** this functions could be found in attachement files from this thesis)

Main functions

coeficients(N,k).m – calculate the number of tones from each type for a certain N input tones at baseband frequency $k\Delta$

direct_conversion(N).m – Calculate all nonlinear contributions at DC an baseband tones when excited by a input signal with N-tones. This function also presents a graphic with the results

Auxiliary functions

aaaa_DC,...., abcd_DC – generic function that calculates the number of tones at DC with N tones

aaaa,...., abcd – same as the previous but for a $k\Delta$ baseband tone

graph_aaaa_DC, ... – represents a graphic with the behaviour from each term

Appendix D

4th order baseband products – Example since DC to *k*=8

(Note: this appendix shows the nonlinear products that influence the k baseband tone and respective number of elements)

4th order –> DC values

2 Tones

ω2- ω2+ ω2- ω2; ω2- ω2+ ω1- ω1; ω1- ω1+ ω1- ω1 (2 +1)

- **3 terms**

3 Tones

ω3- ω3+ ω3- ω3; ω3- ω3+ ω2- ω2; ω3- ω3+ ω1- ω1; (3)

ω3- ω2 + ω1- ω2 (x2);(2) + 2 tones factors

- **5+3 =8 terms**

4 Tones

ω 4- ω4+ ω4- ω4; ω4- ω4+ ω3- ω3; ω4- ω4+ ω2- ω2; ω4- ω4+ ω1- ω1; (4)

ω4-ω3+ω2-ω3 (x2); ω4-ω3+ω1-ω2 (x2); (4) + 3 tones factors

- **8+8 =16 terms**

5 Tones

ω5-ω5+ω5-ω5; ω5-ω5+ω4-ω4; ω5-ω5+ω3-ω3; ω5-ω5+ω2-ω2;ω5- ω5+ ω1- ω1; (5)

ω5-ω4+ω3-ω4 (x2); ω5-ω4+ω2-ω3 (x2); ω5-ω4+ω1-ω2 (x2); (6)

ω5-ω3+ω1-ω3 (x2); (2) + 4 tones factors

- **13+16 =29 terms**

6 Tones

ω6-ω6+ω6-ω6; ω6-ω6+ω5-ω5; ω6-ω6+ω4-ω4; ω6-ω6+ω3-ω3; ω6-ω6+ω2-ω2; ω6- ω6+ ω1- ω1; (6)

ω6-ω5+ω4-ω5(x2); ω6-ω5+ω3-ω4(x2); ω6-ω5+ω2-ω3(x2); ω6-ω5+ω1-ω2(x2); (8)

ω6-ω4+ω2-ω4 (x2); ω6-ω4+ω1-ω3 (x2); (4) + 5 tones factors

- **18+29 =47 terms**

7 Tones

ω7-ω7+ω7-ω7; ω7-ω7+ω6-ω6; ω7-ω7+ω5-ω5; ω7-ω7+ω4-ω4; ω7-ω7+ω7-ω7; ω7-ω7+ω2-ω2; ω7- ω7+ ω1- ω1; (7)

ω7-ω6+ω5-ω6 (x2); ω7-ω6+ω4-ω5 (x2); ω7-ω6+ω3-ω4 (x2); ω7-ω6+ω2-ω3 (x2); ω7-ω6+ω1-ω2 (x2); (10)

ω7-ω5+ω3-ω5 (x2); ω7-ω5+ω2-ω4 (x2); ω7-ω5+ω1-ω3 (x2); (6)

ω7-ω4+ω1-ω4 (x2); (2) + 6 tones factors (4)

- **25+47 =72 terms**

8 Tones

ω8-ω8+ω8-ω8; ω8-ω8+ω7-ω7; ω8-ω8+ω6-ω6; ω8-ω8+ω5-ω5;ω8-ω8+ω4-ω4; ω8-ω8+ω3-ω3; ω8-ω8+ω2-ω2;ω8-ω8+ω1-ω1; (8)

ω8-ω7+ω6-ω7(x2); ω8-ω7+ω5-ω6(x2); ω8-ω7+ω4-ω5(x2); ω8-ω7+ω3-ω4(x2); ω8-ω7+ω2-ω3(x2); ω8-ω7+ω1-ω2 (x2); (12)

ω8-ω6+ω4-ω6 (x2); ω8-ω6+ω3-ω5 (x2); ω8-ω6+ω2-ω4 (x2); ω8-ω6+ω1-ω3 (x2); (8)

ω8-ω5+ω2-ω5 (x2); ω8-ω5+ω1-ω4 (x2); (4) + 7 tones factors

- **32+72 =104 terms**

9 Tones

ω9-ω9+ω9-ω9; ω9-ω9+ω8-ω8; ω9-ω9+ω7-ω7; ω9-ω9+ω6-ω6; ω9-ω9+ω5-ω5; ω9-ω9+ω4-ω4; ω9-ω9+ω3-ω3; ω9-ω9+ω2-ω2; ω9-ω9+ω1-ω1; (9)

ω9-ω8+ω7-ω8(x2); ω9-ω8+ω6-ω7(x2); ω9-ω8+ω5-ω6(x2); ω9-ω8+ω4-ω5(x2); ω9-ω8+ω3-ω4(x2); ω9-ω8+ω2-ω3(x2); ω9-ω8+ω1-ω2 (x2); (14)

ω9-ω7+ω5-ω7 (x2); ω9-ω7+ω4-ω6 (x2); ω9-ω7+ω3-ω5 (x2); ω9-ω7+ω2-ω4 (x2); ω9-ω7+ω1-ω3 (x2); (10)

ω9-ω6-ω6+ω3 (x2); ω9-ω6-ω5+ω2 (x2); ω9-ω6-ω4+ω1 (x2); (6)

ω9-ω5-ω5+ω1 (x2); (2) + 8 tones factors

- **41+104 =145 terms**

10 Tones

ω10-ω10+ ω10-ω10; ω10-ω10+ω9-ω9; ω10-ω10+ω8-ω8; ω10-ω10+ω7-ω7; ω10-ω10+ω6-ω6; ω10-ω10+ω5-ω5; ω10-ω10+ω4-ω4; ω10-ω10+ω3-ω3; ω10-ω10+ω2-ω2; ω10-ω10+ω1-ω1; (10)

ω10-ω9+ω8-ω9(x2); ω10-ω9+ω7-ω8(x2); ω10-ω9+ω6-ω7(x2); ω10-ω9+ω5-ω6(x2); ω10-ω9+ω4-ω5(x2); ω10-

ω9+ω3-ω4(x2); ω10-ω9+ω2-ω3(x2); ω10-ω9+ω1-ω2 (x2); (16)

ω10-ω8+ω6-ω8 (x2); ω10-ω8+ω5-ω7 (x2); ω10-ω8+ω4-ω6 (x2); ω10-ω8+ω3-ω5 (x2); ω10-ω8+ω2-ω4 (x2); ω10-ω8+ω1-ω3 (x2); (12)

ω10-ω7+ω4-ω7 (x2); ω10-ω7+ω3-ω6 (x2); ω10-ω7+ω2-ω5 (x2); ω10-ω7+ω1-ω4 (x2); (8)

ω10-ω6+ω2-ω6 (x2); ω10-ω6+ω1-ω5 (x2); (4) + 8 tones factors

- **50+145 =195 terms**

11 Tones

ω11-ω11+ω11-ω11; ω11-ω11+ω10-ω10; ω11-ω11+ω9-ω9; ω11-ω11+ω8-ω8; ω11-ω11+ω7-ω7; ω11-ω11+ω6-ω6; ω11-ω11+ω5-ω5; ω11-ω11+ω4-ω4; ω11-ω11+ω3-ω3; ω11-ω11+ω2-ω2; ω11-ω11+ω1-ω1; (11)

ω11-ω10+ω9-ω10(x2); ω11-ω10+ω8-ω9(x2); ω11-ω10+ω7-ω8(x2); ω11-ω10+ω6-ω7(x2); ω11-ω10+ω5-ω6(x2); ω11-ω10+ω4-ω5(x2); ω11-ω10+ω3-ω4(x2); ω11-ω10+ω2-ω3(x2); ω11-ω10+ω1-ω2 (x2); (18)

ω11-ω9+ω7-ω9 (x2); ω11-ω9+ω6-ω8 (x2); ω11-ω9+ω5-ω7 (x2); ω11-ω9+ω4-ω6 (x2); ω11-ω9+ω3-ω5 (x2); ω11-ω9+ω2-ω4 (x2); ω11-ω9+ω1-ω3 (x2); (14)

ω11-ω8+ω5-ω8 (x2); ω11-ω8+ω4-ω7 (x2); ω11-ω8+ω3-ω6 (x2); ω11-ω8+ω2-ω5 (x2); ω11-ω8+ω1-ω4 (x2); (10)

ω11-ω7+ω3-ω7 (x2); ω11-ω7+ω2-ω6 (x2); ω11-ω7+ω1-ω5 (x2); (6)

ω11-ω6+ω1-ω6 (x2); (2) + 8 tones factors

- **61+195 =256 terms**

12 Tones

ω12-ω12+ω12-ω12; ω12-ω12+ω11-ω11; ω12-ω12+ω10-ω10; ω12-ω12+ω9-ω9; ω12-ω12+ω8-ω8; ω12-ω12+ω7-ω7; ω12-ω12+ω6-ω6; ω12-ω12+ω5-ω5; ω12-ω12+ω4-ω4; ω12-ω12+ω3-ω3; ω12-ω12+ω2-ω2; ω12-ω12+ω1-ω1; (12)

ω12-ω11+ω10-ω11(x2); ω12-ω11+ω9-ω10(x2); ω12-ω11+ω8-ω9(x2); ω12-ω11+ω7-ω8(x2); ω12-ω11+ω6-ω7(x2); ω12-ω11+ω5-ω6(x2); ω12-ω11+ω4-ω5(x2); ω12-ω11+ω3-ω4(x2); ω12-ω11+ω2-ω3(x2); ω12-ω11+ω1-ω2 (x2); (20)

ω12-ω10+ω8-ω10 (x2); ω12-ω10+ω7-ω9 (x2); ω12-ω10+ω6-ω8 (x2); ω12-ω10+ω5-ω7 (x2); ω12-ω10+ω4-ω6 (x2); ω12-ω10+ω3-ω5 (x2); ω12-ω10+ω2-ω4 (x2); ω12-ω10+ω1-ω3 (x2); (16)

ω12-ω9+ω6-ω9 (x2); ω12-ω9+ω5-ω8 (x2); ω12-ω9+ω4-ω7 (x2); ω12-ω9+ω3-ω6 (x2); ω12-ω9+ω2-ω5 (x2); ω12-ω9+ω1-ω4 (x2); (12)

ω12-ω8+ω4-ω8 (x2); ω12-ω8+ω3-ω7 (x2); ω12-ω8+ω2-ω6 (x2); ω12-ω8+ω1-ω5 (x2); (8)

ω12-ω7+ω2-ω7 (x2); ω12-ω7+ω1-ω6 (x2); (4) + 8 tones factors

- **72+256 =328 terms**

4th order –> +ΔW

2 Tones

ω2- ω2+ ω2- ω1; ω2- ω1+ ω1- ω1; (1+1)

- **2 terms**

3 Tones

ω3- ω3+ ω3- ω2; ω3- ω3+ ω2- ω1; (2)

ω3- ω2- ω2+ ω2; ω3- ω2- ω1+ ω1; + 2 tones factors (2)

- **4+2 =6 terms**

4 Tones

ω4-ω4+ ω4-ω3; ω4-ω4+ ω3-ω2; ω4-ω4+ ω2-ω1; (3)

ω4-ω3-ω3+ω3; ω4-ω3-ω2+ω2; ω4-ω3-ω1+ω1; (3)

ω4-ω2-ω2+ω1; + 3 tones factors (1)

- 7+6 =13 terms

5 Tones

ω5-ω5+ω5-ω4; ω5-ω5+ω4-ω3; ω5-ω5+ ω3-ω2; ω5-ω5+ ω2-ω1; (4)

ω5-ω4+ω4-ω4; ω5-ω4+ω3-ω3; ω5-ω4+ω2-ω2; ω5-ω4+ω1-ω1; (4)

ω5-ω3-ω3+ω2; ω5-ω3-ω2+ω1; (2) + 4 tones factors

- 10+13 =23 terms

6 Tones

ω6-ω6+ω6-ω5; ω6-ω6+ω5-ω4; ω6-ω6+ω4-ω3; ω6-ω6+ω3-ω2; ω6-ω6+ ω2- ω1; (5)

ω6-ω5+ω5-ω5; ω6-ω5+ω4-ω4; ω6-ω5+ω3-ω3; ω6-ω5+ω2-ω2; ω6-ω5-ω1+ω1; (5)

ω6-ω4-ω4+ω3; ω6-ω4-ω3+ω2; ω6-ω4-ω2+ω1; (3)

ω6-ω3-ω3+ ω1; + 5 tones factors (1)

- **14+23 = 37 terms**

7 Tones

ω7-ω7+ω7-ω6; ω7-ω7+ω6-ω5; ω7-ω7+ω5-ω4; ω7-ω7+ω4-ω3; ω7-ω7+ω3-ω2; ω7-ω7+ω2-ω1; (6)

ω7-ω6-ω6+ω6; ω7-ω6-ω5+ω5; ω7-ω6-ω4+ω4; ω7-ω6-ω3+ω3; ω7-ω6-ω2+ω2; ω7-ω6-ω1+ω1; (6)

ω7-ω5-ω5+ω4; ω7-ω5-ω4+ω3; ω7-ω5-ω3+ω2; ω7-ω5-ω2+ω1; (4)

ω7-ω4-ω4+ω2; ω7-ω4-ω3+ω1 (2) + 6 tones factors

- **18+37 =55 terms**

8 Tones

ω8-ω8+ω8-ω7; ω8-ω8+ω7-ω6; ω8-ω8+ω6-ω5; ω8-ω8+ω5-ω4; ω8-ω8+ω4-ω3; ω8-ω8+ω3-ω2; ω8-ω8+ω2-ω1; (7)

ω8-ω7-ω7+ω7; ω8-ω7-ω6+ω6; ω8-ω7-ω5+ω5; ω8-ω7-ω4+ω4; ω8-ω7-ω3+ω3; ω8-ω7-ω2+ω2; ω8-ω7-ω1+ω1; (7)

ω8-ω6-ω6+ω5; ω8-ω6-ω5+ω4; ω8-ω6-ω4+ω3; ω8-ω6-ω3+ω2; ω8-ω6-ω2+ω1; (5)

ω8-ω5-ω5+ω3; ω8-ω5-ω4+ω2; ω8-ω5-ω3+ω1 (3)

ω8-ω4-ω4+ω1; (1) + 7 tones factors

- 23+55 = 78 terms

9 Tones

ω9-ω9+ω9-ω8;ω9-ω9+ω8-ω7; ω9-ω9+ω7-ω6; ω9-ω9+ω6-ω5; ω9-ω9+ω5-ω4; ω9-ω9+ω4-ω3; ω9-ω9+ω3-ω2; ω9-ω9+ω2-ω1; (8)

ω9-ω8+ω8-ω8; ω9-ω8+ω7-ω7; ω9-ω8+ω6-ω6; ω9-ω8+ω5-ω5; ω9-ω8+ω4-ω4; ω9-ω8+ω3-ω3; ω9-ω8+ω2-ω2;ω9-ω8+ω1-ω1; (8)

ω9-ω7-ω7+ω6; ω9-ω7-ω6+ω5; ω9-ω7-ω5+ω4; ω9-ω7-ω4+ω3; ω9-ω7-ω3+ω2; ω9-ω7-ω2+ω1; (6)

ω9-ω6-ω6+ω4; ω9-ω6-ω5+ω3; ω9-ω6-ω4+ω2; ω9-ω6-ω3+ω1; (4)

ω9-ω5-ω5+ω2; ω9-ω5-ω4+ω1; (2) + 8 tones factors

- 28+78 = 106 terms

10 Tones

ω10-ω10+ω10-ω9;ω10-ω10+ω9-ω8; ω10-ω10+ω8-ω7; ω10-ω10+ω7-ω6; ω10-ω10+ω6-ω5; ω10-ω10+ω5-ω4; ω10-ω10+ω4-ω3; ω10-ω10+ω3-ω2; ω10-ω10+ω2-ω1; (9)

ω10-ω9+ω9-ω9; ω10-ω9+ω8-ω8; ω10-ω9+ω7-ω7; ω10-ω9+ω6-ω6; ω10-ω9+ω5-ω5; ω10-ω9+ω4-ω4; ω10-ω9+ω3-ω3; ω10-ω9+ω2-ω2; ω10-ω9+ω1-ω1; (9)

ω10-ω8-ω8+ω7; ω10-ω8-ω7+ω6; ω10-ω8-ω6+ω5; ω10-ω8-ω5+ω4; ω10-ω8-ω4+ω3; ω10-ω8-ω3+ω2; ω10-ω8-ω2+ω1; (7)

ω10-ω7-ω7+ω5; ω10-ω7-ω6+ω4; ω10-ω7-ω5+ω3; ω10-ω7-ω4+ω2; ω10-ω7-ω3+ω1; (5)

ω10-ω6-ω6+ω3; ω10-ω6-ω5+ω2; ω10-ω6-ω4+ω1; (3)

ω10-ω5-ω5+ω1; (1) + 9 tones factors

- 34+106 = 140 terms

11 Tones

ω11-ω11+ω11-ω10; ω11-ω11+ω10-ω9; ω11-ω11+ω9-ω8; ω11-ω11+ω8-ω7; ω11-ω11+ω7-ω6; ω11-ω11+ω6-ω5; ω11-ω11+ω5-ω4; ω11-ω11+ω4-ω3; ω11-ω11+ω3-ω2; ω11-ω11+ω2-ω1; (10)

ω11-ω10+ω10-ω10; ω11-ω10+ω9-ω9; ω11-ω10+ω8-ω8; ω11-ω10+ω7-ω7; ω11-ω10+ω6-ω6; ω11-ω10+ω5-ω5; ω11-ω10+ω4-ω4; ω11-ω10+ω3-ω3; ω11-ω10+ω2-ω2; ω11-ω10+ω1-ω1; (10)

ω11-ω9-ω9+ω8; ω11-ω9-ω8+ω7; ω11-ω9-ω7+ω6; ω11-ω9-ω6+ω5; ω11-ω9-ω5+ω4; ω11-ω9-ω4+ω3; ω11-ω9-ω3+ω2; ω11-ω9-ω2+ω1; (8)

ω11-ω8-ω8+ω6; ω11-ω8-ω7+ω5; ω11-ω8-ω6+ω4; ω11-ω8-ω5+ω3; ω11-ω8-ω4+ω2; ω11-ω8-ω3+ω1; (6)
ω11-ω7-ω7+ω4; ω11-ω7-ω6+ω3; ω11-ω7-ω5+ω2; ω11-ω7-ω4+ω1; (4)
ω11-ω6-ω6+ω2; ω11-ω6-ω5+ω1; (2) + 10 tones factors
- 40+140 = 180 terms

12 Tones
ω12-ω12+ω12-ω11; ω12-ω12+ω11-ω10; ω12-ω12+ω10-ω9; ω12-ω12+ω9-ω8; ω12-ω12+ω8-ω7; ω12-ω12+ω7-ω6; ω12-ω12+ω6-ω5; ω12-ω12+ω5-ω4; ω12-ω12+ω4-ω3; ω12-ω12+ω3-ω2; ω12-ω12+ω2-ω1; (11)
ω12-ω11+ω11-ω11; ω12-ω11+ω10-ω10; ω12-ω11+ω9-ω9; ω12-ω11+ω8-ω8; ω12-ω11+ω7-ω7; ω12-ω11+ω6-ω6; ω12-ω11+ω5-ω5; ω12-ω11+ω4-ω4; ω12-ω11+ω3-ω3; ω12-ω11+ω2-ω2; ω12-ω11+ω1-ω1; (11)
ω12-ω10-ω10+ω9; ω12-ω10-ω9+ω8; ω12-ω10-ω8+ω7; ω12-ω10-ω7+ω6; ω12-ω10-ω6+ω5; ω12-ω10-ω5+ω4; ω12-ω10-ω4+ω3; ω12-ω10-ω3+ω2; ω12-ω10-ω2+ω1; (9)
ω12-ω9-ω9+ω7; ω12-ω9-ω8+ω6; ω12-ω9-ω7+ω5; ω12-ω9-ω6+ω4; ω12-ω9-ω5+ω3; ω12-ω9-ω4+ω2; ω12-ω9-ω3+ω1; (7)
ω12-ω8-ω8+ω5; ω12-ω8-ω7+ω4; ω12-ω8-ω6+ω3; ω12-ω8-ω5+ω2; ω12-ω8-ω4+ω1; (5)
ω12-ω7-ω7+ω3; ω12-ω7-ω6+ω2; ω12-ω7-ω5+ω1; (3)
ω12-ω6-ω6+ω1; (1) +11 tones factors
- 47+180 = 140 terms

----------//----------

4th order –> +2ΔW

2 Tones
ω2-ω1+ω2-ω1; (1)

- **1 terms**

3 Tones
ω3-ω3+ω3-ω1; (1)
ω3-ω2+ω3-ω2; ω3-ω2+ω2-ω1; (2)
ω3-ω1+ω1-ω1; (1) + 2 tones factors

- **4+1 = 5 terms**

4 Tones
ω4-ω4+ω4-ω2; ω4-ω4+ω3-ω1; (2)
ω4-ω3+ω4-ω3; ω4-ω3+ω3-ω2; ω4-ω3+ω2-ω1; (3)
ω4-ω2+ω2-ω2; ω4-ω2+ω1-ω1;(2) + 3 tones factors (2)

- **7+5 =12 terms**

5 Tones
ω5-ω5+ω5-ω3; ω5-ω5+ω4-ω2; ω5-ω5+ω3-ω1; (3)
ω5-ω4+ω5-ω4; ω5-ω4+ω4-ω3; ω5-ω4+ω3-ω2; ω5-ω4+ω2-ω1; (4)
ω5-ω3+ω3-ω3; ω5-ω3+ω2-ω2; ω5-ω3+ω1-ω1; (3)
ω5-ω2-ω2+ω1; (1) + 4 tones factors

- **11+12 =23 terms**

6 Tones
ω6-ω6+ω6-ω4; ω6-ω6+ω5-ω3; ω6-ω6+ω4-ω2; ω6-ω6+ω3-ω1; (4)
ω6-ω5+ω6-ω5; ω6-ω5+ω5-ω4; ω6-ω5+ω4-ω3; ω6-ω5+ω3-ω2; ω6-ω5+ω2-ω1; (5)
ω6-ω4+ω4-ω4; ω6-ω4+ω3-ω3; ω6-ω4+ω2-ω2; ω6-ω4+ω1-ω1; (4)
ω6-ω3-ω3+ω2; ω6-ω3-ω2+ω1; + 5 tones factors (2)

- **15+23 = 38 terms**

7 Tones
ω7-ω7+ω7-ω5; ω7-ω7+ω6-ω4; ω7-ω7+ω5-ω3; ω7-ω7+ω4-ω2; ω7-ω7+ω3-ω1; (5)
ω7-ω6+ω7-ω6; ω7-ω6+ω6-ω5; ω7-ω6+ω5-ω4; ω7-ω6+ω4-ω3; ω7-ω6+ω3-ω2; ω7-ω6+ω2-ω1; (6)
ω7-ω5+ω5-ω5; ω7-ω5+ω4-ω4; ω7-ω5+ω3-ω3; ω7-ω5+ω2-ω2; ω7-ω5+ω1-ω1; (5)
ω7-ω4-ω4+ω3; ω7-ω4-ω3+ω2; ω7-ω4-ω2+ω1; (3)
ω7-ω3-ω3+ω1;(1) + 6 tones factors
20+38 =58 terms

8 Tones
ω8-ω8+ω8-ω6; ω8-ω8+ω7-ω5; ω8-ω8+ω6-ω4; ω8-ω8+ω5-ω3; ω8-ω8+ω4-ω2; ω8-ω8+ω3-ω1; (6)
ω8-ω7+ω8-ω7; ω8-ω7+ω7-ω6; ω8-ω7+ω6-ω5; ω8-ω7+ω5-ω4; ω8-ω7+ω4-ω3; ω8-ω7+ω3-ω2; ω8-ω7+ω2-ω1; (7)
ω8-ω6+ω6-ω6; ω8-ω6+ω5-ω5; ω8-ω6+ω4-ω4; ω8-ω6+ω3-ω3; ω8-ω6+ω2-ω2; ω8-ω6+ω1-ω1; (6)
ω8-ω5-ω5+ω4; ω8-ω5-ω4+ω3; ω8-ω5-ω3+ω2; ω8-ω5-ω2+ω1; (4)
ω8-ω4-ω4+ω2; ω8-ω4-ω3+ω1;(2) + 7 tones factors
25+58 =83 terms

9 Tones
ω9-ω9+ ω9-ω7; ω9-ω9+ω8-ω6; ω9-ω9+ω7-ω5; ω9-ω9+ω6-ω4; ω9-ω9+ω5-ω3; ω9-ω9+ω4-ω2; ω9-ω9+ω3-ω1; (7)
ω9-ω8+ω9-ω8; ω9-ω8+ω8-ω7; ω9-ω8+ω7-ω6; ω9-ω8+ω6-ω5; ω9-ω8+ω5-ω4; ω9-ω8+ω4-ω3;

ω9-ω8+ω3-ω2; ω9-ω8+ω2-ω1; (8)
ω9-ω7+ω7-ω7; ω9-ω7+ω6-ω6; ω9-ω7+ω5-ω5; ω9-ω7+ω4-ω4; ω9-ω7+ω3-ω3; ω9-ω7+ω2-ω2;
ω9-ω7+ω1-ω1; (7)
ω9-ω6-ω6+ω5; ω9-ω6-ω5+ω4; ω9-ω6-ω4+ω3; ω9-ω6-ω3+ω2; ω9-ω6-ω2+ω1; (5)
ω9-ω5-ω5+ω3; ω9-ω5-ω4+ω2; ω9-ω5-ω3+ω1; (3)
ω9-ω4-ω4+ω1; (1) + 8 tones factors
31+83 =114 terms

10 Tones
ω10-ω10+ω10-ω8; ω10-ω10+ω9-ω7; ω10-ω10+ω8-ω6; ω10-ω10+ω7-ω5; ω10-ω10+ω6-ω4;
ω10-ω10+ω5-ω3; ω10-ω10+ω4-ω2; ω10-ω10+ω3-ω1; (8)
ω10-ω9+ω10-ω9; ω10-ω9+ω9-ω8; ω10-ω9+ω8-ω7; ω10-ω9+ω7-ω6; ω10-ω9+ω6-ω5; ω10-ω9+ω5-ω4;
ω10-ω9+ω4-ω3; ω10-ω9+ω3-ω2; ω10-ω9+ω2-ω1; (9)
ω10-ω8+ω8-ω8; ω10-ω8+ω7-ω7; ω10-ω8+ω6-ω6; ω10-ω8+ω5-ω5; ω10-ω8+ω4-ω4; ω10-ω8+ω3-ω3;
ω10-ω8+ω2-ω2; ω10-ω8+ω1-ω1; (8)
ω10-ω7-ω7+ω6; ω10-ω7-ω6+ω5; ω10-ω7-ω5+ω4; ω10-ω7-ω4+ω3; ω10-ω7-ω3+ω2; ω10-ω7-ω2+ω1; (6)
ω10-ω6-ω6+ω4; ω10-ω6-ω5+ω3; ω10-ω6-ω4+ω2; ω10-ω6-ω3+ω1; (4)
ω10-ω5-ω5+ω2; ω10-ω5-ω4+ω1; (2) + 9 tones factors
37+114 =151 terms

11 Tones
ω11-ω11+ω11-ω9; ω11-ω11+ω10-ω8; ω11-ω11+ω9-ω7; ω11-ω11+ω8-ω6; ω11-ω11+ω7-ω5;
ω11-ω11+ω6-ω4; ω11-ω11+ω5-ω3; ω11-ω11+ω4-ω2; ω11-ω11+ω3-ω1; (9)
ω11-ω10+ω11-ω10; ω11-ω10+ω10-ω9; ω11-ω10+ω9-ω8; ω11-ω10+ω8-ω7; ω11-ω10+ω7-ω6; ω11-ω10+ω6-ω5; ω11-ω10+ω5-ω4; ω11-ω10+ω4-ω3; ω11-ω10+ω3-ω2; ω11-ω10+ω2-ω1; (10)
ω11-ω9+ω9-ω9; ω11-ω9+ω8-ω8; ω11-ω9+ω7-ω7; ω11-ω9+ω6-ω6; ω11-ω9+ω5-ω5; ω11-ω9+ω4-ω4; ω11-ω9+ω3-ω3; ω11-ω9+ω2-ω2; ω11-ω9+ω1-ω1; (9)
ω11-ω8-ω8+ω7; ω11-ω8-ω7+ω6; ω11-ω8-ω6+ω5; ω11-ω8-ω5+ω4; ω11-ω8-ω4+ω3; ω11-ω8-ω3+ω2; ω11-ω8-ω2+ω1; (7)
ω11-ω7-ω7+ω5; ω11-ω7-ω6+ω4; ω11-ω7-ω5+ω3; ω11-ω7-ω4+ω2; ω11-ω7-ω3+ω1; (5)
ω11-ω6-ω6+ω3; ω11-ω6-ω5+ω2; ω11-ω6-ω4+ω1; (3)
ω11-ω5-ω5+ω1; (1)+ 10 tones factors
44+151 =195 terms

4th order –> +3ΔW

3 Tones
ω3-ω2+ω3-ω1;
ω3-ω1+ω2-ω1>; (1)
- 2 terms

4 Tones
ω4-ω4+ω4-ω1; (1)
ω4-ω3+ω4-ω2; ω4-ω3+ω3-ω1; (2)
ω4-ω2+ω3-ω2; ω4-ω2+ω2-ω1; (2)
ω4-ω1+ω1-ω1; (1) + 3 tones factors
- 6+2 =8 terms

5 Tones
ω5-ω5+ω5-ω2; ω5-ω5+ω4-ω1; (2)
ω5-ω4+ω5-ω3; ω5-ω4+ω4-ω2; ω5-ω4+ω3-ω1; (3)
ω5-ω3+ω4-ω3; ω5-ω3+ω3-ω2; ω5-ω3+ω2-ω1; (3)
ω5-ω2+ω2-ω2; ω5-ω2+ω1-ω1; (2) + 4 tones factors
- **10+7 =18 terms**

6 Tones
ω6-ω6+ω6-ω3; ω6-ω6+ω5-ω2; ω6-ω6+ω4-ω1; (3)
ω6-ω5+ω6-ω4; ω6-ω5+ω5-ω3; ω6-ω5+ω4-ω2; ω6-ω5+ω3-ω1; (4)
ω6-ω4+ω5-ω4; ω6-ω4+ω4-ω3; ω6-ω4+ω3-ω2; ω6-ω4+ω2-ω1; (4)
ω6-ω3+ω3-ω3; ω6-ω3+ω2-ω2; ω6-ω3+ω1-ω1; (3) + 5 tones factors (2)
ω6-ω2-ω2+ω1(1);
- **15+18 = 33 terms**

7 Tones
ω7-ω7+ω7-ω4; ω7-ω7+ω6-ω3; ω7-ω7+ω5-ω2; ω7-ω7+ω4-ω1; (4)
ω7-ω6+ω7-ω5; ω7-ω6+ω6-ω4; ω7-ω6+ω5-ω3; ω7-ω6+ω4-ω2; ω7-ω6+ω3-ω1; (5)
ω7-ω5+ω6-ω5; ω7-ω5+ω5-ω4; ω7-ω5+ω4-ω3; ω7-ω5+ω3-ω2; ω7-ω5+ω2-ω1; (5)
ω7-ω4-ω4+ω4; ω7-ω4-ω3+ω3; ω7-ω4-ω2+ω2; ω7-ω4-ω1+ω1; (4)
ω7-ω3-ω3+ω2; ω7-ω3-ω2+ω1; (2) + 6 tones factors
20+33 =53 terms

8 Tones
ω8-ω8+ω8-ω5; ω8-ω8+ω7-ω4; ω8-ω8+ω6-ω3; ω8-ω8+ω5-ω2; ω8-ω8+ω4-ω1; (5)
ω8-ω7+ω8-ω6; ω8-ω7+ω7-ω5; ω8-ω7+ω6-ω4; ω8-ω7+ω5-ω3; ω8-ω7+ω4-ω2; ω8-ω7+ω3-ω1; (6)
ω8-ω6+ω7-ω6; ω8-ω6+ω6-ω5; ω8-ω6+ω5-ω4; ω8-ω6+ω4-ω3; ω8-ω6+ω3-ω2; ω8-ω6+ω2-ω1; (6)

ω8-ω5-ω5+ω5; ω8-ω5-ω4+ω4; ω8-ω5-ω3+ω3; ω8-ω5-ω2+ω2; ω8-ω5-ω1+ω1; (5)
ω8-ω4-ω4+ω3; ω8-ω4-ω3+ω2; ω8-ω4-ω2+ω1; (3)
ω8-ω3-ω3+ω1; (1) + 7 tones factors
26+53 =79 terms

9 Tones
ω9-ω9+ω9-ω6; ω9-ω9+ω8-ω5; ω9-ω9+ω7-ω4; ω9-ω9+ω6-ω3; ω9-ω9+ω5-ω2; ω9-ω9+ω4-ω1; (6)
ω9-ω8+ω9-ω7; ω9-ω8+ω8-ω6; ω9-ω8+ω7-ω5; ω9-ω8+ω6-ω4; ω9-ω8+ω5-ω3; ω9-ω8+ω4-ω2; ω9-ω8+ω3-ω1; (7)
ω9-ω7+ω8-ω7; ω9-ω7+ω7-ω6; ω9-ω7+ω6-ω5; ω9-ω7+ω5-ω4; ω9-ω7+ω4-ω3; ω9-ω7+ω3-ω2; ω9-ω7+ω2-ω1; (7)
ω9-ω6-ω6+ω6; ω9-ω6-ω5+ω5; ω9-ω6-ω4+ω4; ω9-ω6-ω3+ω3; ω9-ω6-ω2+ω2; ω9-ω6-ω1+ω1; (6)
ω9-ω5-ω5+ω4; ω9-ω5-ω4+ω3; ω9-ω5-ω3+ω2; ω9-ω5-ω2+ω1; (4)
ω9-ω4-ω4+ω2; ω9-ω4-ω3+ω1; (2) + 7 tones factors
32+81 =111 terms

10 Tones
ω10-ω10+ω10-ω7; ω10-ω10+ω9-ω6; ω10-ω10+ω8-ω5; ω10-ω10+ω7-ω4; ω10-ω10+ω6-ω3; ω10-ω10+ω5-ω2; ω10-ω10+ω4-ω1; (7)
ω10-ω9+ω10-ω8; ω10-ω9+ω9-ω7; ω10-ω9+ω8-ω6; ω10-ω9+ω7-ω5; ω10-ω9+ω6-ω4; ω10-ω9+ω5-ω3; ω10-ω9+ω4-ω2; ω10-ω9+ω3-ω1; (8)
ω10-ω8+ω9-ω8; ω10-ω8+ω8-ω7; ω10-ω8+ω7-ω6; ω10-ω8+ω6-ω5; ω10-ω8+ω5-ω4; ω10-ω8+ω4-ω3; ω10-ω8+ω3-ω2; ω10-ω8+ω2-ω1; (8)
ω10-ω7-ω7+ω7; ω10-ω7-ω6+ω6; ω10-ω7-ω5+ω5; ω10-ω7-ω4+ω4; ω10-ω7-ω3+ω3; ω10-ω7-ω2+ω2; ω10-ω7-ω1+ω1; (7)
ω10-ω6-ω6+ω5; ω10-ω6-ω5+ω4; ω10-ω6-ω4+ω3; ω10-ω6-ω3+ω2; ω10-ω6-ω2+ω1; (5)
ω10-ω5-ω5+ω3; ω10-ω5-ω4+ω2; ω10-ω5-ω3+ω1; (3)
ω10-ω4-ω4+ω1; (1) + 9 tones factors
39+113 =150 terms

11 Tones
ω11-ω11+ω11-ω8; ω11-ω11+ω10-ω7; ω11-ω11+ω9-ω6; ω11-ω11+ω8-ω5; ω11-ω11+ω7-ω4; ω11-ω11+ω6-ω3; ω11-ω11+ω5-ω2; ω11-ω11+ω4-ω1; (8)
ω11-ω10+ω11-ω9; ω11-ω10+ω10-ω8; ω11-ω10+ω9-ω7; ω11-ω10+ω8-ω6; ω11-ω10+ω7-ω5; ω11-ω10+ω6-ω4; ω11-ω10+ω5-ω3; ω11-ω10+ω4-ω2; ω11-ω10+ω3-ω1; (9)
ω11-ω9+ω10-ω9; ω11-ω9+ω9-ω8; ω11-ω9+ω8-ω7; ω11-ω9+ω7-ω6; ω11-ω9+ω6-ω5; ω11-ω9+ω5-ω4; ω11-ω9+ω4-ω3; ω11-ω9+ω3-ω2; ω11-ω9+ω2-ω1; (9)
ω11-ω8-ω8+ω8; ω11-ω8-ω7+ω7; ω11-ω8-ω6+ω6; ω11-ω8-ω5+ω5; ω11-ω8-ω4+ω4; ω11-ω8-ω3+ω3; ω11-ω8-ω2+ω2; ω11-ω8-ω1+ω1; (8)
ω11-ω7-ω7+ω6; ω11-ω7-ω6+ω5; ω11-ω7-ω5+ω4; ω11-ω7-ω4+ω3; ω11-ω7-ω3+ω2; ω11-ω7-ω2+ω1; (6)
ω11-ω6-ω6+ω4; ω11-ω6-ω5+ω3; ω11-ω6-ω4+ω2; ω11-ω6-ω3+ω1; (4)
ω11-ω5-ω5+ω2; ω11-ω5-ω4+ω1; (2) + 10 tones factors
46+152 =196 terms

----------//----------

4th order –> +4ΔW
3 Tones
ω3-ω1+ω3-ω1;
- 1 terms
4 Tones
ω4-ω3+ω4-ω1; (1)
ω4-ω2+ω4-ω2; ω4-ω2+ω3-ω1; (2)
ω4-ω1+ω2-ω1; (1) + 3 tones factors
- **4+1 =5 terms**

5 Tones
ω5-ω5+ω5-ω1; (1)
ω5-ω4+ω5-ω2; ω5-ω4+ω4-ω1; (2)
ω5-ω3+ω5-ω3; ω5-ω3+ω4-ω2; ω5-ω3+ω3-ω1; (3)
ω5-ω2+ω3-ω2; ω5-ω2+ω2-ω1; (2)
ω5-ω1+ω1-ω1; (1) + 4 tones factors
- **9+5 =14 terms**

6 Tones
ω6-ω6+ω6-ω2; ω6-ω6+ω5-ω1; (2)
ω6-ω5+ω6-ω3; ω6-ω5+ω5-ω2; ω6-ω5+ω4-ω1; (3)
ω6-ω4+ω6-ω4; ω6-ω4+ω5-ω3; ω6-ω4+ω4-ω2; ω6-ω4+ω3-ω1; (4)
ω6-ω3+ω4-ω3; ω6-ω3+ω3-ω2; ω6-ω3+ω2-ω1; (3) + 5 tones factors
ω6-ω2-ω2+ω2; ω6-ω2-ω1+ω1 (2);
- **14+14 = 28 terms**

7 Tones
ω7-ω7+ω7-ω3; ω7-ω7+ω6-ω2; ω7-ω7+ω5-ω1; (3)
ω7-ω6+ω7-ω4; ω7-ω6+ω6-ω3; ω7-ω6+ω5-ω2; ω7-ω6+ω4-ω1; (4)

ω7-ω5+ω7-ω5; ω7-ω5+ω6-ω4; ω7-ω5+ω5-ω3; ω7-ω5+ω4-ω2; ω7-ω5+ω3-ω1; (5)
ω7-ω4+ω5-ω4; ω7-ω4+ω4-ω3; ω7-ω4+ω3-ω2; ω7-ω4+ω2-ω1; (4)
ω7-ω3-ω3+ω3; ω7-ω3-ω2+ω2; ω7-ω3-ω1+ω1; (3)
ω7-ω2-ω2+ω1;(1) + 6 tones factors
20+28 =48 terms

8 Tones
ω8-ω8+ω8-ω4; ω8-ω8+ω7-ω3; ω8-ω8+ω6-ω2; ω8-ω8+ω5-ω1; (4)
ω8-ω7+ω8-ω5; ω8-ω7+ω7-ω4; ω8-ω7+ω6-ω3; ω8-ω7+ω5-ω2; ω8-ω7+ω4-ω1; (5)
ω8-ω6+ω8-ω6; ω8-ω6+ω7-ω5; ω8-ω6+ω6-ω4; ω8-ω6+ω5-ω3; ω8-ω6+ω4-ω2; ω8-ω6+ω3-ω1; (6)
ω8-ω5+ω6-ω5; ω8-ω5+ω5-ω4; ω8-ω5+ω4-ω3; ω8-ω5+ω3-ω2; ω8-ω5+ω2-ω1; (5)
ω8-ω4-ω4+ω4; ω8-ω4-ω3+ω3; ω8-ω4-ω2+ω2; ω8-ω4-ω1+ω1; (4)
ω8-ω3-ω3+ω2; ω8-ω3-ω2+ω1; (2) + 7 tones factors
26+48 =74 terms

9 Tones
ω9-ω9+ω9-ω5; ω9-ω9+ω8-ω4; ω9-ω9+ω7-ω3; ω9-ω9+ω6-ω2; ω9-ω9+ω5-ω1; (5)
ω9-ω8+ω9-ω6; ω9-ω8+ω8-ω5; ω9-ω8+ω7-ω4; ω9-ω8+ω6-ω3; ω9-ω8+ω5-ω2; ω9-ω8+ω4-ω1; (6)
ω9-ω7+ω9-ω7; ω9-ω7+ω8-ω6; ω9-ω7+ω7-ω5; ω9-ω7+ω6-ω4; ω9-ω7+ω5-ω3; ω9-ω7+ω4-ω2;
ω9-ω7+ω3-ω1; (7)
ω9-ω6+ω7-ω6; ω9-ω6+ω6-ω5; ω9-ω6+ω5-ω4; ω9-ω6+ω4-ω3; ω9-ω6+ω3-ω2; ω9-ω6+ω2-ω1; (6)
ω9-ω5-ω5+ω5; ω9-ω5-ω4+ω4; ω9-ω5-ω3+ω3; ω9-ω5-ω2+ω2; ω9-ω5-ω1+ω1; (5)
ω9-ω4-ω4+ω3; ω9-ω4-ω3+ω2; ω9-ω4-ω2+ω1; (3)
ω9-ω3-ω3+ω1; (1) + 8 tones factors
33+74 =107 terms

10 Tones
ω10-ω10+ω10-ω6; ω10-ω10+ω9-ω5; ω10-ω10+ω8-ω4; ω10-ω10+ω7-ω3; ω10-ω10+ω6-ω2;
ω10-ω10+ω5-ω1; (6)
ω10-ω9+ω10-ω7; ω10-ω9+ω9-ω6; ω10-ω9+ω8-ω5; ω10-ω9+ω7-ω4; ω10-ω9+ω6-ω3; ω10-ω9+ω5-ω2; ω10-ω9+ω4-ω1; (7)
ω10-ω8+ω10-ω8; ω10-ω8+ω9-ω7; ω10-ω8+ω8-ω6; ω10-ω8+ω7-ω5; ω10-ω8+ω6-ω4; ω10-ω8+ω5-ω3; ω10-ω8+ω4-ω2; ω10-ω8+ω3-ω1; (8)
ω10-ω7+ω8-ω7; ω10-ω7+ω7-ω6; ω10-ω7+ω6-ω5; ω10-ω7+ω5-ω4; ω10-ω7+ω4-ω3; ω10-ω7+ω3-ω2; ω10-ω7+ω2-ω1; (7)
ω10-ω6-ω6+ω6; ω10-ω6-ω5+ω5; ω10-ω6-ω4+ω4; ω10-ω6-ω3+ω3; ω10-ω6-ω2+ω2; ω10-ω6-ω1+ω1; (6)
ω10-ω5-ω5+ω4; ω10-ω5-ω4+ω3; ω10-ω5-ω3+ω2; ω10-ω5-ω2+ω1; (4)
ω10-ω4-ω4+ω2; ω10-ω4-ω3+ω1; (2) + 9 tones factors
40+107 =147 terms

11 Tones
ω11-ω11+ω11-ω7; ω11-ω11+ω10-ω6; ω11-ω11+ω9-ω5; ω11-ω11+ω8-ω4; ω11-ω11+ω7-ω3; ω11-ω11+ω6-ω2; ω11-ω11+ω5-ω1; (7)
ω11-ω10+ω11-ω8; ω11-ω10+ω10-ω7; ω11-ω10+ω9-ω6; ω11-ω10+ω8-ω5; ω11-ω10+ω7-ω4; ω11-ω10+ω6-ω3; ω11-ω10+ω5-ω2; ω11-ω10+ω4-ω1; (8)
ω11-ω9+ω11-ω9; ω11-ω9+ω10-ω8; ω11-ω9+ω9-ω7; ω11-ω9+ω8-ω6; ω11-ω9+ω7-ω5; ω11-ω9+ω6-ω4; ω11-ω9+ω5-ω3; ω11-ω9+ω4-ω2; ω11-ω9+ω3-ω1; (9)
ω11-ω8+ω9-ω8; ω11-ω8+ω8-ω7; ω11-ω8+ω7-ω6; ω11-ω8+ω6-ω5; ω11-ω8+ω5-ω4; ω11-ω8+ω4-ω3; ω11-ω8+ω3-ω2; ω11-ω8+ω2-ω1; (8)
ω11-ω7-ω7+ω7; ω11-ω7-ω6+ω6; ω11-ω7-ω5+ω5; ω11-ω7-ω4+ω4; ω11-ω7-ω3+ω3; ω11-ω7-ω2+ω2; ω11-ω7-ω1+ω1; (7)
ω11-ω6-ω6+ω5; ω11-ω6-ω5+ω4; ω11-ω6-ω4+ω3; ω11-ω6-ω3+ω2; ω11-ω6-ω2+ω1; (5)
ω11-ω5-ω5+ω3; ω11-ω5-ω4+ω2; ω11-ω5-ω3+ω1; (3)
ω11-ω4-ω4+ω1; (1) + 10 tones factors
48+147 =195 terms

4th order –> +5ΔW

4 Tones

ω4-ω2+ω4-ω1; (1)

ω4-ω1+ω3-ω1; (1)

- **2 terms**

5 Tones

ω5-ω4+ω5-ω1; (1)

ω5-ω3+ω5-ω2; ω5-ω3+ω4-ω1; (2)

ω5-ω2+ω4-ω2; ω5-ω2+ω3-ω1; (2)

ω5-ω1+ω2-ω1; (1) + 4 tones factors

- **6+2 =8 terms**

6 Tones

ω6-ω6+ω6-ω1; (1)

ω6-ω5+ω6-ω2; ω6-ω5+ω5-ω1; (2)

ω6-ω4+ω6-ω3; ω6-ω4+ω5-ω2; ω6-ω4+ω4-ω1; (3)

ω6-ω3+ω5-ω3; ω6-ω3+ω4-ω2; ω6-ω3+ω3-ω1; (3)

ω6-ω2+ω3-ω2; ω6-ω2+ω2-ω1; (2);

ω6-ω1-ω1+ω1; (1); + 5 tones factor

- **12+8 = 20 terms**

7 Tones

ω7-ω7+ω7-ω2; ω7-ω7+ω6-ω1; (2)

ω7-ω6+ω7-ω3; ω7-ω6+ω6-ω2; ω7-ω6+ω5-ω1; (3)

ω7-ω5+ω7-ω4; ω7-ω5+ω6-ω3; ω7-ω5+ω5-ω2; ω7-ω5+ω4-ω1; (4)

ω7-ω4+ω6-ω4; ω7-ω4+ω5-ω3; ω7-ω4+ω4-ω2; ω7-ω4+ω3-ω1; (4)

ω7-ω3+ω4-ω3; ω7-ω3+ω3-ω2; ω7-ω3+ω2-ω1; (3)

ω7-ω2 +ω2-ω2; ω7-ω2 +ω1-ω1; (2) + 6 tones factors

18+20 =38 terms

8 Tones

ω8-ω8+ω8-ω3; ω8-ω8+ω7-ω2; ω8-ω8+ω6-ω1; (3)

ω8-ω7+ω8-ω4; ω8-ω7+ω7-ω3; ω8-ω7+ω6-ω2; ω8-ω7+ω5-ω1; (4)

ω8-ω6+ω8-ω5; ω8-ω6+ω7-ω4; ω8-ω6+ω6-ω3; ω8-ω6+ω5-ω2; ω8-ω6+ω4-ω1; (5)

ω8-ω5+ω7-ω5; ω8-ω5+ω6-ω4; ω8-ω5+ω5-ω3; ω8-ω5+ω4-ω2; ω8-ω5+ω3-ω1; (5)

ω8-ω4+ω5-ω4; ω8-ω4+ω4-ω3; ω8-ω4+ω3-ω2; ω8-ω4+ω2-ω1; (4)

ω8-ω3+ω3-ω3; ω8-ω3+ω2-ω2; ω8-ω3+ω1-ω1; (3)

ω8-ω2-ω2+ω1; (1) + 7 tones factors

25+38 =63 terms

9 Tones

ω9-ω9+ω9-ω4; ω9-ω9+ω8-ω3; ω9-ω9+ω7-ω2; ω9-ω9+ω6-ω1; (4)

ω9-ω8+ω9-ω5; ω9-ω8+ω8-ω4; ω9-ω8+ω7-ω3; ω9-ω8+ω6-ω2; ω9-ω8+ω5-ω1; (5)

ω9-ω7+ω9-ω6; ω9-ω7+ω8-ω5; ω9-ω7+ω7-ω4; ω9-ω7+ω6-ω3; ω9-ω7+ω5-ω2; ω9-ω7+ω4-ω1; (6)

ω9-ω6+ω8-ω6; ω9-ω6+ω7-ω5; ω9-ω6+ω6-ω4; ω9-ω6+ω5-ω3; ω9-ω6+ω4-ω2; ω9-ω6+ω3-ω1; (6)

ω9-ω5+ω6-ω5; ω9-ω5+ω5-ω4; ω9-ω5+ω4-ω3; ω9-ω5+ω3-ω2; ω9-ω5+ω2-ω1; (5)

ω9-ω4+ω4-ω4; ω9-ω4+ω3-ω3; ω9-ω4+ω2-ω2; ω9-ω4+ω1-ω1; (4)

ω9-ω3-ω3+ω2; ω9-ω3-ω2+ω1; (2) + 8 tones factors

32+63 =95 terms

10 Tones

ω10-ω10+ω10-ω5; ω10-ω10+ω9-ω4; ω10-ω10+ω8-ω3; ω10-ω10+ω7-ω2; ω10-ω10+ω6-ω1; (5)

ω10-ω9+ω10-ω6; ω10-ω9+ω9-ω5; ω10-ω9+ω8-ω4; ω10-ω9+ω7-ω3; ω10-ω9+ω6-ω2; ω10-ω9+ω5-ω1; (6)

ω10-ω8+ω10-ω7; ω10-ω8+ω9-ω6; ω10-ω8+ω8-ω5; ω10-ω8+ω7-ω4; ω10-ω8+ω6-ω3; ω10-ω8+ω5-ω2; ω10-ω8+ω4-ω1; (7)

ω10-ω7+ω9-ω7; ω10-ω7+ω8-ω6; ω10-ω7+ω7-ω5; ω10-ω7+ω6-ω4; ω10-ω7+ω5-ω3; ω10-ω7+ω4-ω2; ω10-ω7+ω3-ω1; (7)

ω10-ω6+ω7-ω6; ω10-ω6+ω6-ω5; ω10-ω6+ω5-ω4; ω10-ω6+ω4-ω3; ω10-ω6+ω3-ω2; ω10-ω6+ω2-ω1; (6)

ω10-ω5+ω5-ω5; ω10-ω5+ω4-ω4; ω10-ω5+ω3-ω3; ω10-ω5+ω2-ω2; ω10-ω5+ω1-ω1; (5)

ω10-ω4-ω4+ω3; ω10-ω4-ω3+ω2; ω10-ω4-ω2+ω1; (3)

ω10-ω3-ω3+ω1; (1) + 8 tones factors

40+95 =135 terms

----------/ /----------

4th order –> +6ΔW

4 Tones

ω4-ω1+ω4-ω1; (1)

- **1 term**

5 Tones

ω5-ω3+ω5-ω1; (1)

ω5-ω2+ω5-ω2; ω5-ω2+ω4-ω1; (2)

ω5-ω1+ω3-ω1; (1) + 4 tones factors

- **4+1 =5 terms**

6 Tones

ω6-ω5+ω6-ω1; (1)

ω6-ω4+ω6-ω2; ω6-ω4+ω5-ω1; (2)

ω6-ω3+ω6-ω3; ω6-ω3+ω5-ω2; ω6-ω3+ω4-ω1; (3)

ω6-ω2+ω4-ω2; ω6-ω3+ω3-ω1; (2)

ω6-ω1+ω2-ω1; (1) + 5 tones factors

- **9+5 =14 terms**

7 Tones

ω7-ω7+ω7-ω1; (1)

ω7-ω6+ω7-ω2; ω7-ω6+ω6-ω1; (2)

ω7-ω5+ω7-ω3; ω7-ω5+ω6-ω2; ω7-ω5+ω5-ω1; (3)

ω7-ω4+ω7-ω4; ω7-ω4+ω6-ω3; ω7-ω4+ω5-ω2; ω7-ω4+ω4-ω1; (4)

ω7-ω3+ω5-ω3; ω7-ω3+ω4-ω2; ω7-ω3+ω3-ω1; (3)

ω7-ω2+ω3-ω2; ω7-ω2+ω2-ω1; (2)

ω7-ω1+ω1-ω1; (1) + 6 tones factors

- **16+14 =30 terms**

8 Tones

ω8-ω8+ω8-ω2; ω8-ω8+ω7-ω1; (2)

ω8-ω7+ω8-ω3; ω8-ω7+ω7-ω2; ω8-ω7+ω6-ω1; (3)

ω8-ω6+ω8-ω4; ω8-ω6+ω7-ω3; ω8-ω6+ω6-ω2; ω8-ω6+ω5-ω1; (4)

ω8-ω5+ω8-ω5; ω8-ω5+ω7-ω4; ω8-ω5+ω6-ω3; ω8-ω5+ω5-ω2; ω8-ω5+ω4-ω1; (5)

ω8-ω4+ω6-ω4; ω8-ω4+ω5-ω3; ω8-ω4+ω4-ω2; ω8-ω4+ω3-ω1; (4)

ω8-ω3+ω4-ω3; ω8-ω3+ω3-ω2; ω8-ω3+ω2-ω1; (3)

ω8-ω2+ω2-ω2; ω8-ω2+ω1-ω1; (2) + 7 tones factors

23+30 = 53 terms

9 Tones

ω9-ω9+ω9-ω3; ω9-ω9+ω8-ω2; ω9-ω9+ω7-ω1; (3)

ω9-ω8+ω9-ω4; ω9-ω8+ω8-ω3; ω9-ω8+ω7-ω2; ω9-ω8+ω6-ω1; (4)

ω9-ω7+ω9-ω5; ω9-ω7+ω8-ω4; ω9-ω7+ω7-ω3; ω9-ω7+ω6-ω2; ω9-ω7+ω5-ω1; (5)

ω9-ω6+ω9-ω6; ω9-ω6+ω8-ω5; ω9-ω6+ω7-ω4; ω9-ω6+ω6-ω3; ω9-ω6+ω5-ω2; ω9-ω6+ω4-ω1; (6)

ω9-ω5+ω7-ω5; ω9-ω5+ω6-ω4; ω9-ω5+ω5-ω3; ω9-ω5+ω4-ω2; ω9-ω5+ω3-ω1; (5)

ω9-ω4+ω5-ω4; ω9-ω4+ω4-ω3; ω9-ω4+ω3-ω2; ω9-ω4+ω2-ω1; (4)

ω9-ω3+ω3-ω3; ω9-ω3+ω2-ω2; ω9-ω3+ω1-ω1; (3)

ω9-ω2+ω1-ω2; (1) + 8 tones factors

31+53 = 84 terms

10 Tones

ω10-ω10+ω10-ω4; ω10-ω10+ω9-ω3; ω10-ω10+ω8-ω2; ω10-ω10+ω7-ω1; (4)

ω10-ω9+ω10-ω5; ω10-ω9+ω9-ω4; ω10-ω9+ω8-ω3; ω10-ω9+ω7-ω2; ω10-ω9+ω6-ω1; (5)

ω10-ω8+ω10-ω6; ω10-ω8+ω9-ω5; ω10-ω8+ω8-ω4; ω10-ω8+ω7-ω3; ω10-ω8+ω6-ω2; ω10-ω8+ω5-ω1; (6)

ω10-ω7+ω10-ω7; ω10-ω7+ω9-ω6; ω10-ω7+ω8-ω5; ω10-ω7+ω7-ω4; ω10-ω7+ω6-ω3; ω10-ω7+ω5-ω2; ω10-ω7+ω4-ω1; (7)

ω10-ω6+ω8-ω6; ω10-ω6+ω7-ω5; ω10-ω6+ω6-ω4; ω10-ω6+ω5-ω3; ω10-ω6+ω4-ω2; ω10-ω6+ω3-ω1; (6)

ω10-ω5+ω6-ω5; ω10-ω5+ω5-ω4; ω10-ω5+ω4-ω3; ω10-ω5+ω3-ω2; ω10-ω5+ω2-ω1; (5)

ω10-ω4+ω4-ω4; ω10-ω4+ω3-ω3; ω10-ω4+ω2-ω2; ω10-ω4+ω1-ω1; (4)

ω10-ω3+ω2- ω3; ω10-ω3+ω1-ω2; (2) + 8 tones factors

39+84 =123 terms

----------//----------

4th order –> +7ΔW

5 Tones

ω5-ω2+ω5-ω1; (1)

ω5-ω1+ω4-ω1; (1)

- **2 terms**

6 Tones

ω6-ω4+ω6-ω1; (1)

ω6-ω3+ω6-ω2; ω6-ω3+ω5-ω1; (2)

ω6-ω2+ω5-ω2; ω6-ω3+ω4-ω1; (2)

ω6-ω1+ω3-ω1; (1) + 5 tones factors

- **6+2 =8 terms**

7 Tones

ω7-ω6+ω7-ω1; (1)

ω7-ω5+ω7-ω2; ω7-ω5+ω6-ω1; (2)

ω7-ω4+ω7-ω3; ω7-ω4+ω6-ω2; ω7-ω4+ω5-ω1; (3)

ω7-ω3+ω6-ω3; ω7-ω3+ω5-ω2; ω7-ω3+ω4-ω1; (3)

ω7-ω2+ω4-ω2; ω7-ω2+ω3-ω1; (2)

ω7-ω1+ω2-ω1; (1) + 6 tones factors

- **12+8 =20 terms**

8 Tones

ω8-ω8+ω8-ω1; (1)

ω8-ω7+ω8-ω2; ω8-ω7+ω7-ω1; (2)

ω8-ω6+ω8-ω3; ω8-ω6+ω7-ω2; ω8-ω6+ω6-ω1; (3)

ω8-ω5+ω8-ω4; ω8-ω5+ω7-ω3; ω8-ω5+ω6-ω2; ω8-ω5+ω5-ω1; (4)

ω8-ω4+ω7-ω4; ω8-ω4+ω6-ω3; ω8-ω4+ω5-ω2; ω8-ω4+ω4-ω1; (4)

ω8-ω3+ω5-ω3; ω8-ω3+ω4-ω2; ω8-ω3+ω3-ω1; (3)

ω8-ω2+ω3-ω2; ω8-ω2+ω2-ω1; (2)

ω8-ω1+ω1-ω1; (1) + 7 tones factors

- **20+20 = 40 terms**

9 Tones

ω9-ω9+ω9-ω2; ω9-ω9+ω8-ω1; (2)

ω9-ω8+ω9-ω3; ω9-ω8+ω8-ω2; ω9-ω8+ω7-ω1; (3)

ω9-ω7+ω9-ω4; ω9-ω7+ω8-ω3; ω9-ω7+ω7-ω2; ω9-ω7+ω6-ω1; (4)

ω9-ω6+ω9-ω5; ω9-ω6+ω8-ω4; ω9-ω6+ω7-ω3; ω9-ω6+ω6-ω2; ω9-ω6+ω5-ω1; (5)

ω9-ω5+ω8-ω5; ω9-ω5+ω7-ω4; ω9-ω5+ω6-ω3; ω9-ω5+ω5-ω2; ω9-ω5+ω4-ω1; (5)

ω9-ω4+ω6-ω4; ω9-ω4+ω5-ω3; ω9-ω4+ω4-ω2; ω9-ω4+ω3-ω1; (4)

ω9-ω3+ω4-ω3; ω9-ω3+ω3-ω2; ω9-ω3+ω2-ω1; (3)

ω9-ω2+ω2-ω2; ω9-ω2+ω1-ω1; (2) + 8 tones factors

28+40 = 68terms

10 Tones

ω10-ω10+ω10-ω3; ω10-ω10+ω9-ω2; ω10-ω10+ω8-ω1; (3)

ω10-ω9+ω10-ω4; ω10-ω9+ω9-ω3; ω10-ω9+ω8-ω2; ω10-ω9+ω7-ω1; (4)

ω10-ω8+ω10-ω5; ω10-ω8+ω9-ω4; ω10-ω8+ω8-ω3; ω10-ω8+ω7-ω2; ω10-ω8+ω6-ω1; (5)

ω10-ω7+ω10-ω6; ω10-ω7+ω9-ω5; ω10-ω7+ω8-ω4; ω10-ω7+ω7-ω3; ω10-ω7+ω6-ω2; ω10-ω7+ω5-ω1; (6)

ω10-ω6+ω9-ω6; ω10-ω6+ω8-ω5; ω10-ω6+ω7-ω4; ω10-ω6+ω6-ω3; ω10-ω6+ω5-ω2; ω10-ω6+ω4-ω1; (6)

ω10-ω5+ω7-ω5; ω10-ω5+ω6-ω4; ω10-ω5+ω5-ω3; ω10-ω5+ω4-ω2; ω10-ω5+ω3-ω1; (5)

ω10-ω4+ω5-ω4; ω10-ω4+ω4-ω3; ω10-ω4+ω3-ω2; ω10-ω4+ω2-ω1; (4)

ω10-ω3+ω3- ω3; ω10-ω3+ω2-ω2; ω10-ω3+ω1-ω1; (3)

ω10-ω2+ω1- ω2; (1) + 9 tones factors

37+68 =105 terms

11 Tones

ω11-ω11+ω11-ω4;ω11-ω11+ω10-ω3; ω11-ω11+ω9-ω2; ω11-ω11+ω8-ω1; (4)

ω11-ω10+ω11-ω5; ω11-ω10+ω10-ω4; ω11-ω10+ω9-ω3; ω11-ω10+ω8-ω2; ω11-ω10+ω7-ω1; (5)

ω11-ω9+ω11-ω6; ω11-ω9+ω10-ω5; ω11-ω9+ω9-ω4; ω11-ω9+ω8-ω3; ω11-ω9+ω7-ω2; ω11-ω9+ω6-ω1;(6)

ω11-ω8+ω11-ω7; ω11-ω8+ω10-ω6; ω11-ω8+ω9-ω5; ω11-ω8+ω8-ω4; ω11-ω8+ω7-ω3; ω11-ω8+ω6-ω2; ω11-ω8+ω5-ω1; (7)

ω11-ω7+ω10-ω7; ω11-ω7+ω9-ω6; ω11-ω7+ω8-ω5; ω11-ω7+ω7-ω4; ω11-ω7+ω6-ω3; ω11-ω7+ω5-ω2; ω11-ω7+ω4-ω1; (7)

ω11-ω6+ω8-ω6; ω11-ω6+ω7-ω5; ω11-ω6+ω6-ω4; ω11-ω6+ω5-ω3; ω11-ω6+ω4-ω2; ω11-ω6+ω3-ω1; (6)

ω11-ω5+ω6-ω5; ω11-ω5+ω5-ω4; ω11-ω5+ω4-ω3; ω11-ω5+ω3-ω2; ω11-ω5+ω2-ω1; (5)

ω11-ω4+ω4- ω4; ω11-ω4+ω3- ω3; ω11-ω4+ω2-ω2; ω11-ω4+ω1-ω1; (4)

ω11-ω3+ω2- ω3; ω11-ω3+ω1- ω2; (2) + 9 tones factors

46+105 =151 terms

----------/ /----------

4th order –> +8ΔW

5 Tones

ω5-ω1+ω5-ω1; (1)

- **1 terms**

6 Tones

ω6-ω3+ω6-ω1; (1)

ω6-ω2+ω6-ω2; ω6-ω2+ω5-ω1; (2)

ω6-ω1+ω4-ω1; (1) + 5 tones factors

- **4+1 = 5 terms**

7 Tones

ω7-ω5+ω7-ω1; (1)

ω7-ω4+ω7-ω2; ω7-ω4+ω6-ω1; (2)

ω7-ω3+ω7-ω3; ω7-ω3+ω6-ω2; ω7-ω3+ω5-ω1; (3)

ω7-ω2+ω5-ω2; ω7-ω2+ω4-ω1; (2)

ω7-ω1+ω3-ω1; (1) + 6 tones factors

- **9+5 =14 terms**

8 Tones

ω8-ω7+ω8-ω1; (1)

ω8-ω6+ω8-ω2; ω8-ω6+ω7-ω1; (2)

ω8-ω5+ω8-ω3; ω8-ω5+ω7-ω2; ω8-ω5+ω6-ω1; (3)

ω8-ω4+ω8-ω4; ω8-ω4+ω7-ω3; ω8-ω4+ω6-ω2; ω8-ω4+ω5-ω1; (4)

ω8-ω3+ω6-ω3; ω8-ω3+ω5-ω2; ω8-ω3+ω4-ω1; (3)

ω8-ω2+ω4-ω2; ω8-ω2+ω3-ω1; (2)

ω8-ω1+ω2-ω1; (1) + 7 tones factors

- **16+14 = 30 terms**

9 Tones

ω9-ω9+ω9-ω1; (1)

ω9-ω8+ω9-ω2; ω9-ω8+ω8-ω1; (2)

ω9-ω7+ω9-ω3; ω9-ω7+ω8-ω2; ω9-ω7+ω7-ω1; (3)

ω9-ω6+ω9-ω4; ω9-ω6+ω8-ω3; ω9-ω6+ω7-ω2; ω9-ω6+ω6-ω1; (4)

ω9-ω5+ω9-ω5; ω9-ω5+ω8-ω4; ω9-ω5+ω7-ω3; ω9-ω5+ω6-ω2; ω9-ω5+ω5-ω1; (5)

ω9-ω4+ω7-ω4; ω9-ω4+ω6-ω3; ω9-ω4+ω5-ω2; ω9-ω4+ω4-ω1; (4)

ω9-ω3+ω5-ω3; ω9-ω3+ω4-ω2; ω9-ω3+ω3-ω1; (3)

ω9-ω2+ω3-ω2; ω9-ω2+ω2-ω1; (2)

ω9-ω1+ω1-ω1; (1) + 8 tones factors

25+30 = 55terms

10 Tones

ω10-ω10+ω10-ω2; ω10-ω10+ω9-ω1; (2)

ω10-ω9+ω10-ω3; ω10-ω9+ω9-ω2; ω10-ω9+ω8-ω1; (3)

ω10-ω8+ω10-ω4; ω10-ω8+ω9-ω3; ω10-ω8+ω8-ω2; ω10-ω8+ω7-ω1; (4)

ω10-ω7+ω10-ω5; ω10-ω7+ω9-ω4; ω10-ω7+ω8-ω3; ω10-ω7+ω7-ω2; ω10-ω7+ω6-ω1; (5)

ω10-ω6+ω10-ω6; ω10-ω6+ω9-ω5; ω10-ω6+ω8-ω4; ω10-ω6+ω7-ω3; ω10-ω6+ω6-ω2; ω10-ω6+ω5-ω1; (6)

ω10-ω5+ω8-ω5; ω10-ω5+ω7-ω4; ω10-ω5+ω6-ω3; ω10-ω5+ω5-ω2; ω10-ω5+ω4-ω1; (5)

ω10-ω4+ω6-ω4; ω10-ω4+ω5-ω3; ω10-ω4+ω4-ω2; ω10-ω4+ω3-ω1; (4)

ω10-ω3+ω4-ω3; ω10-ω3+ω3-ω2; ω10-ω3+ω2-ω1; (3)

ω10-ω2+ω2-ω2; ω10-ω2+ω1-ω1; (2) + 9 tones factors

34+55 =89 terms

11 Tones

ω11-ω11+ω11-ω3;ω11-ω11+ω10-ω2; ω11-ω11+ω9-ω1; (3)

ω11-ω10+ω11-ω4; ω11-ω10+ω10-ω3; ω11-ω10+ω9-ω2; ω11-ω10+ω8-ω1; (4)

ω11-ω9+ω11-ω5; ω11-ω9+ω10-ω4; ω11-ω9+ω9-ω3; ω11-ω9+ω8-ω2; ω11-ω9+ω7-ω1; (5)

ω11-ω8+ω11-ω6; ω11-ω8+ω10-ω5; ω11-ω8+ω9-ω4; ω11-ω8+ω8-ω3; ω11-ω8+ω7-ω2; ω11-ω8+ω6-ω1;(6)

ω11-ω7+ω11-ω7; ω11-ω7+ω10-ω6; ω11-ω7+ω9-ω5; ω11-ω7+ω8-ω4; ω11-ω7+ω7-ω3; ω11-ω7+ω6-ω2; ω11-ω7+ω5-ω1; (7)

ω11-ω6+ω9-ω6; ω11-ω6+ω8-ω5; ω11-ω6+ω7-ω4; ω11-ω6+ω6-ω3; ω11-ω6+ω5-ω2; ω11-ω6+ω4-ω1; (6)

ω11-ω5+ω7-ω5; ω11-ω5+ω6-ω4; ω11-ω5+ω5-ω3; ω11-ω5+ω4-ω2; ω11-ω5+ω3-ω1; (5)

ω11-ω4+ω5- ω4; ω11-ω4+ω4- ω3; ω11-ω4+ω3-ω2; ω11-ω4+ω2-ω1; (4)

ω11-ω3+ω3-ω3; ω11-ω3+ω2- ω2; ω11-ω3+ω1-ω1; (3)

ω11-ω2+ω1-ω2; (1) + 10 tones factors

- **44+89 =133 terms**

----------/ /----------

4th order –> +9ΔW

6 Tones

ω6-ω2+ω6-ω1; (1)

ω6-ω1+ω5-ω1; (1)

- **2 terms**

7 Tones

ω7-ω4+ω7-ω1; (1)

ω7-ω3+ω7-ω2; ω7-ω3+ω6-ω1; (2)

ω7-ω2+ω6-ω2; ω7-ω2+ω5-ω1; (2)

ω7-ω1+ω4-ω1; (1) + 6 tones factors

- **6+2 =8 terms**

8 Tones

ω8-ω6+ω8-ω1; (1)

ω8-ω5+ω8-ω2; ω8-ω5+ω7-ω1; (2)

ω8-ω4+ω8-ω3; ω8-ω4+ω7-ω2; ω8-ω4+ω6-ω1; (3)

ω8-ω3+ω7-ω3; ω8-ω3+ω6-ω2; ω8-ω3+ω5-ω1; (3)

ω8-ω2+ω5-ω2; ω8-ω2+ω4-ω1; (2)

ω8-ω1+ω3-ω1; (1) + 7 tones factors

- **12+8 = 20 terms**

9 Tones

ω9-ω8+ω9-ω1; (1)

ω9-ω7+ω9-ω2; ω9-ω7+ω8-ω1; (2)

ω9-ω6+ω9-ω3; ω9-ω6+ω8-ω2; ω9-ω6+ω7-ω1; (3)

ω9-ω5+ω9-ω4; ω9-ω5+ω8-ω3; ω9-ω5+ω7-ω2; ω9-ω5+ω6-ω1; (4)

ω9-ω4+ω8-ω4; ω9-ω4+ω7-ω3; ω9-ω4+ω6-ω2; ω9-ω4+ω5-ω1; (4)

ω9-ω3+ω6-ω3; ω9-ω3+ω5-ω2; ω9-ω3+ω4-ω1; (3)

ω9-ω2+ω4-ω2; ω9-ω2+ω3-ω1; (2)

ω9-ω1+ω2-ω1; (1) + 8 tones factors

20+20 = 40 terms

10 Tones

ω10-ω10+ω10-ω1; (1)

ω10-ω9+ω10-ω2; ω10-ω9+ω9-ω1; (2)

ω10-ω8+ω10-ω3; ω10-ω8+ω9-ω2; ω10-ω8+ω8-ω1; (3)

ω10-ω7+ω10-ω4; ω10-ω7+ω9-ω3; ω10-ω7+ω8-ω2; ω10-ω7+ω7-ω1; (4)

ω10-ω6+ω10-ω5; ω10-ω6+ω9-ω4; ω10-ω6+ω8-ω3; ω10-ω6+ω7-ω2; ω10-ω6+ω6-ω1; (5)

ω10-ω5+ω9-ω5; ω10-ω5+ω8-ω4; ω10-ω5+ω7-ω3; ω10-ω5+ω6-ω2; ω10-ω5+ω5-ω1; (5)

ω10-ω4+ω7-ω4; ω10-ω4+ω6-ω3; ω10-ω4+ω5-ω2; ω10-ω4+ω4-ω1; (4)

ω10-ω3+ω5-ω3; ω10-ω3+ω4-ω2; ω10-ω3+ω3-ω1; (3)

ω10-ω2+ω3-ω2; ω10-ω2+ω2-ω1; (2)

ω10-ω1+ω1-ω1; (1) + 9 tones factors

30+40 =70 terms

11 Tones

ω11-ω11+ω11-ω2;ω11-ω11+ω10-ω1; (2)

ω11-ω10+ω11-ω3; ω11-ω10+ω10-ω2; ω11-ω10+ω9-ω1; (3)

ω11-ω9+ω11-ω4; ω11-ω9+ω10-ω3; ω11-ω9+ω9-ω2; ω11-ω9+ω8-ω1; (4)

ω11-ω8+ω11-ω5; ω11-ω8+ω10-ω4; ω11-ω8+ω9-ω3; ω11-ω8+ω8-ω2; ω11-ω8+ω7-ω1; (5)

ω11-ω7+ω11-ω6; ω11-ω7+ω10-ω5; ω11-ω7+ω9-ω4; ω11-ω7+ω8-ω3; ω11-ω7+ω7-ω2; ω11-ω7+ω6-ω1; (6)

ω11-ω6+ω10-ω6; ω11-ω6+ω9-ω5; ω11-ω6+ω8-ω4; ω11-ω6+ω7-ω3; ω11-ω6+ω6-ω2; ω11-ω6+ω5-ω1; (6)

ω11-ω5+ω8-ω5; ω11-ω5+ω7-ω4; ω11-ω5+ω6-ω3; ω11-ω5+ω5-ω2; ω11-ω5+ω4-ω1; (5)

ω11-ω4+ω6-ω4; ω11-ω4+ω5- ω3; ω11-ω4+ω4-ω2; ω11-ω4+ω3-ω1; (4)

ω11-ω3+ω4-ω3; ω11-ω3+ω3- ω2; ω11-ω3+ω2-ω1; (3)

ω11-ω2+ω2-ω2; ω11-ω2+ω1-ω1; (2) + 10 tones factors

40+70 =110 terms

12 Tones

ω12-ω12+ω12-ω3; ω12-ω12+ω11-ω2; ω12-ω12+ω10-ω1; (3)

ω12-ω11+ω12-ω4; ω12-ω11+ω11-ω3; ω12-ω11+ω10-ω2; ω12-ω11+ω9-ω1; (4)

ω12-ω10+ω12-ω5; ω12-ω10+ω11-ω4; ω12-ω10+ω10-ω3; ω12-ω10+ω9-ω2; ω12-ω10+ω8-ω1; (5)

ω12-ω9+ω12-ω6; ω12-ω9+ω11-ω5; ω12-ω9+ω10-ω4; ω12-ω9+ω9-ω3; ω12-ω9+ω8-ω2; ω12-ω9+ω7-ω1; (6)

ω12-ω8+ω12-ω7; ω12-ω8+ω11-ω6; ω12-ω8+ω10-ω5; ω12-ω8+ω9-ω4; ω12-ω8+ω8-ω3; ω12-ω8+ω7-ω2; ω12-ω8+ω6-ω1;(7)

ω12-ω7+ω11-ω7; ω12-ω7+ω10-ω6; ω12-ω7+ω9-ω5; ω12-ω7+ω8-ω4; ω12-ω7+ω7-ω3; ω12-ω7+ω6-ω2; ω12-ω7+ω5-ω1; (7)

ω12-ω6+ω9-ω6; ω12-ω6+ω8-ω5; ω12-ω6+ω7-ω4; ω12-ω6+ω6-ω3; ω12-ω6+ω5-ω2; ω12-ω6+ω4-ω1; (6)

ω12-ω5+ω7-ω5; ω12-ω5+ω6-ω4; ω12-ω5+ω5-ω3; ω12-ω5+ω4-ω2; ω12-ω5+ω3-ω1; (5)

ω12-ω4+ω5- ω4; ω12-ω4+ω4- ω3; ω12-ω4+ω3-ω2; ω12-ω4+ω2-ω1; (4)

ω12-ω3+ω3-ω3; ω12-ω3+ω2- ω2; ω12-ω3+ω1-ω1; (3)

ω12-ω2+ω1-ω2; (1) + 11 tones factors

51+70 =122 terms